ISSN 0514–8790

AKADEMIE DER WISSENSCHAFTEN DER DDR
Forschungsbereich Geo- und Kosmoswissenschaften
ZENTRALINSTITUT FÜR PHYSIK DER ERDE

Veröffentlichungen des Zentralinstituts für Physik der Erde
Nr. 102

6th International Symposium „Geodesy and Physics of the Earth"

GDR Potsdam, August 22–27, 1988

PROCEEDINGS

Part III

Recent Crustal Movements

Herausgeber: Der Direktor des Zentralinstituts für Physik der Erde

Als Manuskript gedruckt
Potsdam 1989

III-12-12 Ag 521 426 89

C O N T E N T S
I N H A L T S V E R Z E I C H N I S

Part III
Teil III

RECENT CRUSTAL MOVEMENTS

PRESENT STATE AND PROSPECTS OF MONITORING RECENT CRUSTAL MOVEMENTS

Pavel Vyskočil, Research Institute of Geodesy, Topography and Cartography, Zdiby, Czechoslovakia

ABSTRACT

The recent crustal movement studies are one of the main tasks of present geophysical and geological sciences. It is the result of common experiences, as volcanic and seismic activity, that the Earth is not stable as has been supposed early. In order to diminish the seismic and volcanic risk affected the environment of the mankind, the properties of recent crustal movements are studied by various methods. One of the sources of such information are also the geodetic repeated measurements, offered the exact numerical values of the rates of movements. In addition to the temporal Inter-Union Projects as Upper Mantle Project, Geodynamics Project and Litosphere Project, the studies are coordinated by the permanent Commission on Recent Crustal Movements of the IAG. The main goal of this effort is to understand the laws controled the Earth's dynamics. In order to achieve this goal, the studies are carried out separately in global and regional or local scale till now, but finally, the results of both aproaches must be in agreement. Such a final result will have the improtance for earthguake prediction and other practical applications. The present paper discussed the up to date results and main directions for further extension and improvement of recent crustal movement studies with respect to modern technique available.

DOI: https://doi.org/10.2312/zipe.1989.102.03

INTRODUCTION

Of about two thousand years ago Eratosthenes determined the approximative value of the Earth's radius by the measurement of the geocentrical angle and surface distance between Aswan and Alexandria at the territory of present Egypt. In spite of the low accuracy, his idea and work could be considered as the fundamental stone of the building called GEODESY. Many centuries later was the same value determined more exact, but not enough for present requirements. It was established the branch of geodesy aimed to the studies of present dimensions and shape of the Earth's body. It was discovered the polar motion and the present studies are aimed to understand the mutual connection between the core dynamics and Earth's rotation. At the beginning of this century Wegener presented his theory on the movement of continents as the fundamental idea for the plate tectonic theory, extended after the Second World War. Nevertheless, at the 3rd General Assembly of IUGG held in Praha, Czechoslovakia in 1927, it was recommended to establish the system of permanent stations to determine the changes of geographical coordinates, due to the movement of continents. All these studies were started and are performed with the aim to understand the global mechanism of Earth's body dynamics.

After the catastrophic earthquake occured in San Francisco, Calif. in 1906 as well as after the similar events in Japan, the detail studies of recent crustal movements in local scale were iniciated there by means of repeated geodetic measurements. The significance of such studies was appreciated by IAG in fiftieths and the Commission on Recent Crustal Movements (CRCM) was established in early sixtieths. We commemorated this turning point in recent crustal movement studies at the CRCM International Symposium held in Tallin, Est.SSR in 1986. With respect to the observing technique of that time, the Commission started with the main task to

DOI: https://doi.org/10.2312/zipe.1989.102.03

construct the maps of vertical crustal movements with additional studies at the test areas of local importance. During last 27 years the Commission extended its activity practically at all continents, and, using the more precise technique improved also its studies. At the present stage, the work of the CRCM is focused at the local and regional studies, i.e. at the second part of the common research of the dynamics of our Planet. Nevertheless, each local or regional study of recent crustal movements is unique, and contributes essentially to detail understanding of the Earth's dynamics. The history of the CRCM is described in more detail in the paper presented by Yu.D. Boulanger and P. Vyskočil at the mentioned above CRCM Symposium in Tallin 1986.

PRESENT STATE OF PROBLEM

The history of recent crustal movement studies during last 27 years is directly connected with the work of the CRCM. It is why, discussing the present state of studies, we have to use the results achieved within this Commission and by its cooperation with the Inter-Union Projects. And moreover, following the development of the CRCM we can better understand the present achievements in recent crustal movement research throughout the world.

The first stage of the CRCM work is related to the data collection and studies of their processing by simple way. With respect to the simplicity of levelling and availability of its repeated measurements, the regional and national maps of vertical movements were constructed at parts of Europe, Northern America as well as Japan. Studies of horizontal movements were limited at local test areas for not accurate results of determination of movements at long distances by means of repeated determinations of geographic coordinates. The unique results were achieved in Japan, where the horizontal movements were determined at whole country by the analy-

DOI: https://doi.org/10.2312/zipe.1989.102.03

sis of repeated triangulation. Due to the lack of proper repeated geodetic measurements in Africa, Southern America and most part of Asia, no information were available from these regions. Moreover, most countries at these continents had neither proper economical background to support financially the crustal movement studies nor proper knowledge on the importance of such works. From this view point, the extension of our studies in developing countries is related to the education "how can help the information on recent crustal movements to their national economy". Unfortunately, the predominant source of geodynamical information from developing countries is based on the geological research and gravity measurements, focused mainly at oil and gas prospection.

Continuous improvement of recent crustal movement studies in sixtieths and seventieths is related to improvement of measurement instrumentation as distance meters, precise absolute and relative gravity meters and space technique. The proper procedures for data processing and analysis are elaborated simultaneously with respect to improvements of measurement instrumentation and technique as well as to improvements in construction and capability of computors. Such a way, the first stage of our studies, characterized by collection of data and description of movements is changed in second stage, starting approximatively at the end of seventieths. This change is continuous and is accompanied by more close cooperation among various branches of science and improvement of theoretical basis. The description of movements is changed in analysis and modelling of dynamical phenomena using the information on crustal structure and movements at its surface. We started to transform the simple movements in the field of deformations as a qualitatively new phenomenon to describe the dynamics. Such an approach is the first step to further description and definition of driving forces in local or regional scale ets. But only the first step till now!

DOI: https://doi.org/10.2312/zipe.1989.102.03

From theoretical studies we understand the mutual connaction between movements and secular changes in gravity field. Unfortunately, with exception of some seismoactive areas, we did not register the real non tidal gravity changes. Due to the lack of underground information and difficulties in computations, the geodynamical models are very simplified. We achieved some knowledge on relations between the surface movements and deformations and seismicity, but the procedures for earthquake prediction is at the starting point. The developing countries are more interested in recent crustal movement studies but the financial questions brake the extension of works till now.

In spite of the pesimistic comments given above, we did anything and we achieved qualitatively new results and knowledge on the dynamical porperties of the Earth's crust. These information in detail you can learn in Proceedings of last CRCM regional and international symposia as well as of symposia of other bodies of the IUGG. Also the papers to be presented here will give the evidence on progress in our work. In addition to increase of amount of data and areas under study, the theoretical basis for further research is extended intensively. The results of applications of space technique gave us the first information on movements of continents, and offer us the further achievements as weel as possibilities to combine the global and regional or local results. From this view point, the present stage of our studies can be characterized as the preparation of initial conditions for further stage of complex geodynamical research.

FUTHER TASKS AND DEVELOPMENT

The main task of the CRCM given by its first President Prof. Mesherikov was to cover all continents by the maps of recent crustal movements, in first stage of their vertical components. Unfortunately, this task was not realized

DOI: https://doi.org/10.2312/zipe.1989.102.03

till now, and can not be simply achieved at main parts of lands of the Earth in near future. Nevertheless, the rapid development of space and computing technique gives us the tool to follow this task more easy and really at all drylands. It is also the reason why the CRCM established the close contacts with the IAG Commission No. VIII, responsible for the applications of space technique in geodynamics. The first common symposium of both Commissions will be held at the IAG General Meeting in Edinburg, UK, August 1989. This cooperation should result in more rapid covering of not yet studied eraes and regions by proper, at the first stage scattered data on crustal movements in Africa, Southern America and Asia. The close cooperation of both Commissions offer also the possibility to perform the studies of global plate movements.

Obviously, the applications of space technique in our studies will not replace the local and regional measurements by means of terrestrial methods. These works will serve for improvements of complex modelling technique using the detail, and more dense data. In addition, the construction of maps of vertical movements should be finished in the areas where the proper data are available. Simultaneously, we have to follow the projects for monitoring the secular gravity changes in order to apply these data to the other information on surface movements. All these works, supposed to be performed at proper scientific level should be based at the more close international and interdisciplinary cooperation. The CRCM is good basis for such a cooperation, but all its possibilities did not used till now. It concerns especially the establishment of international projects for monitoring recent crustal movements at classical territories as well as in developing countries. In order to follow this idea, some test area in very active zone could be chosen as a working place for specialized groups of scientists from various countries etc. In addition, the active participation at the projects of the Commission VIII is desirable.

DOI: https://doi.org/10.2312/zipe.1989.102.03

As has been said early, we have now the unique chance for qualitatively new improvements in recent crustal movement studies. The topics of these works could be summarized as follows:

- to establish the initial epoch of regional or global network measured by means of space technique, with special respect to its connection to present local test areas,

- to establish the initial epoch of precise gravity measurements for studies of mutual connections between the surface movements and deformations and gravity changes,

- to improve the international and interdisciplinary cooperation by preparation of international projects focused at very active areas, including the seimoactive zones,

- to improve the recent crustal movement and deformation studies in seismoactive zones, aimed to the earthquake prediction,

- to focuse the scientific effort at the improvement of processing methods as well as geodynamical modelling,

- to continue by the compilation of maps of movements and deformations covering the regions of the Earth.

CONCLUSION

The CRCM during its work achieved valuable results and knowledge on the recent crustal movements a deformations at various areas and regions. For processing and analysis of data the proper theoretical basis was established, including modelling of geodynamical phenomena. Unfortunately, the covering of all drylands by information we are interested is very slow.

The applications of space technique offer us the unique oportunity for rapid extension of the geodynamical studies,

DOI: https://doi.org/10.2312/zipe.1989.102.03

especially in areas not studied till now. In order to improve our works the more close international and interdisciplinary cooperation should be established, and focused at the most active areas, especially in developing countries. The theoretical studies and geodynamical modelling should be improved continuously, and testad in accordance with increase of amount of data, including real gravity changes.

Following the given above topics we prepare the good basis for the use of qualitatively new and worldwide data sets during next decade. Such a way we can expect the essential extension of our knowledge on geodynamical properties of our Planet till the end of present century. It will be also our contribution to the understanding of the origin of the dynamics of the Earth's crust.

DOI: https://doi.org/10.2312/zipe.1989.102.03

Zu einigen methodisch-instrumentellen Fragen bei geodynamischen Messungen mit hydrostatischen Niveauvariometern

J. Byl, Potsdam[+]

Summary

In general, tiltmeters are used for observing ground deformation at periods of minutes to days. Small-scale lateral inhomogeneities at the instrument sites distort signals up to 25 % ... 40 %. An other point of view - beside site location and geometry - is the question of tiltmeter design and attaching the instrument to the ground, especially for observing longperiodic crustal movements. Basic design techniques of short base and longbase tiltmeters, problems of stability of instruments and results of comparison tests are discussed. Repeated experience has shown the long base tiltmeter (Michelson-type), when well built, to be superior to all other types, proving end-monument stability to be a dominant source of noise.

Zusammenfassung

Allgemein werden Neigungsmesser zur Beobachtung von Untergrunddeformationen im Periodenbereich von Minuten bis Tagen verwandt. Lokale laterale Inhomogenitäten in der Umgebung des Beobachtungsortes verfälschen das Signal bis zu 40 %. Neben der Stationslage und -geometrie spielen Fragen der mechanischen Gestaltung des Instruments und der Ankopplung an den Untergrund insbesondere dann eine wesentliche Rolle, wenn das Langzeitverhalten der Kruste untersucht werden soll.

[+] Akademie der Wissenschaften der DDR, Zentralinstitut für Physik der Erde, 1561 Potsdam, Telegrafenberg

DOI: https://doi.org/10.2312/zipe.1989.102.03

Es werden verschiedene Grundtypen von Neigungsmessern, Probleme der Ankopplung der Instrumente an den Untergrund und Ergebnisse von Instrumentenvergleichen diskutiert. Dabei zeigt sich, daß longbase-Neigungsmesser vom Michelsontyp anderen Varianten überlegen sind, wenn die Stabilität der Sensorgefäße beachtet wird.

1. Problemstellung

Geodynamische Prozesse sind durch komplexe Bewegungsvorgänge in unterschiedlichen Maßstabs- und Periodenbereichen gekennzeichnet, die in der oberen Erdkruste und an der Erdoberfläche geometrisch und physikalisch meßbar in Erscheinung treten. Sie stehen in enger Beziehung zum Erdschwerefeld. Höhen- und Massenveränderungen führen zu Schwereänderungen. Andererseits verursachen durch endogene und exogene Kräfte hervorgerufene Variationen des Schwerefeldes Massen- und Höhenveränderungen.
Bewegungen der Erdoberfläche gegenüber den Niveauflächen des Erdschwerefeldes stellen sich als vertikale Verschiebungen und Neigungen dar. Ihre Bestimmung erfordert Nivellements sowie Beobachtungen des örtlichen und zeitlichen Verhaltens des Schwerevektors. Aus der Frage nach der Richtung, d. h. nach dem Neigungsverhalten, ergibt sich das Problem der Bestimmung der Lotrichtung bzw. der Niveaufläche mit Bezug auf die Erdoberfläche. Ein direktes Verfahren besteht in der Bestimmung der Differenz der gezeitenbedingten Deformationen der Meeresoberfläche gegenüber denen der festen Erdoberfläche. Auswertungen langjähriger Messungen der Pegelstände der Meere hauptsächlich durch Darwin und Schweydar ermöglichten so erste quantitative Informationen über das globale elastische Verhalten der festen Erde / 1 /.
Die ersten kontinuierlichen Erdkrustenbeobachtungen hat Kühnen zur Feststellung von Neigungen und vertikalen Bewegungen auf dem Telegraphenberg bei Potsdam angestellt / 2 /. Zu diesem Zweck

DOI: https://doi.org/10.2312/zipe.1989.102.03

wurde um die Kuppe des Telegraphenberges ein etwa 400 m langes hydrostatisches System längs einer Höhenlinie verlegt und an 4 Stellen über 10 Jahre beobachtet.
In der folgenden Zeit hat das Horizontalpendel allgemeine Verbreitung gefunden. Es ermöglicht bei einfacher mechanischer Gestaltung kontinuierliche Beobachtungen der Lotbewegung mit hoher Empfindlichkeit. Die nach dem Internationalen Geophysikalischen Jahr 1956/57 mit verschiedenen Varianten des Horizontalpendels gewonnenen Beobachtungsreihen waren trotz z. T. erheblicher systematischer Instrumenteneffekte geeignet, die harmonischen Konstanten des wesentlichen Teils des kurzperiodischen Gezeitenspektrums sowie der 14tägigen und 4wöchigen Mondwelle zu bestimmen.
Beobachtungen der Gezeiten der festen Erde lassen sich mit Hilfe von Spektralfunktionen in der Form

$$S_T(f) = L_T(f) + E_T(f) + M_T(f), \qquad (1)$$

darstellen

$L_T(f)$ - lokaler, stationsbedingter Anteil,

$E_T(f)$ - Erdgezeitenanteil,

$M_T(f)$ - maritimer und meteorologischer Anteil.

Die einzelnen Glieder werden durch trigonometrische Funktionen beschrieben, deren Frequenzen, Amplituden und Phasen entweder durch den Quellprozeß vorgegeben sind oder aus den Beobachtungsreihen ermittelt werden. Das Horizontalpendelsignal wird wesentlich durch den lokalen Term beeinflußt. Häufig zeigt sich, daß die stationsbedingten lokalen Effekte bei Lotschwankungsmessungen mit Horizontalpendeln bis zu $\pm$ 40 % in der Gesamtamplitude der NS-Komponente und bis zu $\pm$ 15 % in der EW-Komponente von M_2 betragen können; Fehler in den Phasenverschiebungen der beobachteten gegenüber den Modellgezeitenwellen bis

DOI: https://doi.org/10.2312/zipe.1989.102.03

zu ± 20 % sind verbreitet / 3 /. Die anzustrebende repräsentative Bandbreite der Lotschwankungssignale umfaßt über den Anteil der sektoriellen und tesseralen Gezeiten hinaus Informationen über quasiperiodische und saisonale Neigungsvorgänge. Die Unterdrückung des hauptsächlich störenden kurzwelligen Signalanteils wird einmal mit Hilfe der üblichen Signalfilterung angestrebt, zum anderen auch über mechanisch-konstruktive Lösungen mit gegenüber dem Horizontalpendel wesentlich vergrößerten Instrumentenbasen. Die Forderung nach wenig aufwendiger Installation an beliebigen Orten bei gleichzeitig größerer Repräsentativität des langperiodischen Signalanteils führte zu verschiedenen Entwicklungen von Bohrlochneigungsmessern, unter denen das Vertikalpendel Bedeutung erlangte / 4 / / 5 /. Eine mehrere Meter lange Beton- oder Metallverrohrung des Bohrloches für die Aufnahme des Instruments vergrößert die Instrumentenbasis gegenüber der des Horizontalpendels um eine Größenordnung und reduziert so die bei unterirdischen Observatorien herkömmlicher Art von der Stationsgeometrie abhängigen Hohlraumeffekte / 6 /.

Daneben findet das direkte Verfahren der Niveauflächenbeobachtung mit hydrostatischen Systemen als Ergänzung zu geometrischen Wiederholungsnivellements in Bereichen mit besonderer Krustenmobilität zunehmend Anwendung. Das hydrostatische Niveau bietet grundsätzliche Vorteile im Hinblick auf Genauigkeit und Kontinuität der Signalgewinnung sowohl als Niveauvariometer für die Neigungsbestimmung als auch für Nivellements unter schwierigen Bedingungen in Höhennetzen kleiner Ausdehnung / 7 / / 8 /.

Für unterschiedliche Aufgaben sind Instrumente mit Basislängen von 30 m bis zu mehreren hundert Metern in beiden Grundformen Schlauchwaage und Langwasserhorizont entstanden. Entsprechend den Forderungen an die Signalauflösung - 10^{-8} ... 5 . 10^{-9} rad., d. h. 100 nm vertikale Niveauverschiebung bei einer Instrumentenbasislänge von 100 m - wird eine berührungslose Signalerfassung angestrebt.

DOI: https://doi.org/10.2312/zipe.1989.102.03

2. Die hydrostatische Neigungsmessung

Das hydrostatische Niveauvariometer leitet sich aus dem hydrostatischen Nivellementssystem und der Präzisionsschlauchwaage für die Bauwerksüberwachung ab. Die Messung der Neigung des mechanischen Sensors, der über seine gesamte Länge fest mit dem Untergrund verbunden ist, erfolgt mit Bezug auf die Niveaufläche. Die Neigung ($\tan\varphi = 2h/l$) ergibt sich aus der Instrumentenbasislänge und der vertikalen Verschiebung der Wandlergefäße gegenüber den die Niveaufläche repräsentierenden Flüssigkeitsspiegeln. Das Verfahren ermöglicht die Höhen- bzw. Neigungsbestimmung zwischen beliebigen Punkten in annähernd gleichem Niveau.
Für die Meßstellen gilt:

$$V_o\,(R, \varphi, \lambda\,) = V\,(R + \Delta R, \varphi + \Delta\varphi, \lambda + \Delta\lambda\,), \qquad (2)$$

woraus hinreichend genau folgt:

$$\frac{\partial V}{\partial R}\,\Delta R + \frac{\partial V}{\partial \varphi}\,\Delta\varphi + \frac{\partial V}{\partial \lambda}\,\Delta\lambda = 0 \qquad (3)$$

Das bedeutet: Aus der Kenntnis der Breiten- und Längendifferenzen zweier Meßstellen ist die Höhendifferenz ihrer Niveaus ableitbar (Moulton) / 9 /.
Hydrostatische Systeme mit vorwiegend induktiver oder kapazitiver Signalwandlung sind für geodynamische Untersuchungen von Hagiwara /10/, Yamada /11/, Cook /12/, Kisslinger und Rikitake /13/, Kääriäinen /14/, Peters /15/ und Mathey /16/ entwickelt worden. Bower beschreibt einen empfindlichen Neigungsmesser, der auf dem Prinzip eines von Eaton entwickelten Instruments beruht; die Niveauschwankungen werden über Schwimmerbewegungen induktiv erfaßt /17/, /18/. Hugget et.al. versuchen eine Temperaturkompensation unter Verwendung verschiedener Flüssigkeiten mit unterschiedlichen Temperaturkoeffizienten /19/.
In Japan gehören seit dem Japanese Earthquakeresearch Programme hydrostatische Systeme (Schlauchwaageprinzip) zur Standardausrü-

DOI: https://doi.org/10.2312/zipe.1989.102.03

stung geodynamischer Observatorien.
An mehr als 30 Stationen sind hier Niveauvariometer gemeinsam mit Extensometern und Gravimetern für kleinregionale Deformationsuntersuchungen in mobilen Krustenbereichen installiert, die durch gekoppelte Tilt-Strain-Deformationen gekennzeichnet sind /20/. Schlauchwaage-Niveaus und Extensometer sind meist parallel angeordnet, haben gleiche Abmessungen und gleiche Empfindlichkeit /21/ /22/. Die Basislängen betragen zumeist 30 ... 40 m, die Auflösung der Extensometer 10^{-9} ($\Delta l/l$) und die der Niveaus 10^{-7} ... 10^{-9} ($\Delta h/h$). Die hydrostatischen Niveaus sind damit auch der Gezeitenproblematik angepaßt, dienen aber in erster Linie der Untersuchung des langzeitigen Neigungsverhaltens, oftmals in Verbindung mit im Stationsumfeld durchgeführten Wiederholungsnivellements /23/.
Die andere Variante arbeitet mit einem über die gesamte Instrumentenlänge freien Flüssigkeitsniveau (Langwasserhorizont). Niveauinstrumente dieser Art haben einen kleinen Meßbereich, erfordern eine präzise Horizontierung und bedingen eine entsprechend aufwendige Installation; sie ermöglichen jedoch hohe Empfindlichkeiten und gestatten vom Prinzip her die Reduzierung äußerer Einflüsse. Während hochauflösende Messungen mit Schlauchwaageniveaus eine unterirdische Installation erforderlich machen, stellen Niveauvariometer mit freiem Horizont keine Anforderungen bezüglich der Temperaturkonstanz an den Meßort. Die neueren Instrumentenentwicklungen wurden wesentlich durch diesen Umstand bestimmt.
Der Langwasserhorizont als geodynamischer Sensor führt sich auf Michelson und Gale zurück, denen es mit teils interferometrischer Auflösung der Wasserspiegelschwankungen gelang, halb- und ganztägige Gezeitenwellen nachzuweisen /24/.
Spätere Entwicklungen wurden durch Egedal und Fjeldstad /25/, Kasahara /26/, Bower unc Coutier /27/, Kääriäinen /28/ und Plumb et al. /29/ bekannt.

DOI: https://doi.org/10.2312/zipe.1989.102.03

3. Temperatur- und Luftdruckänderungen, Kapillarität, Eigenschwingungen. Orientierung der Instrumente

Abweichungen der Menisken von der Niveaufläche werden hervorgerufen durch: Temperatureinflüsse,
Luftdruckschwankungen,
den Einfluß der Kapillarität und
Anregungen von Schwingungen

3.1. Temperatur- und Luftdruckeinflüsse

Statische Veränderungen der Flüssigkeitsstände in einem kommunizierenden Gefäß infolge äußerer Einflüsse, wie durch den Luftdruck und die Temperatur, lassen sich mit Hilfe der Bernoullischen Gleichung

$$\frac{1}{2}\rho v^2 + p + \rho g h = \text{const.} \qquad (4)$$

darstellen.

Hierin sind ρ die Dichte der Flüssigkeit,
v ihre (im allgemeinen örtlich veränderliche) Geschwindigkeit,
p der Druck,
g die Schwerebeschleunigung und
h die Vertikalkomponente (Höhe des Sensorgefäßes).

Unperiodische bzw. langperiodische Bewegungsvorgänge der Neigung können als Aufeinanderfolge statischer Gleichgewichtszustände betrachtet werden. Damit wird $v = 0$, und es ergibt sich für das Gleichgewicht in einem kommunizierenden Gefäß gemäß Abb. 1a

$$p_1 + \rho_1 g_1 h_1 = p_2 + \rho_2 g_2 h_2 \quad ^{1)} \qquad (5)$$

---

1) bei unterschiedlichen Dichten ρ_1, ρ_2 und entsprechend unterschiedlichen Höhen h_1, h_2 in den vertikalen Gefäßteilen

DOI: https://doi.org/10.2312/zipe.1989.102.03

Aus der Differentiation der Parameter p, ϱ und g nach h folgen Luftdruck-, Temperatur- und Schwerekorrektion.
Aus Gleichung (4) folgt durch Differentiation nach den Parametern ϱ und h: $d\varrho\, g\, h + \varrho\, g\, dh = 0$,

$$dh = -\frac{d\varrho\, h}{\varrho} \quad . \tag{6}$$

Die Dichte ϱ ist eine Funktion der Temperatur ϑ. Mit $\varrho = \varrho(\vartheta)$ folgt:

$$dh = -\frac{\frac{d\varrho}{d\vartheta}}{\varrho}\, h\, d\vartheta \quad . \tag{7}$$

Der Temperatureinfluß ist somit dem vertikalen Anteil des Flüssigkeitsbehälters (Sensorgefäß), dem Ausdehnungskoeffizienten der Flüssigkeit und der Temperaturdifferenz proportional. Hiernach ist die Temperaturstörung durchgehender Niveaus nach dem Prinzip des Langwasserhorizonts gleich Null, während Schlauchwaagesysteme entsprechend der Höhe des Sensorgefäßes gestört sind. Die Korrektion wegen unterschiedlicher Temperaturen in den Vertikalkomponenten des Flüssigkeitsgefäßes ist bei hydrostatischen Nivellements von besonderer Bedeutung / 7 / / 8 /.

Luftdruckbedingte Fehler entstehen durch unterschiedlichen Luftdruck über den Flüssigkeitsständen der Sensorgefäße. Die Druckdifferenz dp zwischen den Meßstellen führt zu einer Differenz der Flüssigkeitsstände dh von der Größe

$$dh = -\frac{dp}{\varrho\, g} \tag{8}$$

Wird die Druckdifferenz in mm Hg gemessen, so beträgt die Korrektur der Niveaumessung

$$dh\,(p)_{mm} = \frac{\varrho_{Hg}}{\varrho_{Fl}}\, dp \quad ^{2)} \tag{9}$$

---

2) Wurde der Anschaulichkeit halber benutzt; entsprechende Umrechnungseinheit: $1\ hPa = 1\ mb$.

DOI: https://doi.org/10.2312/zipe.1989.102.03

h - für die vertikalen Teile des Flüssigkeitsbehälters - ist in (8) nicht enthalten; d. h. der Einfluß von Luftdruckdifferenzen ist, unabhängig von der geometrischen Form des Meßsystems, in jedem Falle wirksam.
(9) läßt weiterhin erkennen, daß die luftdruckbedingte Meniskenverschiebung von der Dichte der Flüssigkeit abhängig ist. Sie wird mit zunehmender Dichte geringer und erreicht bei Verwendung von Quecksilber weniger als ein Zehntel des Betrages von Wasser. Üblicherweise wird Wasser als Füllung benutzt, seltener Äthylalkohol o. ä.. Bei einer Luftdruckdifferenz von 1 mm Hg zwischen den Menisken entstehen bei diesen Flüssigkeiten relative Verschiebungen von etwa 13,6 bzw. 17,0 mm.
Die einfachste Lösung bezüglich horizontaler Luftdruckdifferenzen ermöglicht wieder der Langwasserhorizont in der seinerzeit von Michelson und später von Kääriäinen angewendeten Form eines nach außen abgeschlossenen teilgefüllten Behälters.

3.2. Die Kapillarität

Die Resultierende der Kohäsionskräfte innerhalb der Flüssigkeit und der zwischen den Gefäßwänden und der Flüssigkeit wirkenden Adhäsionskräfte bewirkt Höhen- und Formänderungen der Flüssigkeitsspiegel (Abb. 1b).
Für den allgemeinen Fall einer nicht vollständigen Benetzung der Gefäßwände entsteht eine Höhenänderung, die sich durch die Beziehung

$$dh = \frac{2\sigma}{\rho g r} \cdot \cos\Theta \qquad (10)$$

darstellen läßt, wobei

- r der Gefäßradius,
- σ die Oberflächenspannung,
- ρ die Dichte der Flüssigkeit und
- Θ den Randwinkel zwischen der Gefäßwand und der Tangente der Flüssigkeitsoberfläche in der Kontaktlinie bezeichnen.

DOI: https://doi.org/10.2312/zipe.1989.102.03

Kapillarascension oder Kapillardepression werden durch das Verhältnis von Adhäsion und Kohäsion zueinander bestimmt und durch das Vorzeichen des Faktors cos Θ beschrieben.
Der Kapillarfehler ist hiernach umgekehrt proportional der Oberfläche des Meniskus.

Tektonische Problemstellungen erfordern Instrumente mit erheblichen Basislängen (200 m bis zu 1000 m), die bereits mechanisch langwelligen Signalen nach Möglichkeit angepaßt sind. Von Interesse sind Bewegungsabläufe in der Erdkruste im Kilometerbereich mit Perioden von einigen Tagen bis zu einem Jahr und mit Amplituden bis zu 10^{-5} rad.
Nach Plumb et al. ist für die Erfassung von Straindeformations- und Neigungsvorläufern im Zusammenhang mit entfernteren Erdbeben eine Verminderung des Rauschpegels auf weniger als 10^{-8} rad notwendig, während im langperiodischen tektonischen Signalbereich ein Rauschpegel von maximal 10^{-7} rad als Stabilitätskriterium anzustreben ist bei einer gleichzeitigen Empfindlichkeit von ca. 5×10^{-9} rad.
Eine Störpegelamplitude von maximal 10^{-7} rad erfordert eine vertikale Standfestigkeit der Wandler einer 200 m - 300 m langen Anlage von 25 /um. Plumb et al. berichten von Messungen unter günstigen Aufstellungsbedingungen, die eine vertikale Langzeitstabilität der Wandler von 20 /um relativ zueinander über 6 Monate ermöglichten /30/. Die Instrumentenbasislänge betrug 250 m.
Eine Empfindlichkeit von 10^{-9} rad einer 100 m langen Anlage erfordert Auflösungen der Niveauschwankungen von 100 nm (entsprechend einer Druckänderung von 10^{-3} Pa).

3.3. Eigenschwingungen

Aufschluß über die seismische Störanfälligkeit eines hydrostatischen Systems gibt seine Eigenfrequenz.
Sie folgt aus der Lösung der **Bewegungsdifferentialgleichung** einer Flüssigkeit in kommunizierenden Gefäßen. Für eine Anlage von etwa

DOI: https://doi.org/10.2312/zipe.1989.102.03

200 m Länge und 30 mm Rohrdurchmesser und einem Durchmesser der Wandlergefäße (Steigrohre) von 70 mm ergibt sich eine Eigenperiode von 50 ... 60 sek. - laminare Strömung vorausgesetzt.
Bei geotektonischen Instrumenten großer Basislänge gestaltet sich das Signal-Rauschverhältnis noch günstiger. Im Fall der Messung mit kurzen Anlagen - die Mehrzahl der japanischen Instrumente arbeitet mit Basislängen von ca. 30 m - werden kleine Rohrdurchmesser bevorzugt, die zu einer aperiodischen Dämpfung führen.
Die Langwasserhorizonte vom Michelsontyp haben durch entsprechende Gefäßgestaltung eine große Eigenperiode. Die Eigenperiode des Long-baseline fluid tiltmeters beim U. S. Geological Survey (Basislänge 240 m) beträgt 7,5 min; hierdurch wird eine hohe Stabilität erreicht. Ein lokales Erdbeben in 7 km Entfernung (mag = 2,9) verursachte während des Durchgangs der P-Wellen nur einen Versatz eines Interferometers um einige Interferenzstreifen /29/.

3.4. Die Orientierung der Instrumente

Problematisch ist die Bestimmung der Phase der Gezeitendeformation aus Horizontalpendelbeobachtungen infolge des ständig sich ändernden Pendelazimuts. Das Pendelazimut müßte streng für jeden Meßwert bestimmt werden. Azimutangaben von Horizontalpendeln beziehen sich daher auf eine mittlere Lage des Gehänges, um die erfahrungsgemäß die Pendelbewegung über längere Zeit erfolgt.
Darüber hinaus erweist sich die Bestimmung des Azimuts des arretierten Horizontalpendels auf Grund der konstruktiven Gegebenheiten als schwierig. Daraus ergibt sich eine Gesamtunsicherheit der horizontalen Komponente der Richtung des Schwerevektors von 20 - 30 Bogenminuten. Die relativen Unsicherheiten in der Phasendifferenz $\varkappa = \varphi_{obs} - \varphi_{vg}$ [3] werden damit erheblich, da $\varkappa$ nur kleine Werte annehmen kann. Die Erde reagiert gegenüber

3) φ_{obs} : instrumentell ermittelte Gezeitenphase
φ_{vg} : Gezeitenphase einer starren Modellerde

DOI: https://doi.org/10.2312/zipe.1989.102.03

äußeren Kräften insgesamt elastisch. α müßte also gleich 0 sein. Real bestehende kleine Phasendifferenzen ($\alpha \neq 0$) geben somit Aufschluß über Vorgänge in der Erdkruste einschließlich maritimer und meteorologischer Prozesse. Aus geeigneten Modellierungen solcher Prozesse folgen Phasenverschiebungen von $\pm 1^{0} \ldots 1{,}5^{0}$. Das festinstallierte starre hydrostatische Niveau ermöglicht eine Genauigkeit in der Richtungsbestimmung der Sensoren von 1,5 Bogenminuten /28/.

4. Das Michelson-Niveau

Die Möglichkeiten des Langwasserhorizonts für hochauflösende kontinuierliche Beobachtungen der Niveaufläche zeigten zuerst Michelson und Gale am Yerkes-Observatorium, Wisconsin. Es gelang hier mit Hilfe einer interferometrischen Auflösung der Meniskusschwankungen, gezeitenbedingte Niveauflächenänderungen bei gleichzeitig guter Langzeitstabilität nachzuweisen. Die Niveauflächenschwankung wurde aus den Differenzen der Menisken jedes Rohres ermittelt. Voraussetzung für die angewandte Differenzmessung sind geringe horizontale Temperaturgradienten im Instrumentenbereich. Die Rohre wurden unter Terrain im Meridian und im ersten Vertikal horizontal verlegt; sie hatten eine Länge von 153 m und einen Durchmesser von 15 cm. Sie waren bis zur Hälfte mit Wasser gefüllt und in den Meßköpfen durch Paraffinöl gegen Verdunstung gesichert. Die Untersuchung verdient insofern Beachtung, da während der folgenden fünf Jahrzehnte in Nordamerika keine weiteren Arbeiten zur Bestimmung gezeitenbedingter Lotschwankungen angestellt wurden.
Egedal und Fjeldstad haben mit ähnlichen hydrostatischen Niveaus (Prinzip der Kanalwaage, halb mit Wasser gefüllt, 2 Rohre je 110 m lang, 2,7 cm Durchmesser) in Bergen (Norwegen) Messungen dieser Art wiederholt. Die Signalanzeige erfolgte hier mittels eines schwimmergekoppelten Hebels über Spiegel und Lichtzeiger auf Film. Die so gewonnenen Aufzeichnungen ermöglichten die Be-

DOI: https://doi.org/10.2312/zipe.1989.102.03

stimmung der Amplituden der Hauptgezeitenwellen M_2 und O_1 /25/. Über jüngere Ergebnisse von Messungen mit Langwasserhorizonten berichten Kasahara, Bower und Coutier /26/ /27/. Weiterführende Untersuchungen zum Problem des fennoskandischen Uplifts mittels hydrostatischer Niveaus hat Kääriäinen angestellt /28/.
Mit Blick auf isostatische und gezeitenbedingte Krustenbewegungen wurden am Finnischen Geodätischen Institut verschiedene hydrostatische Anlagen entwickelt. In Finnland treten im Zusammenhang mit der postglazialen Landhebung jährlich vertikale Krustenbewegungen von 0,05 mm pro 1 km Horizontalerstreckung in Erscheinung, das sind 1 µm/km und Woche. Zur Untersuchung dieser Landhebung in ihrer Zeitabhängigkeit schlug Kukkamäki vor, mit Hilfe eines etwa 1 km langen hydrostatischen Nivellements (quecksilbergefülltes Stahlrohr) in einem Gebiet mit extremen Hebungsgradienten orthogonal zu den Isobasen kontinuierlich über längere Zeit zu messen. Die Anlage gestattet schon von der Dimensionierung her ohne Schwierigkeit Empfindlichkeiten von 0,2 "/mm, so daß innerhalb einer Woche auftretende Deformationen sichtbar werden /30/.
Kääriäinen hat gezeitenbedingte und unperiodische Krustendeformationen mit Schlauch- und Kanalwaageniveaus untersucht. Er experimentierte zunächst mit einer 50 m langen Metallrohrlibelle und konnte aus kleineren Serien die Amplituden und Phasen der Gezeitenwellen M_2 und K_1 sowie Korrelationen des Langzeitverhaltens der Bodenneigung zum Luftdruck ableiten /14/. Die Signalgewinnung erfolgte interferometrisch. Ein später hieraus abgeleitetes Michelson-Niveau hat eine Länge von 177 m. Die Bewegungen der Flüssigkeitsoberfläche werden interferometrisch gemessen und photographisch registriert. Die Ablesegenauigkeit beträgt $\pm$ 0,02 µm. Das entspricht einer Neigung von $\pm 5 \cdot 10^{-2}$ ($\triangleq 2 \cdot 10^{-7}$ rad) zwischen 2 aufeinanderfolgenden stündlichen Ablesungen. Die Anlage wird seit 1977 betrieben. Das Datenmaterial wurde bezüglich des kurzperiodischen Gezeitenanteils analysiert und mit den Ergebnissen von in der Nähe angestellten Horizontalpendelmessungen (Verbaandert-Melchior) verglichen (Tafel 1a und 1b). Die Ergebnisse zeigen systematische Abweichungen in den Verminderungsfaktoren der Lot-

DOI: https://doi.org/10.2312/zipe.1989.102.03

richtung γ zwischen den Horizontalpendeln und dem Niveauvariometer. Die γ-Werte des Niveauvariometers sind mit kleineren inneren Fehlern behaftet und streuen innerhalb der einzelnen Tiden in geringerem Maße als die der Horizontalpendel; besondere Beachtung verdienen dabei die zugrundeliegenden Datenmengen. Interessant ist das Driftverhalten beider Instrumente, d. h. der Signalanteil nach Abzug des kurzperiodischen Gezeitenbandes. Das hydrostatische Niveau hat eine höhere Langzeitstabilität als das Horizontalpendel. Besonders deutlich wird dies bei Berücksichtigung des horizontalen Luftdruckgradienten (Abb. 2 und 3) /34/.

Die derzeit leistungsfähigste Variante des Michelsonniveaus ist die Konstruktion von Beavan, Bilham, Evans und Plumb. An Hand verschiedener Modellvarianten werden methodische und konstruktive Probleme bei hydrostatischen Niveaus diskutiert, so u. a.:

- Konzeption für den Flüssigkeitsbehälter im Hinblick auf das Signal-Rauschverhalten,
- erreichbare Empfindlichkeit und Langzeitstabilität für Gezeitenbewegungen und nichtperiodische Krustendeformationen,
- Möglichkeiten der Reduzierung äußerer Einflußgrößen,
- Möglichkeiten der Eichung, der Signalgewinnung und -verarbeitung.

Aus zahlreichen Experimenten entstanden zwei Instrumente mit Basislängen von 60 m und 240 m; eine kalifornische Variante arbeitet mit Basislängen von 535 m /29/ /31/ /32/.

Mit Blick auf das Signal-Rauschverhalten, problemlose Skalenwertbestimmung und geringe Temperaturanfälligkeit entschieden sich Plumb et al. bei dem 240-m-Instrument für ein Michelson-Niveau mit Laserinterferometern. Die optisch-elektrische Signalgewinnung erübrigt eine zusätzliche Eichung und ermöglicht eine weitgehende Linearität im gesamten Signalbereich; bei 3 cm Vertikalverschiebung des Flüssigkeitsniveaus beträgt die relative

DOI: https://doi.org/10.2312/zipe.1989.102.03

Abweichung von der Linearität des Skalenwerts 10^{-5}.
Die Anlage wird üblicherweise mit Hilfe eines Helium-Neon-Lasers betrieben, sie gestattet jedoch auch die Montage eines einfachen interferometrischen Wandlers mit schwacher inkohärenter Lichtquelle, die einen größeren optischen Aufwand erforderlich macht (einfaches Michelson-Interferometersystem).

In Anlehnung an das 240-m-Instrument vom Lamont Doherty Geological Observatory wurden geotektonische Varianten des Michelson-Niveaus vom Piñon Flat-Geophysical Observatory in Kalifornien entwickelt. Zwei 535 m lange Instrumente wurden oberflächennah installiert und zur Stabilisierung mit 30 m tiefen wassergefüllten Bohrungen unterhalb der Wandler verbunden. Es entstehen so Michelson-Niveaus mit extrem großen Wandlergefäßen und einer entsprechend günstigen Frequenzcharakteristik. Später wurden hier zwei weitere 50-m-Niveaus gemeinsam mit Laserstrainmetern, Gravimetern, Bohrlochneigungsmessern etc. eingerichtet /33/.

Hauptsächlich aus den hier gewonnenen Resultaten ergibt sich folgendes Bild:

Hydrostatische Longbase-Neigungsmesser stellen eine besondere Kategorie geodynamischer Neigungsmeßinstrumente dar. Ihre mechanische Dimensionierung ermöglicht bereits bei geringer Signalvergrößerung extrem hohe Empfindlichkeiten ($5 \cdot 10^{-9}$ rad) bei gleichzeitig gewährleisteter Langzeitstabilität von ca. 10^{-7} rad pro Jahr. Das Langzeitsignal ist offensichtlich nur in geringem Maße durch instrumentelle Effekte beeinflußt. Es zeigt sich hier eine deutlich bessere Kohärenz mit den Ergebnissen nivellitischer Untersuchungen, als zwischen den Langzeit-Neigungssignalen konventioneller Neigungsmesser und denen von Nivellements. Hydrostatische Neigungsmesser mit großer Instrumentenbasis nach dem Michelson-Prinzip vereinigen in sich die Empfindlichkeit von Gezeitenneigungsmessern mit einer hohen regionalen Repräsentativität. Sie können so als das Bindeglied zwischen Bohrloch-Instrumentenarrays und Präzisionsnivellements angesehen werden.

DOI: https://doi.org/10.2312/zipe.1989.102.03

Schlußbemerkungen

Die Untersuchung von Erdkrustendeformationen im Maßstabsbereich der terrestrischen Verfahren (0 ... 100 km) erfordert neben geometrischen Messungen vertikaler und horizontaler Bewegungen der Erdoberfläche kontinuierliche Beobachtungen des Strains, der Schwerebeschleunigung und der Lotrichtung gegenüber der physischen Erdoberfläche. Für die Messung des zeitlichen Verhaltens der Lotrichtung bot sich zunächst das Horizontalpendel wegen seiner erreichbaren Empfindlichkeit von etwa 10^{-3}"/mm Registrierausschlag an. Die mit diesem Instrument gewonnenen Meßreihen haben indessen nur im Bereich der kurzperiodischen Gezeiten diskutable Ergebnisse erbracht. Der lokale Signalanteil aus dem Umfeld der Station erreicht beim Horizontalpendel die Größenordnung der Gezeitenamplituden. Eine Aussage über langwellige Lot- bzw. Niveauflächenbewegungen gegenüber der physischen Erdoberfläche erfordert eine größere Kontaktbasis des Instruments mit dem Untergrund. Eine Lösung des Problems ist mit hydrostatischen Niveaus möglich. Besondere Probleme bei höchstempfindlichen Instrumenten dieser Art sind

- die Temperaturempfindlichkeit und
- die Bestimmung des Skalenwertes (reziproke Empfindlichkeit).

Das exogene Neigungssignal (Gezeiten) hat eine maximale Amplitude von 3×10^{-2}", die auf besser als 1 % bestimmbar sein sollte. Entsprechende Forderungen sind an die Eichung zu stellen. Ähnliche Bedingungen bestehen bei der Messung unperiodischer Krustenbewegungen; von Bedeutung ist hier die instrumentelle Stabilität - der Nullpunktgang - über längere Zeit (5×10^{-2}"/Jahr), die mit Hilfe eines unabhängigen Verfahrens bestimmt werden kann. Die interferometrische Signalgewinnung ermöglicht eine kontinuierliche, sichere Skalenwertbestimmung für jedes gemessene Signal. Hydrostatische Niveaumessungen bieten gegenüber geometrischen Nivellements und trigonometrischen Höhenmessungen den Vorteil der kontinuierlichen Signalgewinnung bei gleichzeitig höherer Signalauflösung. Bei stationären Neigungsmessungen ermöglichen sie die

DOI: https://doi.org/10.2312/zipe.1989.102.03

Eliminierung der kleinmaßstäblichen Neigungs-Deformationssignale. Jüngere konstruktive Entwicklungen haben das Verfahren sowohl für das Nivellement als auch für die Neigungsmessung verbessert und für krustendynamische Untersuchungen vielfältig anwendbar gemacht.

Tabelle 2 enthält einen Vergleich der stationären Verfahren der Neigungs- und Lotschwankungsbeobachtung. Hydrostatische Neigungsmessungen werden zunehmend in Störungszonen mit ausgeprägter Mobilität angestellt. Im zirkumpazifischen Bereich werden empfindliche Schlauchwaagen mit vorwiegend induktiver oder kapazitativer Signalgewinnung eingesetzt. Die Instrumente sind störanfällig gegenüber Temperatureffekten und daher aufwendig unterirdisch installiert.
Eine optimale Lösung des hydrostatischen Verfahrens für geodynamische Observatoriumsbeobachtungen ist der Langwasserhorizont in Form des Michelsonniveaus mit interferometrischer Signalgewinnung; er erfüllt in hohem Maße wesentliche Forderungen für die Messung von Erdkrustendeformationen gegenüber der Niveaufläche in einem großen Periodenbereich:

1. Der Maßstab (Skalenwert) der Niveauverschiebung ergibt sich aus dem interferometrisch gewonnenen Signal; damit erübrigt sich eine Eichung.
2. Die große Instrumentenbasis ermöglicht
   - eine hohe mechanische Auflösung und
   - eine geringe seismische Störanfälligkeit des Systems auf Grund großer Eigenperiode.
3. Das Azimut der Anlage ist während der Messung unveränderlich und mit großer Genauigkeit bestimmbar.
4. Das Instrument ist unempfindlich gegenüber Änderungen des Temperaturgradienten.

DOI: https://doi.org/10.2312/zipe.1989.102.03

Tafel 1a

Station [4]	O_1	$P_1S_1K_1$	M_2	S_2K_2	N_2
WT	0,710	0,725	0,701	0,704	0,694
(96 Tage)	± 9	± 6	± 2	± 3	± 9
LO	0,698	-	0,641	-	0,628
(780 Tage)	± 11		± 3		± 17
Ai	0,679	0,706	0,663	0,665	0,680
(192 Tage)	± 29	± 9	± 9	± 16	± 42

Amplitudenquotienten aus den Messungen an den skandinavischen klinometrischen Stationen (EW-Komponente) /34/

Tafel 1b

Station [4]	O_1	$P_1S_1K_1$	M_2	S_2K_2	N_2
WT	- 2,39	- 2,98	- 2,26	- 1,18	- 2,81
	± 0,73	± 0,12	± 0,12	± 0,25	± 0,73
LO	+ 1,73	-	- 2,43	-	- 0,29
	± 0,92		± 0,27		± 1,53
Ai	+ 0,27	- 4,71	- 5,83	- 4,53	- 3,43
	± 2,44	± 1,63	± 0,73	± 1,39	± 3,50

Phasendifferenzen an den skandinavischen klinometrischen Stationen (in Grad)
(EW-Komponente) /34/

DOI: https://doi.org/10.2312/zipe.1989.102.03

Tafel 2

	co-Seismic	1 Tag	1 Woche	1 Monat	1 Jahr	5 Jahre	10 Jahre
Hydrost. Niveau-variometer	1×10^{-7}	5×10^{-8} - 1×10^{-7}	5×10^{-8} - 1×10^{-7}	1×10^{-7}	2×10^{-7}	3×10^{-7}	3×10^{-7}
Horizontal-pendel		3×10^{-8} - 1×10^{-7}	2×10^{-7} - 1×10^{-7}	5×10^{-7} - 1×10^{-6}	1×10^{-6} - 5×10^{-6}	5×10^{-6}	
Bohrloch-vertikal-pendel		5×10^{-8}		2×10^{-7}	3×10^{-7}	5×10^{-7}	
Extenso-meter	5×10^{-9} - 1×10^{-8}	5×10^{-9}	1×10^{-8}	5×10^{-8}	2×10^{-7} - 1×10^{-6}	5×10^{-7} - 5×10^{-6}	1×10^{-6} - 5×10^{-6}

Tafel 2: Abschätzung der synthetischen Zuverlässigkeit verschiedener Instrumententypen

DOI: https://doi.org/10.2312/zipe.1989.102.03

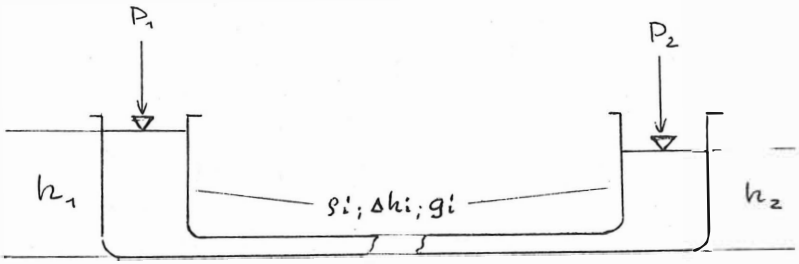

Abb. 1a:

Zum Gleichgewicht in einem kommunizierenden Gefäß

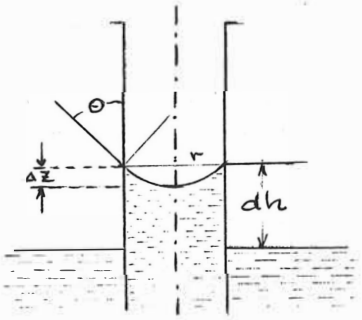

Abb. 1b:

Zur Höhen- und Formänderung der Flüssigkeitsspiegel infolge der Kapillarität

DOI: https://doi.org/10.2312/zipe.1989.102.03

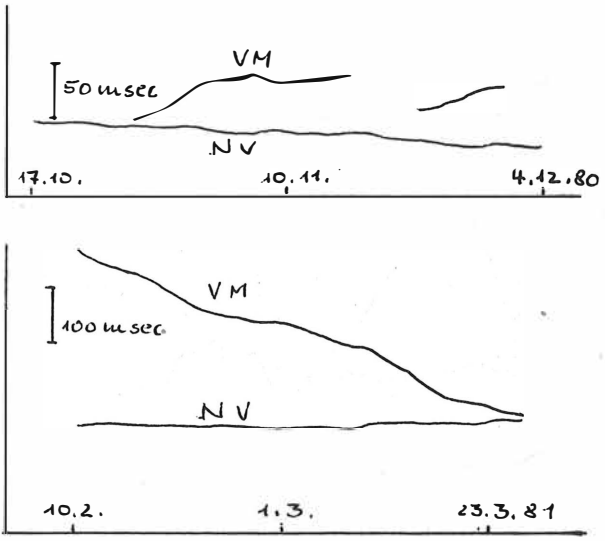

Abb. 2: [1]

Gangverhalten von Horizontalpendel und hydrostatischem Niveau (VM: Horizontalpendel, NV: Hydrostatisches Niveau)

DOI: https://doi.org/10.2312/zipe.1989.102.03

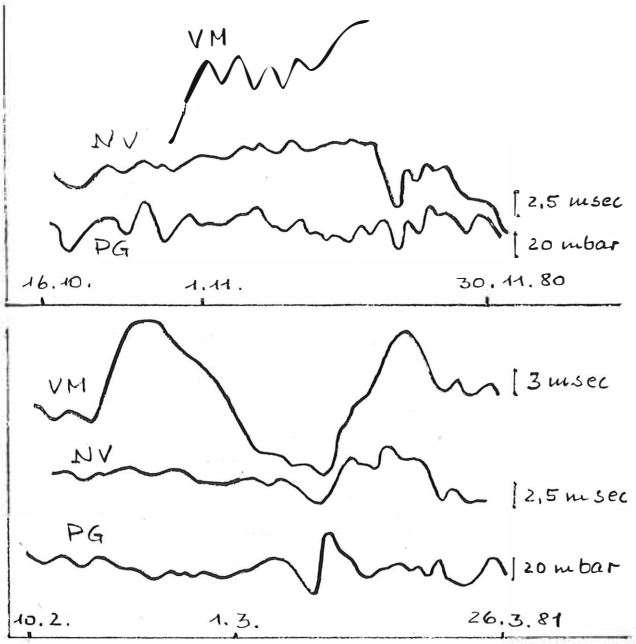

Abb. 3: [1]

Beziehung zwischen Instrumentengängen und Luftdruckgradient (VM: Horizontalpendel, NV: Hydrostatisches Niveau, PG: Horizontaler Luftdruckgradient)

[1] nach /34/

DOI: https://doi.org/10.2312/zipe.1989.102.03

Literatur

/ 1 / Tomaschek, R.: Tides of the solid Earth - Handbuch der Physik, Geophysik 2, Bd. 48, Berlin (1957)

/ 2 / Kühnen, F.: Hydrostatische Höhenvergleichung von 4 Festpunkten auf dem Telegraphenberg bei Potsdam - Geodät. Inst. Potsdam, N. F. Nr. 37 (1908)

/ 3 / King, G. C. P.; R. G. Bilham: Tidal tilt measurement in Europe - Nature, 243, London-Washington (1973)

/3a / Baker, T. F.; G. W. Lennon: Tidal tilt anomalies - Nature, 243, London-Washington (1973)

/ 4 / Cabaniss, G. H.: Crustal tilt in coastal New England - An experimental study, PhD Thesis, Boston Univ., Boston (1974)

/ 5 / Edge, R. J.; T. F. Baker; G. Jeffries: Borehole tilt measurements, a periodic crustal tilt in an aseismic area - Tectonophysics, 71, Amsterdam-London (1981)

/ 6 / Harrison, J. C.: Cavity and topographic effects on tilt and strain measurements - J. Geophys. Res., 81, Washington D. C. (1976)

/ 7 / Waalewijn, A.: Hydrostatic measurement of vertical movements in the coast dependent on the tide - Symp. on coastal geodesy, München (1970)

/ 8 / Sandig, H. U.; G. Scheel: Hydrostatische Stromübergänge im Gezeitengebiet - Deutsche Geodätische Kommission, R. B., Nr. 6, Frankfurt/M. (1952)

/ 9 / Moulton, F. R.: Theory of tides in pipes on a rigid earth - Astroph. J., 50, Chicago Ill. (1919)

/10 / Hagiwara, T.: Observations of changes in the inclination of the earth's surface at Mt. Tsukuba (3 rd report). Bull. Earthquake Res. Inst., Univ. Tokyo, 25 (1947)

DOI: https://doi.org/10.2312/zipe.1989.102.03

/11/ Yamada, J.: A water-tube tiltmeter and its applications to crustal movement studies. Spec. Bull. Earthquake Res. Inst. Tokyo, 10 (1973)

/12/ Cook, K. L.: Granite mountains records vault 15 miles south of Salt lake City, Utah., Rep. pres. to the 4th U.S.-Japan Conference on Earthquake pred. San Francisco (1973)

/13/ Kisslinger, C.; T. Rikitake: US-Japan seminar on Earthquake prediction and control, Eos, Trans. Geophys. Union, 55, Washington (1974)

/14/ Kääriäinen, J.: Über die 50 m lange Rohrlibelle zur Untersuchung der Neigung der Erdkruste - Mitt. des Finnischen Geod. Instituts, Helsinki (1973)

/15/ Peters, J. A.: Results from a new 22 metre baselength mercury tiltmeter - 8th Intern. Symp. on Earth Tides, Bonn (1977)

/16/ Manthey, W.: Erprobung der registrierenden Schlauchwaage - Ein methodischer Beitrag zur Beobachtung rezenter Krustenbewegungen - Geod. Geophys. Veröff. R. 3, H. 11, Berlin (1968)

/17/ Bower, D. R.: A sensitive water-level tiltmeter - Phil. Trans. R. Soc-London, A-274 (1973)

/18/ Eaton, J. P.: A portable water tube tiltmeter - Bull. Seism. Soc. America, 49, El Cervito (Cal.) (1959)

/19/ Hugget et al.: Precision levelling with a two fluid tiltmeter - Geophys. Res. Letters, 3, Washington (1976)

/20/ Rikitake, T.: Japanese National Programm on earthquake prediction - Tectonophysics, Vol. 23, Nr. 3, Elsevier Amsterdam (1974)

/21/ Kato, M.: Observations of crustal movements by newly-designed horizontal pendulum and water-tube tiltmeters with electromagnetic transducers - Bull. Dis. Prev. Inst., Kyoto Univ. 27, Kyoto (1977)

DOI: https://doi.org/10.2312/zipe.1989.102.03

/22/ Okada, Y.; S. Watanabe: Observation of crustal deformation at the Futjigawa Observatory, Central Honsku, Japan (1) (2) (3) - J. Geod. Soc. Japan, Vol 18, 1 (1974), 22, 2 (1976), 26, 4 , Kitasato (1980)

/23/ Kasahara, K.: Tiltmeter observations in complement with precise levellings - J. Geod. Soc. Japan, 19, Kitasato (1973)

/24/ Michelson, A. A.; H. G. Gale: The regidity of the earth - Astroph. Journ. 50, 330-345, Chicago Ill. (1919)

/25/ Egedal, I.; I. E. Fjelstad: Observations of tidal motions of the earth's crust - Geof. Publ., Bd. XI, Oslo (1937)

/26/ Kasahara, K.: Earthquake fault studies in Japan - Phil. Trans. Roy. Soc., London A 274 (1973)

/27/ Bower, D. R.; N. Courtier: Long baseline tilt observations in a mine near Ottawa - Canad. Geophys. Union Meeting, London, Ontario (1978)

/28/ Kääriäinen, J.: Observing the earth tides with a long watertube tilt meter - Annales Acad. Scientiarum Fennicae, Ser. A, VI. Physica, 424, Helsinki (1979)

/29/ Plumb, R.; R. Bilham; J. Beavan: A stable long-baseline fluid tiltmeter for tectonic studies - U. S. Geological Survey, open-file report 79-370, Washington D. C. (1979)

/30/ Kukkamäki, T. J.: Recording of the secular land tilting with pipe level. - Proceedings of the second International Symposium on Recent Crustal Movements, Aulanko, Finnland, August 3. - 7. 1965. Annales Academiae Scientiarum Fennicae, Series A. III, Helsinki (1966)

/31/ Bilham, R.; R. Plumb; J. Beavan: Design considerations in an ultra stable long baseline tiltmeter - results from a Lasertiltmeter - Proc. Conf. Terrestrial and Space Techniques in Earthquakeprediction Research, Strasbourg (1979)

DOI: https://doi.org/10.2312/zipe.1989.102.03

/32/ Bilham, R.; J. Beavan; K. Evans: Long baseline fluid-tube tiltmeter geometry and the detection of flexure and tilt - Proc. 9. Intern. Symp. on Earth Tides, Stuttgart (1983)

/33/ Wyatt, F.; J. Berger: Investigations of tilt measurements using shallow borehole tiltmeters - J. Geoph. Res. Vol. 85, Nr. 138, Washington D. C. (1980)

/34/ Kääriäinen, J.; I. Välimäki: Some results from the tidal measurements at the Lohja Clinometric station, Finnland, NKG Meeting, 13. - 17. Sept. 1982, Gäule (1982)

DOI: https://doi.org/10.2312/zipe.1989.102.03

Jan Cisak
Maria Dobrzycka
Zbigniew Drożdżewski

Institute of Geodesy and Cartography
Warszawa, Poland

Contribution of Henryk Arctowski Polish Polar Station to the Intercosmos Doppler Campaign

A b s t r a c t

In January of 1988 the Arctowski Antarctic Polar Station at the King George Island has participated in the Intercosmos Doppler Campaign (ICOOC). The observations were executed using the Polish Doppler receiver DOG 3 and reduced by the single point method using a set of Geodop program version 5, with WGS 72 ellipsoidal parameters. From 311 passes accepted by program following co-ordinates of the main geodetic point of Arctowski station were obtained:

LAT = -62°09´41".56
LON = 301°31´49".99
H = 30,68 m

Вклад Польской полярной станции им.Арктовского в международную допплеровскую кампанию "Интеркосмос"

Резюме

В январе 1988 года антарктическая станция им. Арктовского на острове Кинг Джорж участвовала в кампании допплеровских наблюдений "Интеркосмос".

Наблюдения были произведены польским допплеровским приёмником "DOG 3". Эти наблюдения были вычислены с помощью метода "single point" с использованием программы "GEODOP" , версия 5, с параметрами эллипсоида "WGS 72"

Из 311 прохождений, принятых программой, получились следующие координаты векового пункта станции им. Арктовского:

φ = - 62°09 41.56
λ = 301°31 49.99
H = 30.68 м.

DOI: https://doi.org/10.2312/zipe.1989.102.03

In January of 1988 the Arctowski Polar Station at the King George Island has participated in the Intercosmos Doppler Campaign (ICDOC).The aim of this campaign was to link regular and probable future Intercosmos stations in a common, coherent co-ordinate system.

ICDOC campaign was divided into two fortnightly subcampaigns. The first was carried out in the first half of December, 1987, the second in the later half of January,1988. Sixsteen stations were supposed to participate in this campaign: two Antarctic stations -Georg Forster (GDR) and Arctowski (Poland) and: Heluan (Egypt), Khartum (Sudan), Maputo (Mozambique), Bamako (Mali), Simeiz (USSR), Zvenigorod (USSR), Penc (Hungary), Potsdam (GDR), Borowiec (Poland), Ondrejov (Czechoslovakia), Santiago de Cuba, Nhatrang (Viet-Nam), Bangalore (India), Ulhan Bator (Mongolia). Some of these stations, who do not possess Doppler receivers of their own, were to be helped by teams from Poland, GDR, Czechoslovakia, USSR and Bulgaria. Whole operation is coordinated by the Hungarian station Penc.

The results of satelite observations are to be elaborated using single point method, multilocation and orbital methods. Data bank is to be set up and kept at Penc in Hungary. The final results - having been agreed among different methods of elaboration - are to be presented at the meeting of the 4-th Intercosmos section in May 1989.

At the Arctowski station 348 passes of satelites have been observed from 8-th to 21-st of January 1988. The observations were executed using the Polish Doppler receiver DOG3, owned by the Institute of Geodesy and Cartography. The observations were reduced by the single point method using a set of GEODOP programs, version V, with WGS 72 ellipsoidal parameters. Since King George Island is far removed from other participating in the ICDOC campaign there is no use using multilocation method.Thus the results quoted below may be considered as the final ones.They may be revised if either a new program,

DOI: https://doi.org/10.2312/zipe.1989.102.03

better than GEODOP, be introduced or if other options relating to the refraction model and gravity field model could be used.

From 311 passes accepted by program following geocentric co-ordinates were obtained:

X = 1 561 693.7 m ± 1.4 m
Y = -2 545 679.2 m ± 1.7 m
Z = -5 616 855.9 m ± 1.0 m

They correspond to:

LAT = -62°09′33".31 ± 0".05
LON = 301°31′40".08 ± 0".05
H = 35.31 m ± 1.5 m

Using conventional geodetic method these co-ordinates were projected on the main geodetic point of Arctowski station (Fig.1). Its co-ordinates in WGS 72 system are:

LAT = -62°09′41".56
LON = 301°31′49".99
H = 30.68 m

The co-ordinates of the lighthouse at the Admiralty Bay like manner obtained are:

LAT = -62°09′28".9
LON = 301°32′02".3

During the same polar expedition in January 1988 its participants have attempted to improve the astronomical position of the main geodetic point. Its position was preliminary determined by Jerzy Jasnorzewski in 1977 /1/. However, due to poor weather conditions only several series of longitude, latitudo and azimuth from Sun observations could be performed. Following results were obtained:

LAT = -62°09′39" ± 2"
LON = 301°31′32" ± 3"
AZ = 34°13′06" ± 2"

Azimuth is referred to a very distinctive triangulation mark on the Ulman peninsula at the Admiralty Bay.

Literature

/1/ Jasnorzewski J.: Astronomical observations for determining... Polish Polar Research, vol.2, No 3-4, 1981.

DOI: https://doi.org/10.2312/zipe.1989.102.03

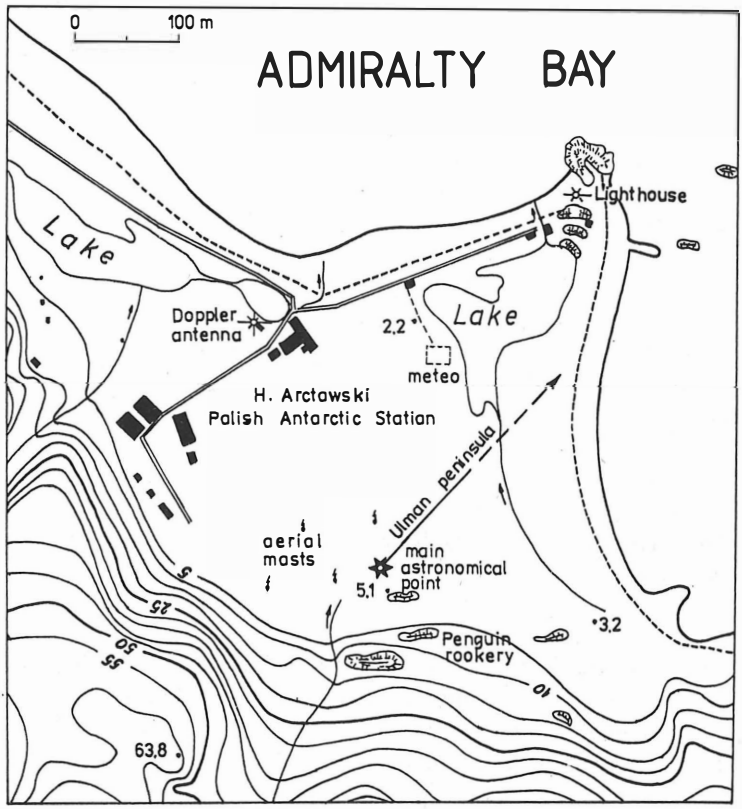

Fig. 1

The work was done within the Project CPBP 03.03 granted by Polish Academy of Sciences

DOI: https://doi.org/10.2312/zipe.1989.102.03

НОВЫЕ ДАННЫЕ О СОВРЕМЕННЫХ ТЕКТОНИЧЕСКИХ ДВИЖЕНИЯХ ЗАПАДНОЙ КУБЫ

Х.Л.ДИАС /I/ и Д.А.ЛИЛИЕНБЕРГ /2/

РЕЗЮМЕ: Исследования по современной геодинамике Западной Кубы рассматриваются, как геоморфологическая проблема национального характера, так и в международных научных программах. На основе геолого-геоморфологических и сейсмических исследований, а также повторных нивелирований с интервалами IC и 25 лет было составлено I8 комплексных профилей и карта современных тектонических движений.

Современная геодинамика территории характеризуется общими и регисиальными закономерностями в пространственно-временном определении и тесной взаимосвязью с надвигово-блоковыми морфоструктурами различного типа, категории и возраста. Преобладает умеренная интенсивноть вертикальных движений порядка первых мм/год и слабая сейсмичность. Определено несколько кинематических типов взаимосвязей между морфоструктурными узлами и миграцией во времени сейсмоактивной зоны.

/I/ Институт географии АН Кубы

/2/ Институт географии АН СССР

DOI: https://doi.org/10.2312/zipe.1989.102.03

NEW DATA ABOUT RECENT TECTONIC MOVEMENTS OF WESTERN CUBA

J.L. DIAZ (1) and D. A. LILIENBERG (2)

ABSTRACT. Researches about Western Cuba recent geodynamics are analyzed into the framework of domestic and foreign scientific programs. Based on seismic and geologic-geomorphological studies as well as the repeated graduation with intervals between 10 and 25 years, the map of recent movements at 1:500 000 scale and 18 complex profiles are been made.

General and regional regularities of the spatio-temporal differentiation of the recent geodynamics and its strong interrelation with block-overthrow morphostructures of different types, categories and ages were detected. Through the territory a moderate intensity of vertical movements ranging of firsts mm/year and a weak seismicity are predominant. Kinematic types of morphostructural interrelations, morphostructural knots and the migration of seismoactive zones in time were determined.

(1) Institute of Geography. Academy of Sciences of Cuba.

(2) Institute of Geography. Academy of Sciences of USSR.

DOI: https://doi.org/10.2312/zipe.1989.102.03

В структурно-геодинамическом плане Западная Куба представляет одну из модельных областей сотрсвной дуги Больших Антилл. Основные черты ее современной морфоструктуры сложились в результате обдукции позднемелового вулканической дуги на край Багамской плиты и сложного сочетания горизонтальных и вертикальных блоковых движений в процессе завершения раскрытия Юкатанской впадины на неотектоническом этапе. В последние годы здесь был проведен взаимосвязанный комплекс геодезических, сейсмологических и геолого-геоморфологических исследований, результаты которых обобщены Советско-Кубинской экспедицией и являются частью международного проекта КАПГ /I-4/. На базе повторных нивелировок за период I0-25 лет и морфоструктурного анализа составлена предварительная схема тенденций современной геодинамики и 25 комплексных профилей. В связи с отсутствием на Кубе длиннорядных и непрерывных уровнемерных данных, величины скоростей движений приводятся не в "абсолютных", а в относительных значениях /по отношению к пункту Гуано/.

В целом Кубинский архипелаг рассматривается нами в качестве морфоструктурного мегаблока, а Западная Куба - в качестве макроблока, отделенного системой диагональных разрывов Карденас-Кочинос /2,5/. В пределах последнего выделяются соответственно три морфоструктурных мезоблока, разделенных региональными морфолинеаментами: Пинар-дель-Рио, Гавана-Матансас и с-в Хувентуд /Пинос/. Каждый из них отличается специфическим рисунком полей современных вертикальных движений, их интенсивностью и направленностью, характером проявления сейсмичности. Наименее интенсивными движениями /от -0,7 до +2 мм/год/ и их слабой дифферен-

DOI: https://doi.org/10.2312/zipe.1989.102.03

рованностью характеризуется о-в Хувентуд. Мезоблок Пинар-дель-Рио выделяется умеренной геодинамикой /от -2 до +2,5 мм/год/. При этом в полях современных движений проявляются в первую очередь продольные морфоструктуры, а поперечные носят наложенный характер. Для мезоблока Гавана-Матансас характерна наибольшая интенсивность /от -2,5 до +10 мм/год и более/, резкая контрастность и блоковая мозаичность вертикальных движений. В полях современной геодинамики проявляются прежде всего поперечно-диагональные морфоструктуры.

В целом для Западной Кубы отчетливо проявляется тенденция нарастания интенсивности и контрастности современных движений с запада на восток, а также общий наклон морфоструктурного макроблока с севера на юг, соответствующий тенденции тектонического развития и четвертичное и голоценовое время /2,5/. Важной закономерностью является установление блокового характера проявления современной геодинамики. На всех комплексных профилях кривые скоростей движений имеют ступенчатое строение. Границы сопряжения блоков выражены высокоградиентными участками. Размеры морфоструктурных блоков колеблятся от нескольких километров до 100-150 км. Выделяется большое разнообразие кинематических форм современных смещений по разломам, фиксируемых повторными нивелировками. Преобладают простые формы с разнонаправленными смещениями крыльев, "пиками" поднятий или опусканий, а также сложные ступенчатые формы при наличии мелкоблокового дробления. Но все современные деформации обычно локализуются в узкой зоне самого разлома.

Главной морфоструктурно-геодинамической осью Пинар-дель-Рио является Пинарский трансформный шов. Большинством геологов он обычно считается отмершим в плиоцен-четвертичное время. Однако аэрокосмические материалы, анализ русловых форм и повторные нивелировки показывают

DOI: https://doi.org/10.2312/zipe.1989.102.03

его значительную активность на современном этапе. Градиенты смещений на отдельных участках колеблятся от 0,1 - 0,2 на западе до 0,5 -1,5 мм/год/км - на востоке. Кроме того, это главная сейсмогенная зона Западной Кубы. Важную геодинамическую роль играет также поперечно-диагональный сдвиг Сан-Диего, который разделяет осевую горную систему Гуанигуанико на два разноприподнятых блока: Лос-Органос /-0,5 + +1,0 мм/год/ и Росарио /+1 + +1,5 мм/год/. На Северной Пинарской равнине он разграничивает западный +1 + +2 мм/год/ и восточный /-1 + -2,5 мм/год/ блоки; аналогично на Южной Пинарской равнине также - западный /с нейтральными движениями и слабыми опусканиями/ и восточный /0 + +2 мм/год/ блоки. Таким образом, противостоящие морфоструктурные блоки Северной и Южной равнин находятся как бы в противофазах современных вертикальных движений, а разделяющие их горы Гуанигуанико и Пинарский трансформный шов играют шарнирную роль. При этом сопряженные вертикальные перемещения морфоструктурных блоков горной системы Гуанигуанико по отношению к Южной Пинарской равнине, отделенной от них Пинарским швом, образуют клавишную систему: блок Кантадорес-Кабрас испытывает нейтральные движения, Виньялес - слабые поднятия /0,5-1,0 мм/год/, Росарио - умеренные опускания /до 1-6 мм/год/, возвышенности Мариель - умеренные поднятия /1-2 мм/год/.

Горы Гуанигуанико отличаются слабой интенсивностью современных вертикальных движений, что, возможно, обусловлено их покровно-надвиговой структурой, когда значительная часть вертикальной составляющей поднятий в известной мере компенсируется горизонтальной составляющей /1,3/. Некоторые фронтальные участки покрытых пластин иногда дают ступенчатые перегибы до 0,5 - 1,0 мм/год на графиках скоростей движений. Это может

DOI: https://doi.org/10.2312/zipe.1989.102.03

свидетельствовать, что эпоха горизонтальных перемещений не кончилась, как считается, в эоцене, а вряде случаев продолжается и на современном этапе. В локальных полях геодинамики отчетливо проявляются отдельные горстовые поднятия, равнины-грабены, сеть продольных и поперечных разломов.

Цоколь Северная Пинарская равнина выделяется наиболее мелкой блоковой дифференциацией современных вертикальных движений. Моноклинальная Южная равнина более монолитна по характеру геодинамики; только на участке Гуане и п-ве Гуанаакабибес движения приобретают резкую контрастность.

Горстовые и горст-антиклинальные возвышенности Гавана-Матансас испытывают общие относительные и абсолютные современные поднятия до 4-8 мм/год. На этом фоне грабен-синклинальные плато Тапасте, Агуакате отстают в поднятиях /2-4 мм/год/, т.е., выступают как блоки относительных опусканий. Градиенты смещений по разломам составляют 0,5-1,0 мм/год/км, местами достигая весьма высоких значений порядка 1-3 мм/год/км. Отчетливо прослеживаются линейные зоны прогибаний вдоль поперечно-диагональных морфолинеаментов Вахай-Эль-Габриэль, Харуко-Камачо, Мариель-Батабано.

Важную региональную морфоструктурно-геодинамическую роль играет линеамент Харуко-Камачо, к востоку от которого современные поднятия ступенеобразно резко возрастают. Так, Северная равнина Гаваны испытывает слабые относительные опускания, достигающие максимума -2,5 мм/год в районе бухты Гаванн, представляющей грабен растяжения, а Северная равнина Матансаса к востоку от Санта-Крус-дель-Норте и Харуко втянута в нарастающие интенсивные ступенчато-блоковые поднятия до 6-8 мм/год, достигающие в пределах равнины Карденас-Марти 10-12 мм/год и более, что является максимальным для Западной Кубы и может быть сопоставлено лишь с наиболее

DOI: https://doi.org/10.2312/zipe.1989.102.03

мобильными районами Юго-Восточной Кубы. Южная равнина Гавана-Матансас к западу от указанного морфолинеамента входит в область слабых относительных поднятий /0-2 мм/год/, а к востоку интенсивность современных поднятий нарастает до 4-6 мм/год. На этом фоне в качестве зоны относительных опусканий /отставания в поднятиях/ проявляется субмеридиональная равнина Колон-Хсвельянос, представляющая морфоструктурную границу с Центральной Кубой. Заболоченная грабен-синклинальная равнина Западная Сапата испытывает опускания до -2 мм/год.

Западная Куба относится к сейсмоактивным территориям Антильской островной дуги, хотя здесь преобладают слабые и средние землетрясения. За последние 300 лет /1678-1983 г.г./ здесь зафиксировано около 70 землетрясений с интенсивностью III-VI баллов, в том числе - одно разрушительное /I=VII, M=6,3/ - Сан-Кристобаль, 1880 г. /6/. В их динамике намечается исторически направленная тенденция нарастания сейсмической активности в пространстве и времени, с распространением от севера Гаванн-Матансаса на Пинар-дель-Рио к концу XIX в. и на всю Западную Кубу во второй половине XX в. Можно выделить три главных морфоструктурно-геодинамических типа мест возникновения землетрясений. Наиболее сложным являются морфоструктурные узлы сочленения блоков разного генезиса, возраста и ранга. Примером может служить бухта-грабен растяжения Гаваны, мелкоблоковое дробление которой находит прямое отражение в плейстоцен-голоценовом рельефе и современных движениях. Другой тип образуют линейные сейсмогенерирующие зоны. Ярким примером является Пинарский трансформный разлом, вдоль которого сосредоточено около половины очаговых зон Западной Кубы. Они группируются вдоль шва, но не в морфоструктурных узлах, а в местах пересечения его частными разломами, проявившими активность по данным повторного нивелирования и характеризующимися повы-

DOI: https://doi.org/10.2312/zipe.1989.102.03

ленными градиентами движений. Например, изосейста УШ баллов землетрясения Сан-Кристобаль почти точно оконтуривает блок современных поднятий до 2-2,5 мм/год, расположенный на границе со Сьеррой-дель-Росарио, испытывающей локальную инверсию движений, т.е. на стыке разнонаправленных движений. Линейной сейсмогенной зоной выделяется также линеамент Чатансас-Мадруга-Батабано. Третьим типом являются дизъюнктивные узлы в местах пересечения разноориентированных разломов и линеаментов.

Некоторые очаговые зоны находятся в определенной динамической взаимосвязи и активизируются последовательно, мигрируя вдоль зоны разломов /Сан Кристобаль-Гавана/ и свидетельствуя об их раскрытии.

В целом проявление как медленных вертикальных, так и быстрых /сейсмических/ современных движений Западной Кубы обнаруживает четкую взаимосвязь с морфоструктурной дифференциацией Антильской островной дуги. Выявленные здесь пространственно-временные закономерности современной геодинамики носят, по-видимому, не только региональный, но и более общий характер, поскольку они сопоставимы с аналогичными закономерностями Западно-Тихоокеанских островных дуг /Япония, Сахалин/.

Институт географии Академии наук СССР, Москва
Институт географии Академии наук Кубы, Гавана

Цитируемая литература:

I. Д.А.Лилиенберг. Современные движения земной коры /Теория, методы, прогноз. М.:Наука, 1980а. 2. Д.А.Лилиенберг, Современ.движения земной коры /Методика и результаты исслед. Киев: Наук.думка, 1980а. 3. Д.А.Лилиенберг, Х.Л.Диас, К.Паскуаль и др. Докл. АН СССР, 1977, т. 234, № 4. 4. Д.А. Лилиенберг, М.Е.Маркес. Современные движения

DOI: https://doi.org/10.2312/zipe.1989.102.03

на геодинамических полигонах. Петропавловск-Камчат.: ИВ ДВНЦ АН СССР, 1981 г. 5. Х.Л.Диас, Морфоструктуры и современные движения Западной Кубы. Автореф. канд. дисс., М: ИГ АН СССР, 1986. 6. T. Chuy, B. González. Investigaciones sismológicas en Cuba. IGA, Acc, 1980, No. 1.

Сведения об авторах:

1. ДИАС ДИАС ХОРХЕ ЛУИС - Зам.директора по науке Института географии АН Кубы, канд. геогр. наук., научный сотрудник. Адрес: Calle 11 No. 514 entre D y E. Vedado. La Habana 4. CUBA.

2. ЛИЛИЕНБЕРГ ДМИТРИЙ АНАТОЛЬЕВИЧ - Лауреат Государственной премии СССР, канд. геогр. наук, ведущий научный сотрудник Института географии АН СССР. Адрес домашний: Москва 103062, Подсосенский пер. 13, кв.5, тел.дом 297-66-15, служ. 237-03-60

DOI: https://doi.org/10.2312/zipe.1989.102.03

GAUSSIAN CURVATURE OF POSTGLACIAL REBOUND AND THE DISCOVERY OF CAVES CREATED BY MAJOR EARTHQUAKES IN FENNOSCANDIA

MARTIN EKMAN

National Land Survey
Division of Geodetic Research
S - 801 82 Gävle, Sweden

Abstract

The Gaussian curvature of the postglacial rebound of Fennoscandia at the end of the deglaciation is computed. The result is used for investigating the origin of boulder caves, where the bed-rock has been split into caves and accumulations of huge boulders. It is concluded that the three large boulder caves, concentrated at the Swedish coast of the southern part of the Gulf of Bothnia, most probably are created by major earthquakes produced by the Gaussian postglacial curvature about ten thousand years ago. The Gaussian curvature theory explains both the location and the character of the boulder accumulations and caves. Also, the curvature seems to be great enough to allow major earthquakes to occur. On the other hand the theory as applied here fails to explain the distribution of the many small boulder caves. Finally, an earlier conclusion of the author on the origin of today's minor earthquakes in central Fennoscandia is here considered doubtful.

DOI: https://doi.org/10.2312/zipe.1989.102.03

1. Introduction

In recent years attention has been drawn to certain types of caves in Sweden. Their common characteristic is that they are formed within accumulations of huge boulders. R Sjöberg (1987) has shown these caves to be of postglacial origin. His main arguments for this are that the boulders are glacially striated, proving that they accumulated after the advance of the inland ice, and that scarcely any weathering products are found on the floors of the caves. Sjöberg suggests that the boulder caves were created by major earthquakes occurring at the end of the deglaciation, when the isostatic rebound was very rapid; cf. Mörner (1985).

The caves are more or less labyrinthine. Most of them have a length of about 100 m or less, but three caves are considerably larger having a length of the order of 1 km. These three large caves are situated within a common area. Since there seems to be no other reason for their size they may be suspected to represent the strongest postglacial earthquakes.

A mathematical method using the concept of curvature was developed by Ekman (1985) for trying to study postglacial uplift as a possible origin of earthquakes. This curvature theory will now be applied to the boulder caves. We first give an outline of the theory, then apply it to the land uplift at the end of the deglaciation as revealed by ancient shore lines, and finally compare the result with the location and character of the caves.

DOI: https://doi.org/10.2312/zipe.1989.102.03

2. Postglacial curvature theory

Postglacial land uplift, like any function on a sphere, may be expanded in a series of surface spherical harmonics,

$$U = \sum_{n=0}^{\infty} \sum_{m=0}^{n} (\bar{a}_{nm} \cos m\lambda + \bar{b}_{nm} \sin m\lambda)\, \bar{P}_{nm}(\sin \varphi) \qquad (1)$$

(see e.g. Heiskanen & Moritz, 1967). The coefficients are given by

$$\bar{a}_{nm} = \frac{1}{4\pi} \int_0^{2\pi} \int_0^{\pi} U(\varphi, \lambda)\, \bar{P}_{nm}(\sin \varphi) \cos \varphi \cos m\lambda \, d\varphi d\lambda$$

$$\bar{b}_{nm} = \frac{1}{4\pi} \int_0^{2\pi} \int_0^{\pi} U(\varphi, \lambda)\, \bar{P}_{nm}(\sin \varphi) \cos \varphi \sin m\lambda \, d\varphi d\lambda \qquad (2)$$

Here φ denotes latitude, λ longitude, and $\bar{P}_{nm}$ the normalized Legendre functions.

The uplift U to be used here is the absolute uplift, which is the apparent uplift - according to the shore line observations - corrected for the change of the geoid and for eustatic changes of the water level. The uplift may be thought of either as a vertical velocity or as a height change between different epochs; it will be used in both senses in the following.

Now, postglacial uplift causes the Earth's crust not only to rise (and to tilt) but also to curve. The postglacial curvature, especially the Gaussian curvature, serves as a kind of measure of the amount of postglacial stress and strain produced in the crust. This may be realized through the geometric interpretation of the Gaussian curvature, or through the "Theorema egregium" of Gauss, stating that a surface which is bent without being strained does not change its Gaussian curvature (cf. e.g. Lipschutz, 1969).

DOI: https://doi.org/10.2312/zipe.1989.102.03

A formula for the Gaussian postglacial curvature has been derived, starting form (1), by Ekman (1985):

$$
\begin{aligned}
K = \frac{1}{R^4} \sum_{n=0}^{N} \sum_{m=0}^{n} & (\bar{a}_{nm} \cos m\lambda + \bar{b}_{nm} \sin m\lambda) \\
& \left[\left(- n(n+1) + (n+1) \tan^2\varphi + \frac{m^2}{\cos^2\varphi} \right) \bar{P}_{nm}(\sin\varphi) \right. \\
& \left. - \frac{\sqrt{(2n+1)(n+m+1)(n-m+1)}\, \sin\varphi}{\sqrt{2n+3}\, \cos^2\varphi} \bar{P}_{n+1,m}(\sin\varphi) \right] \\
& \sum_{n=0}^{N} \sum_{m=0}^{n} (\bar{a}_{nm} \cos m\lambda + \bar{b}_{nm} \sin m\lambda) \\
& \left[\left(- (n+1) \tan^2\varphi - \frac{m^2}{\cos^2\varphi} \right) \bar{P}_{nm}(\sin\varphi) \right. \qquad (3) \\
& \left. + \frac{\sqrt{(2n+1)(n+m+1)(n-m+1)}\, \sin\varphi}{\sqrt{2n+3}\, \cos^2\varphi} \bar{P}_{n+1,m}(\sin\varphi) \right] \\
& - \frac{1}{R^4} \left(\sum_{n=0}^{N} \sum_{m=0}^{n} (\bar{a}_{nm} \sin m\lambda - \bar{b}_{nm} \cos m\lambda) \right. \\
& \left[- \frac{(n+2)m \sin\varphi}{\cos^2\varphi} \bar{P}_{nm}(\sin\varphi) \right. \\
& \left. \left. + \frac{\sqrt{(2n+1)(n+m+1)(n-m+1)}\, m}{\sqrt{2n+3}\, \cos^2\varphi} \bar{P}_{n+1,m}(\sin\varphi) \right] \right)^2
\end{aligned}
$$

DOI: https://doi.org/10.2312/zipe.1989.102.03

Here R is the radius of the Earth; the other symbols have already been explained. For obvious reasons the series expansion is cut off at some large number n = N, the coefficients (2) being then calculated by summation over a lot of surface elements (squares) of a corresponding size.

3. Gaussian curvature at the end of the deglaciation

Let us now apply the formula (3) to the postglacial rebound of Fennoscandia some eight thousand years ago, when the ice had recently melted away.

The first step is to determine the apparent uplift at that time. This can be accomplished for the Baltic Sea area by using two maps of Eronen (1983), showing the heights above present sea level of the shore lines at about 7000 B.C. and 5500 B.C. The difference between them represents the apparent uplift between the mentioned years, turning out to be 170 m at its maximum. For the Atlantic coast area we use the shore displacement curves compiled in Hafsten (1983), together with a few additional curves (Mörner, 1980; Donner, 1980).

The apparent uplift should then be corrected for changes in the amount of water. In the Baltic Sea area the eustatic change of the water level is composed of two parts: the lowering of the Ancylus Lake between approximately 7000 B.C. and 6500 B.C., c. 15 m (Björck, 1987), and the rise of the sea approximately from 6500 B.C. to 5500 B.C., c. 10 m (Mörner, 1980). The two parts nearly cancel out. The influence of the rise of the geoid, being slightly reduced by the existence of the Ancylus Lake, does nowhere exceed 10 m (cf. Ekman, 1987). These corrections may be considered insignificant for our further computations. In the Atlantic coast area, on the other hand, we should correct for the eustatic rise of sea level during the whole period; it amounts to c. 25 m (Mörner, 1980).

DOI: https://doi.org/10.2312/zipe.1989.102.03

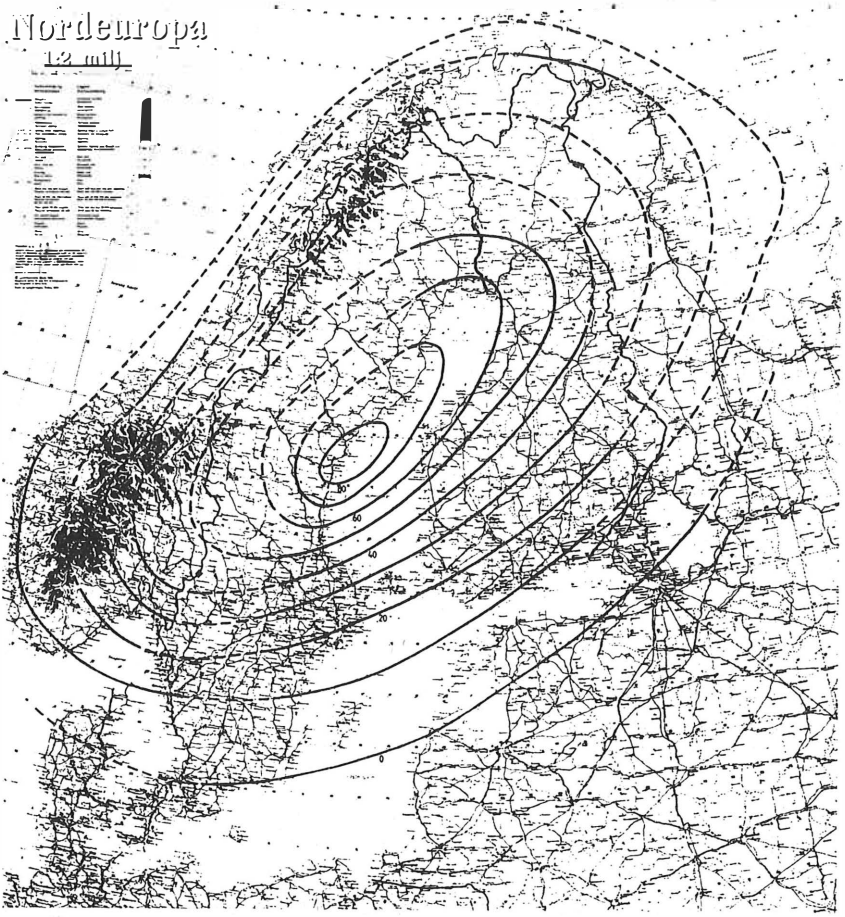

Figure 1. Absolute uplift of Fennoscandia in mm/year at about 6000 B.C.

DOI: https://doi.org/10.2312/zipe.1989.102.03

Applying the correction above we obtain the absolute uplift between 7000 B.C. and 5500 B.C. From this we easily find the absolute uplift rate at about 6000 B.C., the map of which is shown in Figure 1. Its maximum value is more than 80 mm/year, nearly 10 times the value of today (cf. Ekman, 1987).

From Figure 1 we next determine mean values of the uplift rate within squares of 1^{o} x 1^{o} (1^{o} latitude x 2^{o} longitude). Using these values the coefficients $\bar{a}_{nm}$ and $\bar{b}_{nm}$ can now be calculated according to (2).

Finally we compute the Gaussian postglacial curvature K applying the formula (3). Thereby the maximum possible value of N is 180, corresponding to the minimum wave-length 1^{o}. To examine the stability of the solutions for various values of N some computations of K for $180 \geq N \geq 120$ were made, leading to quite similar results. The result for N = 150 is shown as a Gaussian curvature map in Figure 2.

From the map we see that the Gaussian curvature of one century of postglacial uplift is great - $K > 5 \cdot 10^{-27}$ mm^{-2} - within a rather small area located at the Swedish coast of the southern part of the Gulf of Bothnia. The maximum is $K = 20 \cdot 10^{-27}$ mm^{-2}.

Now, Figure 2 shows the situation at about 6000 B.C. when the ice did no longer exist. However, the peak rate of land uplift here was probably reached about 2000 years earlier, before the ice had disappeared completely (Mörner, 1980). The Gaussian curvature at that time can only be estimated through an attempt to extrapolate back to 8000 B.C.: First, the uplift rate then was at least three times larger (Mörner, 1980), making the Gaussian curvature one order of magnitude larger. Second, although the general pattern of the land uplift has kept remarkably unchanged up till today the maximum point has slowly migrated to the north-northeast by nearly half a degree per millenium. This can be seen by studying e.g. Eronen's (1983) map of the uplift since the Ancylus Lake, his

DOI: https://doi.org/10.2312/zipe.1989.102.03

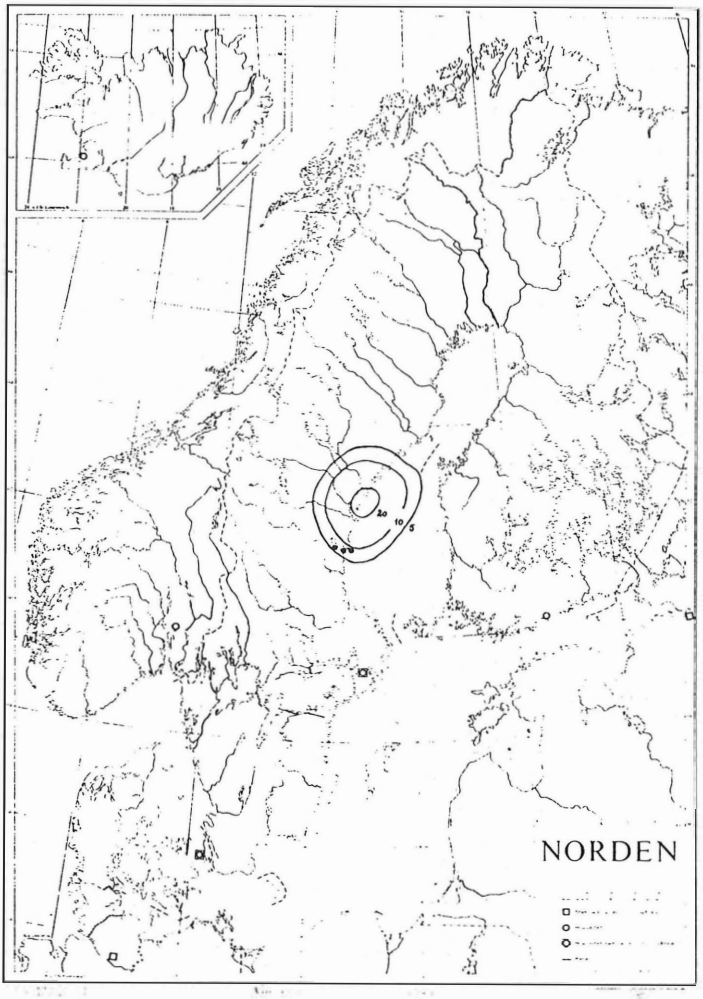

Figure 2. Gaussian curvature K of the postglacial uplift of Fennoscandia at about 6000 B.C. (N = 150). Unit of K for one century of uplift: 10^{-27} mm^{-2}. Dots denote large boulder caves.

DOI: https://doi.org/10.2312/zipe.1989.102.03

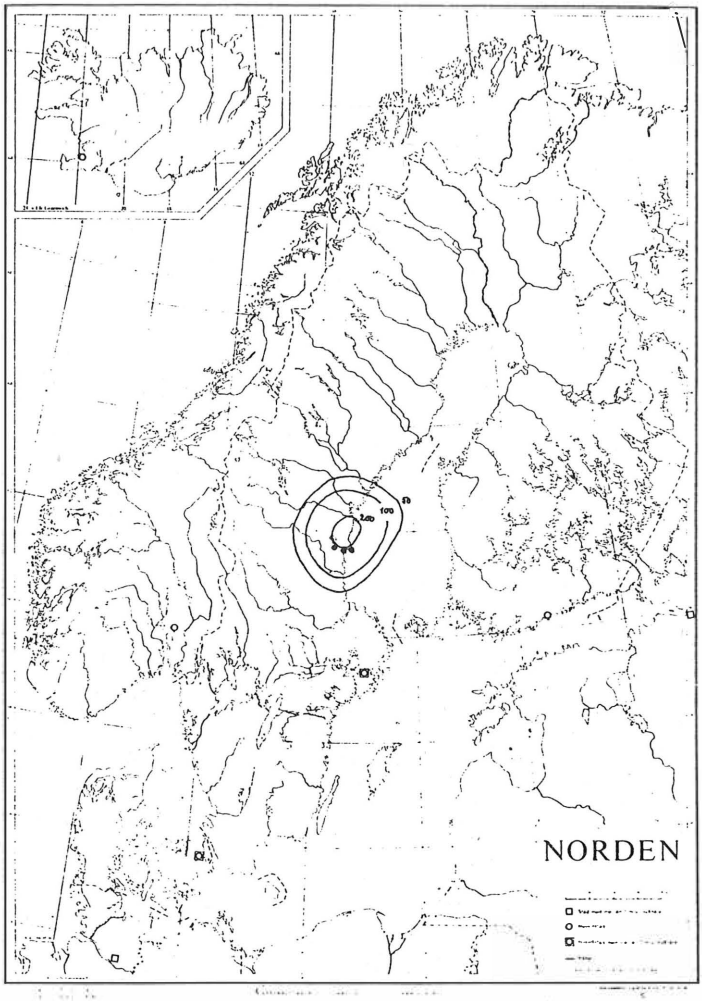

Figure 3. Estimated Gaussian curvature K of the postglacial uplift of Fennoscandia at about 8000 B.C. (N = 150). Unit of K for one century of uplift: 10^{-27} mm^{-2}. Dots denote large boulder caves.

DOI: https://doi.org/10.2312/zipe.1989.102.03

map of the uplift since the early Litorina Sea, and a geodetic map of the present uplift. Assuming that this process had started not later than 8000 B.C. the area with large K values was at that time located nearly one degree further to the south-southwest, as illustrated in Figure 3.

4. Gaussian curvature, earthquakes and boulder caves

The character of the boulder caves is in good accordance with what one should expect from a positive Gaussian post-glacial curvature (as we have in Figures 2 and 3). Positive values of K, i.e. elliptic curvature, should here correspond to tension in all directions. According to R Sjöberg (1987) the accumulation of boulders forming the caves clearly show that the bed-rock was split by tensional forces in all directions.

If postglacial rebound is the origin of the earthquakes that seem to have created the boulder caves, then the largest boulder accumulations should be found where the Gaussian postglacial curvature is great. As was mentioned in the Introduction there are three large boulder caves, all of them situated within a common area. They are marked by dots in Figures 2 and 3. In Figure 2, representing 6000 B.C., we find the large boulder caves close to the Gaussian curvature maximum. In Figure 3, representing the more realistic 8000 B.C., we find the large boulder caves almost coinciding with the Gaussian curvature maximum. We must, however, bear in mind that the extrapolation makes Figure 3 uncertain. In any case, the large caves are situated very close to where predicted by the Gaussian postglacial curvature.

One would now also expect to find some correlation between the Gaussian curvature and the small boulder caves, but this is not the case. Most of the twenty small caves are scattered in the whole eastern part of Sweden. Our mathematical method fails to explain this.

DOI: https://doi.org/10.2312/zipe.1989.102.03

Finally we note that the maximum Gaussian curvature of one century of postglacial rebound amounts to $K = 10^{-25}$ mm^{-2} or more. This may be compared with the Gaussian curvature of the earth tide which is 10^{-34} mm^{-2} (Ekman, 1985). The secular postglacial curvature is thus of the order of 10^{9} times the tidal curvature, i.e. the secular postglacial strain may be roughly estimated to 10^{4} - 10^{5} times the tidal strain. This should allow major postglacial earthquakes to occur (cf. Heaton, 1975, and Johnston, 1987).

Before summarizing the conclusions a few words ought to be said about the long postglacial fault in northernmost Sweden, the Pärvie fault (Lundqvist & Lagerbäck, 1976). This fault might have been formed by a zone of great mean curvature of postglacial rebound. However, whether this is so cannot be determined since no shore lines exist to give information on the postglacial curvature there.

Conclusions: The three large boulder caves, concentrated at the Swedish coast of the southern part of the Gulf of Bothnia, most probably are created by major earthquakes produced by the Gaussian curvature of the postglacial rebound of Fennoscandia. The Gaussian curvature theory explains both the location and the character of the boulder accumulations and caves. Also, the curvature seems to be great enough to allow major earthquakes to occur. On the other hand the theory as applied here fails to explain the distribution of the small boulder caves. In the light of this the conclusion on the origin of today's minor earthquakes in central Fennoscandia drawn by the author a few years ago (Ekman, 1985) must be considered doubtful; it rather seems that nothing could yet be concluded in that matter.

A picture of the split bed-rock above the largest cave system, the Boda caves, is shown in Figure 4. According to our curvature calculations the picture could be mathematically described as Nature's own illustration of the Theorema egregium of Gauss!

DOI: https://doi.org/10.2312/zipe.1989.102.03

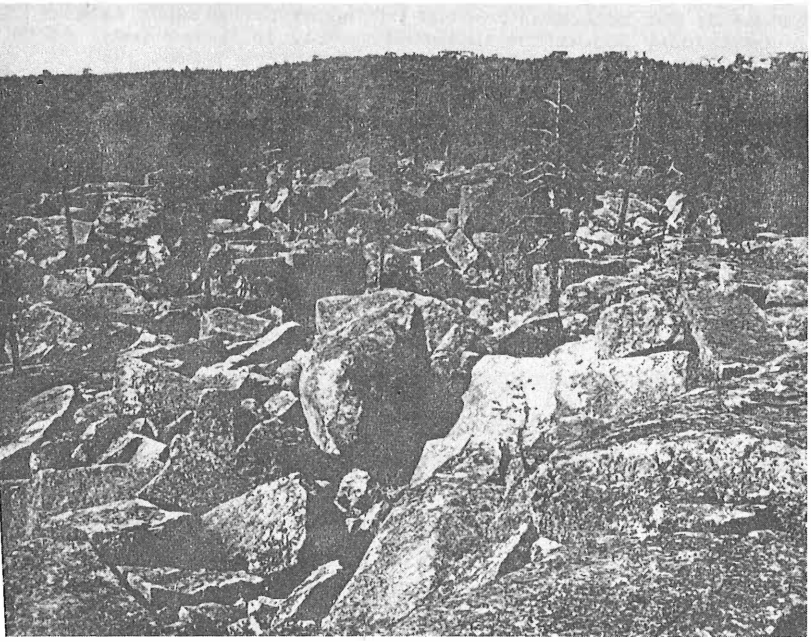

Figure 4. Split bed-rock above the largest boulder cave (Boda).

DOI: https://doi.org/10.2312/zipe.1989.102.03

References

Björck S: An Answer to the Ancylus Enigma? - Presentation of a Working Hypothesis. Geologiska Föreningens i Stockholm Förhandlingar, 109, 1987.

Donner J: The Determination and Dating of Synchronous Late Quaternary Shorelines in Fennoscandia. In Mörner (ed): Earth Rheology, Isostasy and Eustasy. John Wiley & Sons 1980.

Ekman M: Gaussian and Mean Curvatures of Earth Tides and Post-glacial Land Uplift, and Their Effects on Earthquakes. Doctoral dissertation, Uppsala 1985.

Ekman M: Postglacial Uplift of the Crust in Fennoscandia and Some Related Phenomena. International Association of Geodesy (Section V: Geodynamics), XIX General Assembly, Vancouver 1987.

Eronen M: Late Weichselian and Holocene Shore Displacement in Finland. In Smith & Dawson (eds): Shorelines and Isostasy. Academic Press 1983.

Hafsten U: Biostratigraphical Evidence for Late Weichselian and Holocene Sea-level Changes in Southern Norway. In Smith & Dawson (eds): Shorelines and Isostasy. Academic Press 1983.

Heaton T: Tidal Triggering of Earthquakes. Geophysical Journal of the Royal Astronomical Society, 43, 1975.

Heiskanen W A & Moritz H: Physical Geodesy. W. H. Freeman & Co. 1967.

Johnston A C: Suppression of Earthquakes by Large Continental Ice Sheets. Nature, 330, 1987.

Lipschutz M: Theory and Problems of Differential Geometry. Schaum's Outline Series, McGraw-Hill Book Co. 1969.

Lundqvist J & Lagerbäck R: The Pärve Fault: A Late-glacial Fault in the Precambrian of Swedish Lapland. Geologiska Föreningens i Stockholm Förhandlingar, 98, 1976.

Mörner N-A: The Fennoscandian Uplift: Geological Data and Their Geodynamical Implication. In Mörner (ed): Earth Rheology, Isostasy and Eustasy. John Wiley & Sons 1980.

Mörner N-A: Paleoseismicity and Geodynamics in Sweden. Tectonophysics, 117, 1985.

Sjöberg R: Caves as Indicators of Neotectonics in Sweden. Zeitschrift f¯r Geomorphologie, Suppl.-Bd. 63, 1987.

Acknowledgement

I thank S. Björck for kindly having provided information on the shore line data.

DOI: https://doi.org/10.2312/zipe.1989.102.03

S.V.Enman and O.E.Popov

Periodic patterns in land displacements based on geodetic data

The problem of periodicities in land displacements arose with the recent progress in the study of recent crustal movements, the prediction of earthquakes and volcanic eruptions, the study of earth structure by instrumental (geodetic, gaging, geophysical) and non-instrumental (geologic, geomorphological, historical and archeological) methods.

Publications of the early 1960s on the rhythm, cyclicity in the oscillations of land surface were mainly based on the results of geological, geomorphological, archeological, gaging and partly levelling studies. Quite frequently, these studies aimed at elucidating, corroborating whether the rates of recent vertical crustal movements based on levelling measurements really reflect long-term, slow patterns in the displacements. It was pointed out that, if the effect of observation epoch were confirmed by extensive statistical material, then levelling data and gage measurements would have to be reduced to the same observation epoch (Matskova,1963; Sinyagina,1965).

The regular periodicity of tectonic processes is due to the effect of certain relations between gravity forces acting from outside the Earth on the Earth's interiors (B.L.Lichkov, see Kozlovsky,1965). It is supposed that secular movements of the same direction in north-west zones can be regarded as tide-like waves propagating on the surface of our planet. These waves are associated with the formation of geologic structures and vary in amplitude within structures (Kozlovsky,1965). Some geological, geomorphic, and historical and

DOI: https://doi.org/10.2312/zipe.1989.102.03

archeological evidence suggests a period of secular movements at least 600-700 years. Land uplifts and subsidences occur in close relation, the areas involved in the two types of movement being different. Geodetic data reveal waves of recent movements on the order 600-800 km (for the Russian Platform) and 180-250 km (for Japan)(Meshcheryakov,1963).

Kozlovsky(1965) finds tectonic waves of 500-600 yr period in his historical and archeological studies in Chersonese excavations, Crimea . Meshcheryakov(1963), Kalashnikova and Magnitsky(1978) report a complete cycle of land oscillations about 2,000 years as determined from displacements in the columns of a Roman market within a mobile volcanic area of Italy, in Pazzuole. The thickness of flysch deposits has been used to determine cyclicities of land displacements with 500 and 4,000 years (Kozlovsky,1965).

A harmonic analysis of the rates of recent vertical crustal movements along a number of lines in the USA, Japan, USSR traversing platforms and mountain regions reveals common wavelengths for the same type of area. The values for the platforms are 630, 330, 210, 130, 120, 100, 80, 70, 65-55 km, the shape of the spectral curves being different for different tectonic zones; it is smoother for the platforms (Kalashnikova,1968). A spectral analysis of recent crustal movements along great-circle arcs (Helsinki-Tashkent, Ljubljana-Chardjou, Stockholm-Dubrovino, Ohrid-Pechora) yields the spatial dimensions of areas of recent vertical crustal movements having the same sign and constituting a

DOI: https://doi.org/10.2312/zipe.1989.102.03

hierarchical system of three ranks: I for platform areas ~1,500-2,000 km, for folded areas ~1,000 km with average amplitudes of 7 and 5-6 mm/yr; II ~300 km with an average amplitude of 3 mm/yr; III ~100-150 km (Golovkov and Narmirzaev,1985).

Yu.A.Meshcheryakov wrote as early as 1965 that secular crustal movements are complicated by short-period oscillations of different origins which are little known, except the solid-earth tides, so that little that is definite can be stated about their periods, amplitudes, patterns of occurrence in nature (Meshcheryakov,1963). As more instrumental data (levelling and geodimeter measurements) are being accumulated, including results from the use of various geophysical techniques, papers appear that contain attempts to deal with these problems.

V.G.Rikhter (1957) discovered a 5-yr period of land surface pulsations from an analysis of gage data. V.A.Matskova examined data at 12 gage stations to obtain patterns in the variations of the rate of crustal displacements in 15-year and at a number of sites in 30-year periods (Matskova,1963). Sha has also revealed (Matskova,1973) a period of 30-40 years from an analysis of long gage data series (as long as 80-100 years) at 50 sites in the Baltic Sea and the North Sea. An analysis of mean annual levels at gage stations in Lake Baykal area. has shown the shore oscillations to have a regular periodicity and wavelike propagation across the Baykal Basin towards the northwest. The duration of the micropul-

DOI: https://doi.org/10.2312/zipe.1989.102.03

sation period is 8-9 years. The wave amplitude reaches 4-6 cm. The wavelength is 50-80 km. The velocity of the micropulsation waves is greater and the wavelength is less than the respective values in the northern part of the lake, particularly near the western shore (Lamakin, 1965).

The discrepant rates of vertical land movements derived from levelling measurements for different intervals of time provide evidence that the displacements can be represented as a sum of individual components (Tyapkin and Bondaruk, 1983). Researchers have also tried to determine the period spectrum from geodetic data. V.S.Vereda discovers an activation of movements with a period of 5-6 years from analyses of multiple levelling data in the Donbass (Vereda,1974; Vereda, Yurchenko, Surovtsev, and Urmantsev,1980). Investigations in the Krivoy Rog area have shown that correcting levelling measurements for temperature and pressure does not exclude an annual component of land surface movements with amplitudes as large as 5-6 mm. In addition, sinusoidal movements of 6-yr period and 1-mm amplitude have been identified (Denisov,1987). Tyapkin and Bondaruk (1983) present compelling evidence that there is an annual componentwith an amplitude reaching 30 mm/yr in recent vertical crustal movements. These authors recommend to incorporate the component into the rate of movements, whatever is the cause of the component. These form a basis on which a rotational hypothesis of feature formation in the earth's crust is being developed. V.I.Volkov (1983) hypothesized a systematic influence of upper-crustal

DOI: https://doi.org/10.2312/zipe.1989.102.03

thermoelastic oscillations due to seasonal temperature waves on recent vertical crustal movements. An analysis of long-continued geodimeter observations in the Maricope area along the San Andreas Fault zone has revealed cyclic deformations of 6.5-9-year period and $1.5 \cdot 10^{-6}$ amplitude (Greensfelder and Bennett, 1973).

Measurements of deformation in Japan and Western Cordillera reveal displacements of deformations at a velocity of 10-100 km/yr landwards (Kasahara,1979). Migration of shear deformation was discovered in northeastern Honshu from southeast to northwest at a velocity of 38 km/yr based on strainmeter observations at 5 stations. Analysis of variance applied to the variations of strain curves at different stations has revealed the deformation front propagating at velocities of 100-300 km/yr (Ishii, Takagi and Suzuki, 1979).

Many authors have found migration of large and moderate earthquakes along faults in a number of areas. The migration fits into the hypothesis of cyclicity manifested by the impulses of tectonic movements, since the spatio-temporal earthquake sequences repeat themselves on each fault (Nikonov, 1977). The rates of seismic migration yield the following velocities of the deformation front: 80 km/yr from east to west for the Anatolian Fault (Mogi,1968), 50 km/yr westwards and 10 km/yr eastwards of 39° meridian for the northern Anatolian Fault (Dewey,1976), 110 km/yr from west to east for the epicentral area of the Haicheng earthquake (Scholz,1977), 3.5 km/yr in Central California (San Andreas Fault System)

DOI: https://doi.org/10.2312/zipe.1989.102.03

(Wood and Allen,1973), 95 km/yr for South America (by an application of the analysis of variance to the distribution of seismicity)(Delsemme and Smith,1979). Vilkovich, Guberman and Keilis-Borok(1974) have examined the spatio-temporal structure of the seismic field for California, Chile, Panama to discover propagation of tectonic deformation waves along major north-south faults at a velocity of 34-86 km/yr in association with earthquakes with M 6.5.

A study of changes in various seismological parameters in the Garm area has shown a spatial migration of deformation from southeast to northwest at a velocity of 33 ± 7 km/yr. A number of seismological parameters indicate sinusoidal variations of 2.75 year period (Lukk and Nersesov,1982).

An analysis of the investigations quoted shows that land surface displacements involve periodic patterns of oscillations with periods from a year to hundreds or thousands of years, different amplitudes of velocities of propagation whose superposition forms a complex tectonic process. Some possible causes for the migration of deformation waves have been suggested.

The Garm Geodynamic Test Area is one of the oldest of its kind in the USSR. It lies in the basins of the Surkhob and Obi-Khingou Rivers and their mountain margin (Southern Tien-Shan, Northern Pamir) and occupies an area of about 14,000 km^2. First geodetic works (levelling, microtriangulation) started along Runou Brook in 1948, precise levelling being conducted along the Garm circle and in the Nimichi area since 1957. The geodetic network was later made more dense

DOI: https://doi.org/10.2312/zipe.1989.102.03

and extended. Repeated geodetic observations are concentrated in some individual areas of special study traversing the frontal part of the Vakhsh Thrust. More than 100 repeated measurements have been made in some areas (the Garm circle). Since 1972 geodimeter measurements have been conducted in the Test Area for networks of different ranks with sides ranging between 0.5-1 and 30 km.

Geodetic work has identified, on the left bank of the Surkhob River, the frontal part of the Vakhsh Thrust where the rocks of the Tadjik Depression creep northwards. There is a ridge of the Thrust in the frontal part in the Garm area with a maximum vertical amplitude of +14.6 mm/yr relative to the quiet right bank of the Surkhob River where the rates of displacement do not exceed 0.1 mm/yr. The thrust amplitude decreases on both sides. It is ~10 mm/yr at a distance of 2 km and ~4 mm/yr at 4 km. As one moves away from the frontal part of the Thrust, the displacement amplitude decreases, being at the minimum at a distance of 0.7-0.9 km from the ridge crest. Two more thrust plates occur over a distance of 9 km into the Peter the First Range.

The rates of horizontal displacements derived from geodimeter measurements of the Sari-Pul deformation network across the frontal part of the Thrust during the period 1972-1984 are 9-16 mm/yr over different lines of 0.4-1.9 km length, the measurement sites in the Thrust move nearly from south to north (A=350°)(Guseva,1986). The deformation rapidly decreases within the frontal part of the Thrust (as inferred

DOI: https://doi.org/10.2312/zipe.1989.102.03

from strain measurements in the Sari-pul tunnel, see Latynina et al.,1978) and become as low as $1\text{-}2\cdot10^{-6}$ at a distance of 100 m.

V.A.Matskova(1963) in an attempt to evaluate the period of recent vertical crustal movements from levelling measurements came to the conclusion that the movements retain their direction and rate within 50 years. Yu.A.Meshcheryakov(1963) thinks that an interval of 20-25 years between measurements is long enough for the effects of short-period oscillations and measurement errors to be compensated or suppressed by secular movements. With trend movements present in geodetic data and assuming that the rate of slow movements persist through observation periods of 10-40 years, one could hope to eliminate trend displacements from the observed results. This paper deals with regular patterns of movements superimposed on the slow trend.

Regression and spectral analyses have been carried out for a long series of geodetic measurements in the Garm part of the geodynamic test area (Figure 1). The displacement rates were obtained from the results of repeated measurements along individual sections in the levelling and in the lines of the deformation network based on the regression equation $Y=C+VX$. The rates of slow vertical crustal movements V were determined for a period of 10-27 years with repetitions 10-100 in number. The accuracy of the resulting rates is characterized by the values $m_V=\pm 0\text{-}0.15$ mm/yr. The initial displacement rates C were also determined for each benchmark on the initial date of measurement. An attempt to de-

DOI: https://doi.org/10.2312/zipe.1989.102.03

tect a relationship between V and C for individual lines has not established any correlation, showing the two displacements were different in origin. Superposed on these are the deformation processes controlled by the rate C.

Figure 2,a shows plots of V and C for benchmarks in the segment 3040-1248 on the right bank of the Surkhob River (the Gissar side of the Garm circle) where V does not exceed 0.1 mm/yr. The length of the segment is 4 km, the direction from west to east. The segment has 20 benchmarks, at intervals of 200 m on an average. Observations in the sections 3040-3433-3179 have been conducted since 1957, those at closely spaced benchmarks since 1972. The curves of V and C are different in character. The plot of C ($m_{Cmean}=\pm 0.08$ mm/yr) shows a regular deformation curve of maximum amplitude 2.6 mm at site 53, 3.3 km of the initial benchmark 3040. If we assume this to be 1/4 of the wavelength, then the full wavelength is $\lambda \approx 13$ km, $A_n \approx 5$ mm. Other waves are probably superposed on this deformation, ones of lesser wavelength and amplitude. There is also a similar regular variation in C from west to east for benchmarks lying in the frontal part of the Thrust on the left bank of the Surkhob River (the Peter the First, mobile side of the run), the maximum amplitude being 2.5 times greater, Figure 2,b. It seems impossible to identify such patterns from the large displacements across the frontal part of the Thrust with so few measurement sites. Figure 3 shows plots of C for the lines Runou and Chogdabion. The rate C varies smoothly. The maximum amplitudes are 3.5

DOI: https://doi.org/10.2312/zipe.1989.102.03

and 0.6 mm/yr, respectively. The difference is probably due to the different directions of the lines (nearly perpendicular to each other) and initial dates of measurement (1970, 1974). One can see a jump in C of 3 mm/yr for the line Chogdabion where the seconf thrust plate comes to the surface (fault zone).

Calculation of polynomials of degree 2 to 6 for two lines about 1.7 km in length, 3040-3433 and 3433-3179 on the Gissar side of the Test Area shows identical coefficients and behaviour of the curves, indicating the same nature of oscillatory movements along these sections, Figure 4. The coefficients for both lines retain the same sign, the difference in value being below 20-30 percent. The displacement in phase approximately characterizes the velocity of wave propagation ~ 3.5-4 km/yr from west to east.

A spectral analysis has been carried out to identify high-frequency components in land movements superposed on the trend. The most convenient form for identifying characteristic harmonic components in the observational series was thought to be an analysis of amplitude (A_n) and phase φ_n spectra obtained by expanding the basic data into the Fourier series:

$$f(t) = 0.5\, a_0 + \sum_{n=1}^{\infty} (a_n \cos \omega_n t + b_n \sin \omega_n t)$$

where a_n, b_n are Fourier coefficients

$$|A_n| = (a_n^2 + b_n^2)^{1/2}; \quad \varphi_n = \tan^{-1}(b_n / a_n)$$

DOI: https://doi.org/10.2312/zipe.1989.102.03

The number of terms in the Fourier series was chosen to be 40 for levelling data and 20 for geodimeter observations; this is determined by the measurement sampling rate and follows from the Nyquist theorem giving the main frequency range of a discretized function. As the time series under study are not uniform, the data were interpolated using piecewise polynomial functions after eliminating the linear trend:

$$S(x) = a_i + b_i (x - x_{i-1}) + c_i (x - x_{i-1})^2 + d_i (x - x_{i-1})^3$$

$$x_{i-1} \leq x \leq x_i$$

Typical periodograms obtained for levelling and geodimeter observation series are given in Figure 5, 6. An analysis of the periodograms along the levelling line reveals the following features:

- The characteristic periods along the quiet portion (the right bank of the Surkhob, sections 3040-3433, 3433-3179, 3179-1248) are T $\approx$ 13, 4, 1.2 years with amplitudes of the order $A_n \approx$ 0.2-1.0 mm.
- The characteristic periods across the Surkhob valley, as far as the Thrust (section 1248-16356) are T $\approx$ 4, 2, 1 year with amplitudes 0.3-0.5 mm.
- When one crosses the frontal line of the Thrust (section 16356-829), the characteristic periods 4, 2, 1 year have greater amplitudes $A_n \approx$ 1-2 mm compared with the other sections.
- A poorly defined spectrum is recorded for section 829-3187 in the frontal part of the Thrust, the mean amplitude maximum being about 0.3 mm within 10 to 2 years.

DOI: https://doi.org/10.2312/zipe.1989.102.03

A similar analysis of periodograms was carried out for geodimeter observation series of the Sari-Pul deformation network. The following can be noted for the most representative, sufficiently well sampled and uniform series:

- The characteristic period for the lines 50-3179, 3179-830 (the Gissar side of the network, the most quiet tectonically) is $T \approx 4\text{-}4.5$ years with amplitude $A_n \approx 2\text{-}2.5$ mm.

-For the line 24-829 on the Thrust, we have $T \approx 2, 1$ year, $A_n \approx 2, 1.5$ mm.

- The characteristic periods for the lines 24-50, 24-830 which traverse the Thrust line are $T \approx 4, 1.5$ year, but the amplitude is greater than that in the other lines; $A_n \approx 3.5\text{-}5$ mm for $T \approx 4$.

A comparison of the results from the spectral analysis of vertical and linear observation series has revealed a number of features in the character of oscillatory crustal movements:

(1) Presence of characteristic periodic components with similar periods 4, 2, 1 year for vertical and linear observation series.

(2) An identical distribution of amplitudes in the harmonics of vertical and horizontal crustal movements: the maximum amplitudes are recorded on lines traversing tectonically active zones (the Vakhsh Thrust). However, the amplitudes of harmonic components in the geodimeter observation series are about twice as great as those of levelling data.

DOI: https://doi.org/10.2312/zipe.1989.102.03

References

Delsemme J. and Smith A.T., 1979. Spectral analysis of earthquake migration in South America. PAGEOPH, Basel, pp.1271-1285.

Denisov A.I., 1987. The study and construction of a predictive map for recent vertical crustal movements in the Krivoy Rog area. Thesis for Cand.techn.sci. (in Russian).

Dewey J.W., 1976. Seismicity of Northern Anatolia. Bull. Seism.Soc.Amer., v.66, pp.843-868.

Golovkov V.P. and Narmirzaev V.D., 1985. The spatial structure of recent vertical crustal movements and its relation to geotectonics. Uzb.geol.zhurnal, No.8, p.14-17.

Greensfelder R.W. and Bennett J.H., 1973. Characteristics of strain variation along the San Andreas fault from geodimeter measurements. In: Proceedings of the Conference on Tectonic Problems of the San Andreas Fault System. Stanford, p.54-63.

Guseva T.V., 1986. Recent Crustal Movements in the Transition Zone between the Pamirs and Tien-Shan. Moscow, 171pp.(in Russian).

Ishii H., Takagi A. and Suzuki Z., 1979. Characteristic movement of crustal deformation in Northeast Honshu, Japan. Gerl. Beitr.Geophysik, Leipzig, v.88, No.2, p.163-169.

Kalashnikova I.V., 1968. A method for expanding recent vertical movements into the Fourier series and a comparison of spectra for different tectonic areas. In: Recent Crustal Movements. Moscow, p.104-119 (in Russian).

Kalashnikova I.V. and Magnitsky V.A., 1978. On the inherited character of recent crustal movements. Izvestiya AN SSSR,

DOI: https://doi.org/10.2312/zipe.1989.102.03

Fizika Zemli (Solid Earth), No.10, p.13-20.

Kasahara K., 1979. Migration of crustal deformation. Tectonophysics, v.53, No.1-4, p.329-341.

Kozlovsky D.A., 1965. On the rhythm of secular crustal movements. In: Recent Crustal Movements, No.2, Tartu, p.62-70 (in Russian).

Lamakin V.V., 1965. Crustal micropulsations and research in this field. In: Recent Crustal Movements, No.2, Tartu, p.71-80 (in Russian).

Latynina L.A., Guseva T.V., Zharinov N.A., Karmaleeva N.M., Nikiforova O.D., Pevnev A.K. and Khobot'ko A.A., 1978. On movements recorded in the Surkhob fault zone at the Sari-Pul station. In: Recent Crustal Movements, Novosibirsk, Nauka, p.92-99 (in Russian).

Lukk A.A. and Nersesov I.L., 1982. Temporal variations of various parameters of the seismotectonic process. Izvestiya ANSSSR, Fizika Zemli (Solid Earth), No.3, p.10-27.

Matskova V.A., 1963. An improved map of the rate of recent vertical crustal movements for the western European USSR and some considerations as to the origin of these processes. In: Recent Crustal Movements, No.1, Izd.AN SSSR, Moscow, p.73-87 (in Russian).

Matskova V.A., 1973. A map of the gradient of the rate of recent vertical crustal movements in the European USSR and studies in the periodicity of the movements. In: Recent Crustal Movements, No.5, Tartu, p.42-48 (in Russian).

Meshcheryakov Yu.A., 1963. Secular crustal movements. Sum-

DOI: https://doi.org/10.2312/zipe.1989.102.03

ming-up and perspectives. In: Recent Crustal Movements, Moscow, Izd-vo AN SSSR, p.7-24 (in Russian).

Mogi K., 1968. Migration of seismic activity. Bull.Earthq. Res.Inst., Tokyo, v.46, p.53-74.

Nikonov A.A., 1977. Holocene and Recent Crustal Movements. Moscow, Nauka, 240pp.(in Russian).

Rikhter V.G., 1957. On evaluating the method of repeated levelling for studying recent tectonic movements. Byull. MOIP, otd.geol., v.32, No.2, p.105-120.

Scholz C., 1977. The Haicheng Earthquake Prediction (A Physical Interpretation). U.S.-Japan seminar on theoretical and experimental investigation of earthquake precursors.

Sinyagina M.I., 1965. On the principles underlying the construction of a map of the rate of recent movements over a large area. In: Recent Crustal Movements, No.2, Tartu, p.32-37 (in Russian).

Tyapkin K.F. and Bondaruk A.G., 1983. On the annual component of recent vertical crustal movements. Geofizicheskii zhurnal, v.5, No.1, p.23-31.

Vereda V.S., 1974. On the character of recent vertical tectonic crustal movements in the Donetsk coal basin. Dokl.AN SSSR, v.218, No.8, p.651-652.

Vereda V.S., Yurchenko B.K., Surovtsev V.G. and Urmantsev F.M., 1980. Some results from studies in recent crustal movements in the Donbass Geodynamic Test Area for the years 1966-1977. In: Recent Crustal Movements, Kiev, Naukova Dumka, p.190-195 (in Russian).

DOI: https://doi.org/10.2312/zipe.1989.102.03

Vilkovich E.V., Guberman Sh.A. and Keilis-Borok V.I., 1974. Waves of tectonic deformation on large faults. Dokl. AN SSSR, v.219, No.1, p.77-80.

Volkov V.I., 1983. On evaluating the effect of hydrometeorological factors on recent crustal movements. In: Recent Crustal Movements and Deformation in Geodynamic Test Areas. Moscow, Nauka, p.150-153 (in Russian).

Wood M.D. and Allen S.S., 1973. Recurrence of seismic migrations along the Central California segment of the San Andreas Fault System. Nature, v.244, p.213-215.

DOI: https://doi.org/10.2312/zipe.1989.102.03

Figure Captions

for the paper"Periodic patterns in land displacements based on geodetic data" by S.V.Enman and O.E.Popov

Figure 1. The part of the Garm Test Area where regression and spectral analyses of geodetic data were carried out. The inset shows the Sari-Pul geodimeter network. (1) levelling benchmarks, (2) sites of the geodimeter network, (3) the Sari-Pul geodimeter network, (4) Vakhsh Thrust line

Figure 2. Variation of the rates V and C along the Garm circle

(a) the Gissar side of the network, the tectonically quiet one (the initial measurement of 1972)

(b) the Peter the First side, the highly mobile one (the initial measurement of 1969)

Figure 3. Variation of the rates V and C along the lines Runou (a) and Chogdabion (b).

Figure 4. Variation of elevation in time between benchmarks 3040-3433 (a), 3433-3179 (b). The curved line indicates vertical crustal movements fitted by a polynomial of degree 6.

Figure 5. Periodograms for sections of the levelling work:

(a) 3433-3179, a quiet segment, $V \leq 0.1$ mm/yr

(b) 1248-16356, across the Surkhob valley, as far as the Thrust line

(c) 16356-829, the section traverses the frontal line of the Thrust

(d) 829-3187, this section in the frontal part of the Thrust

Figure 6. Periodograms for lines of the geodimeter network:

DOI: https://doi.org/10.2312/zipe.1989.102.03

(a) 3179-830, the quiet Gissar side of the network

(b) 24-50, 24-830, the lines traverse the frontal line of the Thrust

(c) 24-829, this line is in the frontal part of the Thrust

DOI: https://doi.org/10.2312/zipe.1989.102.03

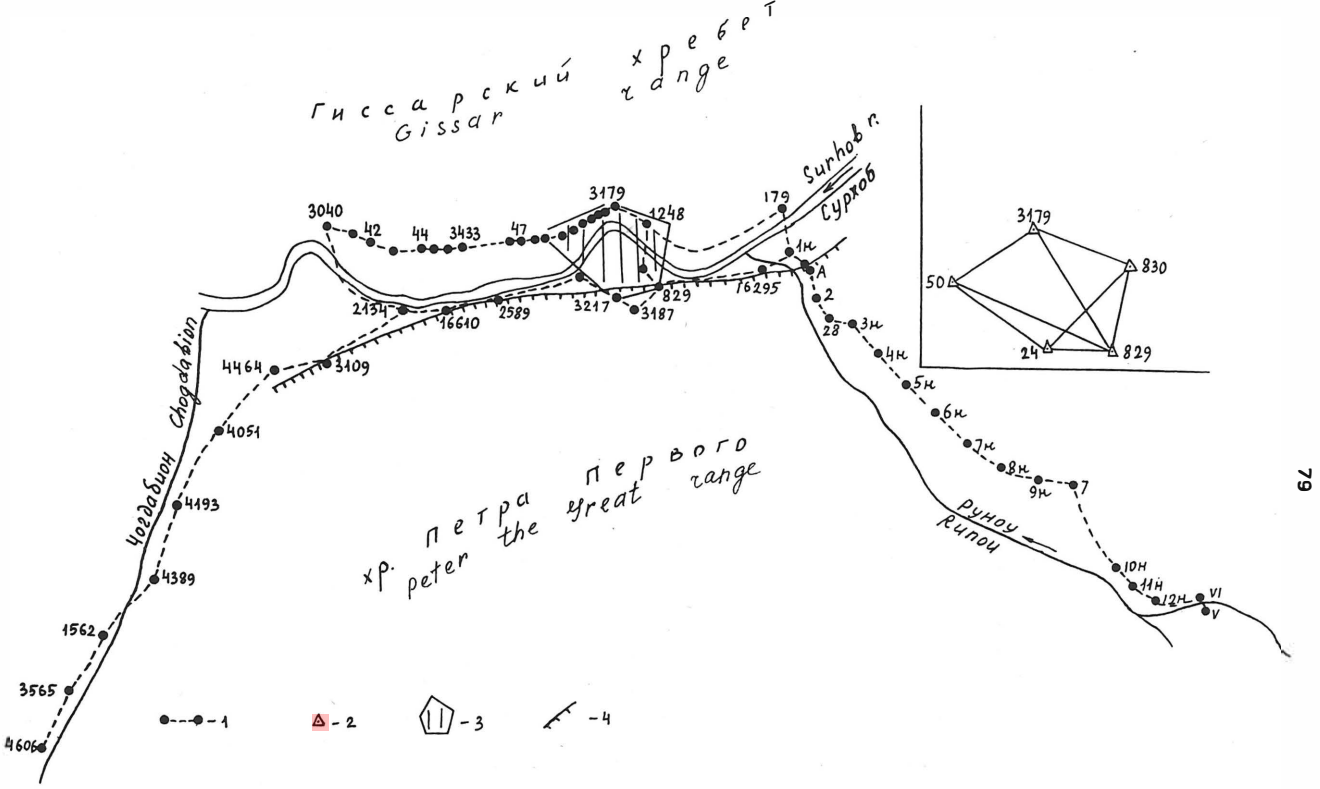

Fig. 1

DOI: https://doi.org/10.2312/zipe.1989.102.03

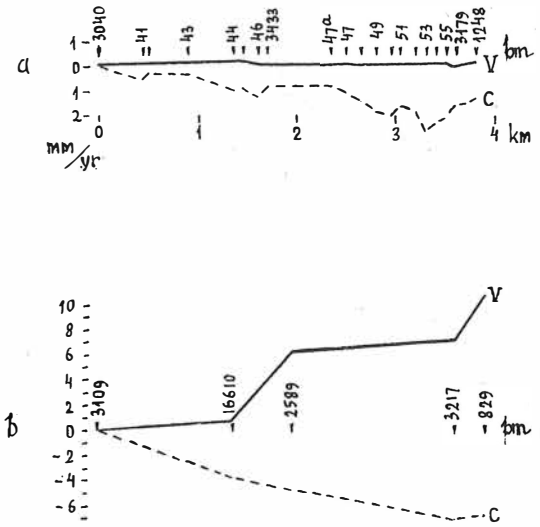

Fig. 2

DOI: https://doi.org/10.2312/zipe.1989.102.03

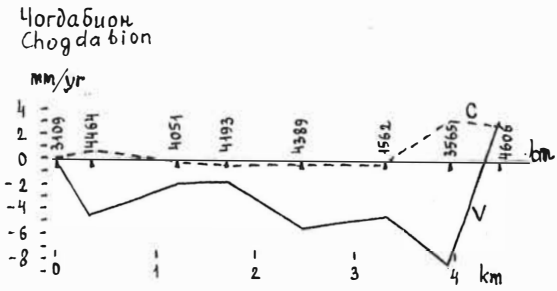

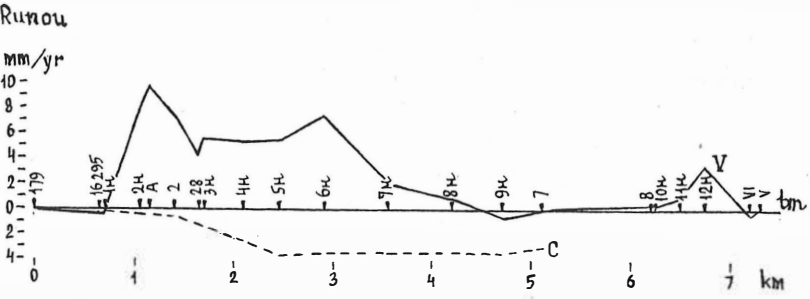

Fig. 3

DOI: https://doi.org/10.2312/zipe.1989.102.03

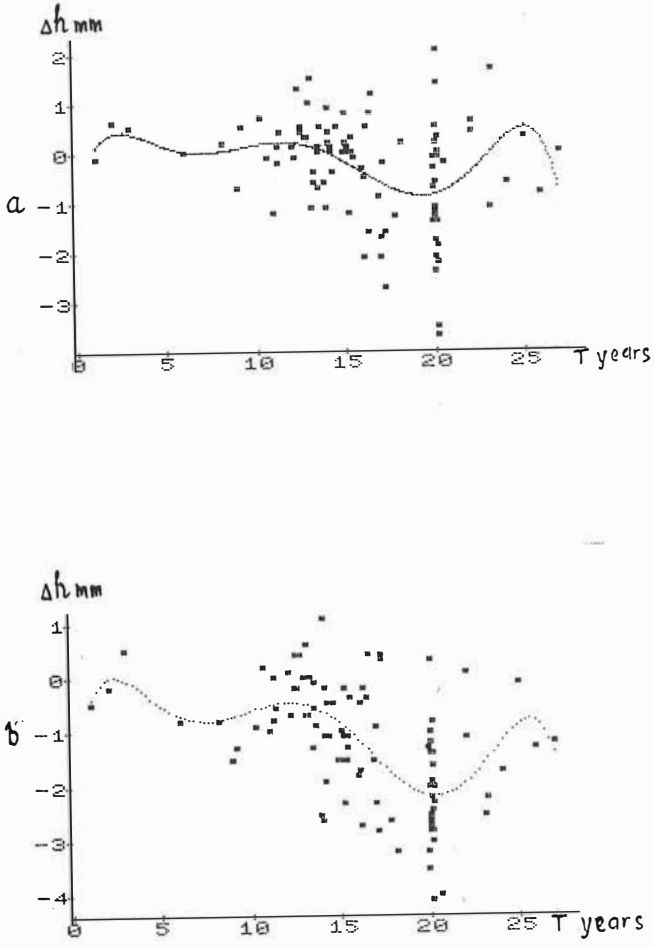

Fig. 4

DOI: https://doi.org/10.2312/zipe.1989.102.03

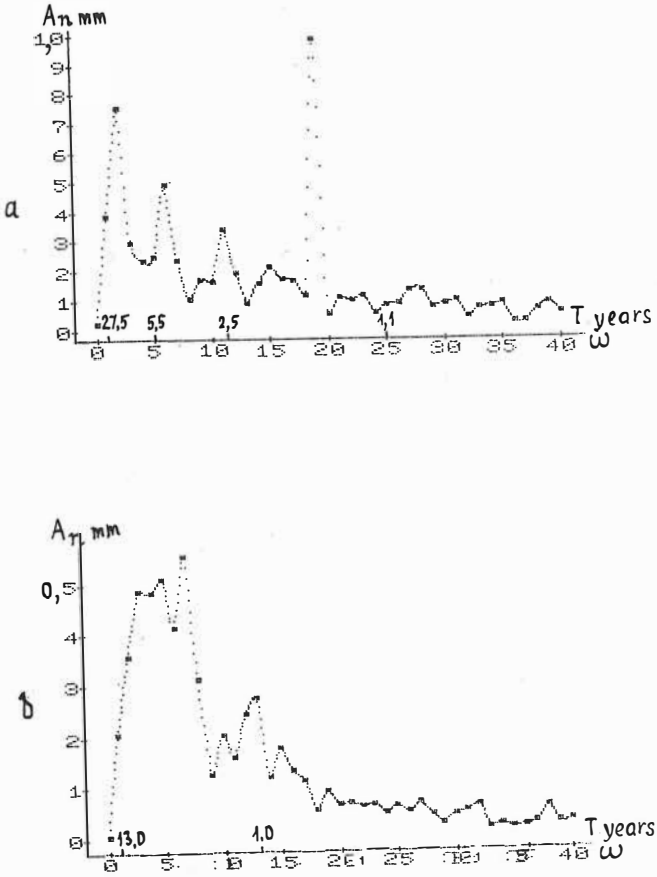

Fig. 5

DOI: https://doi.org/10.2312/zipe.1989.102.03

c

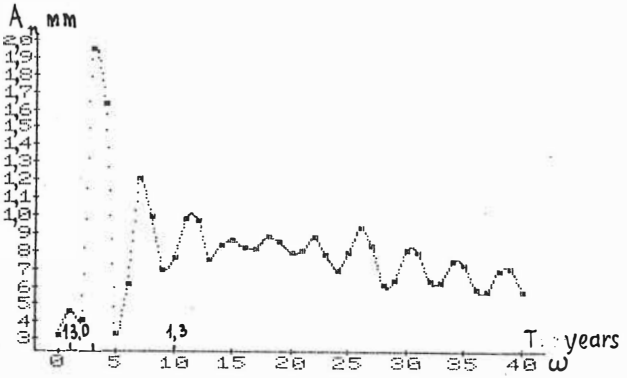

d

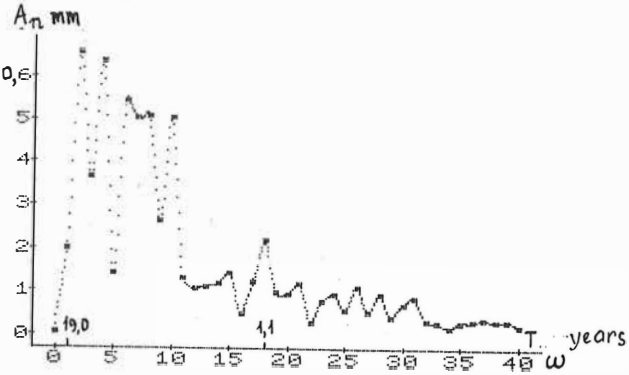

Fig. 5

DOI: https://doi.org/10.2312/zipe.1989.102.03

a

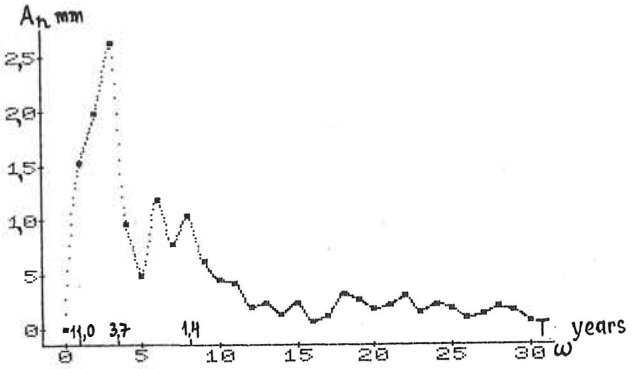

b

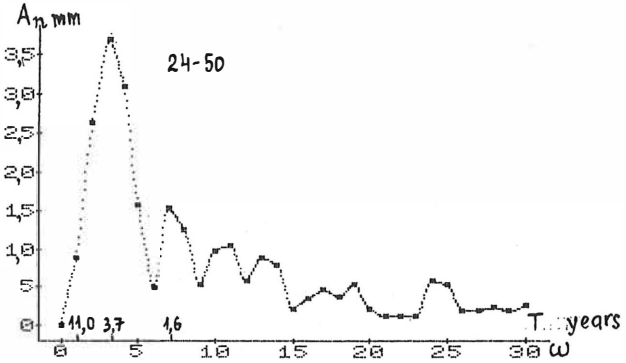

Fig. 6

DOI: https://doi.org/10.2312/zipe.1989.102.03

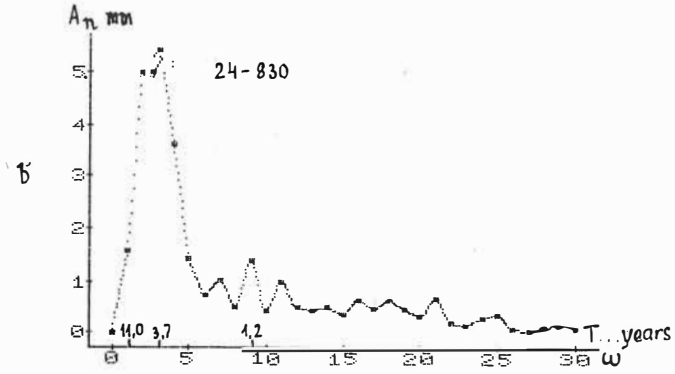

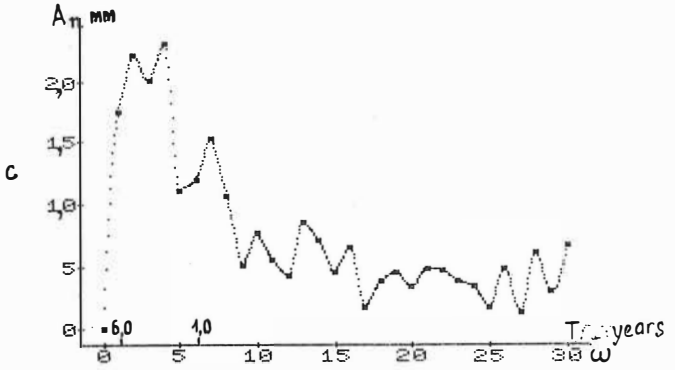

Fig. 6

DOI: https://doi.org/10.2312/zipe.1989.102.03

GENERAL REGULARITIES AND REGIONAL SPECIFICS UNDER CONDITIONS OF LASER LOCATION OF ARTIFICIAL EARTH'S SATELLITES FOR GEODYNAMIC INVESTIGATIONS ACCORDING TO THE PROGRAMME OF THE INTERNATIONAL PROJECT IDEAL

N.Iv. Georgiev and Iv. N. Totomanov
Bulgarian Academy of Sciences - Central Laboratory for Geodesy, Block No. 1,1113 Sofia

Abstract. The fundamental scientific and the applied objectives, the first results and prospects of the project IDEAL (Investigations on the Dynamics of the European -Asian Lithosphere) are outlined. The model argumentation of the intercontinental regional geodetic network of ground stations of INTERCOSMOS and artificial satellites of circular orbits tracked by laser rangefinders of an accuracy of nearly 25 cm is presented. Estimates are obtained, separately for the Carpatho-Balkan and the Ponto-Caspian regions of the Alpo-Himalayan orogen, for the optimum parameters height and inclination of the satellite orbits which provide a root mean square error of 3-4 cm in the length and orientation components of geocentric vectors and chord geokinematic vectors.

Conclusions are drawn which could be summarized in the following:

a) the laser rangefinders available allow a reliable geodetic verification of the meridian-oriented subduction processes, and

b) the accuracy of the laser tracking and the con-

DOI: https://doi.org/10.2312/zipe.1989.102.03

figuration of the network of space geodetic observatories are not satisfactory with regard to the determination of the parallel-oriented slip-collision interplate geodynamic processes within the region studied.

The paper entitled "Comparative analysis of satellite laser positioning within Carpatho-Balkan and Ponto-Caspian regions according to the programme of the international project IDEAL" is published in Comptes rendus de l'Académie bulgare des Sciences, tome 41, No. 4, pp. 33-35.

DOI: https://doi.org/10.2312/zipe.1989.102.03

DETERMINATION OF THE TECTONIC PLATE PARAMETERS FROM POINT COORDINATE SHIFTS

V.M.Gorban'

Ukrainian Academy of Sciences, Gravimetrical Observatory,
Poltava, USSR.

SUMMARY. A method for determining of the kinematics of plate tectonics from point positioning measurements is described. Fortran program PLAMOT was developed to realize the algorithm. Some results of classical, Dopler, and VLBI data processing are presented.

1. Modern observation techniques like VLBI, SLR, LLR and GPS provide information about time derivatives of angles between plumb lines of two points (direction measurements) or distances between points (range measurements) in a time scale of one or two years. In output of data analyses one can obtain "absolute" point position changes - cartesian components (range measurements) or spherical components (angle measurements) of the point radius vector in some terrestrial reference frame.

Radius vector of a site S_i situated at a plate P_k :

$$\underline{R}_i^k = \begin{bmatrix} x_i^k \\ y_i^k \\ z_i^k \end{bmatrix} \Longleftrightarrow \begin{bmatrix} \rho_i^k \\ \varphi_i^k \\ \lambda_i^k \end{bmatrix} \qquad (1)$$

Baseline vector from a site S_i at a plate P_k to a site S_j at a plate P_ℓ :

$$\underline{\zeta}_{ij}^{k\ell} = \begin{bmatrix} \Delta x_{ij}^{k\ell} \\ \Delta y_{ij}^{k\ell} \\ \Delta z_{ij}^{k\ell} \end{bmatrix} \Longleftrightarrow \begin{bmatrix} b_{ij}^{k\ell} \\ \psi_{ij}^{k\ell} \\ \nu_{ij}^{k\ell} \end{bmatrix} \qquad (2)$$

DOI: https://doi.org/10.2312/zipe.1989.102.03

Here and downward the first column vector contains cartesian components, the second one contains spherical components. One can obtain such data sets (a dot denotes time derivatives) :

$\{\dot{x}_i^k, \dot{y}_i^k, \dot{z}_i^k\}$; $\{\Delta\dot{x}_{ij}^{kl}, \Delta\dot{y}_{ij}^{kl}, \Delta\dot{z}_{ij}^{kl}\}$; $\{\dot{b}_{ij}^{kl}\}$

$\{\dot{\varphi}_i^k, \dot{\lambda}_i^k\}$; $\{\dot{B}_{ij}^{kl}\}$; $i,j=\overline{1,N}$; $k,l=\overline{1,M}$.

Spherical distance between two points S_i and S_j can be expressed by $\varphi_i^k, \varphi_j^l, \lambda_i^k, \lambda_j^l$.

2. Any motion of a rigid body (a tectonic plate) on surface of a sphere (Earth's surface) can be described as a rotation around an instantaneous geocentrical axis with the rotation vector:

$$\underline{\Omega}_k = \begin{bmatrix} \Omega_k^x \\ \Omega_k^y \\ \Omega_k^z \end{bmatrix} \Longleftrightarrow \begin{bmatrix} \Omega_k \\ \varnothing_k \\ \Lambda_k \end{bmatrix} \qquad (3)$$

The vector components are kinematic plate parameters. One may regard a relative rotational vector between two plates:

$$\underline{\Omega}_{kl} = \underline{\Omega}_l - \underline{\Omega}_k \qquad (4)$$

or one plate may be kept fixed with respect to the other. On the basis of the geophysical information can be obtain relative plate parameters only. Set of such parameters for some plates form kinematic plate model $\{\underline{\Omega}_{kl}\}$ (for example RM1 and RM2 [5,6]). Fixing the terrestrial system one may obtain "absolute" kinematic plate model $\{\underline{\Omega}_k\}$. For example the model AM1-2 is based on the coordinate system fixed with respect to hot spots in the Earth's mantle [5,6] .

3. The rate of a radial (vertical) displacement is:

$$\dot{\rho}_i^k = \frac{\underline{R}_i^k \cdot \dot{\underline{R}}_i^k}{|\underline{R}_i^k|} \qquad (5)$$

DOI: https://doi.org/10.2312/zipe.1989.102.03

Radius vector of a point on the earth's surface and plate parameters in some terrestrial reference frame are connected by relation:

$$\dot{\underline{R}}_i^{\,k} = \underline{\Omega}_k \times \underline{R}_i^{\,k} \qquad (6)$$

The baseline change rate is scalar triple product:

$$\dot{b}_{ij}^{\,ke} = \frac{(\underline{R}_i^{\,k}, \underline{R}_j^{\,e}, \underline{\Omega}_{ke})}{|\underline{r}_{ij}^{\,ke}|}; \quad \dot{b}_{ij}^{\,ke} = \frac{\underline{r}_{ij}^{\,ke} \cdot \dot{\underline{r}}_{ij}^{\,ke}}{|r_{ij}^{\,ke}|} \qquad (7)$$

The angle between S_i and S_j change with rate:

$$\dot{\beta}_{ij}^{\,ke} = \frac{(\underline{R}_i^{\,k}, \underline{R}_j^{\,e}, \underline{\Omega}_{ke})}{|R_i^{\,k} \times R_j^{\,e}|}; \quad \dot{\beta}_{ij}^{\,ke} = -\frac{\dot{R}_i^{\,k} R_j^{\,e} + R_i^{\,k} \dot{R}_j^{\,e}}{|R_i^{\,k} \times R_j^{\,e}|} \qquad (8)$$

One may express the vector relationship (6) - (8) both in cartesian and in spherical form.

4. Choosing an appropriate relationship for available data set and working out observation equations one can obtain estimates of the plate parameters $\underline{\Omega}_k$ or $\underline{\Omega}_{ke}$ by standard least squares adjustment techiques.

For example let us consider the case of set $\{\dot{x}_i^{\,k}, \dot{y}_i^{\,k}, \dot{z}_i^{\,k}\}$ which contains highest possible information and accept following model:

$$\dot{\underline{R}}_i^{\,k} = \dot{\underline{R}}^{\,0} + \dot{\underline{R}}_T + \dot{\underline{\rho}}_i^{\,k} + \dot{\underline{R}}_L + \underline{\varepsilon} \qquad (10)$$

Where $\underline{R}^{\,0}$ denotes the relative shift of the observational point network with respect to reference system;

$\underline{R}_T$ - the plate tectonic shift (horizontal);

$\underline{R}_L$ - any regional and local motions of the crust (horizontal);

$\underline{\rho}_i^{\,k}$ - radial (vertical) displacement;

$\underline{\varepsilon}$ - observational "noise".

Let N stations are located at M plates. When

$$\dot{\underline{R}}^{\,0} = \frac{1}{N} \sum_{k}^{N} \sum_{i}^{M} \dot{\underline{R}}_i^{\,k} \qquad (10a)$$

DOI: https://doi.org/10.2312/zipe.1989.102.03

$$\dot{\rho}_i'' = \left(x_i'' \dot{x}_i'' + y_i'' \dot{y}_i'' + z_i'' \dot{z}_i''\right)\left((x_i'')^2 + (y_i'')^2 + (z_i'')^2\right)^{-\frac{1}{2}} \qquad (10b)$$

$$\underline{\sigma} = \underline{A}\,\underline{\omega} \qquad (10c)$$

where $\underline{\sigma}$ - 3m-column vector, $\underline{\sigma}^T = [\dot{x}_1'', \ldots \dot{x}_m'', \dot{y}_1'', \ldots \dot{z}_m'']$;
$\underline{\omega}^T = [\Omega_x'', \Omega_y'', \Omega_z'']$ - vector of unknown parameters.
Design matrix (3m x 3) :

$$\underline{A} = \begin{bmatrix} 0 & \dot{z}_1'' & -\dot{y}_1'' \\ 0 & \dot{z}_2'' & -\dot{y}_2'' \\ \cdots & \cdots & \cdots \\ -\dot{z}_1'' & 0 & \dot{x}_1'' \\ \cdots & \cdots & \cdots \\ \dot{y}_m'' & -\dot{x}_m'' & 0 \end{bmatrix} \qquad (11)$$

m - number of points at the plate P_k .
For other types of data set the quantities $\dot{R}^0$, $\dot{\rho}_i''$ are undefined
As regards the local displacement $\dot{R}_i$ it is a part of "noise".

5. The auther developed the program PLAMOT (PLAte MOTion) to realize the foregoing algorithm. The program processes all types of input data set. SVD (singular value decomposition) method [2,4] is applied to inversion of design matrix. The program output contains cartesian and spherical plate tectonic parameters (absolute and/or relative) and the station shift rates. For given sites and/or pair of the sites with its initial coordinates at initial epoch the program computes corrections to site coordinates and/or pair baselines at given epoch.

6. Following data set was at our disposal:
   a) classical time and latitude observations [3] : $\{\dot{\varphi}_i'', \dot{\lambda}_i''\}$.
   b) Dopler satellite observations [2] : $\{\dot{\varphi}_i'', \dot{\lambda}_i''\}$
   c) VLBI measurements from NASA crustal dynamics project [7] : $\{\dot{x}_i'', \dot{y}_i'', \dot{z}_i''\}$.

DOI: https://doi.org/10.2312/zipe.1989.102.03

There is considerable evidence for North American and Eurasian plates only. The data in Table 1,2 suggest rather strongly that plate tectonic motion exist. But the estimations of the plate parameters must be regarded as tentative until more extensive data are available.

Table 1.

Radial point rates (cm/year) from VLBI data.

HRAS085	1.72 ± 1.36	OVRO130	2.07 ± 1.06
NRAO140	-0.11 0.68	MOJAVE12	8.48 4.22
ONSALA60	-1.02 2.07	EFLSBERG	4.61 10.77

Table 2.

Relative spherical plate kinematic parameters.
1 - model RM2; 2 - Dopler data; 3 - VLBI data; 4 - classical data.

		Ω deg/My		$\varnothing$ degree		Λ_E degree	
N.America - Eurasia	1	0.231 ± 0.016		-65.84 ± 13.55		312.48 ± 8.31	
	2	0.254	.201	-61.44	64.1	317.1	152.8
	3	0.507	.918	19.05	389.0	340.73	55.92
	4	2.34	.87	51.96	27.8	41.8	34.5
India - Eurasia	1	0.698	.015	19.71	.56	38.45	1.58
	2	1.39	.65	-12.42	13.0	37.74	12.7
Pacific - Eurasia	1	0.977	.022	-60.64	3.57	101.07	1.30
	2	0.811	.219	-65.85	13.7	158.0	61.6
N.America - Pacific	1	0.85		48.8		286.1	
	2	0.89		66.3	13.5	331.6	50.0

DOI: https://doi.org/10.2312/zipe.1989.102.03

REFERENCES.

1. Форсайт Дж., Малькольм М., Моулер К. Машинные методы математических вычислений. М., Мир, 1980, 279с.

2. Anderle R.J., Malyšev$_a$c C.A. Plate motion computed from Doppler s$_a$tellite observations presented at Symposium 2 of the XVIII Gener$_a$l assembly of IUGG. Mahnurg, 1983.
3. Annual Reports of BIH for 1968 - 1983. Paris, 1969 - 1984.
4. Lawson Ch.L., Hanson R.J. Solving least squares problems. Prentice-Hall, Inc., Englewood Cliffs, N.J., 1974.
5. Minster J.B., Jordan T.H., Molnar P., Haines E. Numerical modelling of instantaneous plate tectonics. - Geophys.J.Roy.Astron.Soc., 1974, 36, p.541-576.
6. Minster J.B., Jordan T.H. Present-day plate tectonics. - J.Geoph. Res., 1978, 83, N B11, p.5331-5354.
7. Ryan J.W., Ma C. Crustal dynamics project. Data analysis. Fixed station VLBI geodetic results. - NASA thechnical memorandum 86229. Goddard space flight center, Greenbelt, 1985.

DOI: https://doi.org/10.2312/zipe.1989.102.03

RECENT CRUSTAL MOVEMENTS AND SEISMICITY OF THE RUSSIAN PLATFORM

Grachev A.F., Kalashnikova I.V., Magnitsky V.A.
Insitute of Physics of the Earth, Academy of Sciences, USSR, Moscow

Abstract

The comparison of earthquakes's epicentres locations with recent crustal and neotectonic deformations is given. The deformations mode is presented by mean curvatures of vertical displacements surface. The main conclusion that can be done is an existence of the close relation of epicentres clusters with the regions of maximum curvatures.

Резюме

Проведен сравнительный анализ сейсмичности и современных и новейших деформаций земной коры Русской платформы. Деформации земной поверхности представлены в виде кривизн современных и новейших вертикальных движений. Сделан вывод, что эпицентры землетрясений приурочены к районам максимальных значений кривизн.

The idea of the relationship between the earthquake origin and the deformations of the Earth's crust and lithosphere is well known. The principal difficulty of its application using for the study of earthqakes and their prediction consists in the absence of a reliable information on the recent crustal movements. As a matter of fact one can get sometimes information dealing with deformation of the

DOI: https://doi.org/10.2312/zipe.1989.102.03

Earth's surface. But such information is usual insufficient to obtain data on the deformations and stresses in the crust and lithosphere.

The information of that kind is obtained as a result of repeatition of geodetic measurements after some time intervals.

In this paper we discuss only the results of measurements of the vertical displacements of the Earth's surface points.We have chosen the western part of the Russian platform as the object of our investigation. The reasons for such a choice are as follows.

The Russian platform is the vast territory of a very low seismicity of tectonic origin. It is covered by a net of repeated precise relevellings with time intervals up to 30-70 years and there are available maps of vertical displacements velocities of the Earth's surface. These values could be expectded being only slightly distored by short period movements of nontectonic origin.

For the present study the map of vertical crustal movements has been chosen compiled with regard to stability of bench-marks (Mescherikov, 1973; Magnitsky et al., 1985).

To characterize the deformation of the surface of the crust it was decided to employ the values of its mean curvatures H given by the equation:

$$H = 1/2 \ (K_1 + K_2),$$

where K_1 and K_2 are maximum and minimum curvatures in any point of the surface.

Sometimes one employs also Gaussian curvatures

$$K = \sqrt{K_1 \cdot K_2}$$

(Ekman, 1985).

DOI: https://doi.org/10.2312/zipe.1989.102.03

For the same purpose attempts have been made also to use tilts or horizontal gradients of the deformations of the surface's crust (Gzovsky, 1963). But unfortunately the relationship between the tilts of the surface and deformations and stresses in the crust is not so favourable as in the case of curvatures. It is easy to construct the model where area of maximal tilts would correspond to zero stresses.

Vertical displacements used in this work must be corrected for the influence of changes of the gravity field due the deformation of the Earth (Heck, Malzer, 1983). Unfortunately it was impossible to make these calculations due to the lack of necessery data. There were no reasons to utilize any approximate method based on any kind of hypothesis (Ekman, 1985; Heck, Malzer, 1983), especially taking into account that the effect of those corrections on curvatures is supposed to be slight.

Therefore calculations of mean curvatures were carried out without any corrections. Procedure adopted was a standard one with averaging data over squares 0.5°x1°.

Hence obtained curvatures given in Fig.1 are not of a local character and can give the picture of the distribution of regions with intensive curvatures as compared with those of low curvatures.

Nevertheless such an approach being the first step is justified as one can see comparing data in Fig.1 with those given in fig.2. The last figure shows the distribution of epicenters of tectonic earthquakes in the same region (Ananyin et al., 1973).

DOI: https://doi.org/10.2312/zipe.1989.102.03

It is easy to see visually the correlation of regions of intensive curvatures in Fig.1 and regions with clusters of epicenters in Fig.2. As an example one can see the region stretching to the north from the Azov sea, the region near the Baltic sea and also those to the east from Kiev and Ljvov.

Of course there are some discrepeances. Some places with sufficient values of curvatures in Fig.1 have no corresponding epicentral clusters in Fig.2. The reasons could be different. For example there are difficulties in obtaining information concerning earthquakes taken place long ago in areas with sparse distribution.

The results obtained in this paper are strongly supported by comparison of data in Fig.2 and curvatures of neotectonic deformations. Those calculations were also carried out by the same method with the map of neotectonics (Nikolaev, 1977), presented in Fig.3 and the similarity of data in Fig.1 and 3 is quite obvious.

The extension of the method under consideration of high seismicity regions is connected with more reliable data for recent crustal movements.

DOI: https://doi.org/10.2312/zipe.1989.102.03

REFERENCES

Ananyin I.V., Lilienberg D.A., Schukin P.K. Problems of a relationship between recent vertical movements, morfostructural pecularities of the Earth's crust and seismocity. In: Recent crustal movements, 1973, n 5 (in Russian).

Ekman M. Gaussian and mean curvatures of postglacial land uplift as expanded in surface. Spherical harmonics and the origin of earthquakes in Fennoscandia. In: Proceedings of the 5-th Internat. Symp. "Geodesy and Physics of the Earth ", part 3, Potsdam, 1985, pp.56-70.

Gzovsky M.V. Geophysical interpretation of data on modern and recent deep tectonic movements. In: Proceedengs of the Symp. " Recent crustal movements ", n 1, Moscow, 1963 (in Russian).

Heck B., Malzer H. Determination of recent crustal movements by levelling and gravity data. Tectonophysics, 1983, vol.97, pp.251-266.

Magnitsky V.A., Grachev A.F., Kalashnikova I.V., Bronguleev V.V. On the relation between recent crustal movements, the surface of the basement complex and neotectonic displacements of the East-European platform. In: Proceedings of the 5-th Internat. Symp. "Geodesy and Physics of the Earth", part 3, Potsdam, 1985, 113-124.

Mescherikov Ju.A., (Ed.). The map of recent crustal movements of the East Europe. Moscow, 1973.

Nikolaev N.I., (Ed.). The neotectonic map of the USSR and adjacent regions in a scale of 1 : 5 000 000. Moscow. 1977.

DOI: https://doi.org/10.2312/zipe.1989.102.03

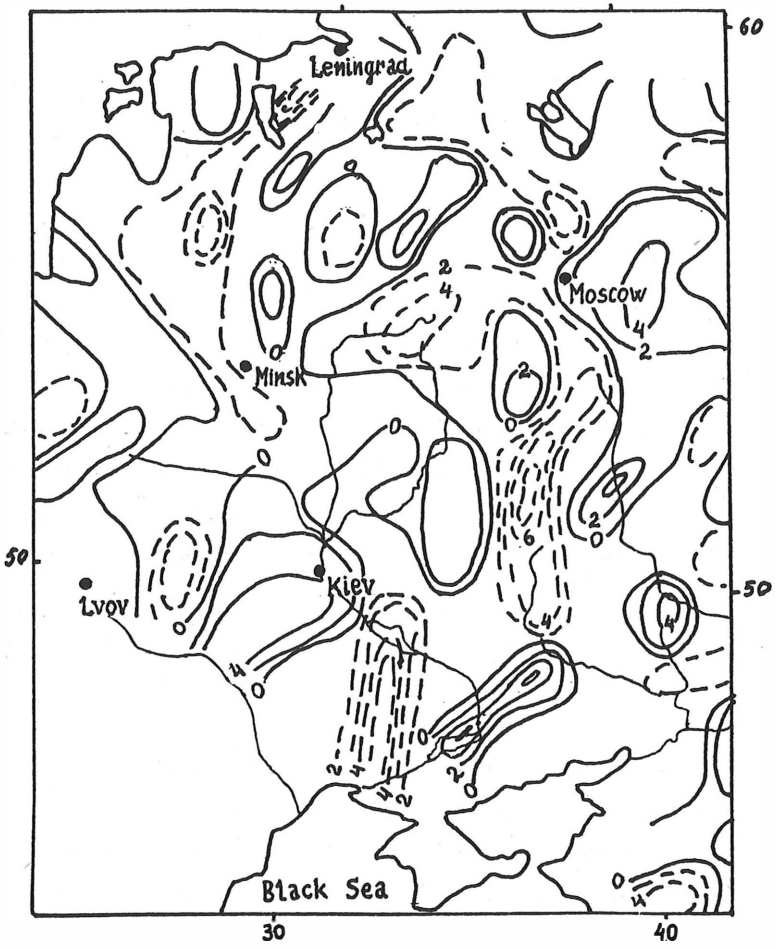

Fig.I Mean curvatures (H) of recent deformations of the crust's surface of the Russian platform. Solid lines - positive values, dash lines - negative ones (arbitrary units).

DOI: https://doi.org/10.2312/zipe.1989.102.03

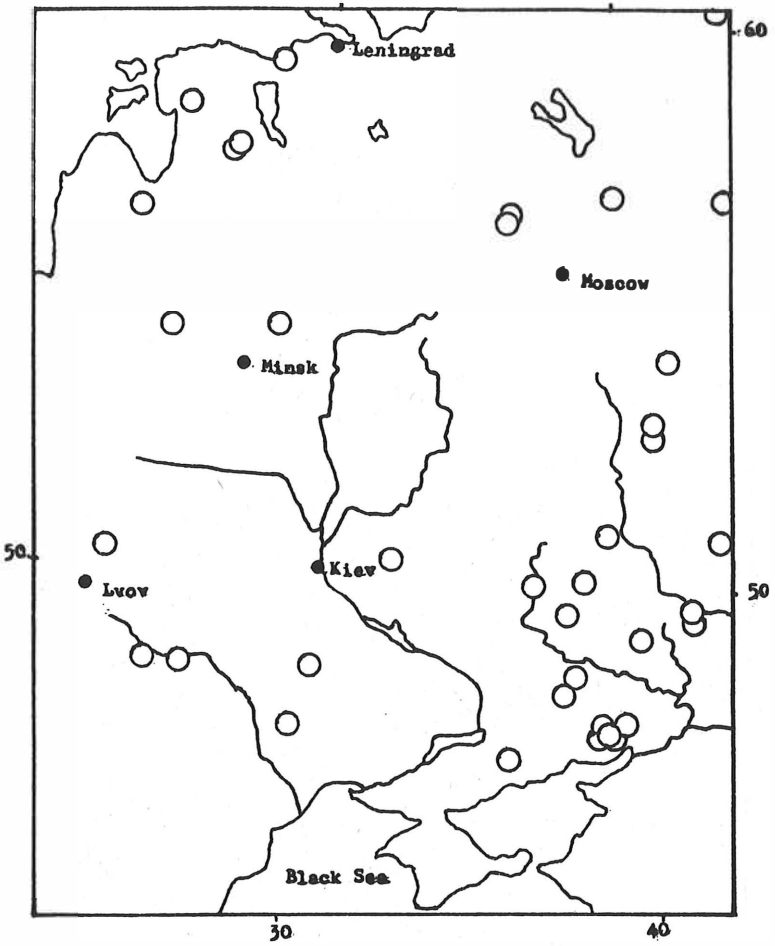

Fig.2 Location of epicenters of tectonic earthquakes on the Russian platform

DOI: https://doi.org/10.2312/zipe.1989.102.03

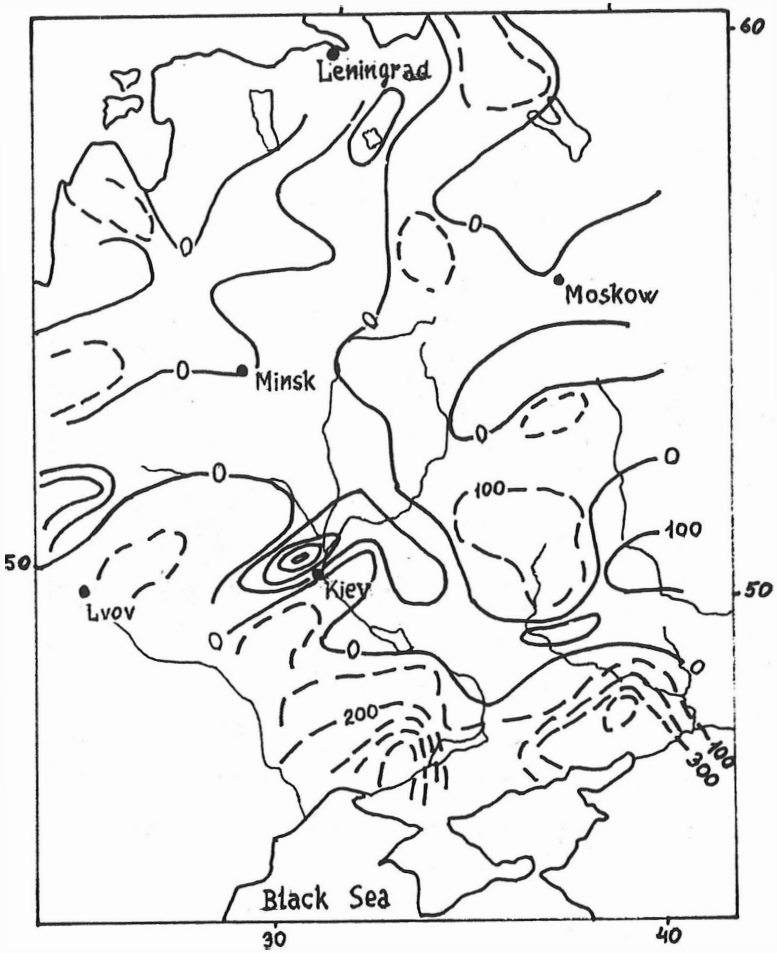

Fig.3 Mean curvatures (H) of neotectonic movements of the Russian platform. Isolines are the same as in Fig.I.

DOI: https://doi.org/10.2312/zipe.1989.102.03

Establishing a Doppler Network in the Astrogeodetic Network of the GDR

Ihde, J.; Rausch, E.

VEB Kombinat Geodäsie und Kartographie
Research Centre

Further development of basic networks with the help of precise, effective geodetic measurement techniques is an important task of geodesy. In the last decade the Doppler measurement technique using the Navy Navigation Satellite System (NNSS) has been used world-wide for this task. The aim of the Doppler network in the Astrogeodetic Network (AGN) of the GDR consists in extensively controlling this network with a technique independent from the terrestrial measurement techniques.

The Doppler network in the Astrogeodetic Network (AGN) of the GDR consists of 5 points with spacings of 150 km to 390 km. Since 1983 several observation campaigns were carried out in translocation and multilocation mode in order to determine the relations between the points. The first available evaluation results were obtained with the program SADOSA from Hungary. The obtained accuracies of the coordinates with reference to Potsdam with an average of $\pm$ 0.2 m come up to the objective of the project. The comparison of Doppler coordinates with the AGN coordinates shows after a 7-parameters similarity transformation a mean residual deviation in the coordinates of $\pm$ 0.23 m. The heights determined in the various Doppler campaigns are in better agreement than the position coordinates and show significant deviations compared to the terrestrially determined heights. In future evaluations are planned with the orbit program POTSDAM-5.

DOI: https://doi.org/10.2312/zipe.1989.102.03

1. Configuration of the Doppler Network

The AGN of the GDR has a precision of $2 \cdot 10^{-6}$ between adjoining points; the precision between points of the about 150 km apart situated terrestrial bases is $1 \cdot 10^{-6}$.
By the efficiency of NNSS Doppler measurements in the multilocation mode in connection with efficient short arc evaluation programs a precision for coordinate differences in the scope of 0.2 m to 0.5 m can be expected, which is nearly independent from distance.
To achieve an adequate precision between the Doppler network and the AGN, an appropriate distance between the Doppler points of 300 km follows.
In projecting the Doppler network, other aspects were considered too.
To create the prerequisites for further research, extensive precise astronomic observations should be available on the points. The choice of points was also influenced by the conditions for receiving Doppler signals and the local prerequisites for establishing a measurement station.
Corresponding to the situation in the AGN of the GDR the final points of former terrestrial calculation bases are suitable for that. The Doppler translocation network consists of 5 AGN points with the point Potsdam as central point.
Between the Doppler points there are distances of 150 km to 390 km (Figure 1).

2. Measurement campaigns

In the period 1983 to 1985 single relations were measured with 2 receivers respectively, which partially were integrated into superior measurement campaigns. In addition to the 2 JMR-4A receivers available in the GDR, one JMR-1A from Hungary had been used. In 1986 one campaign was carried out with a JMR-4A and two MX 1504 as well as a CMA 601 from Bulgaria in the multilocation mode. In 1987 measurements were carried out again with two JMR-4A as part of a superior campaign.

DOI: https://doi.org/10.2312/zipe.1989.102.03

On an average, measurements had been carried out on the stations for 10 days in every campaign. As a result of the 3 campaigns all relations were determined, except one relation because of instrument failure.
Table 1 gives a review of distribution of the quantity of observations in the campaigns, which were utilizable for evaluation.

3. Evaluation results

All observation campaigns were evaluated with the program system SADOSA, which was developed in Hungary.
Table 2 shows obtained precisions of the three campaigns for the coordinates of Doppler points with reference to Potsdam.
Thereby it appeared that

- the longitude is determined less accurately than the two other components,
- in 1986 point C and in 1987 points C and D are determined with comparatively lower precision (reasons unknown),
- the obtained precisions come up to the objective and that a comparison with the AGN is useful for control purposes.

The comparison with the AGN is done by a 7-parameters similarity transformation. The known 3-dimensional Cartesian transformation

$$\begin{pmatrix} X \\ Y \\ Z \end{pmatrix}^{II} = \begin{pmatrix} X \\ Y \\ Z \end{pmatrix}^{I} + \begin{pmatrix} u \\ v \\ w \end{pmatrix} + \begin{pmatrix} 0 & \omega & -\psi \\ -\omega & 0 & \varepsilon \\ \psi & -\varepsilon & 0 \end{pmatrix} \begin{pmatrix} X - X_0 \\ Y - Y_0 \\ Z - Z_0 \end{pmatrix} + m \begin{pmatrix} X - X_0 \\ Y - Y_0 \\ Z - Z_0 \end{pmatrix} \quad (1)$$

is the basis for that.
To enable a better interpretation, an ellipsoidic form was chosen:

$$\begin{pmatrix} B \\ L \\ H \end{pmatrix}^{II} = \begin{pmatrix} B \\ L \\ H \end{pmatrix}^{I} + F(\Delta a, \Delta\alpha, u, v, w, \omega, \psi, \varepsilon, m) \quad (2)$$

DOI: https://doi.org/10.2312/zipe.1989.102.03

The terrestrial ellipsoidic heights H were formed out of normal heights H_n and height anomalies ζ : $H = H_n + \zeta$. The height anomalies are the result of the astrogravimetric levelling according to Molodenskij on the territory of the GDR.
Table 3 shows the residual deviations between Doppler network and AGN of the GDR after the 7-parameters transformation. Considering an estimated precision of the AGN of $1 \cdot 10^{-6}$ in the scope of distance of the Doppler points, the precisions depicted in Table 2 are confirmed with the residual deviations. Hence follows a mean residual deviation of $\pm$ 0.23 m in the coordinates. The Doppler heights are in much better agreement between the campaigns, but they significantly deviate from the terrestrial heights. This fact suggests systematic distortions in the geodetic heights. The reasons are still under investigation.

The last column of Table 3 shows the residual deviations after a preliminary summary of the three measurement campaigns with the weighted mean. In contrast to the heights, significant deviations between the terrestrial and Doppler coordinates show only in two cases in the position coordinates. Herewith the precision of the AGN of the GDR of $1 \cdot 10^{-6}$ in the scope of distance of 150 km is confirmed.

4. Prospects

The measurement campaign of 1987 will be additionally evaluated with the orbit program POTSDAM-5. A gradual increase in precision is expected. Then the Doppler measurement technique is exhausted in its precision potential.
First results of a dynamical adjustment of the Doppler network with the AGN showed an increase in precision in the identical points of about 20 %. The test computations will be continued.

DOI: https://doi.org/10.2312/zipe.1989.102.03

In future special interest has to be devoted to the determination of precise gravimetric geoid or quasi-geoid heights respectively, to create the prerequisites for the use of still more precise satellite observations.

DOI: https://doi.org/10.2312/zipe.1989.102.03

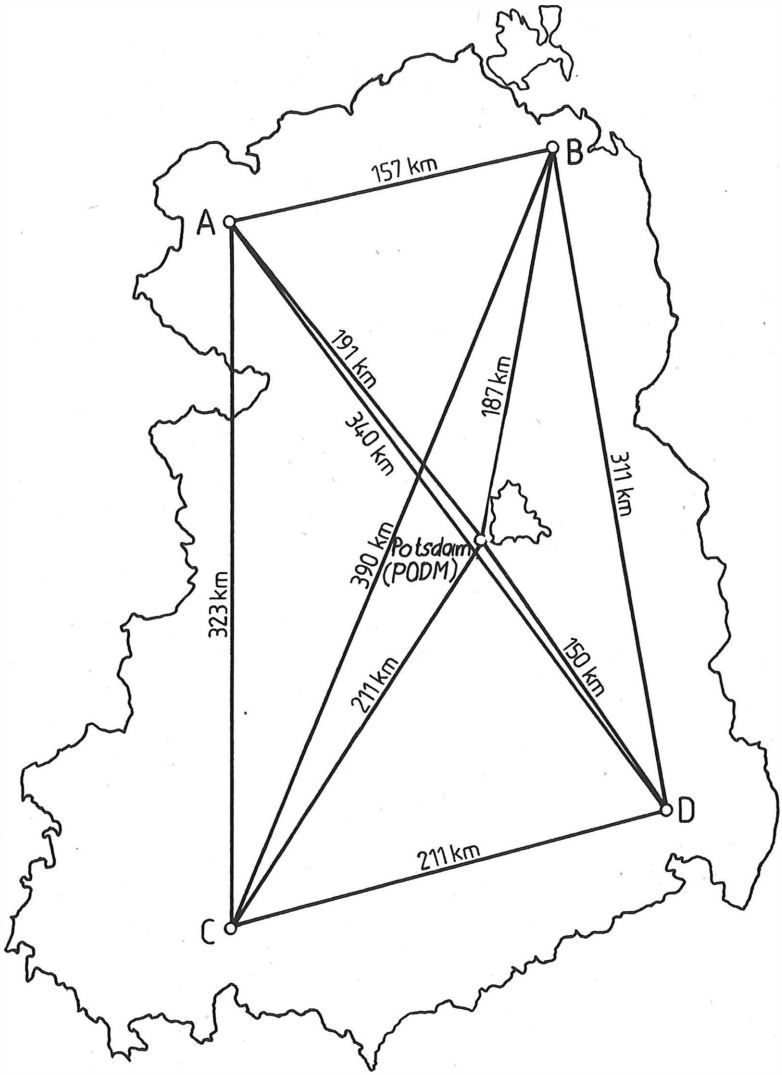

Figure 1

The Doppler Network in the Astrogeodetic Network of the GDR

DOI: https://doi.org/10.2312/zipe.1989.102.03

Table 1
Distribution of synchronous observations of the Doppler campaigns 1983-1987
(Number of passes used for positioning)

Translokation 1983 - 1985, 2 receiver, 267 passes						
station	receiver	PODM	A	B	C	D
PODM	JMR	141	28	27	42	44
A	JMR	28	83	55	-	-
B	MMR	27	55	153	-	71
C	JMR	42	-	-	42	-
D	JMR	44	-	71	-	115
Multilokation 1986, 4 receiver, 154 passes						
station	receiver	PODM	A	B	C	D
PODM	CMA	135	52	60	51	106
A	MX	52	63	30	22	49
B	JMR	60	30	68	-	60
C	JMR	51	22	-	58	34
D	MX	106	49	60	34	120
Translokation 1987, 2 receiver, 297 passes						
station	receiver	PODM	A	B	C	D
PODM	JMR	297	86	108	62	41
A	JMR	86	86	-	-	-
B	JMR	108	-	108	-	-
C	JMR	62	-	-	62	-
D	JMR	41	-	-	-	41

DOI: https://doi.org/10.2312/zipe.1989.102.03

Table 2
Precision of determination of coordinates with reference to Potsdam (in cm) as result of evaluation with the program SADOSA

campaign	number of degrees of freedom f	Coordinate error with reference to Potsdam station	s_B	s_L	s_H	s_P
1983-85		PODM	-	-	-	-
	n = 13177	A	14	22	16	31
	u = 3219	B	13	19	14	26
	f = 9958	C	14	21	16	30
		D	13	18	14	26
1986		PODM	-	-	-	-
	n = 10026	A	14	18	14	27
	u = 2265	B	15	22	15	31
	f = 7761	C	18	31	20	41
		D	10	15	11	21
1987		PODM	-	-	-	-
	n = 12612	A	13	19	14	27
	u = 3579	B	12	19	13	26
	f = 9033	C	23	35	24	48
		D	22	42	24	53

DOI: https://doi.org/10.2312/zipe.1989.102.03

Table 3
Comparison of Doppler network with the AGN of the GDR
(Residual deviations after 7-parameters transformation in cm)

	1983 - 85			1986			1987			weighted (mean)		
	v_B	v_L	v_H	v_B	v_L	v_H	v_B	v_L	v_H	v_B	v_L	v_H
PODM	-25	+ 4	+ 1	-17	70	28	-15	- 6	-17	-19± 3	17±22	2±12
A	-33	+ 9	+50	4	-29	27	- 8	5	39	-15±11	-5±12	39± 6
B	+31	+26	-51	-22	-20	-41	-13	-38	-33	1±16	-9±20	-41± 5
C	-16	-25	-38	19	-42	-29	53	-49	-25	8±19	-36± 7	-32± 4
D	+44	-10	+37	14	20	15	-20	85	36	22±15	14±19	27± 8
mean residual deviation	31	17	40	16	41	29	27	47	31	15	19	31
		31			30			36			23	

DOI: https://doi.org/10.2312/zipe.1989.102.03

INFLUENCE OF THE PERIODICAL VARIATIONS IN SUN DISTURBING POTENTIAL ON THE EARTH SEISMIC ACTIVITY

I.B.Ivanov, V.A.Karagiozov, D.P.Dimitrov
Institute of Mathematics with Comp. Center - BAS
"Acad. G.Bontchev" str. bl.8
SOFIA 1113, BULGARIA

Summary - Based on the developed mathematical model of the Sun tidal force on the Earth, the influence of the long-periodical tides in the Earth body on its shape is investigated. The strain-stress state of a dense elastic sphere (an abstract model of the Earth) subjected to periodical (with periods of one year and 26000 years) forces of tidal type has been analyzed. It is shown that the initial undisturbed spherical shape is being transformed in a pear-like one and vary with the period of the acting forces.
A statistical analysis of the distribution of the large earthquakes (with magnitudes $\geq$ 7) since 1900 till 1978 year has been done and a possible connection between the mass transport through the Equator plane with periods of one year and 26000 years and the triggering of the large earthquakes is discussed.

1. INTRODUCTION

A large number of phenomena and facts has been established in investigation of the global geological process. Some of these phenomena and facts, for example the problem of dislocations of crustal zones, nature of the appearing and developing of Earth's planetary cracks, the periodicity of the global volcano and seismic activities, attract the attention with the incompleteness and unsatisfactory explanations of the causes of their origin. In Ref. [1] a possible connection between the Earth's seismic activity and the annual change in the Sun-Earth radius vector is discussed. A large set of data for strongest earthquakes with magnitude $M \geq 7.0$ is analyzed and the periodicity in distribution of number of strong earthquakes per month is established. This variation is in accordance with the annual variations of Sun-Earth radius vector. A similar dependence concerning earthquakes with magnitude $5.0 < M < 7.0$ (Ref.[2]) and volcano eruptions for last 3447 years (Ref. [3]) are obtained. The reasonable explanation of all these global

DOI: https://doi.org/10.2312/zipe.1989.102.03

phenomena from an uniform point of view is given in Ref. [1] and Ref.[4] – Ref.[8].

It is the purpose of this article to present further theoretical results confirming the hypothesis on Sun gravity influence on Earth and more particular the influence of long-periodical Sun tidal force on Earth's shape. The statistics analysis of earthquakes time and space locations is extended in comparison with Ref.[1], including new data from various sources.

2. THE TIDAL FORCE

The Sun tidal force in any given point L of the Earth, which belongs to the main tidal meridian (MTM) is defined by the vector expression (see Fig. 1)

$$\vec{T}_L = \vec{F}_L - \vec{F}_E, \tag{1}$$

where

$$\vec{F}_L = -\frac{G \cdot M_o}{R_L^2} \cdot \frac{\vec{R}_L}{|\vec{R}_L|}, \qquad \vec{F}_E = -\frac{G \cdot M_o}{R_E^2} \cdot \frac{\vec{R}_E}{|\vec{R}_E|} \tag{2}$$

$$\vec{T}_{LL'} = \vec{T}_L - \vec{T}_{L'} = \vec{F}_L - \vec{F}_{L'}.$$

The distribution of force $T_{LL'}$ for epoch t_1=T+●, t_2=T+6500 and t_3=T+13000 years is shown in Fig.2. Time moment t_1 is associated with Perihelion Earth location on its orbit around the Sun, and t_3 with Aphelion. In Fig.2(b) the force distribution in Equinox location is drawn. At this moment t_2 the distribution of Sun tidal force is symmetric relative to Earth equator. The distribution of the force in Fig.2(a) (Perihelion) is asymmetric relative to equator – a dislocation towards South hemisphere is observed. By analogy the distribution of the force in Fig.2(c) (Aphelion) shows a certain dislocation towards North hemisphere. The values of these forces have the order of 10^{-6} [N] approximately. The asymmetry in distribution of tidal force may be explained with the obliquity of the ecliptic in respect to equator plane. The period of moving the terrestrial axis on precession cone is 26000 years approximately. So the acting forces on the Earth have periodical character (with period of 26000 years or one year) and therefore the induced stresses, strains and

DOI: https://doi.org/10.2312/zipe.1989.102.03

displacements in the Earth must have a periodical character too. The asymmetry in distribution of these forces relative to equator must reflect in asymmetry of the displacements, strains and stresses in the Earth's body. Theoretical validation of this assumption will give a good argument to the hypothesis on the periodical variations in Earth shape due to the influence of Sun tidal forces in Ref.[4], [5] and [8].

3. STRESS-STRAIN STATE OF THE DENSE ELASTIC SPHERE IN A TIDAL FORCE POTENTIAL FIELD

The abstract model of the Earth as a dense homogeneous elastic sphere in a potential field of body tidal forces is under consideration. The potential of the force W is:

$$W = -\frac{G \cdot M_D}{d} \cdot \sum_{n=2}^{\infty} \left[\frac{R^n}{d^n} \cdot P_n(\sin\delta) \cdot P_n(\sin\varphi) \right] \qquad (3)$$

The static equations of elasticity in displacements with the elastic displacement potential (Ref.[9]) Φ and potential of external forces taken into consideration are expressed as:

$$U_i = \Phi_{,i}, \quad X_i = \varrho \cdot W_{,i}, \quad i,j = 1,2,3$$

$$\mu \cdot U_{i,jj} + (\lambda+\mu) \cdot U_{j,ji} + \varrho \cdot W_{,i} = 0 \qquad (4)$$

$$i,j = 1,2,3$$

where U – displacements, X – external forces, comma signify differentiation in respect to appropriate coordinate.

In assumption of axisymmetric in relation to θ coordinate the stress-strain state of the sphere is characterized by the following components:

displacements – U_R, U_φ

strains – ε_{RR}, $\varepsilon_{\varphi\varphi}$, $\varepsilon_{\theta\theta}$, $\varepsilon_{R\varphi}$

stresses – σ_{RR}, $\sigma_{\varphi\varphi}$, $\sigma_{\theta\theta}$, $\sigma_{R\varphi}$

The problem of defining the stress-strain state of the Earth (sphere) is reduced to the solving of non-homogeneous equation:

$$\nabla^2\Phi = -\frac{\varrho \cdot W}{\lambda+2 \cdot \mu}$$

$$\nabla^2 = \frac{\partial^2}{\partial R^2} + \frac{2}{R} \cdot \frac{\partial}{\partial R} + \frac{1}{R^2} \cdot \frac{\partial^2}{\partial \varphi^2} - \mathrm{tg}\varphi \cdot \frac{1}{R^2} \cdot \frac{\partial}{\partial \varphi} \qquad (5)$$

DOI: https://doi.org/10.2312/zipe.1989.102.03

with conditions on the boundary $R = R_0$:

$$\sigma_{RR} = 0, \qquad \sigma_{R\varphi} = 0 \quad \Big|_{R = R_0} \tag{6}$$

which are equivalent to a free of radial σ_{RR} and tangential $\sigma_{R\varphi}$ stresses Earth surface.

The partial solution (function Φ) of the non-homogeneous equation (5)-(6) may be expressed in the form

$$\Phi = \sum_{n=2}^{\infty} \left[B_n \cdot R^{n+2} \cdot P_n(\sin\varphi) \right] \tag{7}$$

and the displacement, strain and stress components from the partial solution, denoted by symbol ^ become

$$\hat{U}_R^{(n)} = B_n' \frac{R^{n+1}}{d^{n+1}}(n+2)P_n(\sin\varphi), \quad \hat{U}_\varphi^{(n)} = B_n' \frac{R^{n+1}}{d^{n+1}} \cos\varphi P_n'(\sin\varphi)$$

$$\hat{\varepsilon}_{RR}^{(n)} = B_n' \frac{1}{d} \cdot \frac{R^n}{d^n}(n+2)(n+1)P_n(\sin\varphi)$$

$$\hat{\varepsilon}_{\varphi\varphi}^{(n)} = B_n' \frac{1}{d} \cdot \frac{R^n}{d^n}\left[(n+2)P_n + \cos^2\varphi P_n'' - \sin\varphi P_n'\right]$$

$$\hat{\varepsilon}_{\theta\theta}^{(n)} = B_n' \frac{1}{d} \cdot \frac{R^n}{d^n}\left[(n+2)P_n - \sin\varphi P_n'\right] \tag{8}$$

$$\hat{\varepsilon}_{R\varphi}^{(n)} = B_n' \frac{1}{d} \cdot \frac{R^n}{d^n}(n+1)\cos\varphi P_n'(\sin\varphi), \quad \hat{e}^{(n)} = B_n' \frac{1}{d} \cdot \frac{R^n}{d^n}(4n+6)P_n'(\sin\varphi)$$

$$\hat{\varepsilon}_{\varphi\varphi}^{(n)} = \frac{1}{1-\nu} \cdot \frac{\bar{B}_n}{d} \cdot \frac{R^n}{d^n}\left[(2\nu n+n+2\nu+2)P_n + (1-2\nu)(\cos^2\varphi P_n'' - \sin\varphi P_n')\right]$$

$$\hat{\varepsilon}_{\varphi\varphi}^{(n)} = \frac{(1-2\nu)n^2+(3-2\nu)n+2(1+\nu)}{1-\nu} \cdot \frac{\bar{B}_n}{d} \cdot \frac{R^n}{d^n} \cdot P_n$$

$$\hat{\varepsilon}_{\theta\theta}^{(n)} = \frac{1}{1-\nu} \cdot \frac{\bar{B}_n}{d} \cdot \frac{R^n}{d^n}\left[(2\nu n+n+2\nu+2)P_n + (1-2\nu)\sin\varphi P_n'\right]$$

$$\hat{\varepsilon}_{R\theta}^{(n)} = \frac{1-2\nu}{1-\nu} \cdot \frac{\bar{B}_n}{d} \cdot \frac{R^n}{d^n} \cdot (n+1)\cos\varphi P_n'$$

where

$$\bar{B}_n = \rho G M_0 \cdot \frac{1}{4n+6} \cdot P_n(\sin\delta) \qquad \left[\frac{N}{m}\right]$$

$$B_n' = \frac{\rho G M_0}{\lambda+2\mu} \cdot \frac{1}{4n+6} \cdot P_n(\sin\delta) \qquad [\,m\,]$$

$$\lambda+2\mu = \frac{E(1-\nu)}{(1+\nu)(1-2\nu)}, \qquad \mu = \frac{E}{2(1+\nu)}$$

DOI: https://doi.org/10.2312/zipe.1989.102.03

The general solution [S] of the homogeneous equation is expressed according to Ref.[10] and equation (5)–(6):

$$[\,S\,] = \sum_{n=2}^{\infty} \left[\, [\,C_n^*\,] + [\,D_n^*\,] \,\right] \tag{9}$$

where

C_n^* :

$$\left[\begin{array}{l}
U_R^{1(n)} = C_n\, n\, R^{n-1}\, P_n(\sin\varphi) \\
U_\varphi^{1(n)} = C_n \cos\varphi\, R^{n-1}\, P_n'(\sin\varphi) \\
\varepsilon_{RR}^{1(n)} = C_n \cos\varphi\, R^{n-2}\, P_n(\sin\varphi) \\
\varepsilon_{\varphi\varphi}^{1(n)} = -\,C_n\, R^{n-2}\,\left[\, n^2\, P_n(\sin\varphi) - \sin\varphi\, P_n'(\sin\varphi)\,\right] \\
\varepsilon_{\theta\theta}^{1(n)} = \quad C_n\, R^{n-2}\,\left[\, n\;\; P_n(\sin\varphi) - \sin\varphi\, P_n'(\sin\varphi)\,\right] \\
\varepsilon_{R\varphi}^{1(n)} = C_n\,(n-1)\cos\varphi\, R^{n-2}\, P_n(\sin\varphi), \qquad e^{1(n)} = 0 \\
\sigma_{RR}^{1(n)} = 2\mu\, \varepsilon_{RR}, \qquad \sigma_{\varphi\varphi}^{1(n)} = 2\mu\, \varepsilon_{\varphi\varphi} \\
\sigma_{\theta\theta}^{1(n)} = 2\mu\, \varepsilon_{\theta\theta} \qquad \sigma_{R\varphi}^{1(n)} = 2\mu\, \varepsilon_{R\varphi}
\end{array}\right. \tag{10a}$$

D_n^* :

$$\left[\begin{array}{l}
U_R^{2(n)} = D_n\,(n+1)\,(n-2+4\nu)\, R^{n+1}\, P_n(\sin\varphi) \\
U_\varphi^{2(n)} = D_n\,(n+5-4\nu)\, R^{n+1}\cos\varphi\, P_n(\sin\varphi) \\
\varepsilon_{RR}^{2(n)} = D_n\,(n+1)^2\,(n-2+4\nu)\, R^n\, P_n(\sin\varphi) \\
\varepsilon_{\varphi\varphi}^{2(n)} = -\,D_n\, R^n\left[(n+1)(n^2+4n-4\nu+2-4\nu n)\, P_n - \right. \\
\qquad\qquad \left. -\,(n+5-4\nu)\,\sin\varphi\, P_n'\,\right] \\
\varepsilon_{\theta\theta}^{2(n)} = D_n\, R^n\,\left[(n+1)(n-2+4\nu)\, P_n - (n+5-4\nu)\sin\varphi\, P_n'\,\right] \\
\varepsilon_{R\varphi}^{2(n)} = D_n\, R^n\,(n^2+2n-1+2\nu)\cos\varphi\, P_n' \\
e^{2(n)} = D_n\, R^n\, 2\,(2\nu-1)(2n+3)(n+1)\, P_n \\
\sigma_{RR}^{2(n)} = 2\mu\, D_n\, R^n\,(n+1)\,(n^2-n-2-2\nu)\, P_n \\
\sigma_{\varphi\varphi}^{2(n)} = -2\mu D_n R^n\left[(n+1)(n^2+4n+2+2\nu)P_n - (n+5-4\nu)\sin\varphi P_n'\right] \\
\sigma_{\theta\theta}^{2(n)} = 2\mu D_n R^n\left[(n+1)(n-2\nu-2-4n\nu)P_n - (n+5-4\nu)\sin\varphi P_n'\right] \\
\sigma_{R\varphi}^{2(n)} = 2\mu D_n R^n\,(n^2+2n-1+2\nu)\cos\varphi\, P_n'
\end{array}\right. \tag{10b}$$

DOI: https://doi.org/10.2312/zipe.1989.102.03

Two sets of arbitrary constants C_n (10a) and D_n (10b) we can define by satisfaction of the boundary conditions

$$\overset{\wedge(n)}{\sigma_{RR}} + \overset{1(n)}{\sigma_{RR}} + \overset{2(n)}{\sigma_{RR}} = 0$$

$$\overset{\wedge(n)}{\sigma_{R\varphi}} + \overset{1(n)}{\sigma_{R\varphi}} + \overset{2(n)}{\sigma_{R\varphi}} = 0 , \qquad R = R_0 .$$

The obtained partial and general solutions give the possibility to define the stress–strain state in an arbitrary point on the Earth and inside it.

Time dependence is defined by the expressions

$$\sin\delta = \cos v \cdot \sin\varepsilon, \qquad v = 2\pi t$$

$$\frac{c}{d} = \frac{1 + e\cdot\cos\bar{v}}{1 - e^2}, \qquad \bar{v} = (2\pi + \frac{\pi}{13000})t \qquad (11)$$

where t has dimension of the year.

4. CONCLUSIONS

The displacements of MTM points due to third mode of Legendre series (n=3) for epoch t_1=T+0, t_2=T+6500 and t_3=T+13000 years are shown in Fig.3(a)–3(c). The intermediate state (Fig.3(b)) corresponds to Earth location in Equinox and the smallest deviations from the initial spheroidal form are observed. Comparing Fig.3(a)–3(c) with Fig.2(a)–2(c) the correspondence of both distributions (this of tidal force and displacement distribution) is obvious. So the asymmetry in force distribution relative to equator plane reflects in asymmetry of the displacements and leads to pear–like variations of the Earth figure. Similarly, the distributions of some other stress–strain characteristics – normal stresses $\sigma_{\varphi\varphi}$ and $\sigma_{\theta\theta}$ shown in Fig.4.1 and Fig.4.2, corroborate the hypothesis on the periodical variations in Earth shape due to the influence of Sun tidal forces in Ref.[4].

The distribution of strong earthquakes with various depth for the period from 1900 till 1978 year is shown in Fig.5.1 and in Fig.5.2 for the shallow shocks. The earthquake data set consist of 1248 records with space and time locations of the registered earthquakes. The number of earthquakes in North hemisphere is 687 while in South hemisphere it is 561, i.e. the exceeding of North hemisphere locations in respect to

DOI: https://doi.org/10.2312/zipe.1989.102.03

the South one is more than 10 percents the total number of earthquakes.

The approach of interpreting the periodicity in earthquake appearance as an element of the global geological process with the influence of Sun gravity field on Earth is of principle importance in view of its unity.

NOTATION

G	gravity constant
$M_\odot$	Sun mass
R_L, R_E	radius vectors Sun–points L and E (Fig.1)
d	distance between Sun arbitrary Earth point
t	time
n	degree of Legendre polynomial
P_n	Legendre polynomial
Φ	elastic displacement potential, see Ref.[9]
δ	angel defined in Fig.1
λ, μ	Lame coefficients
R, φ, θ	spherical coordinates
φ	latitude
θ	longitude
ϱ	density of material
$R_\odot$	mean Earth radius
γ	Poisson's coefficient
E	Young's modulus
e	terrestrial eccentric
v	defined in equation (11)
ε	angel of precession

REFERENCES

[1]. I.B. Ivanov, L.Christoskov, A Possible Connection between the Earth's Seismic Activity and the Annual Change in the Sun–Earth Radius Vector, Compt. rend. Acad. bulg. Sci., 20, 1967, № 5.

[2]. P.N. Kropotkin, A.E. Ljustih, Sezonnaja perioditchnost zemletrjasenii i princip Njutona–Maha, DAN SSSR, 1974, tom 217, № 5 (in Russian).

[3]. S.V. Belov, O perioditchnosti sowremennogo i drevnego vulkanizma Zemli, DAN SSSR, 1986, tom 291, № 3 (in Russian).

[4]. I.B.Ivanov, Effect of the Sun's disturbing potential on the Earth, Comptes rendus de l'Academie bulgare des Sciences, 31, 1978, №12.

[5]. I.B.Ivanov, On the Earth crustal deformations due to the Sun's tidal force, Comptes rendus de l'Academie bulgare des Sciences,33, 1980, №12.,

DOI: https://doi.org/10.2312/zipe.1989.102.03

[6]. I.B.Ivanov, Effect of solar tides on seasonal variations in Earth's rotation, Comptes rendus de l'Academie bulgare des Sciences,37, 1984, №10.

[7]. I.B.Ivanov, Delay in the Earth's rotation velocity, Comptes rendus de l'Academie bulgare des Sciences, 38, 1985, №1.

[8]. I.B.Ivanov, The Largest and the Longest Tide of the Earth, Bulgarian Geophysical Journal, vol. XII, № 3, 1986 (in Russian).

[9]. Lame G., Lesons sur la theorie mathematique de l'elasticite des corps solides, Mallet-Bachelier, Paris, 1852.

[10]. В.Новацкий, Теория упругости, "Мир", Москва, 1975.

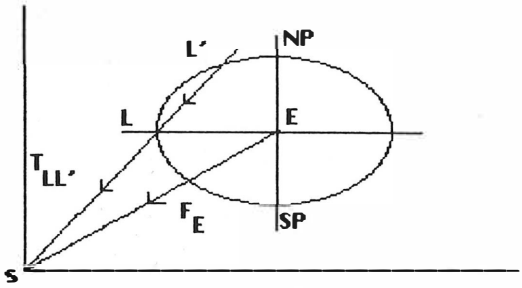

Fig. 1

DOI: https://doi.org/10.2312/zipe.1989.102.03

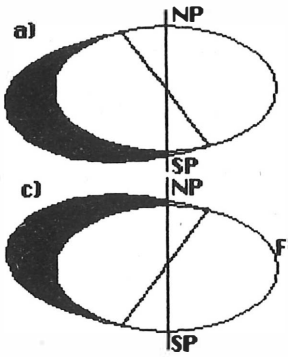

Fig.2. Radial component of Sun tidal force:
a) — t=T+0 year
b) — t=T+6500 (0.25) years
c) — t=T+13000 (0.5) years

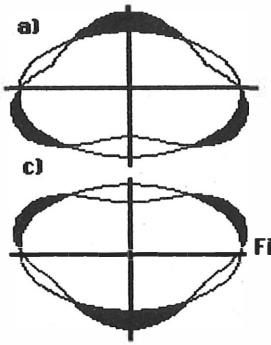

Fig.3. Deviations from Earth's shape:
a) — t=T+0 year
b) — t=T+6500 (0.25) years
c) — t=T+13000 (0.5) years

DOI: https://doi.org/10.2312/zipe.1989.102.03

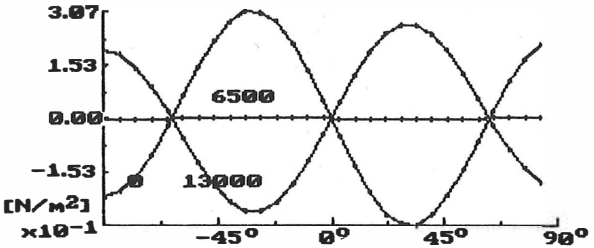

Fig.4.1 Sigmall – stress along meridium. Mode = 3.
Epoch: t=T+0, 6500, 13000 years

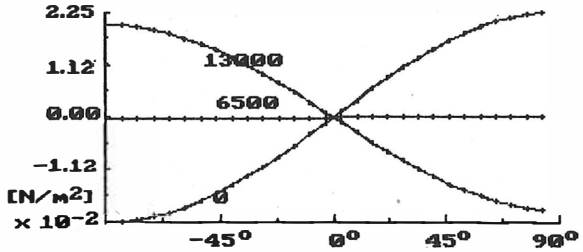

Fig.4.2 Sigmaff – stress along meridium. Mode=3.
Epoch: t=T+0, 6500, 13000 years

DOI: https://doi.org/10.2312/zipe.1989.102.03

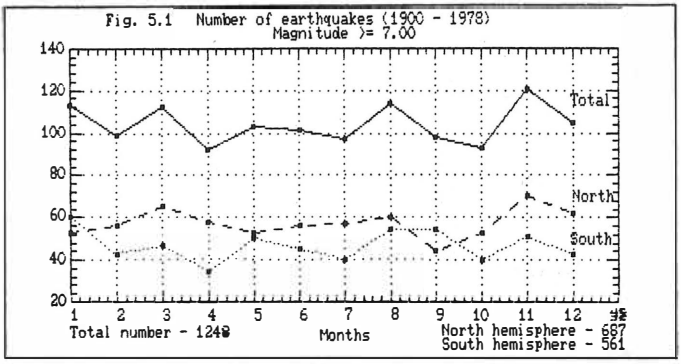

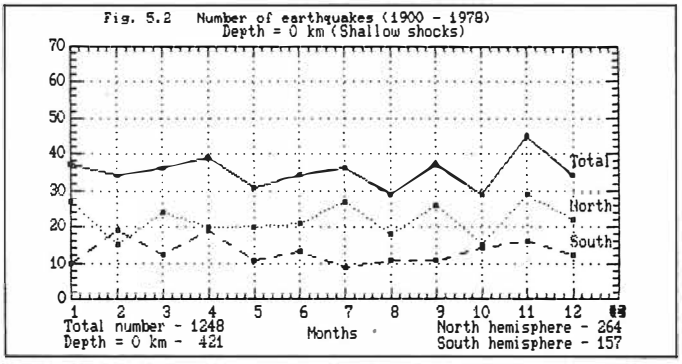

DOI: https://doi.org/10.2312/zipe.1989.102.03

INVESTIGATION OF RECENT SURFACE MOVEMENTS IN THE COUNTRY OF HUNGARY AND IN THE CARPATHO-BALKAN REGION

I. Joó Dr. Sc.

/: College for Surveying and County-planning
of the Unversity of Forestry and Timber Industry
H-8000 Székesfehérvár, Pirosalma u. 1-3. Hungary :/

SUMMARY

Intensive investigation of recent vertical movements is going on in the country of Hungary and in the Carpatho-Balkan Region (CBR). The newer map on the recent vertical movements in CBR was completed in 1985 and demonstrated at the IAG symposium held in Budapest. The map serves well not for only the complex investigation of the earth's crust, but for determining places of special technical objects. The aim of the newer investigations is to gain more complex informations from the repeated precise levellings in the CBR. In this investigation the horizontal gradients of vertical velocities along the lines are derived and supplied in a map completed with detailed geologic and seizmic information. The gradient maps of CBR are to be completed by 1990 and they are to be published in Hungary. Moreover geodynamical investigations have started at various places in Hungary: at the trench of Mór, at the area of the earthquake of 1985 (Berhida-Peremarton). In these local investigations both the vertical and the vertical and horizontal impacts of the movements are studied. The paper gives information on the aim of these investigations with their present stage and probable results.

DOI: https://doi.org/10.2312/zipe.1989.102.03

INTRODUCTION

For long decades the vertical movements of the Earth's crust has been investigated. These examinations have become very intensive since the second half of the sixties. The geophisical co-operation organization of. Academies of Sciences of the socialist countries (KAPG) and the geodetic services took up to their programmes the investigation of recent crustal movements at that time.

As a result of collective and well co-ordinated work, the first map containing the vertical crustal movements in Eastern-Europe was compiled in 1971 [1, 2] . Later more detailed investigations started in the Carpatho--Balkan Region (CBR) and a map on the vertical crustal movements in the CBR was compiled with Hungarian co-ordination [3] . This map was introduced at Canberra in 1979 [4] .

Investigation of vertical movements contiuned both for Eastern-Europe and for the CBR employing the data obtained from newer precise levellings on the one hand, and many geologic and seizmologic informations on the other. As a result of the work carried out in this second stage, an improved map on the vertical movements in the CBR was compiled [5, 6] and it was introduced at an IAG Symposium held at Budapest in 1985.

In a short time an improved map on crustal movements in Easter-Europe was compiled, first at a scale of 1:10 000 000, later at a scale of 1:2 500 000 [7].

RECENT STUDYING OF THE CRUSTAL MOVEMENTS

The repeated investigations of the vertical movements of the Earth's crust namely the surface of the Earth, carried out so far show that need arose for applying other methods in addition to deriving the vertical velocities for more detailed understanding the tendencies of movements.

DOI: https://doi.org/10.2312/zipe.1989.102.03

Therefore deriving the horizontal gradients of the vertical velocities was taken up to the program. Co-ordination of this work within the CBR is carried out by the Hungarian Geodetic Service in the future too, while the Geodetic Service of the Soviet Union carriers out the co-ordination of work in Eastern-Europe.

As a first stage the Research Institute of the Bohemian Geodetic Service (P.Vyskocil) derived the horizontal gradients, employing the velocity data of the available map of crustal movements. An advantage of this method is that it yields the gradients in areal sense, on the other hand it did not employ newer, more ample informations than those ones on which the original map of movements was based.

All those institutions who were active in compiling the original map of movement, take part in the detailed study of gradients of the vertical velocities [10].

A great advantage of the method of the investigation is that the total information content of the data of the geodetic measurements can be derived for the lines of investigation as the horizontal gradient elements are derived for every levelling section. Geologic and seizmologic informations are added and a system of horizontal gradients along the lines comes into existence. (On the method our investigation there will a paper be delivered at the poster session [12].

In accordance with the program of CBR investigations, the countries participating hand over the national materials to the co-ordinating country at the end of 1988. For this reason the Hungarian Geodetic Service has already sent the guiding principle of deriving and descripting the gradients on the one hand, and the cartographic base of the future gradient map at a scale of 1:1 000 000, on the other hand.

DOI: https://doi.org/10.2312/zipe.1989.102.03

In 1989 the national materials will be checked up and preparatory works will be made for publishing the CBR map. According to the plans of the Hungarian Geodetic Service, the map on horizontal gradients will be published in 1990. In accordance with the standpoint of the co-operation of the geodetic services of socialist countries, a version of the horizontal gradient map made by the Chechoslovakian Geodetic Service, will be printed in 1990, too.

RECENT STUDIES ON VERTICAL MOVEMENTS IN HUNGARY

Following institutions take part in the works in Hungary. Hungarian Institute of Geodesy and Remote Sensing (Budapest), College for Surveying and County-planning of the University for Forestry and Timber Industry (Székesfehérvár). Investigations are made at special fields by the following institutions: Geodetic and Geophysical Research Institute of the Academy of Sciences of Hungary (Sopron), Department of Geodesy of Technical University of Budapest and the Military Geodetic Service.

The main fields of the works in Hungary are as follows:

- deriving the gradients along the line and co-ordinating the investigations on the gradients in CBR [8, 9],
- methodological problems of deriving the gradients and their representation in maps,
- detailed investigations of important areas by means of new measurements.

Among the Hungarian investigation areas the following ones could be mentioned separately:

a.) Geodynamic investigations at Mór and its surroundings. The investigations have in view the examination both the vertical and horizontal movements. The Hungarian Geodetic Service assisted in establishing the works with constructing measuring towers of reinforced concrete at he fundamental points of investigation. So far the following works has been carried out:

DOI: https://doi.org/10.2312/zipe.1989.102.03

- a standardization base line of high accuracy was completed, measured with MEKOMETER three times (lenght 1536 m). The reliability is $\pm$0.3 mm for half of the lenght and $\pm$0.8 mm for the total lenght, respectively.
- A micro-net was developed for Inota-Csór fault line. It was measured two time (by means of precise measurement of directions and distance measurement, respectively). The average distance is 400 m, $m_i = \pm 0.4''$ and $m_{distance} = \pm 1.5$ mm.

  Till the end of 1991 the trench of Mór will be tranversally intersected by means of precise levelling, employing the special aid of the Hungarian Academy of Sciences. In this way recent tendencies of the movements can be examined by means of the newer measurements. We also insist on the earliest precise measuring the distances among the six fundamental points of the investigation net at Mór and surroundings.

b.) Around Berhida-Peremarton as a prosecuton of impacts of the arthquake in 1985 the precise levellings are repeated and horizontal investigations are in preparation (also with the aid of MTA) [11] .

c.) The Geodetic and Geophysical Research Institute of the Hungarian Academy of Sciences (Sopron) carries out investigation on movements at the area of the Paks Atomic Power Plants.

d.) The Institute of Geodesy of the Technical University of Budapest establishes an investigation network close to Budapest (at the southern part of the Budai-mountain). It is developed and measured countinously.

e.) The Military Geodetic Service gives valuable assistence in developing the presentation of gradient values on maps.

DOI: https://doi.org/10.2312/zipe.1989.102.03

FUTURE PROSPECTS

Deriving and presenting in maps the horizontal gradients of vertical velocities will assist in better cognition and understanding of processes taking place on the surface of the Earth and in the crust.

As the derivation of horizontal gradients along the lines employs all the informations given by the repeated precise levellings, it is obvious that the maps containing the vertical velocities in CBR and Eastern-Europe should be refined employing the newer informations collected in investigations on gradients.

It sum it can be stated that more and more intensive investigations are in progress in the area of the CBR and Hungary or they are in preparation. These investigations will make the simultaneous and synchronised use of geodetic, geologic and seizmologic informations possible.

DOI: https://doi.org/10.2312/zipe.1989.102.03

REFERENCES

1. Ju.A. Mescherikov et al.: Map of Recent Vertical Crustal Movements of Eastern Europe, scale 1: 2 500 000, Moscow, 1973.

2. Ju.D. Boulanger et al.: Summary Map of the Recent Vertical Crustal Movements for Eastern Europe; XVth. Gen. Assembly of IUGG, Moscow, 1971.

3. I. Joó et al.: Map of Recent Vertical Crustal Movements in the Carpatho-Balkan region, scale 1:1 000 000, Budapest, 1979.

4. I. Joó et al.: Recent Vertical Crustal Movements of the Carpatho-Balkan Region. (XVIIth. Gen. Assambly of IUGG Symp. No.9.), Canberra 2-15 December 1979.

5. I. Joó et al.: Map of Recent Vertical Movements in the Carpatho-Balkan Region, scale 1:1 000 000 (Budapest, 1985.)

6. I. Joó et al.: Explanatory text to the Map of Recent Vertical Movements in the Carpatho-Balkan Region Budapest, 1985.

7. D. Arabadzijski-Ja. Vanko-T.Wyrzykowskij-P.Vyskocil-I. Joó-I.N. Mescerskij-M.Mihaila-M.Madenowski-J.Steinberg: Map of Recent Vertical Movements of Bulgaria, Hungary, GDR, Poland, Romania, USSR, Czechoslovakia, scale 1: 2 500 000, Moscow, 1986.

8. I.Joó-A.Czobor-M.Gazsó-Zs.Németh: The Investigation of Recent Crustal Movements in the Carpatho-Balkan Region and the Co-ordination of the Works(Scientific Report of the College for Surveying and County Planning, Székesfehérévár, 1986. p. 144)

9. I.Joó-A.Czobor-M.Gazsó-Zs.Németh: The Investigation of Recent Crustal Movements in the Carpatho-Balkan Region and the Co-ordination of the Works (Scientific Report of the College for Surveying and County Planning, Székesfehérvár, 1987. p. 276)

DOI: https://doi.org/10.2312/zipe.1989.102.03

10. I.Joó: Basic Results of the Studies on RCM in the Carpatho-Balkan Region (CBR) and in the other Parts of Europe (Tallin, 8-11 Sept. 1986)

11. I.Joó: Contribution to the Study of Interaction of Slow Deformations and Earthquakes (XIXth Gen, Ass. of IUGG, Interdisciplinary Symp. on Slow Deformation and Transmission of Stress im the Earth, Vancouver, Aug. 9-22, 1987)

12. I.Joó - A.Czobor - M.Gazsó - Zs.Németh: RCM Investigation Possibilities by the Horizontal Velocity-Gradients along the Levelling Lines (Symp. Geodesy and Physics of the Earth, Potsdam, Aug. 22-27, 1988)

13. Sz.Csepregi - Gy.Busics: Planning a Network for Examining Crustal Movements near Town Székesfehérvár (Tallin, Sept. 8-11, 1986)

DOI: https://doi.org/10.2312/zipe.1989.102.03

RCM Investigation by horizontal velocity-gradients

I.Joo, Dr.Sc (1)
A.Czobor,Zs.Nemeth,M.Gazso (2)

Summary

At the present state of the investigations a new possibility has been applied. In the previous maps of RCM in the Carpatho-Balkan Region (CBR) the adjusted absolute velocity values have been used to construct isolines. These maps are strongly effected by assumtion of linearity between the fundamental benchmarks. More detailed evaluation can be carried out by horizontal gradients of the raw velocity values. The regression lines together with morphotectonic information provide new possibilities for the interpretation. The paper discusses the present work in detail.

1. Introduction

The basis for the investigation carried out in CBR and also for the maps of movements produced from them is a system of poligonials constructed from national levelling networks. The hights of the junction points have been found from repeated levellings by common adjustment for a selected epoch and the absolute velocities of the points were also determined in units of mm/year.

It has been supposed in each case that the change between the junction points is linear. This supposition is incorporated into the isoline velocity maps [1979,1985; see Fig.1 too].

The detailed information of the sections between the junctions have been smoothed by the integration and the smoothing has been further increased by the construction of the isolines.

The data enable, however, much more detailed investigations, too. The aim of a recent study in CBR is to get maximum information from the available material.

(1), (2) see page 132

DOI: https://doi.org/10.2312/zipe.1989.102.03

2. Horizontal gradients of vertical movements

Repeated levellings enable us to determine the gradients of vertical movements , i.e. the derivatives of the functions of relative velocity. Theoretical considerations about this problem were published in [2,3] , where an example is given too, for the construction of the gradient maps.
The gradients are computed from the height differences of the section, $\Delta H_1, \Delta H_2$ in the epochs T_1 and T_2 :

$$\text{grad } V = \frac{\Sigma \frac{\delta H}{\Delta T}}{L_i} \cdot \rho ["/\text{year}]$$

where $\delta H = \Delta H_1 - \Delta H_2$. Summation is made from a junction to the next one. Thurm [2] determined from the law of error propagation the confidence range which can be used for the qualification of these gradients. According to him, the gradient is significant if

$$| \text{grad } V | > 2.0 \times m_{\text{grad } V} \cdot$$

and strongly significant if

$$| \text{grad } V | > 2.6 \times m_{\text{grad } V} \cdot$$

The gradients themselves are insufficient for an analysis of the movements. Further parameters have to be introduced.

---

(1) College for Surveying and County-planning
of the University of Forestry and Timber Industry
(2) Satellite Geodetic Observatory, Penc

DOI: https://doi.org/10.2312/zipe.1989.102.03

3. Local field survey

In the first step ,the detailed data system of CBR 1I. has been put into a data base [Fig.2.]

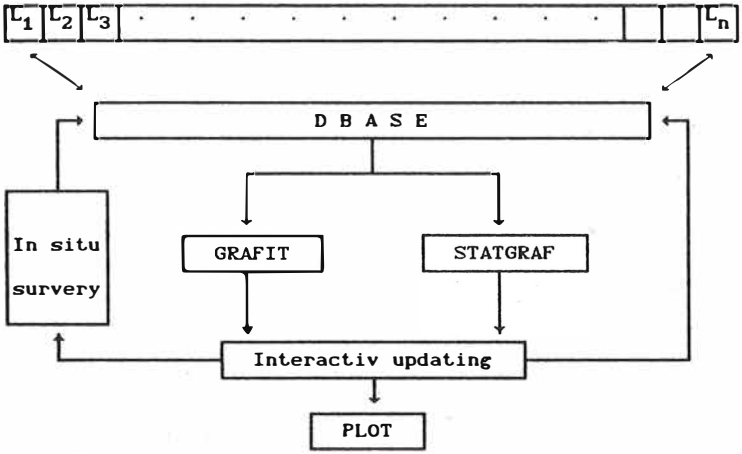

Fig. 2.

A curve as that shown in Fig.3 has been drawn for all lines. The graph contains the longitudinal section of the line, the integrated curve of the raw relative velocities of the sections [Σdv] and the curve of the horizontal gradients deduced from these velocities [grad Σdv]. The prepared material has been supplemented by an in situ survey.

The benchmarks have been photographed and the character of the movements at the points has been tentatively determined .The immediate vicinity of the benchmarks has been described morphologically and tectonically.

The character of the visible surface and the geological structure have been described for each section. Geological, tectonic and morphologic information is summarizingly

DOI: https://doi.org/10.2312/zipe.1989.102.03

Fig. 3.

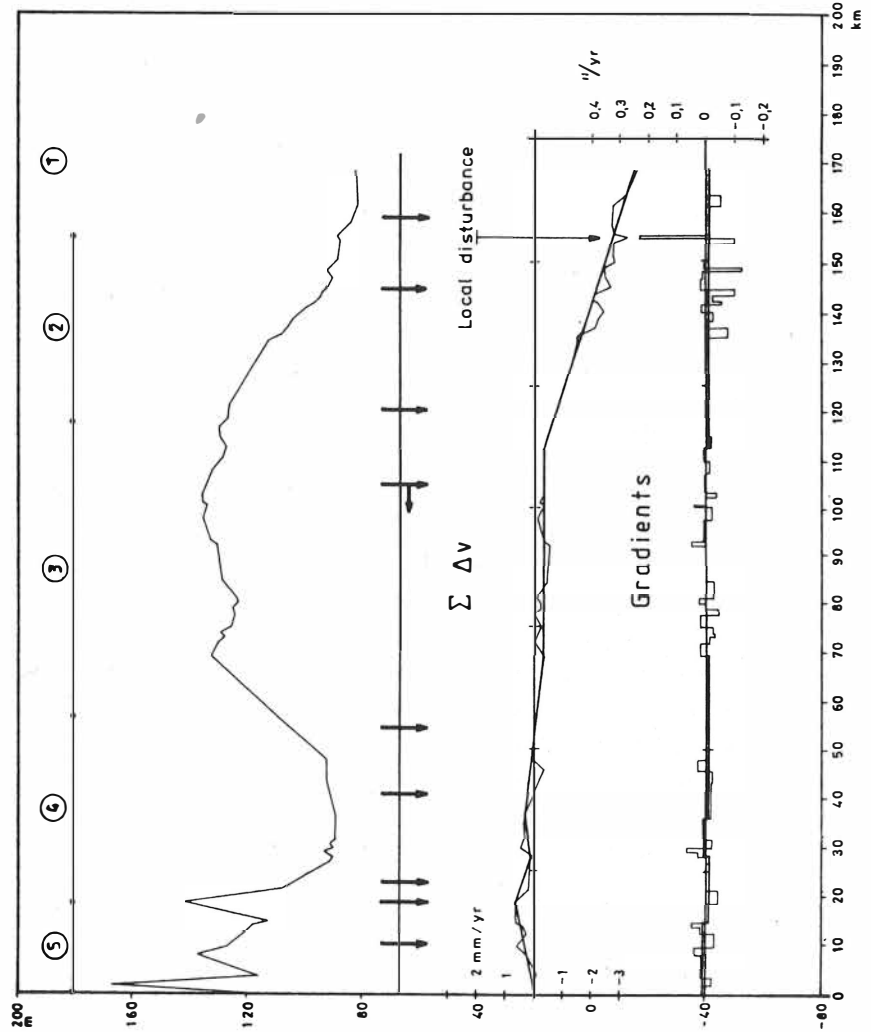

DOI: https://doi.org/10.2312/zipe.1989.102.03

identified with the points within the section [Fig.4].

4. Strategy of the evaluation

Local anomalies in the raw data are filtered out during the in situ survey.

Gradient curves are generalised:

a. Useing mathematical regression,

b. based on morphotectonic characterization.

The generalized values contain significantly more information then gradients for single points as they show the deformation trends free of measurement noises. Discontinuities of the gradient curves indicating differences in the vertical movements between certain points hint at crossings of the tectonic rupture zones at these sites.

In case of lines where the movements change continuously but are of changing sign, the origin of the movements can be determined useing morphologic parameters. These changes may be of a technogene origin [e.g. production of greater oil or water quantities], but lines with a similar pattern result if the deformation is due to an accumulation of stresses in the area crossed.

It is evident that such an interpretation of single lines means rough first approximation as only the projection of the deformations on a line is seen.

An areal interpretation is made possible by a common interpretation of the complete polygonial when geophysical and tectonic information is also to be included.

The strategy for the interpretation is based therefore on preliminary geophysical - techtonic model. The morphotectonic characterization of the lines (see Appendix A.) can be used in digital form as delimiters for the regression. If the trend of the surveying data from repeated levellings confirm the trend

DOI: https://doi.org/10.2312/zipe.1989.102.03

GEOLOGICAL PROFIL

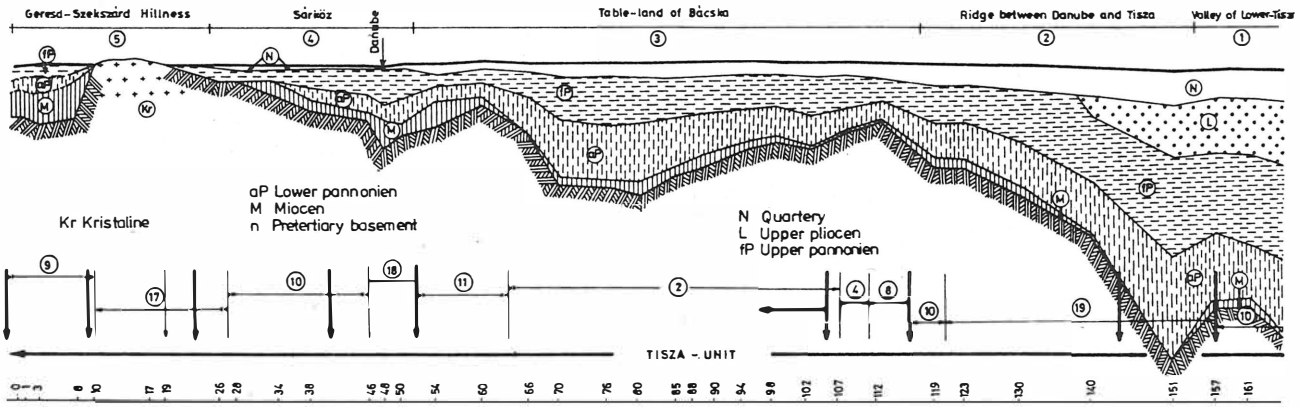

Fig. 4.

DOI: https://doi.org/10.2312/zipe.1989.102.03

Gradient map of the investigated line

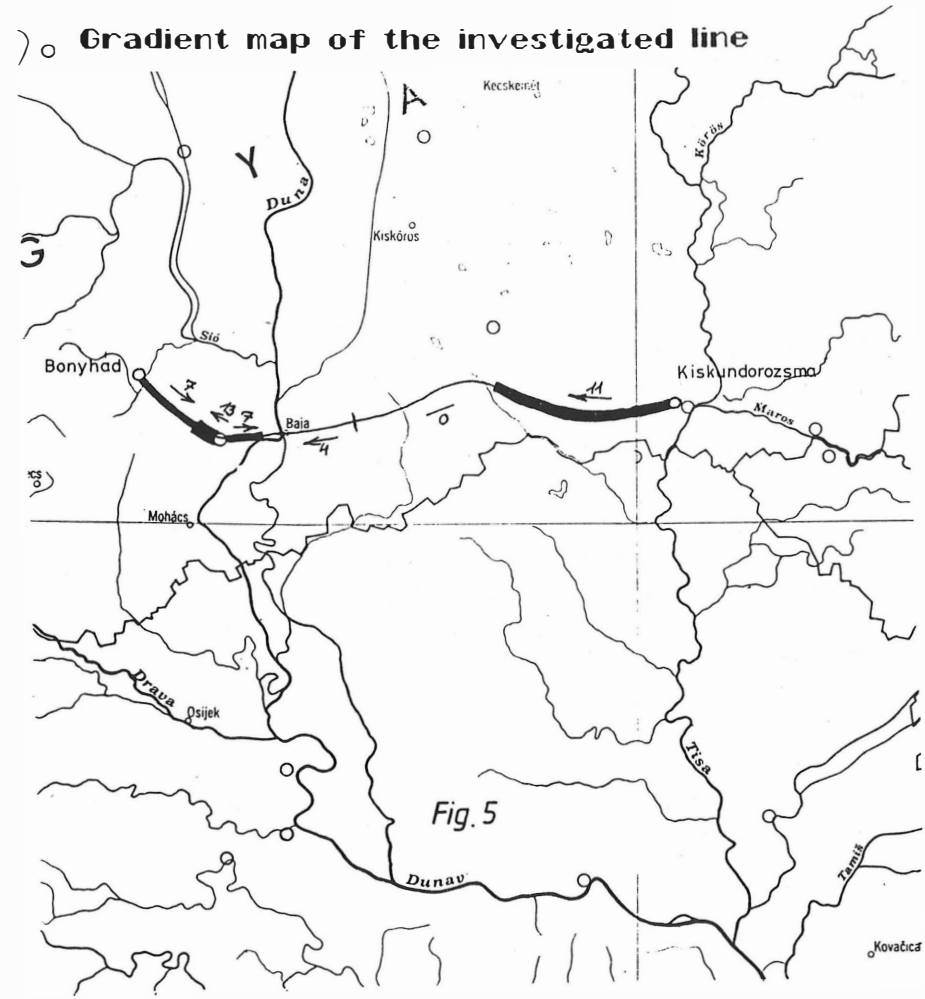

Fig. 5

DOI: https://doi.org/10.2312/zipe.1989.102.03

expected from geophysical data, then numerical values are obtained for these trends. In the opposite case a new prilaminary model is to be constructed. In both cases additional information is obtained from the interpretation. The new gradient map to be produced is expected to contain new information in spite of that it is based on the material of the previous CBK map; the new information will be useful not only in geodesy, but in geophysics, too.
The gradient map of the test line is shown on Fig. 5.

REFERENCES:

1. Joo, I. at al: Explanatory description to the Mapof Recent Vertical Crustal Movements in the CBK. Budapest 1979

2. Thurm, H.: Ableitung von Gradienten rezenter vertikaler Erdkrustbewegungen fur das Gebeit der DDK. Petermanns Geogr. Mitt. 115. Jg 1971.

3 П Выскочил, Определение градиентов скоростей движений и поле деформаций по данным геодезическнх наблюдений 1985

4 Методические указания по составлению карт. Будапешт 1988

DOI: https://doi.org/10.2312/zipe.1989.102.03

Appendix A.

MORPHOTECTONIC CHARACTERIZATION OF THE LINE K - 13 KISKUNDOROZSMA - BONYHÁD

1 . Lower Tisza-region

The whole of the lower Tisza valley is an old structural graben. Its parts sank rythmically during the Pleistocene with different rates.

The western boundary is - in the area of line K-13 - sharp: it is in the line Felgyő-Csánytelek-Baks-Sándorfalva-Röszke.

Generally the flood area below a hight of 85 m above sea level is counted to this region; taking this into account, further that Lake Nagyszéksós near Mórahalom is considered as being at the boundary of the table between Danube and Tisza [in the following: DT-table], the eastern part of this line till Domaszék is considered as belonging to this region.

2. Line K - 13 continues from Domaszék till the county boundary - i.e. Öttömös -Kelebia - on the area of the DT-table.

The DT - table is a remainder of the big alluvial fan of the Pleistocene river Danube.

The material of the alluvial fan is a trough-like depression elongated towards NW-SE which opens in a funnel-shaped form and deepens to 400-800 m in the direction Vecsés-Nagykőrös-Kecskemét - Kiskunfélegyháza-Szeged. It continues without a sharp boundary in the loess table Bácska.

3. Line K-13 continoues from the ranch centre Öttömös - lying at the boundary between counties Csongrád and Bács - on the area of loess table Bácska. The DT-table is bordered to the south at the line Császártöltés-Jánoshalma-Kiskunhalas-Kelebia by the Bácska loess table; a sharp morphologic boundary is

DOI: https://doi.org/10.2312/zipe.1989.102.03

found only towards the river Danube, it was the fan of the Transdanubian Central Mts and of the Baranya Insular Mts towards the edge of Alföld [Great Hungarian Plain] which continued till the depression of the Danube valley to the south of Kalocsa. Later its western edge rose assymmetrically.

In its basement there are two chains of blocks striking NE-SW:

a. The block chain Madaras-Tompa and

b. The block chain Sükösd - Jánoshalma.

The present line K-13 lies between these two chains.

The morphotectonic unit can be divided into two subregions:

a. Sand table of Northern Bácska,

b. oess table of Northern Bácska.

The line lies generally till Felsőszentiván-Csávoly on subregion a., then till the Danube valley at Baja on subregion b.

4. The line leaves at Baja the loess table Bácska and crosses the Alföld Danube valley. The next section of K-13 is called till Bátaszék "Sárköz", being a morphotectonic unit

- with a western boundary at the hilly county of Tolna - Baranya,

- with an eastern boundary at the loess table Bácska specially at the high bank of Kecel-Baja.

The depression Kalocsa-Sárköz is a younger part of the Alföld section of the Danube valley having developed along NE-SW striking fractures.

An analysis of the river sediments has shown that due to a recent sinking a filling of an alluvial fan character continues to develop. Characteristic morphotectonic elements of the area are:

- görönd or gorond : Hungarian name for early Holocene terrace area without any inondation,

- gyűr : Hungarian name for abandoned backwater of a depth of

DOI: https://doi.org/10.2312/zipe.1989.102.03

2 to 3 m, terraces of a width of 1-2 km and relative heigths of 3 to 5 m or 9 to 11 m at the edge of the block of the Pannonian table between Szekszárd and Bátaszék.

5. Line K-13 continoues from Bátaszék to Bonyhád between the hilly counties Geresd and Szekszárd, the latter being built of Neogene sediments over a granitic basement disrupted by late Pleistocene movements and which rose in a block-like form following the valley of the brook Lajvér. The hilly county of Geresd is an ancient granatic block covered by a loess sheet. Line K-13 ends in thee depressional valley of the brook Völgységi which developed in three steps during Pleistocene times near Bonyhád, at the eastern edge of the Bonyhád high basin.

The valley of the brook Lajvér consists of a string of circular widenings with diameters of 200 to 300 m between the two hilly counties having similar basements but different covers.

Before Bonyhad the valley turns to NE and line K-13 crosses a high watershed then descends to valley of the brook Rák which tends to the depression of the brook Völgységi splitting the Börzsöny- Kakasd loess table from the Szekszárd hills.

DOI: https://doi.org/10.2312/zipe.1989.102.03

ON THE RELATIONSHIP BETWEEN GEODYNAMIC AND HYDROGEOLOGIC PROCESSES

Kissin I.G.

Institute of Physics of the Earth, USSR Academy of Sciences, Moscow

Abstract

This paper presents a technique for precision hydrogeologic observations to solve geodynamic problems. It is known that changes in pore and crack pressure or in water level cause a re-distribution of stresses in the saturated rock mass and deformations which should be taken into account in precise geodetic measurements.

The changes in groundwater level or pressure produce a significant gravity effect. This is particularly large for the considerable changes in free-flow water level associated with human activities. Thus, for example, gravity changes caused a groundwater level rise of 0.2-0.3 m Gal in the Ashkhabad Geodynamic Test Area (Kirsta, 1986).

Recent crustal movements have been found to extent a considerable influence on groundwater regime. A good correlation has been found in the Frunze Geodynamic Test Area (Kirghizia) between high-amplitude fluctuations in groundwater level and intensive vertical crustal movements (Kissin, Orolbaev, 1988). Under certain conditions groundwater level observations can very well complement the geodetic methods for studying recent crustal movements. These observations can record effects due to comparatively rapid crustal movements. There are other examples of relationships between

DOI: https://doi.org/10.2312/zipe.1989.102.03

geodynamic processes and groundwater behaviour. Combined geodynamic and hydrogeologic observations are specially needed in areas of high seismicity, pronounced recent crustal movements or intensive human activity.

Резюме

Рассматривается методика прецизионных гидрогеологических наблюдений для решения геодинамических задач. Известно, что изменения давления в порах и трещинах или уровня подземных вод приводят к перераспределению напряжений в насыщенной толще и ее деформациям, которые должны учитываться при высокоточных геодезических измерениях.

Изменения уровня или давления подземных вод дают существенный гравитационный эффект. Особенно велик этот эффект при значительных изменениях уровня безнапорных вод, связанных с деятельностью человека. Например, на Ашхабадском геодинамическом полигоне изменения силы тяжести, обусловленные подъемом уровня грунтовых вод, достигают 0,2-0,3 мГал (Кирста, 1986).

Установлено, что современные движения земной коры могут оказывать существенное влияние на режим подземных вод. На Фрунзенском геодинамическом полигоне(Киргизия), обнаружена хорошая корреляция между высокоамплитудными колебаниями уровня подземных вод и интенсивными вертикальными движениями земной коры(Kissin, Orolbaev , 1988). При определенных условиях наблюдения за уровнем подземных вод могут служить хорошим дополнением к геодезическим методам изучения современных движений земной коры. Эти наблюдения дают возможность регистрировать эффекты относительно быстрых движений земной

DOI: https://doi.org/10.2312/zipe.1989.102.03

коры. Имеются другие примеры взаимного влияния геодинамических процессов и режима подземных вод. Совмещенные геодинамические и гидрогеологические наблюдения особенно актуальны в районах с высокой сейсмичностью, активными современными движениями земной коры или интенсивным развитием деятельности.

Introduction

Ground water, as well as other fluids (oil, gas) that fill pores and cracks in the crust are a powerful factor in the evolution of geodynamic processes. Fluid-related crustal movements occur on a partucularly great scale in areas where the natural fluid behaviour has been drastically altered by drawing ground water, oil or gas, by mining or reclamation activities. Recent geodynamic processes have a strong effect on ground water. The hydrogeologic effects of these processes have been established. A wider study of these effects can provide conditions where they will be used as indicators of recent crustal movements, in particular, relatively rapid movements that cannot be recorded by geodetic methods. An appropriate observation technique should be developed to accomodate the mutual influence of geodynamic and hydrogeologic processes.

Ground Water Regime and its Features that Are Important for Earth Dynamics

Groundwater regime (time changes of its parameters) has a long history of study primarily conducted to provide for the needs of water supply, reclamation, mining. The study of grounwater regime for the needs of geophysics began as

DOI: https://doi.org/10.2312/zipe.1989.102.03

late as the last fifteen years and by now has become a separate branch of geophysical research. Groundwater regime is controlled by two principal factors: changes in groundwater recharge and discharge due to weather, hydrologic or man-made processes; changes in the capacity of pores and cracks due to geodynamic (strain) processes, natural or man-made ones.

Time changes in groundwater parameters (pressure, filtration capacity, chemical composition) affect virtually all geophysical processes. As to geodynamical processes, the main factors are the variations of pressure or groundwater level.* These variations may have a natural or man-made origin. Periodic natural water-level changes, seasonal, 11-year solar ones etc. are well enough known, mostly for gravity groundwater (the shallowest aquifer). Earth-tide water-level fluctuations are periodic too.

The dominant amplitudes of ground water level or pressure fluctuations are of the order (in metres of water column):

Aquifer	Conditions	
	natural	man-made
free-flow water	10^{-1} n ÷ 10^{0} n	10 n
artesian water	10^{-1}	10 n

* We do not consider the changes in the chemical composition of fluids which too may be related to geodynamical processes. However, this relation is much more difficult to identify than for the case of fluid pressure

DOI: https://doi.org/10.2312/zipe.1989.102.03

Here n varies between 1 and 10. The amplitude of water level fluctuations may reach as large values as $10\ n \div 10^2 n$, m in the influence zone of hydrotechnical facilities, particularly in mountainous regions. The depressions of waterbed pressure frequently reach $10^2 n \div 10^3 n$, m in oil or gas fields.

The Effect of Ground Water on Geodynamic Processes

The conditions arising in the deformation of fluid-saturated rocks are sufficiently well known (Nikolaevsky, 1984 and other works). A fluid-dynamic type of recent crustal movements has been identified (Nikonov, 1977). However, geodynamic research in specific areas frequently neglects the influence of fluids.

Changes in water pressure (and in that of other fluids) lead to a redistribution of stresses and are accompanied by density increase (or decrease) in the rocks and sometimes by faulting. Fluid-dynamic compaction occurs more frequently and on a wider scale than density decrease. This is facilitated by the influence of gravity, and by the unilateral man-made effects. When excess water pressure has been dissipated in rocks that possess rheologic properties, a secondary compaction sets in (Mironenko and Shestakov, 1974).

The degree of compaction increase depends on rock compressibility, porosity and filtration capacity. Clays and other fine-grained loose rocks are greatly compacted with decreasing water pressure. The presence of sand interbedding in clays helps remove the water and facilitates compaction.

DOI: https://doi.org/10.2312/zipe.1989.102.03

Rock compaction is also controlled by the amount the fluid pressure has decreased. Since, as pointed out in the Table, this quantity may be one or two orders greater for man-induced factors than for natural ones, there is a corresponding difference in rock compaction.

Land subsidences associated with withdrawal of water, oil and gas, and rock compaction are well known (Konoplyantsev and Yartseva-Popova, 1983). The rate of subsidence reaches some tens of centimetres or even 1-2 metres per year. The deformations due to the natural compaction of thick clay sequences are much slower. This kind of compaction occurs when water is removed from the clay and is an important factor of neotectonic crustal movements. Recent negative movements may have considerable rates in young depressions where compaction continues. For example, the rate of these movements reached 10-15 mm/yr in the sub-Caucasian area and in the Terek-Kumy Depression (Levinson and Meshcheryakov, 1951).

Changes in pore and crack pressure exert a significant influence on rock faulting. The increase in water pressure is known to lower rock strength. This effect of water on the evolution of earthquake sources has been corroborated by numerous cases of induced earthquakes (Kissin, 1972; Gupta, and Rastogi, 1976) and is incorporated in the mechanics of earthquake sources (Rice, 1980). The influence of pore and crack pressure on aseismic movements on faults is still little known. Such movements can apparently be activated during periods of significant pressure increase.

In order to enhance the precision of gravity observa-

DOI: https://doi.org/10.2312/zipe.1989.102.03

tions, one must incorporate the changes in water contained in rocks. The most significant gravity effects are associated with the drying or saturation of pore and crack space. The magnitude of these effects is proportional to the capacity of pores and cracks and to the amplitude of water table fluctuations. The effects of groundwater table fluctuations on gravity was studied in the Ashkhabad Geodynamic Test Area (Kirsta, 1986). It has been found that the gravity effect of groundwater table seasonal fluctuations did not exceed 0.010 - 0.015 mGal, while gravity increased by 0.34 mGal on the bank of the Kara-Kum canal where groundwater table rose by more than 30 m. Special studies are needed to investigate gravity effects caused by pressure changes in head aquifers. In cases where such horizons are not partly dried, the effect in question must be smaller than that for free-flow waters. As to long-continued, very slow changes in gravity, they may be related to compaction and consolidation of clayed sequences and the associated re-distribution of water masses. When undercompacted rocks with excess water overlie denser rocks, convective deformation may arise (Artyushkov, 1965).

Hydrogeological Indicators of Geodynamic Processes

Among hydrogeological effects of recent crustal movements, the effects caused by large earthquakes are relatively well known. These include changes in hydrogeologic situation in the maximum intensity region, periodic fluctuations and sometimes residual displacements in the groundwater level which are observed at great distances

DOI: https://doi.org/10.2312/zipe.1989.102.03

from the epicentre. Recently, studies have been developed of hydrogeodynamic earthquake precursors which manifest themselves as changes in the groundwater level, pressure and output, and changes in the oil and gas output (Kissin, 1984).

In spite of the fact that studies of hydrogeodynamic effects of aseismic crustal movements are yet at a beginning, there are data which confirm the good prospects of using hydrogeological indices as indicators of these movements.

Data on recent vertical crustal movements and groundwater table variations were compared for the 1980-1984 period on the Frunze Geodynamic Test Area in Kirgizia (Kissin and Orolbaev, 1988). For this comparison pairs of observation sites were used, i.e. a well and a multiple levelling benchmark situated nearby. The wells went through aquifers that were free of influences of meteorological and man-made factors. Therefore, one could consider the regime of these horizons to be largely controlled by the influence of changes in the stress-strain state of water-saturated rocks.

A good correlation was found between the variations of groundwater level and the displacements of the relevant benchmarks. The level fluctuated in opposite phase to the vertical movements (Fig. 1). The rate of level change is about two orders greater than that of benchmark movements. As seen from Fig. 1, recent crustal movements (rate, direction) and groundwater level changes are significantly different in character for different sites. The differences depend on the structural positions of observation sites. The greatest benchmark subsidence rates (10 mm/yr) and ground-

DOI: https://doi.org/10.2312/zipe.1989.102.03

water rise (about 2 m/yr) were recorded at sites near the fault-flexural zone.

The out-of-phase groundwater level changes and recent crustal movements indicate that these movements are not associated with fluid dynamics in the Frunze Test Area. Quite the contrary, one would think the fluid dynamics to be controlled by present-day tectonic processes there.

Observations in another region of Kirgizia (Kochkor Depression) show sharp drops of 5 cm to 1 m in amplitude occurring upon the background of a long-continued groundwater rise (Fig. 2). An analysis of hydrogeological conditions has demonstrated that this behavior does not depend on meteorological or man-caused factors there. The groundwater regime obviously reflects the influence of aseismic motions on faults. Such motions are well known in the Kochkor Depression.

Fluctuations of groundwater level having a quasi-2-yr periodicity have been revealed on the basis of long-continued observations of deep (0.5-2.0 km) aquifers in Turkmenia, in the zone of the Frontal Kopet-Dag Fault (Barabanov et al., 1988). The amplitude of the fluctuations reached values of 1-3 m (Fig. 3). They propagated as wave motion along the fault zone towards the west-northwest at a velocity of 49$\pm$ 8 km/yr. These groundwater level fluctuations are not associated with meteorological conditions and man-induced factors. Since the wave-like fluctuations are consistent with seismicity migration, it has been hypothesized that they are caused by the propagation of fronts (waves) of strain. The fluctuations were disturbed in 1981-1982

DOI: https://doi.org/10.2312/zipe.1989.102.03

when tectonic regime began to change in the area.

The above examples serve to illustrate large-amplitude hydrogeologic effects of recent crustal movements. There is another category of these effects only manifesting themselves in charges in the parameters of certain fluctuations of groundwater level or other hydrogeologic indices. These include anomalous changes in the fluctuations due to disturbances such as variations of air pressure, tidal forces and some other factors. Recent crustal movements affect the state of stress and strain in the crust and accordingly the response of the medium to these disturbances.

The observations in the Leninabad Test Area in North Tadjikistan revealed changes in barometric effectivity coefficient which determines the influence of atmospheric pressure on groundwater table within -0.079 to -0.174 cm/GPa (Kissin et al., 1984). There sawtooth fluctuations of groundwater level were also found - a slow rise and a rapid subsidence with 1÷2.5 mm amplitude. The period of these oscillations in one of the wells amounted to 20÷40 min., however, before an earthquake of magnitude 4.4 at a distance of 30 m and during several days after the shock, the period increased to as much as 68÷98 min.

Further studies in hydrogeological effects of recent crustal movements will probably permit a method to be developed for recording rapid movements, which is difficult with geodetic methods. Besides, hydrogeologic effects reflecting the deformation of a water-saturated sequence in some cases provide some clues to the mechanism of recent crustal movements.

DOI: https://doi.org/10.2312/zipe.1989.102.03

The large-amplitude changes in groundwater level (pressure) which are caused by geodynamic processes indicate the necessity of taking account of these processes as a factor influencing the resources and quality of groundwater that is used in regions of intensive recent crustal movements.

Principles of Hydrogeological Study to Solve the Problems of Geodynamics

As already mentioned, two directions of study in the border of hydrogeology and geodynamics exist: the role of groundwater in geodynamic processes and the use of hydrogeologic indices as indicators of these processes. Methodological approaches to solve the problems in each direction are essentially different; however, all of them need combined hydrogeological and geodynamic observations.

Fluid-dynamic motions are generated by sufficiently great changes in groundwater level and pressure. The evolution of these motions can be predicted using hydrogeological data and rock characteristics (Mironenko and Shestakov, 1974). When groundwater (oil) level or pressure was lowered, the land subsidence reached 0.001 to 0.005, and in a single case as much as 0.005 of the lowering (Nikonov, 1977). This means that the monitoring of fluid-dynamic movements does not require precise hydrogeologic measurements. It is sufficient to conduct conventional observations of groundwater regime usual in hydrogeology. The important thing is that such observations sampled areas where fluid-dynamic movements are to be evaluated. When precise monitoring of land surface in the sites of critical facilities is needed, one may require to include

DOI: https://doi.org/10.2312/zipe.1989.102.03

relatively small-amplitude seasonal fluctuations of groundwater level. All these considerations equally apply to hydrogeological observations during precise gravity measurments.

Hydrogeologic effects of geodynamic processes can manifest themselves in a wide rang of amplitude and frequency characteristics of the relevant indices. Such effects must be studied by a special technique which includes precise measurements of ground water level continuously or at a high enough rate of sampling and data processing that eliminates noise and identifies the wanted signal.

At present, the principles of observational methodology are available for use in investigating hydrogeodynamic earthquake precursors (Kissin and Savin, 1986). Its main positions also apply to hydrogeological monitoring of other geodynamic processes and are as follows.

Observation sites are chosen so as to eliminate the significant influence of the noise associated with hydrometeorological and man-induced factors (infiltration of atmospheric precipitation, pumping etc.). The instruments that are used to observe groundwater level are to ensure an automatic continuous or discrete recordings of water level fluctuations with amplitudes between 1 mm and 10 m and as high frequencies as 2 -30 Hz. In some cases it is sufficient to measure groundwater level fluctuations in the range 1cm-1 m at a sampling rate of 1 hour to 1 day.

Computer processing of data is performed by a program that is to eliminate (identify) the component of the observation series associated with the influence of air pressure variations, slow changes of the groundwater level (trends)

DOI: https://doi.org/10.2312/zipe.1989.102.03

of different origins, tidal (or other) fluctuations with a period of less than 24 hours. Each of these components in the groundwater level fluctuations can be regarded as the wanted signal. One can then analyse the overall behaviour of groundwater level, the baromatric or tidal efficiency to determine what is the effect of recent crustal movements on these.

References

1. Artyushkov, E.V., 1965. Formation of convective deformations in poorly consolidated sediments. Izvestiya AN SSSR, ser. geol., No 12 (in Russian).

2. Barabanov, V.L., Grinevsky, A.O., Kissin, I.G. and Milkis, M.R., 1988. Strain waves in the hydrogeologic and seismic regime of the Frontal Kopet-Dag Fault area. Izvestiya AN SSSR, Fizika Zemli (Solid Earth), No 5, pp. 21-31.

3. Gupta, H.K., Rastogi B.K. Dams and earthquakes. Elsevier scientific publishing company, Amsterdam-Oxford-New York, 1976.

4. Kirsta, O.B., 1986. Evaluating the influence of suspended water on gravity in the Ashkhabad Geodynamic Test Area. Izvestiya AN Turkm. SSR, ser. fiz.-teknich., khim. i geol. nauk, No 3, pp. 71-75 (in Russian).

5. Kissin, I.G., 1972. On the problem of earthquakes induced by engineering. Sovetskaya geologiya, No 2, pp. 68-80 (in Russ.)

6. Kissin, I.G., 1984. Hydrogeodynamic precursors in an earthquake prediction system. In: Hydrogeodynamic Earthquake Precursors. Moscow, pp. 3-30 (in Russian).

DOI: https://doi.org/10.2312/zipe.1989.102.03

7. Kissin, I.G., Barabanov, V.L., Grinevsky, A.O. and Markov, V.M., 1984. Variations of groundwater level in the western Fergana Valley. In: Hydrogeodynamic Earthquake Precursors. Moscow, pp.96-119 (in Russian).

8. Kissin, I.G., Orolbaev E.E. Hydrogeological indications of recent movements of the Earth's crust. Journal of Geodynamics, 1988, No 9, pp.63-74.

9. Kissin, I.G. and Savin, I.V., 1986. Methodological Recommendations for Observations Conducted to Identify Hydrodynamic Earthquake Precursors. Moscow, 52 pp. (in Russian).

10. Konoplyantsev , A.A. and Yartseva-Popova, E.N., 1983. Land Subsidence in Relation to Groundwater Lowering. Moscow, VIEMS, 50 pp. (in Russian).

11. Levinson, V.G. and Meshcheryakov, Yu.A., 1951. Recent tectonic movements in the northern sub-Caucasian region as given by repeted levellings. In: Problems of Physical Geography, issue 17. Moscow, Izd. AN SSSR (in Russian).

12. Mironenko, V.A. and Shestakov, V.M., 1974. Principles of Hydrogeomechanics. Moscow, Nedra, 296 pp. (in Russian).

13. Nikolaevsky, V.N., 1984. Mechanics of Porous and Cracked Media. Moscow, Nedra, 232 pp. (in Russian).

14. Nikonov, A.A., 1977. Holocene and Recent Crustal Movements. Moscow, Nauka, 240 pp. (in Russian).

15. Rice J. The mechanics of earthquake rupture. In: Physics of the Earth's interiour Italian physics society. Amsterdam, 1980, pp. 555-649.

DOI: https://doi.org/10.2312/zipe.1989.102.03

Figure Captions

for the paper "On the relationship between geodynamic and hydrogeologic processes" by I.G.Kissin

Figure 1. Changes in groundwater level in relation to the intensity and direction of recent vertical movements in the Frunze Geodynamic Test Area.
(1) groundwater level (H); (2) change in benchmark elevation (Δ h); (3) East-Chuya flexure-faulted zone; (4) observation borehole; (5) benchmark.

Figure 2. Changes in groundwater level in borehole 1254, Kochkor Depression.

Figure 3. Changes in groundwater level recorded in boreholes, Ashkhabad Geodynamic Test Area. The dash-and-dot line shows the coincidence of the lows of quasi-2-yr groundwater level fluctuations (Barabanov et al., 1988).

DOI: https://doi.org/10.2312/zipe.1989.102.03

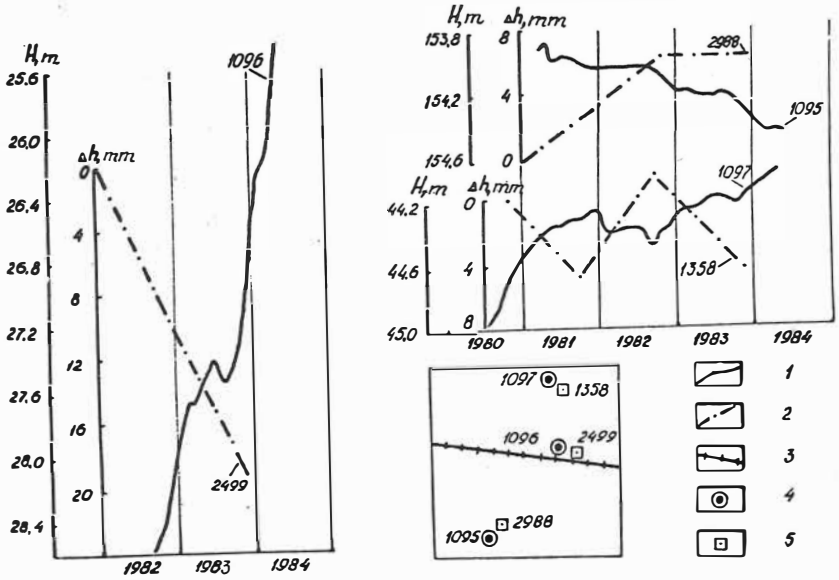

Fig. 1

DOI: https://doi.org/10.2312/zipe.1989.102.03

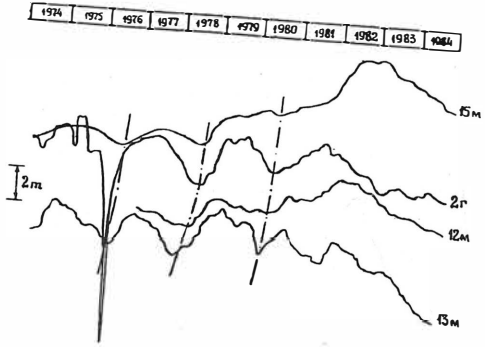

Pig. 3

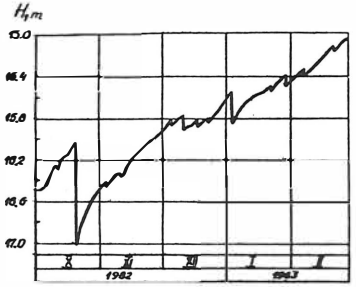

Pig. 2

DOI: https://doi.org/10.2312/zipe.1989.102.03

Академия наук УССР
ПОЛТАВСКАЯ ГРАВИМЕТРИЧЕСКАЯ ОБСЕРВАТОРИЯ
ИНСТИТУТА ГЕОФИЗИКИ им. С.И. СУББОТИНА

М.В. Лубков

ЛОКАЛЬНЫЕ ТЕРМОУПРУГИЕ ДЕФОРМАЦИИ ЗЕМНОЙ ПОВЕРХНОСТИ

Резюме

Исследована трехмерная математическая модель неравномерного нагрева земной поверхности, на основе термоупругой задачи о локальном периодическом нагреве круга на границе однородного полупространства. Получены аналитические выражения в квадратурах для напряжений, наклонов и смещений, определяющие термонапряженное состояние полупространства вследствие неравномерного нагрева его поверхности и учитывающие размеры неоднородности этого нагрева. В качестве иллюстрации приведены графики температурных наклонов, полученные численным интегрированием по методу Симпсона, причем погрешность этого метода не превышает пятого порядка малости. Вычисление функций Бесселя, присутствующих в подинтегральных выражениях осуществлялось численно по стандартной программе.

DOI: https://doi.org/10.2312/zipe.1989.102.03

Введение

Деформации земной поверхности, вызванные гравитационным воздействием Луны и Солнца, изучаются на протяжении многих лет. Получаемая здесь информация важна для изучения геофизических процессов, происходящих внутри Земли. Ряд побочных эффектов существенно влияет на точность регистрации земных приливов, среди которых важно выделить влияние температурных деформаций земной поверхности, вызванных суточным вращением Земли. Амплитуды температурных квазипериодических наклонов и напряжений могут в десятки и более раз превышать значения приливных эффектов.

Проблеме температурных деформаций земной поверхности посвящен ряд работ [5-9] . Но, несмотря на достижение хорошего понимания качественного механизма термоупругих процессов, происходящих в земной поверхности, вопрос практического применения этой информации остается открытым. Это связано прежде всего с тем, что температурные деформации земной поверхности носят сугубо локальный характер, т.е. сильно зависят от неравномерного нагрева поверхности. Двумерные модели, исследованные в работах [5-8] , не в состоянии точно учитывать области локализованного нагрева поверхности, они могут давать только приближенные оценки параметров, учитывающих неравномерный нагрев. Для учета такого рода нагрева необходимо рассматривать трехмерную термоупругую модель с периодическим локальным нагревом области на границе полупространства. Цель настоящей работы состоит в реализации названной выше проблемы. Отметим также, что данная модель может быть использована для учета изменения уровня поверхности Земли вследствии суточного хода температуры.

DOI: https://doi.org/10.2312/zipe.1989.102.03

§ I. Постановка задачи. Разрешающие уравнения

Упругая изотропная однородная среда, заполняющая полупространство $z \geq 0$, имеет начальную температуру $T = 0$. В момент $t = 0$ круговая область радиуса $r = b$ на поверхности $z = 0$ нагревается по периодическому закону $T_0 \cos \omega t$, остальная часть поверхности сохраняет температуру $T = 0$. По истечении некоторого промежутка времени процесс устанавливается и переходный процесс можно не рассматривать. Будем рассматривать периодический процесс нагрева при отсутствии на свободной поверхности полупространства внешней нагрузки. Определение температурного поля полупространства сводится к решению уравнения теплопроводности

$$\frac{1}{r}\frac{\partial}{\partial r}\left(r\frac{\partial T}{\partial r}\right) + \frac{\partial^2 T}{\partial z^2} = \frac{1}{a}\frac{\partial T}{\partial t} \qquad (I.1)$$

при граничном условии на поверхности

$$T = \begin{cases} T_0 \cos \omega t & ; r < b \\ 0 & ; r > b \end{cases} \qquad (I.2)$$

где a - коэффициент температуропроводности.

Напряженно-деформированное состояние определяется статическими уравнениями термоупругости ($\omega \ll 1$):

$$\Delta u - \frac{u}{r^2} + \frac{1}{1-2\mu}\frac{\partial e}{\partial r} = \frac{r(1+\mu)}{1-2\mu}\frac{\partial(\alpha_T T)}{\partial r}$$
$$\Delta w + \frac{1}{1-2\mu}\frac{\partial e}{\partial z} = \frac{r(1+\mu)}{1-2\mu}\frac{\partial(\alpha_T T)}{\partial z} \qquad (I.3)$$

Здесь $e = \frac{\partial u}{\partial r} + \frac{u}{r} + \frac{\partial w}{\partial z}$ - дилатация, μ - коэффициент Пуассона, α_T - коэффициент линейного расширения.

С учетом граничных условий, выражающих отсутствие нормальных и тангенциальных напряжений на поверхности $z = 0$

DOI: https://doi.org/10.2312/zipe.1989.102.03

(I.4)

§ 2. Определение термонапряженного состояния полупространства

Исследуем периодический процесс (задачу рассматриваем без начальных условий). Температуру можно представить в виде

$$T = T^* e^{i\omega t} \tag{2.1}$$

Граничное условие (I.2) представим для удобства в виде

$$T = \begin{cases} T_0 e^{i\omega t} & ; \ z < \delta \\ 0 & ; \ z > \delta \end{cases} \tag{2.2}$$

Уравнение (I.1) с учетом (2.1) приводится к уравнению Пуассона, которое разрешается при помощи преобразования Ханкеля

$$T^* = \int_0^\infty C(\beta) J_0(\beta z) e^{-\sqrt{\beta^2 + \frac{i\omega}{\alpha}}\, z} d\beta \tag{2.3}$$

функция $C(\beta)$ определяется из граничного условия (2.2).

Температура полупространства выразится

$$T = \delta T_0 e^{i\omega t} \int_0^\infty J_1(\beta\delta) J_0(\beta z) e^{-\sqrt{\beta^2 + \frac{i\omega}{\alpha}}\, z} d\beta \tag{2.4}$$

Перепишем уравнение (I.3) в декартовой системе координат

$$\Delta u_i + \frac{1}{1-2\mu} \frac{\partial e}{\partial x_i} = \frac{2(1+\mu)}{1-2\mu} \frac{\partial (\alpha_T T)}{\partial x_i} \tag{2.5}$$

Подставив в уравнение (2.5) $u_i = \frac{\partial \Phi}{\partial x_i}$, получим

$$\frac{2(1-\mu)}{1-2\mu} \frac{\partial}{\partial x_i} (\Delta \Phi) = \frac{2(1+\mu)}{1-2\mu} \frac{\partial (\alpha_T T)}{\partial x_i} \tag{2.6}$$

Здесь Φ — термоупругий потенциал перемещений.

Интегрируя по x_i и приравнивая нулю произвольную функцию, полученную при интегрировании, имеем

DOI: https://doi.org/10.2312/zipe.1989.102.03

$$\Delta\Phi = \frac{1+\nu}{1-\nu}\alpha_T T \qquad (2.7)$$

Компоненты напряжений выражаются через Φ по формуле [2]

$$\sigma_{ik} = 2G\left(\frac{\partial^2\Phi}{\partial x_i \partial x_k} - \Delta\Phi\,\delta_{ik}\right) \qquad (2.8)$$

Дифференцируя уравнение (2.7) по t и учитывая, что $\frac{\partial T}{\partial t} = a\Delta T$ получим

$$\Delta\frac{\partial\Phi}{\partial t} = \frac{1+\nu}{1-\nu}a\alpha_T\Delta T \qquad (2.9)$$

Интегрирование уравнения (2.9) приводит к зависимости

$$\Phi = \frac{1+\nu}{1-\nu}\alpha_T a\int_0^t T\,dt + \Phi_0 + t\,\Phi_1 \qquad (2.10)$$

Поскольку рассматривается периодический процесс, то непериодическую часть потенциала перемещений Φ можно отбросить ($\Phi_1 = 0$). После подстановки выражения (2.4) в (2.10) и интегрирования по времени получим потенциал перемещений Φ в виде:

$$\Phi = \frac{1+\nu}{1-\nu}\frac{\alpha_T a\beta T_0 e^{i\omega t}}{i\omega}\int_0^\infty J_1(\beta\rho)J_0(\beta z)e^{-\sqrt{\beta^2+\frac{i\omega}{a}}\,z}\,d\beta \qquad (2.11)$$

Вводя обозначение $Q = \frac{1+\nu}{1-\nu}\frac{\alpha_T a\beta T_0 e^{i\omega t}}{i\omega}$,

$\gamma = \sqrt{\beta^2+\frac{i\omega}{a}}$ перепишем выражение (2.11) в виде:

$$\Phi = Q\int_0^\infty J_1(\beta\rho)J_0(\beta z)e^{-\gamma z}\,d\beta \qquad (2.12)$$

Исходя из формул (2.8) и (2.12), определим компоненты напряженного состояния в цилиндрической системе координат:

$$\tilde{\sigma}_{zz} = 2GQ\int_0^\infty J_1(\beta\rho)\left(\frac{J_1(\beta z)}{\beta z}e^{-\gamma z}\beta^2 - J_0(\beta z)\gamma^2 e^{-\gamma z}\right)d\beta$$

$$\tilde{\sigma}_{\varphi\varphi} = -2GQ\int_0^\infty J_1(\beta\rho)\left(\frac{J_1(\beta z)}{\beta z}e^{-\gamma z}\beta^2 + J_0(\beta z)e^{-\gamma z}\frac{i\omega}{a}\right)d\beta$$

$$\tilde{\sigma}_{zz} = 2GQ\int_0^\infty J_1(\beta\rho)J_0(\beta z)e^{-\gamma z}\beta^2\,d\beta$$

$$\tilde{\sigma}_{\rho z} = 2GQ\int_0^\infty J_1(\beta\rho)J_1(\beta z)\gamma\beta e^{-\gamma z}\,d\beta \qquad (2.13)$$

DOI: https://doi.org/10.2312/zipe.1989.102.03

Напряженное состояние (2.13) не удовлетворяет граничным условиям (I.4), к нему необходимо добавить некоторое осесимметрическое напряженное состояние, определяемое методом Лява [3]

Окончательно термонапряженное состояние полупространства определяется следующими формулами:

$$\sigma_{rr} = Re\left\{2GQ\int_0^\infty J_1(\beta\rho)\left(\frac{J_1(\beta z)}{\beta z}\beta^2 e^{-\gamma z} - J_0(\beta z)\gamma^2 e^{-\gamma z}\right)d\beta + \right.$$

$$\left. + \frac{2G}{1-2\mu}\int_0^\infty e^{-\beta z}\left[J_0(\beta z)\left(A(2\mu\beta^2+\beta^2-\beta^3 z) - B\beta^3\right) - \frac{J_1(\beta z)}{z}\left(A(\beta z+\beta)+B\beta\right)\right]d\beta\right\}$$

$$\sigma_{\varphi\varphi} = Re\left\{-2GQ\int_0^\infty J_1(\beta\rho)\left(\frac{J_1(\beta z)}{\beta z}\beta^2 e^{-\gamma z} + J_0(\beta z)\frac{i\omega}{\alpha}e^{-\gamma z}\right)d\beta + \right.$$

$$\left. + \frac{2G}{1-2\mu}\int_0^\infty e^{-\beta z}\left[J_1(\beta z)\left(A(\beta-\beta^2 z) - B\beta^2\right) + J_0(\beta z)\cdot A\,2\mu\beta^2\right]d\beta\right\}$$

$$\sigma_{zz} = Re\left\{2GQ\int_0^\infty J_1(\beta\rho)J_0(\beta z)e^{-\gamma z}\beta^2 d\beta + \right. \qquad (2.14)$$

$$\left. + \frac{2G}{1-2\mu}\int_0^\infty e^{-\beta z}J_0(\beta z)\left[A(\beta^2+2\beta^2-2\mu\beta^2) + B\beta^3\right]d\beta\right\}$$

$$\sigma_{rz} = Re\left\{2GQ\int_0^\infty J_1(\beta\rho)J_1(\beta z)\gamma\beta e^{-\gamma z}d\beta + \right.$$

$$\left. + \frac{2G}{1-2\mu}\int_0^\infty e^{-\beta z}J_1(\beta z)\left[A(2\beta^3-2\mu\beta^2) + B\beta^3\right]d\beta\right\}$$

Горизонтальные и вертикальные смещения имеют вид

$$u = Re\left\{-\frac{1+\mu}{1-\mu}\frac{\alpha_T\alpha\beta T_0 e^{i\omega t}}{i\omega}\int_0^\infty J_1(\beta\rho)J_1(\beta z)e^{-\gamma z}\beta\,d\beta + \right.$$

$$\left. + \frac{1}{1-2\mu}\int_0^\infty J_1(\beta z)e^{-\beta z}\left(A(\beta-\beta^2 z) - B\beta^2\right)d\beta\right\} \qquad (2.15)$$

$$w = Re\left\{-\frac{1+\mu}{1-\mu}\frac{\alpha_T\alpha\beta T_0 e^{i\omega t}}{i\omega}\int_0^\infty J_1(\beta\rho)J_0(\beta z)e^{-\gamma z}\gamma\,d\beta + \right.$$

$$\left. + \int_0^\infty J_0(\beta z)e^{-\beta z}\left[A(2\beta-2\beta^2 z) + B\beta^2 + \frac{2\mu}{1-2\mu}(Az+B)\beta^2\right]d\beta\right\}$$

DOI: https://doi.org/10.2312/zipe.1989.102203

Наклоны в направлении X и Y имеют вид

$$\varphi_{x,y} = Re\left\{\frac{1+\mu}{1-\mu}\,\frac{\alpha_T \alpha B T_0 e^{i\omega t}}{i\omega}\int_0^\infty J_1(\beta B) J_1(\beta z) e^{-\gamma z}\,\gamma\beta\,d\beta + \right.$$
$$\left. + \int_0^\infty J_1(\beta z) e^{-\gamma z}\left\{\frac{z-z\mu}{1-z\mu}(Az+B)\beta^2 - A(z\beta^2 - z\gamma) - B\beta^2\right\}\beta\,d\beta\right\}\frac{x}{\sqrt{x^2+y^2}} \quad (2.16)$$

Функции A и B определяются из граничных условий (I.4)

$$A = \frac{(1+\mu)(1-2\mu)}{\mu}\,\frac{\alpha_T \alpha B T_0 e^{i\omega t}}{i\omega}\,\frac{J_1(\beta B)\left(\sqrt{\beta^2 + \frac{i\omega}{\alpha}} - \beta\right)}{\beta}$$

$$B = \frac{(1+\mu)(1-2\mu)}{1-\mu}\,\frac{\alpha_T \alpha B T_0 e^{i\omega t}}{i\omega}\,\frac{J_1(\beta B)\left(\sqrt{\beta^2 + \frac{i\omega}{\alpha}}(2\mu-1) - 2\mu\beta\right)}{\beta^2} \quad (2.17)$$

§ 3. Численный расчет и обсуждение результатов

В § 2 были получены аналитические выражения (2,I4,I5,I6), описывающие термонапряженное состояние полупространства. Интегрирование этих выражений производилось на основе численного метода интегрирования по Симпсону, причем погрешность этого метода не превышала пятого порядка малости. Вычисление функций Бесселя осуществлялось по стандартной программе „BES" вычислительного центра Полтавского инженерно-строительного института.

В качестве примера приведем результаты, полученные для наклонов φ_z (2.I6) на основе исходных данных ($\mu = 0,2$; $T_0 = 10^\circ C$ $\omega = 0,261$ рад/час; $\alpha_T = 12 \cdot 10^{-6}$ 1/°c; $\alpha = 0,9$ дм^2/час). Представленные кривые демонстрируют поведение наклонов с глубиной в фиксированный момент времени (I - $B = 20$ дм, $z = 10$ дм; II - $B = 40$ дм, $z = 20$ дм) Как видно из графиков, наклоны существенно зависят от радиуса нагреваемой области, интересно также отметить, что в начале происходит увеличение амплитуды наклона вплоть до некоторого максимального значения, а затем плавный спад.

Полученные аналитические выражения (2,I4,I5,I6) полностью определяют термонапряженное состояние полупространства вследствие неравномерного нагрева его поверхности, учитывают размеры неоднород-

DOI: https://doi.org/10.2312/zipe.1989.102.03

ТЕМПЕРАТУРНЫЕ НАКЛОНЫ

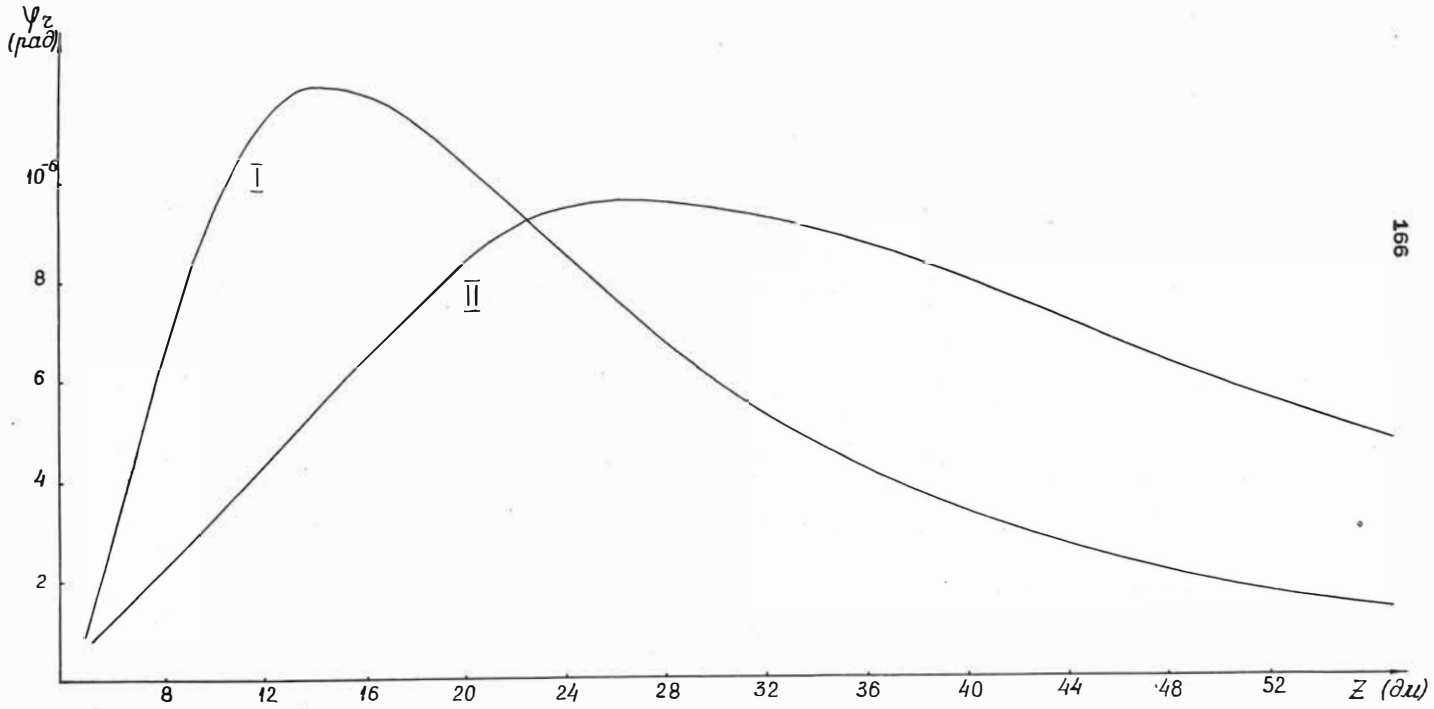

DOI: https://doi.org/10.2312/zipe.1989.102.03

ности этого нагрева и могут служить эффективным орудием при исследовании термоупругих деформаций земной поверхности.

Литература

I. Грей Э., Мэтьюз Г.Б. Функции Бесселя и их приложения к физике и механике.-М.:Изд-во иностр.лит.,1953.-240 с.

2. Паркус Г. Неустановившиеся температурные напряжения.- М.:Физматгиз,1963.-310 с.

3. Мелан Э., Паркус Г. Термоупругие напряжения, вызываемые стационарными температурными полями.-М.:Физматгиз,1958.-220 с.

4. Попов В.В. О температурных деформациях земной поверхности.-Изв. АН СССР. Серия Геофизика.-1960.-№ 7.-С.3-12.

5. Berger J. A note on Thermoelastic strains and Tilts.-J. of Geophysical Research.-1975.-80,N 2.-P.21-30.

6. Jobert G. Perturbations des marees terrestres.-J. of Annales de Geophysique.-16.-1960.-P.3-56.

7. Melchior P. The tides of the planet Earth.-PERGAMON PRESS.-1978.-782 p.

8. Nakano S. She Effect of Surface Temperature on the Crustal Deformations.Disaster Prevention Research Institute Bulletin.-1963.-N 60.- 52 p.

9. Muller G. Thermoelastic Deformations of Hali-Space-A Green's Function.-J. of Geophysics.-1977.-43.-P.52-68.

DOI: https://doi.org/10.2312/zipe.1989.102.03

S. Meier
Technical University Dresden

Stochastic differential geometry versus fractal geometry of the Earth's surface

The qualities of rough surfaces, e. g. of the Earth's surface, can be treated in two ways,

i) by means of the so-called fractals based on the HAUSDORFF measure,

ii) by stochastic differential relations based on two-dimensional random processes.

The first concept, essentially developed by MANDELBROT, may be successfully applied to the domain of microstructures, say in geological sciences. Empirical elements, e. g. formulas for length and area estimations, seem to be prevailing here.

The second concept offers both theoretical and empirical estimation procedures which are consistent with geodetic requirements in the plane and on the sphere, and in the domain of band-limited structures, e. g. estimation of roughness parameters, area estimation, linear filtering of terrain models etc. - As an example of the profitable stochastic differential method, area estimation functions developed by density function transformations (including numerical problems) have been discussed for the planar and spherical case.

The complete theory will be published in the periodical GERLANDS BEITRAEGE ZUR GEOPHYSIK, Leipzig.

DOI: https://doi.org/10.2312/zipe.1989.102.03

VERALLGEMEINERTE DYNAMISCHE MODELLE MIT SPANNUNGEN UND DEFORMATIONEN

Georgi Milev, Prof. Dr.-Ing., Bulgarische Akademie der Wissenschaften, Laboratorium für Geotechnik, Bulgarien, Sofia 1113, Akad. G. Bontschev Str. Bl. 24

Abgeleitet sind die Zusammenhänge zwischen den Trendparametern (Regressionskoeffizienten) oder Faktoren und darauf verursachten Translation, Rotation, Verformungen und Spannungen der untersuchten Objekte in der Zeit. Die gesuchten Parameter sind direkt durch die Koordinaten oder gemessenen Grössen ausgedrückt worden. Damit werden die Ausgleichung, Analyse und Interpretation vereinigt und das Endziel, die mathematisch-geometrische Interpretation realisiert.

GENERALIZED DYNAMIC MODEL WITH STRESSES AND DEFORMATIONS

Georgi Kostov Milev, Prof. Dr. Eng., Bulgarian Akademy of Sciences, Geotechnical Laboratory, Bulgaria, Sofia 1113 Acad. G. Bontchev Srr. Bl. 24

Relationships between trend parameters (regression coefficients), i.e. the factors (loading, underground waters, etc.), and the resulting translations, rotations, deformations and stresses in a given area have been derived. The parameters are expressed directly through the coordinates of the investigated points in the area, their differences or the measured elements. The relations may be used for respective short time forecasts. Further, the steps of equalization, analysis and interpretation are combined and the final aim of deformation studies - mathematical - geometric interpretation - is directly achieved.

DOI: https://doi.org/10.2312/zipe.1989.102.03

1. ALLGEMEINES

Infolge des Einflusses verschiedener Faktoren z.B. von Kräften (Belastung, Grundwasser u.a.) treten in den Ingenieur- und anderen Objekten Veränderungen ein. Im allgemeinen werden sie durch Spannungen, Translationen, Rotationen, Verformungen u.a. Erscheinungen ausgedrückt. Die mathematischen Beziehungen zwischen einigen der genannten Grössen sind in der Elastizitätstheorie vorhanden /9/.

Großes Interesse ruft die Rolle der Geodäsie bei der Festlegung dieser Grössen und Zusammenhänge hervor. Besonders dann, wenn von der Tatsache ausgegangen wird, dass ein Teil dieser Elemente - die Verschiebungen, im Ergebnis der Auswertung der geodätischen Messungen erhalten wird.

In /6/ werden die Zusammenhänge zwischen den geodätisch bestimmten Verschiebungen und Spannungen, Verformungen, Translation und Rotation abgeleitet. Dabei wird durch die gemeinsame Ausgleichung mehrerer Beobachtungszeiten indirekt auch die Zeit eingeschaltet. Somit wird praktisch die Hauptafgabe der Elastizitätstheorie gelöst und zwar als Prozess in der Zeit. Das entspricht der Wirklichkeit, ist naturgemäss und notwendig für die Abschätzung der Stabilität der Objekte.

In /2/, /4/ und /3/ wird die mehrmalige nichtlineare Regression zwischen den geodätisch bestimmten Verschiebungen, der Zeit und den Veränderungen einiger Hauptfaktoren (Parameter), die Verschiebungen verursachen, abgeleitet (eine polynomiale Regression ist vorausgesetzt).

Hier wird der Zusammenhang zwischen den Regressionskoeffizienten (Trendparameter), der Translation, Rotation, den Verformungen und den Spannungen der untersuchten Objekte und der Zeit abgeleitet. Damit wird der allgemeinste Fall (das Modell) der Defor-

DOI: https://doi.org/10.2312/zipe.1989.102.03

mationsuntersuchungen mit Beteiligung der Geodäsie geschaffen.

2. BESTIMMUNG DER REGRESSIONSKOEFFIZIENTEN

Die Lage der Punkte mit der Anzahl n des untersuchten Objekts wird in einem gegebenen Koordinatensystem (O,x,y,z), betrachtet in der Zeit t und unter der Voraussetzung, dass diese Lage von dem Einfluss einer Reihe von Faktoren in einem Beobachtungszeitpunkt t_j entsprechend /2/

$$L_j = L_j(t_j, T_j, p_j, q_j, \ldots) \qquad (1)$$

definiert.

Für den Zeitpunkt t_o gilt

$$L_o = L_o(t_o, T_o, p_o, q_o, \ldots). \qquad (2)$$

Die Lage L_o, b.z.w. L_1 der Punkte wird aufgrund geodätischer Messungen durch Ausgleichung als freies Netz bestimmt. Die Faktoren werden bei der Ausgleichung als unverändert aufgenommen. Ihr Zustand wird auch durch Messungen bestimmt. Unter der Voraussetzung, dass die Funktionen (1) ununterbrochen und differenziert ist und die Veränderungen klein sind, kann sie in der Nähe der Ausgangslage O der Punkte in eine Taylor-Reihe entwickelt werden. Mit der Begrenzung der zu den Gliedern zweiter Potenz und mit der Einführung der in /4/ gegebenen Bezeichnungen kann geschrieben werden

$$\begin{bmatrix} x_1^j \\ y_1^j \\ z_1^j \\ \vdots \\ x_n^j \\ y_n^j \\ z_n^j \end{bmatrix} = \begin{bmatrix} x_1^o \\ y_1^o \\ z_1^o \\ \vdots \\ x_n^o \\ y_n^o \\ z_n^o \end{bmatrix} + \begin{bmatrix} \alpha_o^j & \beta_o^j & \gamma_o^j & \delta_o^j & 0 & 0 & 0 & 0 & 0 & 0 & 0 & 0 \\ 0 & 0 & 0 & 0 & \alpha_o^j & \beta_o^j & \gamma_o^j & \delta_o^j & 0 & 0 & 0 & 0 \\ 0 & 0 & 0 & 0 & 0 & 0 & 0 & 0 & \alpha_o^j & \beta_o^j & \gamma_o^j & \delta_o^j \\ \vdots & \vdots & \vdots & \vdots & \vdots & \vdots & \vdots & \vdots & \vdots & \vdots & \vdots & \vdots \\ \alpha_o^j & \beta_o^j & \gamma_o^j & \delta_o^j & 0 & 0 & 0 & 0 & 0 & 0 & 0 & 0 \\ 0 & 0 & 0 & 0 & \alpha_o^j & \beta_o^j & \gamma_o^j & \delta_o^j & 0 & 0 & 0 & 0 \\ 0 & 0 & 0 & 0 & 0 & 0 & 0 & 0 & \alpha_o^j & \beta_o^j & \gamma_o^j & \delta_o^j \end{bmatrix} \begin{bmatrix} u_1^x \\ u_2^x \\ u_3^x \\ u_4^x \\ u_1^y \\ u_2^y \\ u_3^y \\ u_4^y \\ u_1^z \\ u_2^z \\ u_3^z \\ u_4^z \end{bmatrix} + \qquad (3)$$

DOI: https://doi.org/10.2312/zipe.1989.102.03

Hier bezeichnen $\alpha, \beta, \gamma, \delta$ die Änderungen der Faktoren entsprechend den Anfangsbeobachtungszeitpunkten u^x, u^y und u^z sind die ersten Ableitungen der Funktion, und w^x, w^y, w^z, g^x, g^y, g^z sind die zweiten getrennten und gemischten Ableitungen /4/.

Der Zusammenhang (4), allgemeiner durch ein Symbol bezeichnet, das die drei Koordinaten des Punktes i einschliesse, wird

$$\begin{bmatrix} L_1^j \\ L_2^j \\ \vdots \\ L_n^j \end{bmatrix} = \begin{bmatrix} L_1^o \\ L_2^o \\ \vdots \\ L_n^o \end{bmatrix} + \begin{bmatrix} \alpha_1^j \\ \alpha_2^j \\ \vdots \\ \alpha_n^j \end{bmatrix} b_o^j + 1/2 \begin{bmatrix} \beta_1^j \\ \beta_2^j \\ \vdots \\ \beta_n^j \end{bmatrix} b_1^j. \qquad (5)$$

Für das ganze Objekt gilt

$$\underset{3n1}{L_j} = \underset{3n1}{L_o} + \underset{3n12}{\alpha^j} \underset{121}{b_o^j} + 1/2 \underset{3n30}{\beta^j} \underset{301}{b_1^j} = L_o + \left[\alpha^j \; 1/2\,\beta^j\right] \begin{bmatrix} b_o^j \\ b_1^j \end{bmatrix} \qquad (6)$$

oder

$$\underset{3n1}{L_j} = \underset{3n1}{L_o} + \underset{3n42}{\alpha_j} \underset{421}{b_j^p}. \qquad (7)$$

Indem man die Lösung (2) verfolgt und den Zusammenhang (7) als stochastischen Prozess mit einem determinierten und stochastischen Teil $\mathcal{E}$ betrachtet, folgt

$$L_j = L_o + \alpha_j b_j^p + \mathcal{E} \qquad (8)$$

Unter der Bedingung

$$\mathcal{E}'_j Q_{\delta L} \mathcal{E}_j \Rightarrow \min \qquad (9)$$

Durch die Ausgleichung nach vermittelnden (parametrischen) Beobachtungen (siehe z. B/3/) werden die Regressionskoeffizienten (Trendparameter) bestimmt

$$b_j^p = (\alpha'_j Q_{\delta L}^{-1} \alpha_j)^{-1} \alpha'_j Q_{\delta L}^{-1} \delta L_j = D_j \delta L_j \qquad (10)$$

Die Absolutglieder L_j werden bestimmt, wie bereits, durch eine Ausgleichung als freies Netz, gezeigt wurde, einzeln nach den einzelnen Beobachtungszeitpunkten(unter der Voraussetzung, dass (wenn nötig) die unveränderlichen Punkte dieses Netzes identifiziert und genutzt worden sind) und Bildung der Unterschiede in den Koordinaten oder aber unmittelbar durch die

DOI: https://doi.org/10.2312/zipe.1989.102.03

gemeinsame Ausgleichung der Beobachtungsunterschiede /3/, mit einer entsprechenden Kovarianzmatrix, das heisst

$$\delta L_j = L_j - L_o = \begin{bmatrix} x_j - x_o \\ y_j - y_o \\ z_j - z_o \end{bmatrix} = \begin{bmatrix} \delta x_j \\ \delta y_j \\ \delta z \end{bmatrix} \qquad (11)$$

$$\delta L_j = (A' Q^{-1}_{\delta L} A)^+ + A' Q^{-1}_{\delta L} \quad \delta L_j = Q_{\delta L_j} A' Q^{-1}_{\delta l} \delta l_j$$

$$Q_{\delta L_j} = Q_{L_j} + Q_{L_o}$$

Hier sind A und die entsprechenden Matrizen der Konfigurations - und Kovarianzmatrix der Beobachtungsunterschiede l, die gewöhnlich in der Ausgleichung genutzt werden. Durch + ist die Pseudoinverse Matrix bezeichnet. Durch Ersetzen von (11) in (10), durch die Einführung entsprechender Kürzungen folgt

$$b^p_j = (\alpha' Q^{-1}_{\delta L_j} \alpha_j)^{-1} \alpha'_j Q^{-1}_{\delta L_j} (A' Q^{-1}_{\delta l_j} A)^+ A' Q^{-1}_{\delta l_j} \delta l_j = D_j C_j l_j \qquad (12)$$

421 423n 3n3n 3n1

Dadurch werden die Trendparameter direkt durch Beobachtungen ausgedrückt.

Die Gültigkeit der einzelnen Regressionskoeffizienten kann überprüft werden, indem man der Lösung in (4) folgt.

Die hier angebotene Lösung für die Bestimmung von b^p_j unterscheidet sich von dieser Lösung, die in /4/ gegeben wird praktisch nur durch die Zusammenhänge (4). In /4/ waren diese Zusammenhänge durch die Gruppierung von Koordinaten definiert (an einer Stelle x - Koordinaten aller Punkte, an einem anderen y, beziehungsweise z), und hier ist es nach Punkten i (gemeinsam mit x, y, z). Das ist erforderlich wegen der Festlegung der Zusammenhänge zwischen den Trendparametern (Kräfte, Faktoren), Verformungen u.a.

Wie bereits hervorgehoben, wird bei der Bestimmung von L_j aus (11) vorausgesetzt, dass die tatsächlichen Verschiebungen genutzt werden, d.h., dass sie aufgrund der festgelegten stabilen Punkte des Netzes /3/, /2/ bestimmt sind.

3. Bestimmung der Feldparameter, der Verschiebungsvektoren, der Verformungs- und Spannungstensoren und der anderen Funktionalen

Die Verschiebungen der Punkte i eines gegebenen untersuchten Objektes, das als starrer Körper betrachtet wird (entspre-

DOI: https://doi.org/10.2312/zipe.1989.102.03

chend den angenommenen Voraussetzungen in der Elastizitätstheorie /9/, /6/) können als Verschiebungen auf den Koordinatenachsen u_o, v_o, w_o eines Näherungspunktes O und einer Verschiebungsanomalie dargestellt werden. Wenn der Punkt O im Schwerpunkt der untersuchten Punkte angenommen ist und der Voraussetzungen, die in /6/ angenommen worden sind, die sich auf alle Punkte i des Objektes beziehen, kann man für die Verschiebungen u_1, v_1, w_i (die nach (11) auf den Koordinatenachsen bestimmt sind und bei Beschränkung bis zu linearen Gliedern der Entwicklung /9/, /8/, /2/, /1/) folgendes schreiben

$$\begin{bmatrix} u_1 \\ v_1 \\ w_1 \\ \vdots \\ u_n \\ v_n \\ w_n \end{bmatrix} = \begin{bmatrix} 1 & dx_1 & dy_1 & dz_1 & 0 & 0 & 0 & 0 & 0 & 0 & 0 & 0 \\ 0 & 0 & 0 & 0 & 1 & dx_1 & dy_1 & dz_1 & 0 & 0 & 0 & 0 \\ 0 & 0 & 0 & 0 & 0 & 0 & 0 & 0 & 1 & dx_1 & dy_1 & dz_1 \\ \cdot & \cdot & \cdot & \cdot & \cdot & \cdot & \cdot & \cdot & \cdot & \cdot & \cdot & \cdot \\ 1 & dx_n & dy_n & dz_n & 0 & 0 & 0 & 0 & 0 & 0 & 0 & 0 \\ 0 & 0 & 0 & 0 & 1 & dx_n & dy_n & dz_n & 0 & 0 & 0 & 0 \\ 0 & 0 & 0 & 0 & 0 & 0 & 0 & 0 & 1 & dx_n & dy_n & dz_n \end{bmatrix} \begin{bmatrix} u_o \\ \frac{\partial u}{\partial x} \\ \frac{\partial u}{\partial y} \\ \frac{\partial u}{\partial z} \\ v_o \\ \frac{\partial v}{\partial x} \\ \frac{\partial v}{\partial y} \\ \frac{\partial v}{\partial z} \\ w_o \\ \frac{\partial w}{\partial x} \\ \frac{\partial w}{\partial y} \\ \frac{\partial w}{\partial z} \end{bmatrix} \tag{13}$$

Hier sind dx_i, dy_i, dz_i die Veränderungen der reduzierten Koordinaten der Punkte i gegenüber O /6/, die durch die Koordinaten der Punkte bestimmt sind. Die Elemente des Unbekanntenvektors sind die Verschiebungen des Punktes O (u_o, v_o, w_o) und die ersten Einzelableitungen (Feldparameter der Verschiebungsvektoren) oder

$$\underset{3n1}{\delta L_j} = \underset{3n12}{F_j} \quad \underset{121}{b_j^d} \tag{14}$$

Wenn man das Problem auch hier stochastisch betrachtet, wie bei Punkt 2 und in /6/, so folgt mittels einer Ausgleichung nach vermittelnden Beobachtungen für b_j

$$\underset{121}{b_j^d} = \underset{123n3n3n3n12123n3n3n1}{(F'_j Q_{\delta L}^{-1} F_j)^{-1} F_j Q_{\delta L}^{-1}} \quad \underset{123n\ 3n1}{\delta L_j} = H_j \ \delta L_j \tag{15}$$

DOI: https://doi.org/10.2312/zipe.1989.102.03

Durch das Ersetzen von (11) in (15) folgt

$$b_j^d = (F'_j Q^{-1}_{\delta L_j} F_j)^{-1} F_j Q^{-1}_{\delta L_j} (A' Q^{-1}_{\delta L_j} A)^{+} A'_j Q^{-1}_{\delta l_j} \delta l_j = H_j C_j \delta l_j \quad (16)$$

Den Zusammenhang zwischen den Verschiebungen der Punkte (13) auf den Koordinatenachsen und den Verschiebungen des Näherungspunktes O und den entsprechenden Verschiebungsanomalien /1/, kann man auch folgendermassen darstellen

$$\begin{bmatrix} u_1 \\ v_1 \\ w_1 \\ \vdots \\ u_n \\ v_n \\ w_n \end{bmatrix} = \begin{bmatrix} u_o \\ v_o \\ w_o \\ \vdots \\ u_o \\ v_o \\ w_o \end{bmatrix} + \begin{bmatrix} \frac{\partial u}{\partial x} \frac{\partial u}{\partial y} \frac{\partial u}{\partial z} \cdots 0\ 0\ 0 \\ \frac{\partial v}{\partial x} \frac{\partial v}{\partial y} \frac{\partial v}{\partial z} \cdots 0\ 0\ 0 \\ \frac{\partial w}{\partial x} \frac{\partial w}{\partial y} \frac{\partial w}{\partial z} \cdots 0\ 0\ 0 \\ \cdots\cdots\cdots\cdots \\ 0\ 0\ 0 \cdots \frac{\partial u}{\partial x} \frac{\partial u}{\partial y} \frac{\partial u}{\partial z} \\ 0\ 0\ 0 \cdots \frac{\partial v}{\partial x} \frac{\partial v}{\partial y} \frac{\partial v}{\partial z} \\ 0\ 0\ 0 \quad\ \frac{\partial w}{\partial x} \frac{\partial w}{\partial y} \frac{\partial w}{\partial z} \end{bmatrix} \begin{bmatrix} dx_1 \\ dy_1 \\ dz_1 \\ \vdots \\ dx_n \\ dy_n \\ dz_n \end{bmatrix} \quad (17)$$

$$\underset{3n1}{\delta L_j} = \underset{3n1}{\delta L^j_{oo}} + \underset{3n3n}{T_j} \underset{3n1}{d_j}. \quad (18)$$

Entsprechend /6/ und /9/ kann der Tensor T, unter den üblichen Voraussetzungen für das untersuchte Objekt, als Summe von einem antisymmetrischen T_ω und einem symmetrischen Tensor T_d zerlegt werden, oder

$$\delta L_j = \delta L^j_{oo} + T^j_\omega d^j + T^j_d d^j = \begin{bmatrix} \delta L^j_{oo} T^j T^j_d \end{bmatrix} \begin{bmatrix} E \\ d^j \\ d^j \end{bmatrix} = T_o d_o. \quad (19)$$

(19) definiert die Zerlegung der Verschiebungen als Summe der Translation, Rotation und Verformung des untersuchten Objekts.

Die Elements aus (18) - δL^j_{oo} und T_j, beziehungsweise T^j_ω und T^j_d aus (19) folgen aus (16). Zu diesem Zweck, wie auch bei /6/, mit Rücksicht auf eine Erleichterung durch EDV-Technik werden im voraus zusätzliche Beziehungen, Matrizen und Vektoren eingeführt. Zuerst bestimmt man den Verformungsvektor ε_j und den Rotationsvektor ω_j, danach T^j_ω und T^j_d für die einzelnen Punkte. Festgelegt werden die Spannungsvektoren σ_j und die Spannungstensoren T^j_H bei den einzelnen Punkten unter den traditionellen Voraussetzungen der Elastizitätstheorie.

Die Rotations-, Verformungs- und Spannungstensoren, entsprechend T^j_ω, T^j_d und T^j_H, des untersuchten Objektes können als

DOI: https://doi.org/10.2312/zipe.1989.102.03

Ganzes bestimmt werden, indem man die entsprechenden Tensoren der einzelnen Punkte des Objektes vereinigt, d.h.

$$
\begin{aligned}
T_{\omega}^{j} &= \begin{bmatrix} T_{\omega 1} & 0 & \cdots & 0 \\ 0 & T_{\omega 2} & \cdots & 0 \\ \cdot & \cdot & \cdots & \cdot \\ 0 & 0 & \cdots & T_{\omega n} \end{bmatrix} \\
T_{d}^{j} &= \begin{bmatrix} T_{d1} & 0 & \cdots & 0 \\ 0 & T_{d2} & \cdots & 0 \\ \cdot & \cdot & \cdots & \cdot \\ 0 & 0 & \cdots & T_{dn} \end{bmatrix} \\
T_{H}^{j} &= \begin{bmatrix} T_{H1} & 0 & \cdots & 0 \\ 0 & T_{H2} & \cdots & 0 \\ \cdot & \cdot & \cdots & \cdot \\ 0 & 0 & \cdots & T_{Hn} \end{bmatrix}
\end{aligned}
\qquad (20)
$$

Für die Ausführung dieser Vereinigung durch EDV-Technik müssen zuerst die Rotations, Dehnungs- und Spannungstensoren der einzelnen Punkte bestimmt werden, d.h.

$$
\begin{aligned}
a_{w}' &= \begin{bmatrix} T_{\omega 1} & T_{\omega 2} \cdots T_{\omega n} \end{bmatrix} \\
a' &= \begin{bmatrix} T_{d1} & T_{d2} & & T_{dn} \end{bmatrix} \\
a_{H} &= \begin{bmatrix} T_{H1} & T_{H2} \cdots T_{Hn} \end{bmatrix}
\end{aligned}
\qquad (21)
$$

Eingeführt wird auch die Matrix B_{14}

$$
B_{14} = \begin{bmatrix} 1 & 0 & \cdots & 0 \\ 0 & 1 & \cdots & 0 \\ \cdot & \cdot & \cdots & \cdot \\ 0 & 0 & \cdots & 1 \end{bmatrix} \qquad (22)
$$

Dann bekommt man die Tensoren aus (20)

$$
\begin{aligned}
T_{\omega} &= B_{14} a \\
T_{d} &= B_{14} a_{d} \\
T_{H} &= B_{14} a_{H} .
\end{aligned}
\qquad (23)
$$

Entsprechend dem Translationsvektor t_o aus (19) bekommt man bei der Einführung des Vektors t_o und der Matrix B_{15},

DOI: https://doi.org/10.2312/zipe.1989.102.03

$$t'_o = \begin{bmatrix} u_o v_o w_o \end{bmatrix}$$

$$B_{15} = \begin{bmatrix} 1\,0\,0\,1\,0\,0\,\ldots\,1\,0\,0 \\ 0\,1\,0\,0\,1\,0\,\ldots\,0\,1\,0 \\ \cdot\,\cdot\,\cdot\,\cdot\,\cdot\,\cdot\,\cdot\,\cdot\,\cdot\,\cdot\,\cdot\,\cdot \end{bmatrix} \qquad (24)$$

$$\delta L^j_{oo} = t'_o B_{15}.$$

4. Zusammenhang zuischen den Trendparametern, dem Translationsvektor und den Rotations-, Dehnungs- und Spannungstensoren

Wenn man in (10) L_j aus (19) ersetzt, so entsteht der Zusammenhang

$$b^p_j = D_j \left(\delta L^j_{oo} + T^j_\omega \, d^j + T^j_d \, d^j \right) = D_j T^j_o d^j_o. \qquad (25)$$

Entsprechend /4/ erfolgt der Zusammenhang zwischen dem Verformungsvektor und dem Spannungsvektor aus

$$\varepsilon^j = T \, \sigma^j$$

$$\begin{bmatrix} \varepsilon_x \\ \varepsilon_y \\ \varepsilon_z \\ \gamma_{xy} \\ \gamma_{yz} \\ \gamma_{zx} \end{bmatrix} = \frac{1}{E} \begin{bmatrix} 1 & -\mu & -\mu & 0 & 0 & 0 \\ -\mu & 1 & -\mu & 0 & 0 & 0 \\ -\mu & -\mu & 1 & 0 & 0 & 0 \\ 0 & 0 & 0 & 2(1+\mu) & 0 & 0 \\ 0 & 0 & 0 & 0 & 2(1+\mu) & 0 \\ 0 & 0 & 0 & 0 & 0 & 2(1+\mu) \end{bmatrix} \begin{bmatrix} \sigma_x \\ \sigma_y \\ \sigma_z \\ \tau_{xy} \\ \tau_{yz} \\ \tau_{zx} \end{bmatrix} \qquad (26)$$

Entsprechend dem Dehnungstensor gilt für einen kleinen Raum, dargestellt durch den Punkt i (i=1,..n) und durch Einführung der Matrix B_5, B_6, B_7, B_8, B_9, B_{10}, die aus 0 und 1, oder 0 und 1/2 bestehen, we bei /6/,

$$T^j_{di} = \varepsilon_{10} + \varepsilon_{20} + \varepsilon_{30} = B_5 \varepsilon^j B_8 + B_6 \varepsilon^j B_9 + B_7 \varepsilon^j B_{10} \qquad (27)$$

oder durch den Spannungsvektor ausgedrückt

$$T^j_{di} = B_5 T^d_e \sigma^j B_8 + B_6 T^d_e + \sigma^j_i B_9 + B_7 T^d_e \sigma^j_i B_{10}. \qquad (28)$$

Indem man (21) und (23) in Betracht zieht, so folgt für T

DOI: https://doi.org/10.2312/zipe.1989.102.03

$$T_d^j = B_{14} a_d^j = B_{14} \begin{bmatrix} T_d^j \\ 1 \\ T_d^j \\ \vdots \\ T_{dn}^j \end{bmatrix} = B_{14} \begin{bmatrix} B_5 T_e^d \sigma_1^j B_8 + B_6 T_e^d \sigma_1^j B_9 + B_7 T_e^d \sigma_1^j B_{10} \\ B_5 T_e^d \sigma_2^j B_8 + B_6 T_e^d \sigma_2^j B_9 + B_7 T_e^d \sigma_2^j B_{10} \\ \vdots \\ B\ T_e^d \sigma_n^j B_8 + B_6 T_e^d \sigma_n^j B_9 + B_7 T_e^d \sigma_n^j B_{10} \end{bmatrix}$$

$$T_d^j = B_{14} R^j \qquad (29)$$

Wenn wir (29) in (25) ersetzen, entstehen die Zusammenhänge

$$b_j^p = D_j \left(\delta L_{oo}^j + T_\omega^j d^j + B_{14} R^j d^j \right) = D_j T_1^j d_o^j. \qquad (30)$$

Mit (25) und (30) wird eine Verallgemeinerung und eine direkte Lösung der Hauptaufgabe der Elastizitätstheorie gegeben, indem man die Zeitzwischen zwei Beobachtungszeitpunkten in Betracht zieht. Parallel dazu sind die hier festgestellten Zusammenhänge verallgemeinert, sie stellen praktisch den Allgemeinfall (das Modell) der Untersuchung des Spannungs- und Verformungszustands der Körper dar. Er beinhaltet als Sonderfälle die in den letzten Jahren lancierten /1/, /7/, /8/ Begriffe "statisches", "kinematisches" und "dynamisches" Modell, von denen der Autor einige als nicht genug begründet und korrekt betrachtet, besonders das "statische" Modell /5/. Es muss hervorgehoben werden, dass, auch wenn diese Fälle nicht mit den erwähnten Begriffen genannt werden, für sie bereits prinzipielle Lösungen bereitstehen /2/. In /2/ wird auch eine dreidimensionale Lösung mit entsprechenden Formeln vorgeschlagen.

Die weitere Verallgemeinerung der hier abgeleiteten Zusammenhänge, wie bereits am Aufang erwähnt wurde, findet seinen Ausdruck in ihrer Aufnahme in eine gemeinsame Ausgleichung einiger Beobachtungszeitpunkte in Übereinstimmung mit dem in /4/ und /6/ vorgenommenen.

Die abgeleiteten Zusammenhänge erlauben, eine Prognose für eine kurze Zeitspanne, z.B. der Verschiebungen oder Trendparameter in Abhängigkeit vom Spannungs- und Verformungszustand oder anderer Varianten zusammenzustellen.

Literatur

1. Kahmen, H., Niemeier, W., Pelzer, H. Geodätisches Institut. AVN, 1983, Heft 11-12, S. 452-460.

DOI: https://doi.org/10.2312/zipe.1989.102.03

2.Milev, G. Ausgleichung,Analyse und Interpretation von Deformationsmessungen. 1973, DGK, Reihe C, Nr. 193,

3.Milev, G. Geodätische Methoden zur Untersuchung von Deformationen. Konrad WittwerVerlag, 1985, 286 S.

4.Milev, G. Eine Verallgemeinerung der Trendparameterschätzung. IV. Internationales Symposium über Deformationsmessungen mit geodätischen Methoden. 9.-16. Juni 1985, Katovice, Polen, 10 S.

5.Milev, G. Präzisierung und Verallgemeinerung der Begrisfe und Modelle für Deformationsuntersuchungen. X. Internationaler Kurs für Ingenieurvermessung. 1988. E 10, 7 S.

6.Milev, G. Untersuchung,"Der Spannungs- und Verformungszustand der Körper aus geodätisch bestimmten Verschiebungen." XVIII FIG Kongress, Toronto, Kanada, 1986, Band 6

7.Papo, H., Perelmuter, A. Vierdimensionale Analyse von Deformationen. ZfV, 1 8 , Heft 2, S. 66-72.

8.Pelzer, H. Deformationsuntersuchungen auf der Basis Kinematischer Bewegungsmodelle. AVN, 1987, Heft 2, S. 49-62.

9.Warbanov, Chr. Elastizitätstheorre. Sofia, Technika, 1976.

DOI: https://doi.org/10.2312/zipe.1989.102.03

О.М.Остач, Л.П.Пеллинен
ЦНИИГАиК ГУГК СССР
Москва, СССР

НЕКОТОРЫЕ РЕЗУЛЬТАТЫ ИССЛЕДОВАНИЙ ДЕФОРМАЦИЙ ЗЕМНОЙ КОРЫ НА ГЕОДИНАМИЧЕСКИХ ПОЛИГОНАХ ГУГК СССР

Резюме

Приведены и прокомментированы некоторые результаты анализа деформаций земной коры, полученные на основе регулярных геодезических наблюдений, выполняемых геодезистами ГУГК СССР на специально созданных геодинамических полигонах (ГДП). Такие ГДП размещены в тектонически активных областях, характеризующихся повышенной сейсмичностью или активным вулканизмом. Первоочередная цель проводимых наблюдений состоит в выявлении и детальном изучении развития во времени различных аномальных деформаций земной коры, предваряющих землетрясения и извержения вулканов. Изучению подлежат и постсейсмические деформации, так как они несут ценную информацию о механизмах очагов землетрясений.

Приводимые примеры наглядно иллюстрируют результативность геодезического метода изучения тектонических процессов. Однако наиболее полные данные могут быть получены только с применением новых средств космической геодезии, быстрое совершенствование которых приведет в ближайшее время к широкому размаху геодинамических исследований.

Abstract

O.M.Ostach, L.P.Pellinen

SOME RESULTS OF INVESTIGATIONS ON THE EARTH CRUST DEFORMATIONS IN GEODYNAMIC TEST AREAS OF THE MAIN GEODESY AND CARTOGRAPHY ADMINISTRATION OF THE USSR COUNCIL OF MINISTERS (GUGK)

Some results of analysis of the crustal deformations determined in course of regular geodetic observations carried out by geodesists of the GUGK in special geodynamic test areas are presented and commented upon. Such test areas are layed out at tectonically active regions characterized by increased seismicity or availability of volcanic phenomena. The primary task of observations carried out consists in discovering and detailed studying of the temporal changes of various crustal deformations that take place prior to earthquakes and volcanic eruptions. Postseismic deformations must also be studied because they provide valuable information about the mechanisms of the earthquake focuses.

The examples presented in the paper illustrate clearly the fact that geodetic methods can be efficiently employed for tectonic process studies. At the same time further extension of our knowledge is only possible by employment of modern space geodetic techniques. Rapid improvement of these techniques will bring forth greater scope of geodynamic studies.

DOI: https://doi.org/10.2312/zipe.1989.102.03

I. Цели и задачи исследований на ГДП

По мере возрастания точности и оперативности геодезических измерений расширяется круг проблем, в решение которых существенный вклад может внести современная геодезия. Одной из таких проблем является изучение деформаций земной коры и изменений внешнего гравитационного поля Земли. Эта проблема геодинамики имеет непосредственное отношение к исследованию процессов развития земной коры и верхней мантии, отражающихся в движениях континентальных плит и внутриплитовых деформациях, изучению и прогнозированию землетрясений и извержений вулканов, а также сейсмотектоническому районированию отдельных территорий, важных с экономической точки зрения. Решение указанного круга задач требует проведения специально поставленных высокоточных геодезических измерений на обширных территориях, причем эти измерения должны выполняться с определенной регулярностью. Постановка такой работы возможна только на основе новейших средств наблюдений, появляющихся сейчас в арсенале космической геодезии. Таким образом, это дело самого ближайшего будущего.

Далее мы будем говорить о менее масштабных, но уже ведущихся в СССР работах геодинамической направленности, которые выполняются Главным управлением геодезии и картографии при Совете Министров СССР (ГУГК СССР) с целью изучения деформационных процессов, предваряющих и сопровождающих землетрясения, а также вызываемых техногенными причинами. Эти работы являются частью более обширных исследований по изучению и прогнозированию землетрясений, проводимых совместно с Академией Наук СССР. В данном случае повторные геодезические наблюдения ведутся на ограниченных территориях площадью порядка нескольких тысяч кв. километров, выбираемых с учетом специфики решаемой задачи. Такие специально выбранные территории, на которых созданы контролирующие геодезические построения и ведется регулярный комплекс высокоточных геодезических наблюдений, названы геодинамическими полигонами (ГДП). В зависимости от конкретных решаемых задач ГДП несколько различаются между собой.

DOI: https://doi.org/10.2312/zipe.1989.102.03

Геодинамические полигоны, созданные в сейсмоактивных районах страны, ориентированы в первую очередь на выявление и детальное изучение развития во времени различного вида аномальных деформаций земной поверхности, предваряющих землетрясения. Такие деформации квалифицируются как кинематические предвестники землетрясений.

Значение геодезических измерений в решении проблемы прогноза землетрясений основывается на весьма правдоподобном предположении о том, что столь грандиозное явление как землетрясение, приводящее в результате к очевидным смещениям земной поверхности, не может подготавливаться без каких-либо обнаруживаемых современными измерительными средствами деформаций. Эти деформации в каждый данный момент мало заметны, так как процесс накопления напряжений идет длительное время, измеряемое годами и десятилетиями, но само их существование в период подготовки землетрясений не вызывает сомнений. Задача, таким образом, состоит в исследовании характера их проявления.

Важной составной частью прогностических исследований является изучение смещений земной поверхности, возникающих в результате сильных землетрясений. Такие данные существенно дополняют информацию, необходимую сейсмологам для построения моделей очагов землетрясений, без чего невозможно продвижение вперед в понимании природы этих явлений.

Несколько иное назначение имеют ГДП, создаваемые в районах расположения крупных гидроэлектростанций с высотными плотинами. Предметом изучения здесь являются деформации земной поверхности, происходящие под действием дополнительной нагрузки больших масс воды, изменяющейся к тому же во времени (как при заполнении водохранилища, так и в период эксплуатации ГЭС). Известные в мировой практике явления так называемой "наведенной сейсмичности" придают этим наблюдениям и прогностический смысл.

В местах интенсивной добычи нефти и газа исследуется реакция земной поверхности на откачку указанных флюидов. Созданные там полигоны названы техногенными.

Изучение деформаций земной коры имеет также большое значение для определения общей направленности медленно происходя-

DOI: https://doi.org/10.2312/zipe.1989.102.03

щих тектонических движений криппового характера, что весьма существенно при сейсмотектоническом районировании отдельных территорий, перспективных для возведения крупных инженерных сооружений.

Наблюдения на созданных ГДП, как правило, выполняются специалистами производственных предприятий ГУГК СССР. Научно-методическое руководство работами осуществляет ЦНИИГАиК, который разрабатывает также методику обработки и анализа результатов. Непосредственная обработка результатов выполняется как в предприятиях, так и в ЦНИИГАиК.

Работы на ГДП имеют свою специфику, не позволяющую быстро получать интересующие нас результаты. Так как исследованию подлежат развивающиеся во времени процессы, то единственным средством фиксации их состояний являются периодически повторяемые циклы измерений. Для того чтобы обнаружить характерные особенности изучаемого процесса, требуется как минимум 3-4 цикла таких измерений, которые затем должны быть продолжены с учетом полученных результатов. Учитывая значительную стоимость высокоточных геодезических работ, а также точностные характеристики имеющихся у нас средств измерений, полные повторные циклы на большинстве ГДП выполняются с интервалом 3-5 лет. Для эффективного решения прогнозных задач необходимы, однако, более частые наблюдения, что экспериментально подтверждено уже полученными результатами. Поэтому на нескольких ГДП, которые выделены сейчас как исследовательские (ГДПИ), был сокращен интервал между повторными циклами измерений до двух лет, а также созданы на них локальные построения, где наблюдения выполняются с интервалом в несколько месяцев. Таковыми сейчас являются Алма-Атинский, Ферганский (включая район Ташкента), Петропавловск-Камчатский и Ашхабадский ГДПИ. Кроме того, локальные построения с повышенной периодичностью измерений существуют на ГДП Шеки-Кюрдамир в Закавказье, а также на ГДП ГЭС. В последнем случае наблюдения в периоды заполнения водохранилищ выполняются ежегодно.

Результаты работ на отдельных ГДП по мере накопления наблюдений обрабатываются и анализируются. В конце 1985 года в

DOI: https://doi.org/10.2312/zipe.1989.102.03

рамках совместной работы предприятий ГУГК СССР и ЦНИИГАиК под научно-методическим руководством последнего были по единой программе обобщены накопленные к этому времени материалы наблюдений и выполнен анализ деформаций на тех ГДП, где мы располагали необходимым объемом повторных измерений.

В этом докладе кратко сообщается о некоторых полученных результатах.

2. Некоторые результаты анализа деформаций земной поверхности на ГДП

Камчатка. Этот полуостров является уникальным объектом геодинамических исследований. Его положение вблизи зоны субдукции Еврпзийской и Тихоокеанской тектонических плит обусловило высокую вулканическую и сейсмическую активность. В этом регионе происходит около 80% всех сильных землетрясений в СССР. Сказанное определило создание здесь нескольких ГДП, нацеленных на изучение деформаций земной коры, обусловленных процессами вулканизма, а также аккумуляцией тектонических напряжений в зоне контакта тектонических плит. Эти ГДП созданы ГУГК СССР по предложениям Института вулканологии ДВНЦ АН СССР.

В качестве примера приведем результаты определения деформаций земной поверхности, полученные на Карымском ГДП, созданном в районе вулкана Карымский. Была поставлена задача изучить закономерности указанных деформаций в продолжении полного эруптивного цикла вулкана, который по данным вулканологов составляет 10-12 лет. Сравнительно небольшая продолжительность этого цикла позволила с хорошей детальностью охватить его измерениями. Четыре выполненных здесь цикла геодезических измерений (1975, 1977, 1981, 1983 г.г.) охватывают период, включающий активизацию вулкана, его извержение (1976 г.) и постепенное затухание вулканической деятельности вплоть до ее полного прекращения. На основе анализа имеющихся измерений установлено, что период наибольшей активности вулкана сопровождается интенсивным растяжением территории ГДП. Зона максимальных деформаций, достигающих величин $(+37 \pm 2{,}5)\cdot 10^{-6}$ (дилатация), смещена относительно конуса вулкана и совпадает с участком наибольшей сейсмической активности (см.рис.1). Прекращение активной вулканической

DOI: https://doi.org/10.2312/zipe.1989.102.03

деятельности приводит к обратному процессу, но с гораздо меньшими скоростями деформаций. Этот процесс едва наметился в интервале между третьим и четвертым циклами измерений и только последующие наблюдения могут показать, как он будет развиваться далее. Полученные данные представляют чрезвычайный интерес, ставя ряд вопросов, ответ на которые вулканологам еще предстоит найти. Обширность наблюдаемых деформаций одного знака говорит о значительных глубинах и размерах источника деформаций. По крайней мере их нельзя объяснить давлением в узком вертикальном канале вулкана, что могло бы представляться естественным.

Следует подчеркнуть, что столь детальные количественные данные о деформационных процессах в районе действующего вулкана могли быть получены только на основе специально поставленных высокоточных наблюдений.

Средне-Азиатский регион. Указанный регион был первым, где начали создаваться ГДП для изучения деформаций земной коры в связи с проблемой прогноза землетрясений. Он отличается высокой сейсмичностью, проявившейся в последнее столетие в форме нескольких катастрофических землетрясений. В связи с тем, что в этом регионе расположены крупные административные и промышленные центры с большой плотностью населения, на него обращено особое внимание. Здесь созданы наиболее активно функционирующие ГДП: Алма-Атинский, Ферганский, Фрунзенский, Газлийский, Душанбинский и некоторые другие, а также ГДП Токтогульской, Чарвакской и Нурекской ГЭС.

Как уже говорилось выше, важнейшей задачей геодинамических исследований является поиск и изучение развития во времени кинематических предвестников землетрясений, т.е. аномальных деформаций, которые предваряют возникновение сейсмических толчков. Такая задача может решаться только на основе максимально точных и достаточно частых повторных наблюдений. В настоящее время мы располагаем данными, позволяющими считать, что предвестниковые деформации фиксируются, по крайней мере, в результатах высокоточного нивелирования. Пространственно-временные графики вертикальных смещений по линиям на Алма-Атинском (рис.2) и Ферганском (рис.3) ГДП с нанесенными на эти графики

DOI: https://doi.org/10.2312/zipe.1989.102.03

моментами происшедших землетрясений довольно наглядно показывают это. Однако необходимо со всей определенностью подчеркнуть, что намеченная еще Ю.А.Мещеряковым схема предвестниковых деформаций реализуется не всегда и потребуются дополнительные продолжительные и кропотливые наблюдения, которые позволят установить ее статистическую значимость и внести необходимые коррективы.

Красноречивым примером надежной фиксации медленных тектонических деформаций являются схемы (рис.4), показывающие для Алма-Атинского ГДП развитие таких деформаций. Они зафиксированы двумя парами независимых циклов измерений. Наглядно видно сходство характера деформаций (звено северо-восточного простирания).

Выявленное измерениями общее сжатие в направлении северо-запад - юго-восток хорошо согласуется с представлениями тектоники плит о характере деформаций в Средне-Азиатском регионе (рис.5).

Чрезвычайно интересные и важные результаты получены при изучении распределения деформаций земной коры, явившихся следствием известных Газлийских землетрясений 1976 и 1984 г.г. Вследствие того, что эти землетрясения произошли в районе, где ранее был создан геодинамический полигон, удалось получить детальную картину распределения как вертикальных, так и горизонтальных деформаций. Схемы таких деформаций (рис.6) уже опубликованы в статье В.А.Пискулина и А.П.Райзмана "О деформациях земной поверхности в районе Газли" ("Геодезия и картография", 1985, № 9, с.53-57). Полученные данные являются надежной экспериментальной основой для изучения механизма очагов происшедших землетрясений. Они наглядно показывают также миграцию очагов в западном направлении, давая основания для прогнозирования мест будущих толчков. Следует отметить, что после землетрясения 1984 г. геодезические данные были первыми, позволившими систематизировать разрозненные геофизические наблюдения.

Кавказ и Карпаты. С точки зрения изучения развития молодых складчатых структур показательны результаты, полученные на ГДП Шеки-Кюрдамир, созданном в 1981 г. в Азербайджане в предгорьях Главного Кавказского хребта. Здесь на линии примерно

DOI: https://doi.org/10.2312/zipe.1989.102.03

меридионального направления длиной около 40 км поставлены режимные наблюдения с интервалом между циклами 2-3 месяца. Выполненные до середины 1986 г. 20 циклов повторного нивелирования были обработаны совместно с целью определения надежных значений скоростей вертикальных смещений земной поверхности (рис.7). Полученные результаты со всей определенностью указывали на направленный и устойчивый характер происходящих деформаций, соответствующих как будто бы изостатическому выравниванию территории. Обнаружена тесная обратная корреляция скоростей вертикальных движений и отклонений высот профиля линии от прямой. Привлечение геологических данных позволяет заключить, что указанный процесс четко отражен и в деформациях слоев горных пород. Продолжение наблюдений дало, однако, совершенно неожиданные результаты: последующие пять циклов измерений зафиксировали резкое изменение направленности движений. Наблюдаемое за этот период смещение полностью компенсировало накопившееся за предыдущий период (4,5 года) и даже превзошло его, вновь отразив особенности простирания слоем горных пород.

В качестве иллюстрации деформаций земной коры в районе Прикарпатья приведем результаты анализа двух циклов измерений на Кишиневском ГДП. Эти измерения выполнены в 1982-1984 г.г.

Выявленные горизонтальные смещения пунктов линейно-угловой сети довольно определенно распадаются на три группы, что, по-видимому, связано с принадлежностью этих групп пунктов к различным тектоническим блокам (рис.8). Указанный сейсмологами тектонический разлом хорошо вписывается в полученную картину, что, конечно, повышает ее достоверность. Более определенные выводы можно будет сделать после анализа наблюдений третьего цикла, который выполнялся в текущем году.

ГДП ГЭС. Изучен характер деформирования земной поверхности в районах ГЭС с высотными плотинами. К настоящему времени конкретные числовые данные получены для районов Ингури, Чиркейской, Чарвакской, Нурекской и Токтогульской ГЭС. Надежно фиксируется связь между изменениями уровня воды в водохранилище и изменением высотного положения реперов. На фоне изменений, объясняемых упругой отдачей, наблюдаются и отдельные аномалии.

DOI: https://doi.org/10.2312/zipe.1989.102.03

Примером последних являются интенсивные деформации в зоне Таласо-Ферганского глубинного разлома на ГДП Токтогульской ГЭС (рис.9 и I0). Эти деформации развиваются на участке протяженностью I5 км. Скорости вертикальных движений реперов этого участка достигают в отдельные периоды, а именно при максимальном уровне воды в водохранилище, 20 мм/год. Наиболее деформируемая часть участка близка к Таласо-Ферганскому разлому, как он намечен по тектоническим схемам, но точно не совпадает с ним. Нужно подчеркнуть, что в согласованном движении участвуют не отдельные репера, а значительные толщи верхних слоев земной коры.

Техногенные полигоны. В качестве примера развития техногенных деформаций приведена схема скоростей вертикальных смещений земной поверхности на Апшеронском полуострове, где уже много лет ведется разработка нефтяных месторождений. Эти результаты получены из совместной обработки нескольких циклов нивелирования, выполненных начиная с I949 г. (рис.II).

Существенное место в наших работах было отведено совершенствованию методов обработки наблюдений, выполняемых с целью определения деформаций земной коры. В итоге было разработано и в I985 г. опубликовано методическое пособие "Геодезические методы изучения деформаций земной коры на геодинамических полигонах". Оно содержит изложение существа разработанных к настоящему времени методов анализа деформаций на основе повторных геодезических измерений. Его основные результаты ориентированы на непосредственное практическое использование. Оно явилось основой для анализа деформаций, о котором говорилось выше.

DOI: https://doi.org/10.2312/zipe.1989.102.03

СХЕМА ДИЛАТАЦИИ Δ НА КАРЫМСКОМ ГДП (период 1983-1975)

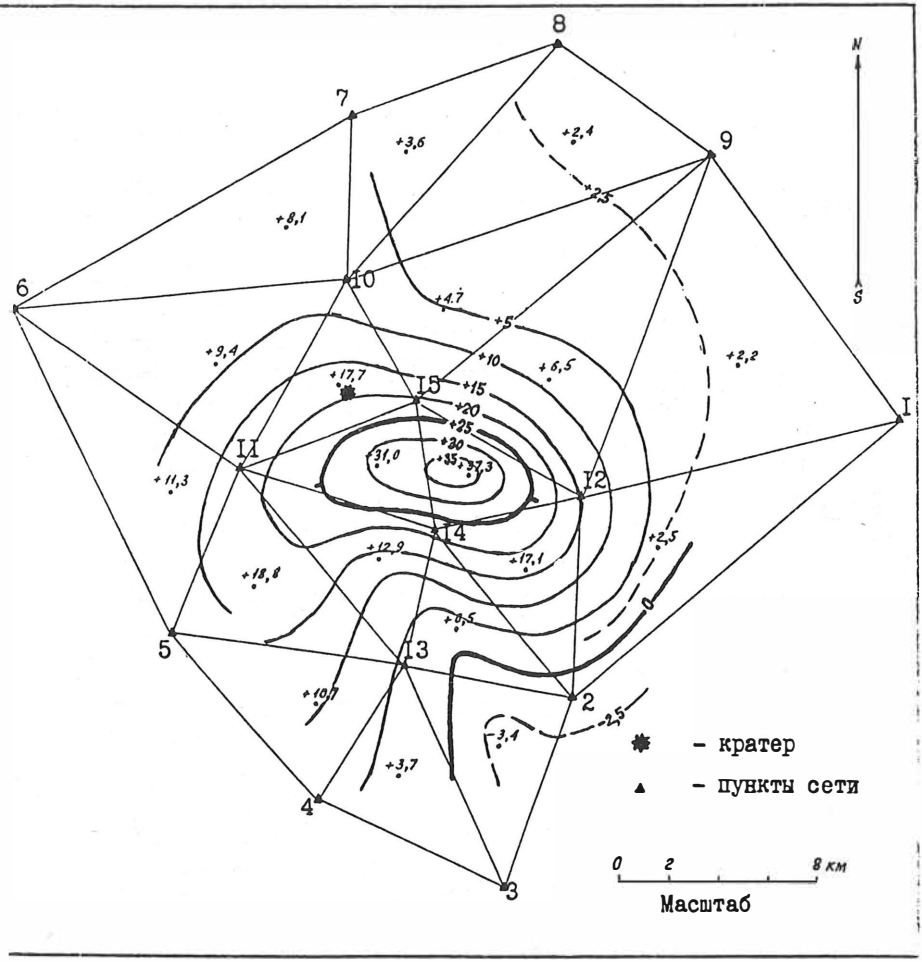

Изолинии проведены через $5 \cdot 10^{-6}$

Рис. I

DOI: https://doi.org/10.2312/zipe.1989.102.03

ПРОСТРАНСТВЕННО-ВРЕМЕННОЙ ГРАФИК СМЕЩЕНИЙ РЕПЕРОВ
Алма-Атинский ГДП

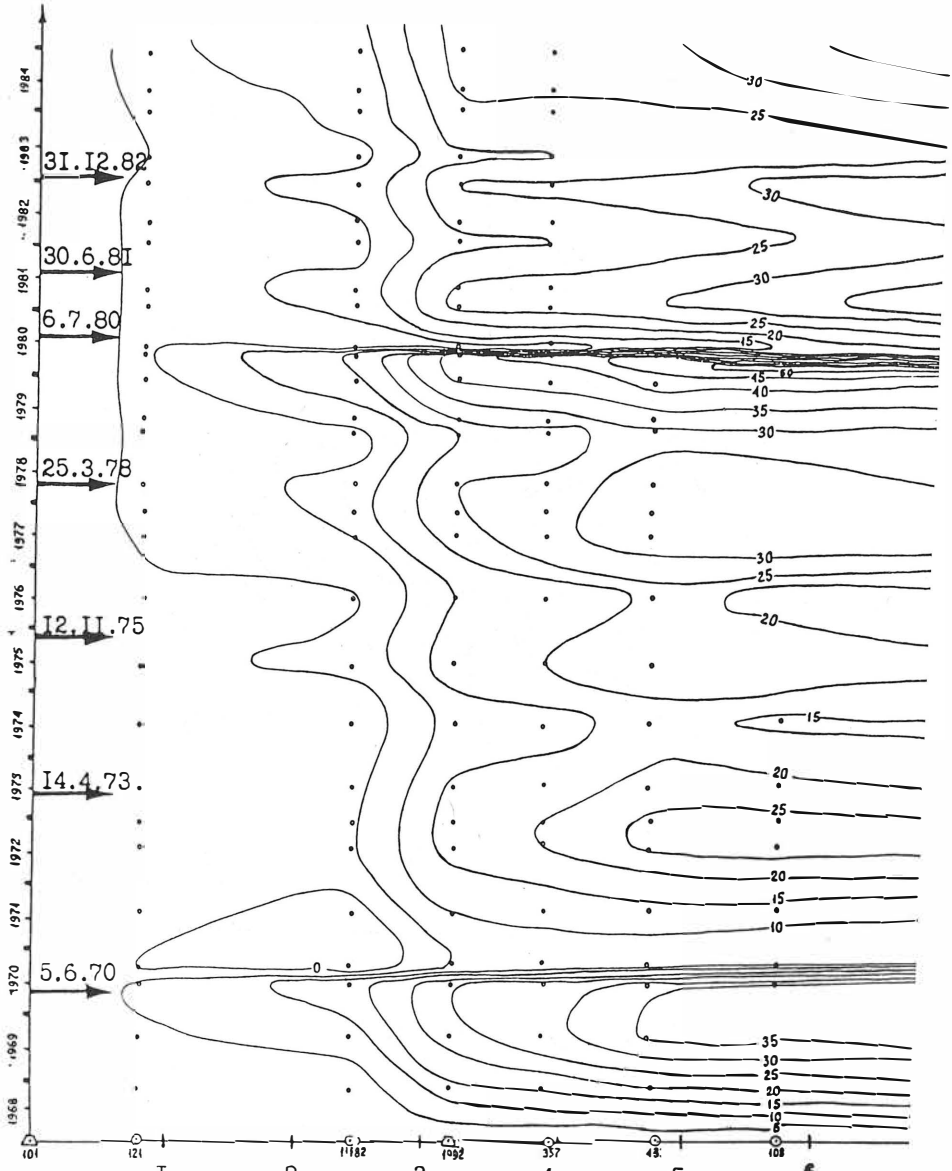

Высота сечения изолиний 5 мм

Рис.2

DOI: https://doi.org/10.2312/zipe.1989.102.03

ПРОСТРАНСТВЕННО-ВРЕМЕННОЙ ГРАФИК СМЕЩЕНИЙ РЕПЕРОВ
Ферганский ГДП

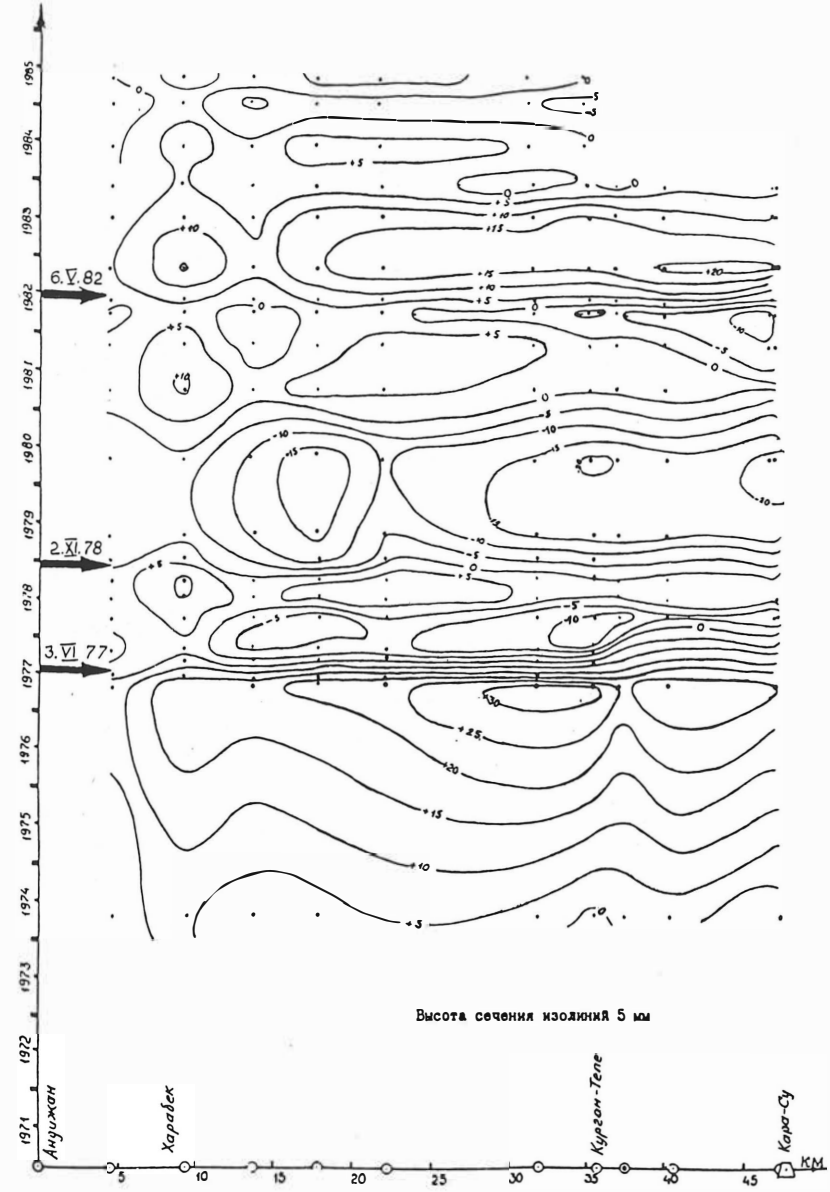

Рис.3

DOI: https://doi.org/10.2312/zipe.1989.102.03

СХЕМА ЛИНЕЙНО-УГЛОВОЙ СЕТИ АЛМА-АТИНСКОГО ГДП С КОМПОНЕНТАМИ ДЕФОРМАЦИЙ

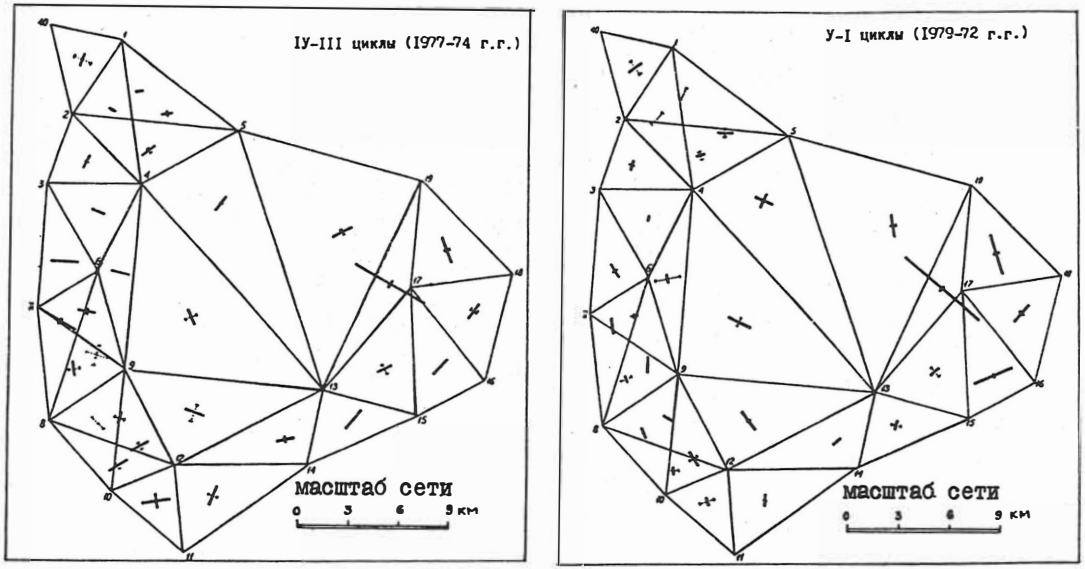

Условные обозначения:

Главные деформации E_1 и E_2 (▬ сжат., ▬ растяж.)

Масштаб компонент деформаций (в ед. 10^{-6})

0 10 20

Рис. 4

DOI: https://doi.org/10.2312/zipe.1989.102.03

СХЕМА ВЕКТОРОВ СМЕЩЕНИЙ НА АЛМА-АТИНСКОМ ГДП
(1979-1972)

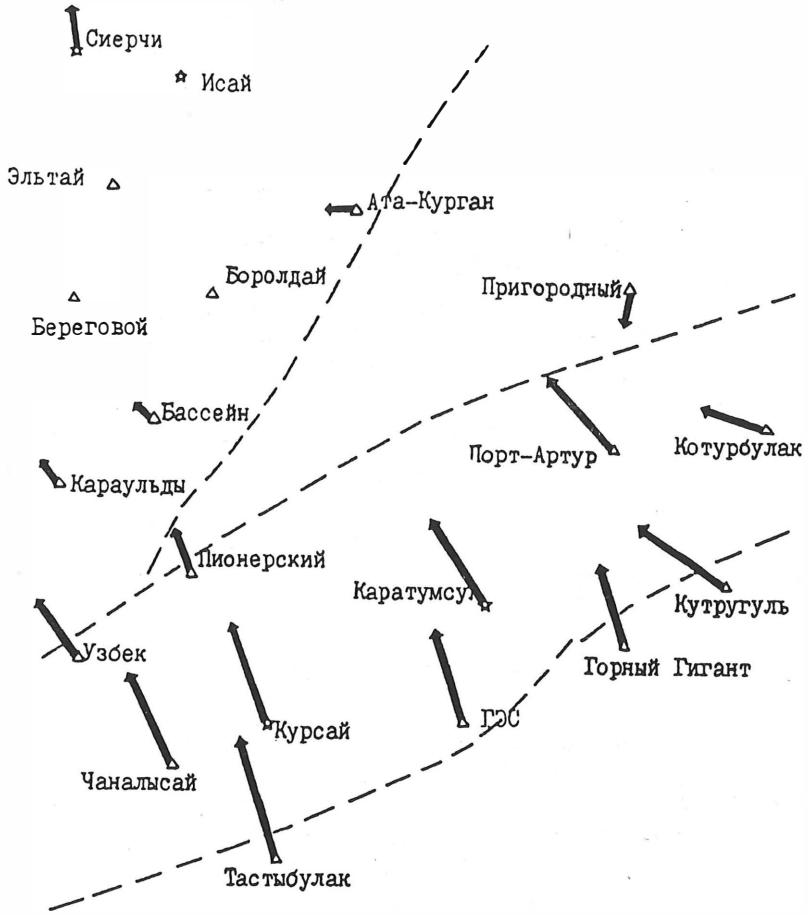

Масштаб I: 200 000

Условные обозначения

Глубинные разломы

Векторы смещений пунктов

0 2см 4см Масштаб векторов

Рис.5

DOI: https://doi.org/10.2312/zipe.1989.102.03

КАРТА ВЕРТИКАЛЬНЫХ ДЕФОРМАЦИЙ ЗЕМНОЙ КОРЫ
в эпицентральной зоне газлийских землетрясений

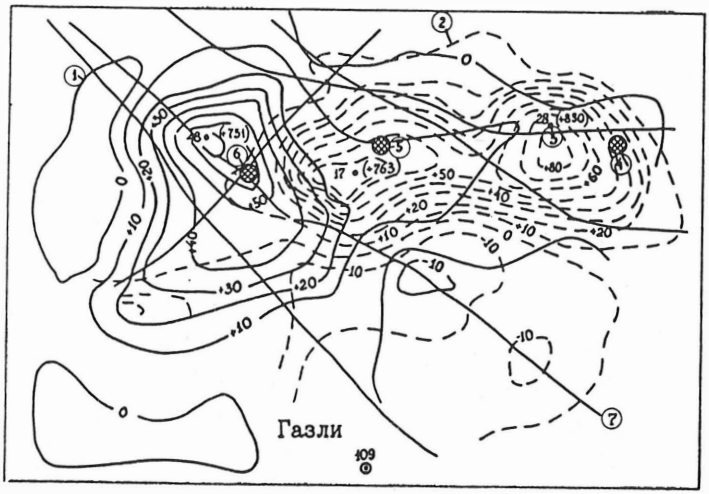

Ⅰ - изолинии равных верт.деформаций, проведённые через I0 см (I984 г.);
② - то же (I976 г.);
③ - характерный пункт нивелирования, его номер и относительное изменение высоты, мм;
④ - 8 апреля I976 г.
⑤ - эпицентры землетрясений I7 мая I976 г.
⑥ - 20 марта I984 г.
⑦ - разломы в земной коре.

Рис. 6

DOI: https://doi.org/10.2312/zipe.1989.102.03

DOI: https://doi.org/10.2312/zipe.1989.102.03

ВЕРТИКАЛЬНЫЕ ДЕФОРМАЦИИ ЗЕМНОЙ ПОВЕРХНОСТИ
на ГДП Шеки-Кордамир

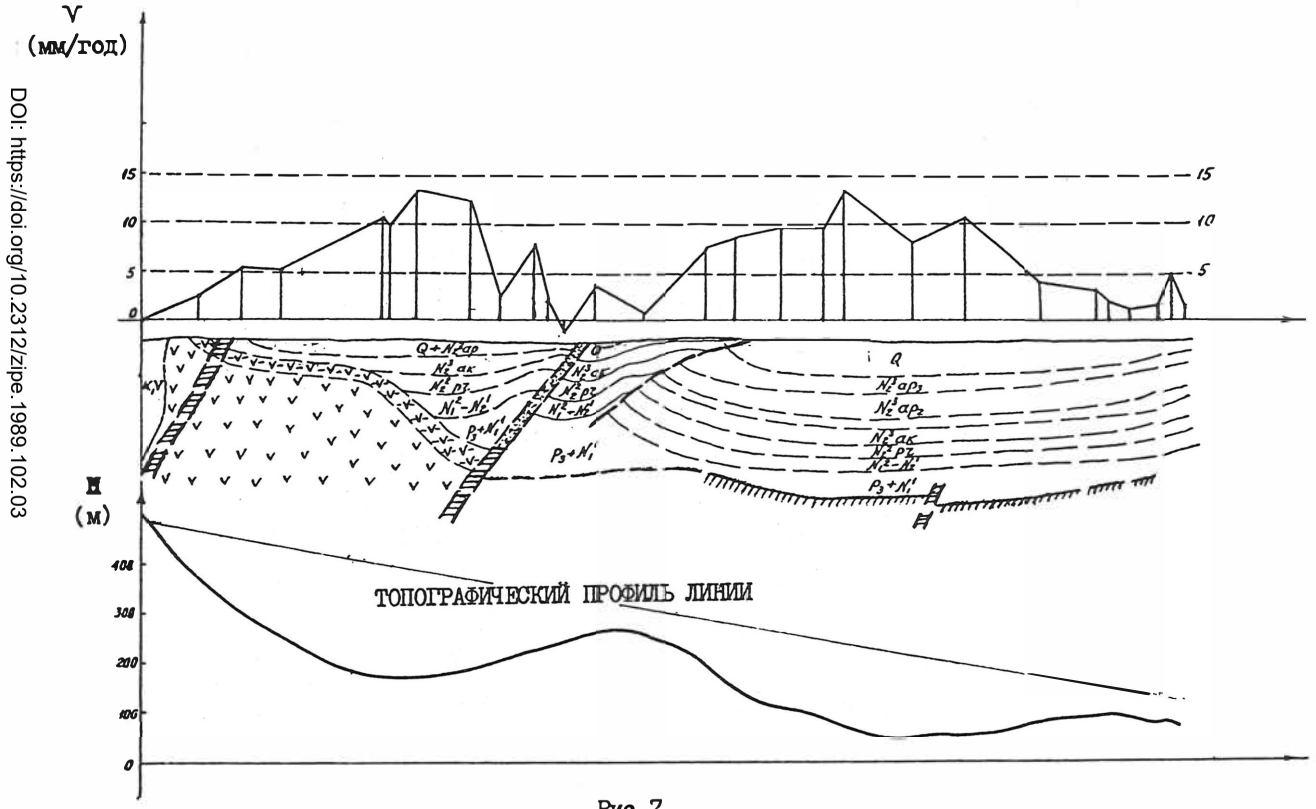

Рис.7

СХЕМА ГОРИЗОНТАЛЬНЫХ ДЕФОРМАЦИЙ
Кишинёвский ГДП

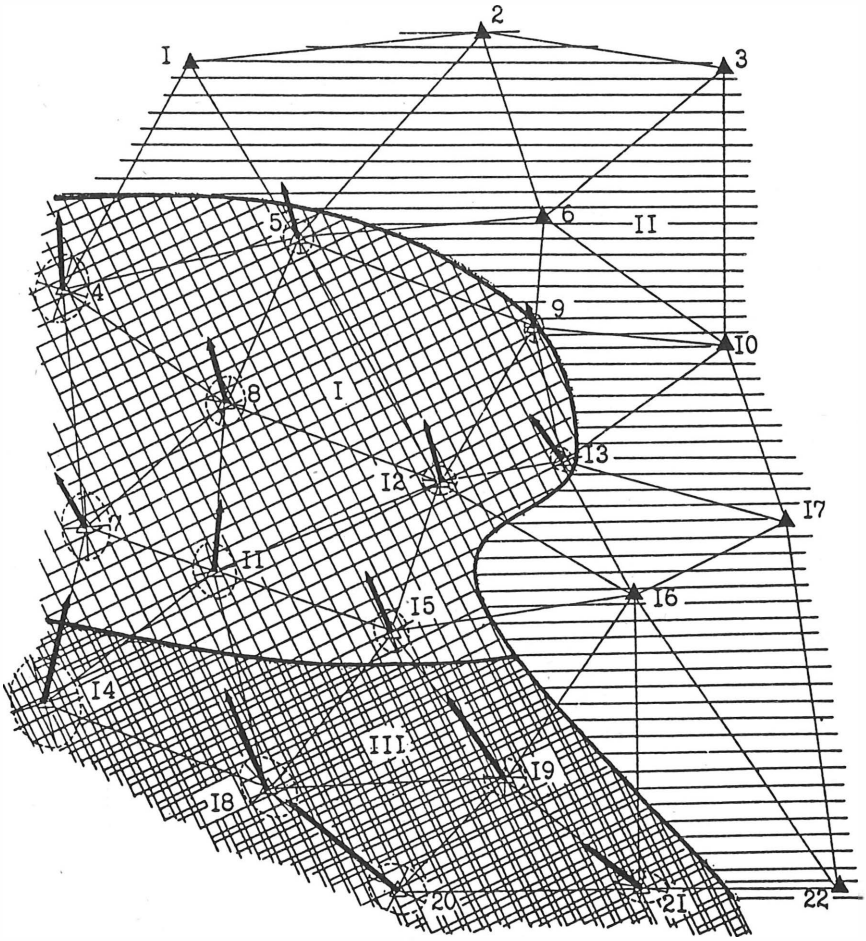

0 ——— 30 мм масштаб векторов

I, II, III- номера блоков

▲ - пункты, принятые за исходные.

Рис. 8

DOI: https://doi.org/10.2312/zipe.1989.102.03

ПРОСТРАНСТВЕННО-ВРЕМЕННОЙ ГРАФИК ВЕРТИКАЛЬНЫХ СМЕЩЕНИЙ

ГДП Токтогульской ГЭС

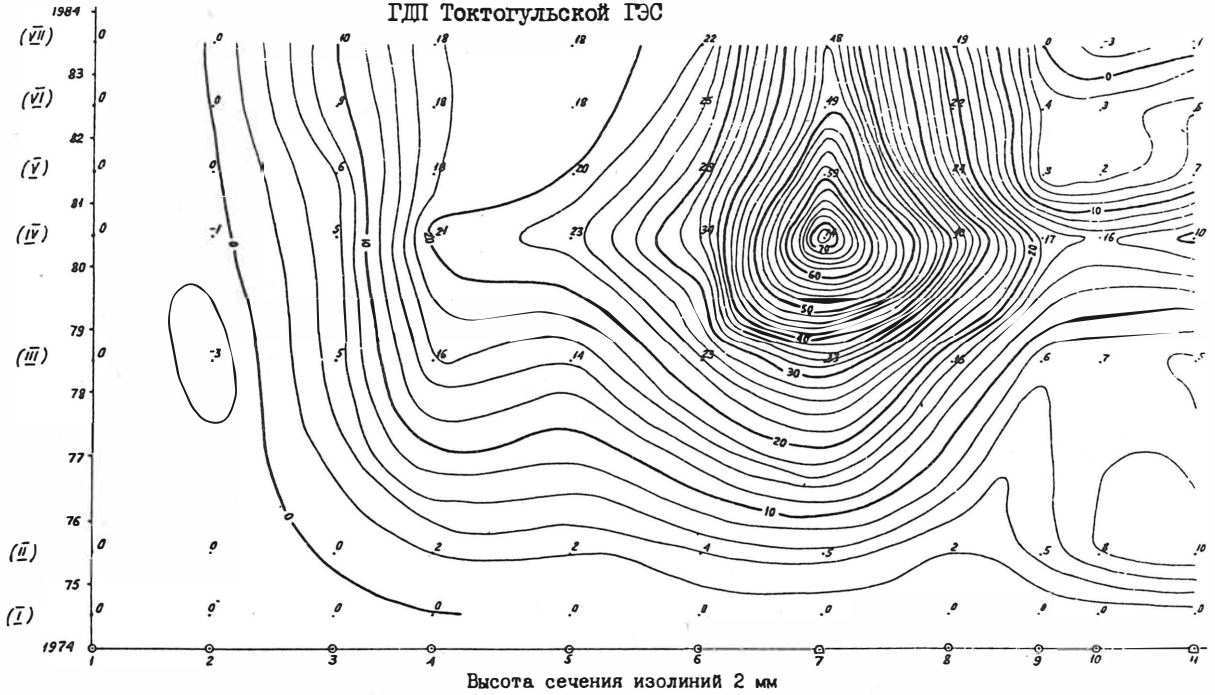

Высота сечения изолиний 2 мм

Рис.9

DOI: https://doi.org/10.2312/zipe.1989.102.03

ПРОСТРАНСТВЕННО-ВРЕМЕННОЙ ГРАФИК СКОРОСТЕЙ ВЕРТИКАЛЬНЫХ ДВИЖЕНИЙ

ГДП Токтогульской ГЭС

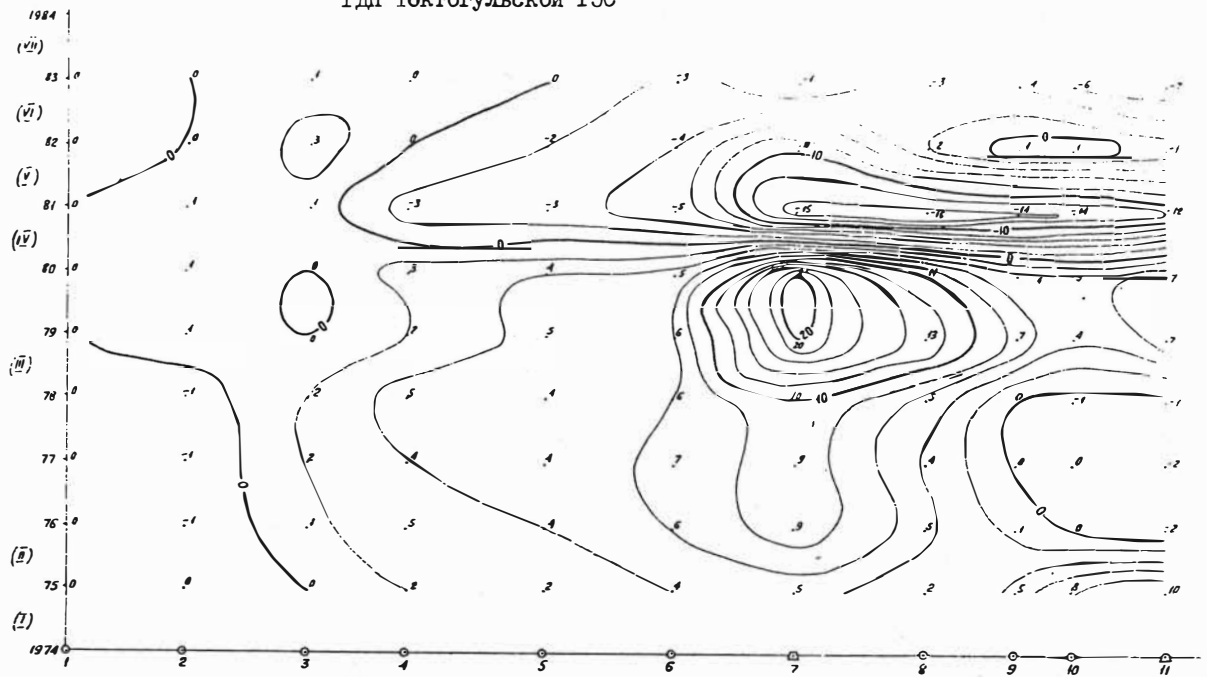

Высота сечения изолиний 2 мм/год

Рис. 10

DOI: https://doi.org/10.2312/zipe.1989.102.03

СХЕМА ВЕРТИКАЛЬНЫХ ДВИЖЕНИЙ ЗЕМНОЙ ПОВЕРХНОСТИ НА АПШЕРОНСКИЙ ПОЛУОСТРОВ

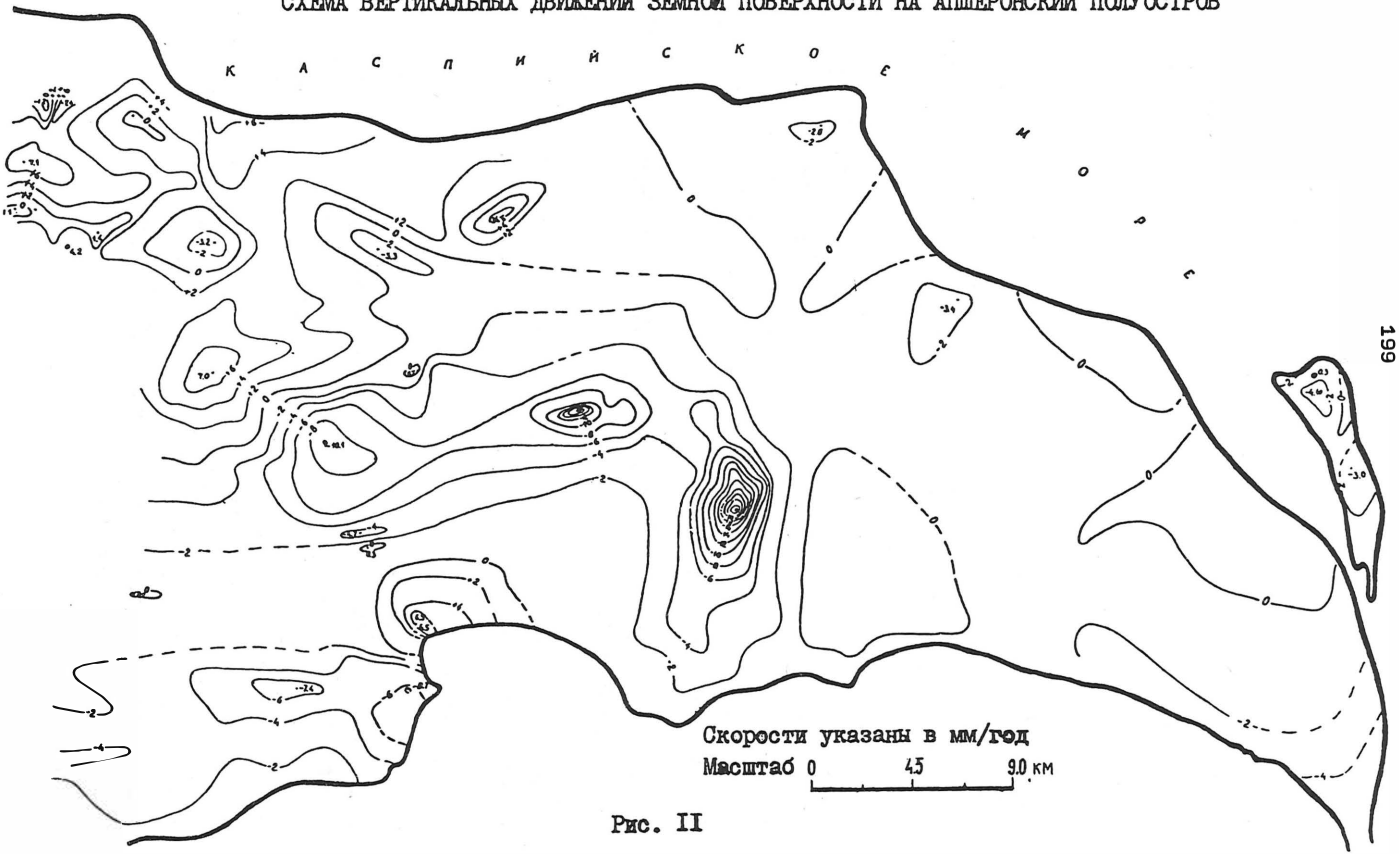

Рис. II

DOI: https://doi.org/10.2312/zipe.1989.102.03

FAULTING IN THE CONTINENTAL LITHOSPHERE AND MOVEMENTS IN THE NEAR-FAULT ZONES

S.I.SHERMAN
Institute of the Earth Crust, Siberian Branch of the USSR Academy of Sciences
Irkutsk, USSR

Abstract

Faulting in the lithosphere obeys physical laws of deformation and destruction of viscoelastic bodies. It is established that amplitudes of displacements along faults are functionally related with the fault length. The width of the zone of dynamic effect of the fault depends on the thickness of the deformed layer, its rheology and the state of stress. It is shown that the distribution of movements in such zones is irregular. Other relationships between main parameters controling the systematic fault net are discussed. It is underlined that it is reasonable to consider the factors, which "disturb" the crust movements near large faults.

РАЗВИТИЕ РАЗЛОМОВ КОНТИНЕНТАЛЬНОЙ ЛИТОСФЕРЫ И ДВИЖЕНИЯ В ПРИРАЗЛОМНЫХ ЗОНАХ

С.И.ШЕРМАН
Институт земной коры Сибирского отделения Академии наук СССР
Иркутск, СССР

Аннотация

Развитие разломов в литосфере подчиняется законам разрушения упруго-вязких тел. Установлено, что амплитуды смещений по разломам функционально связаны с их длиной, ширина зоны динамического влияния разломов зависит от толщины слоя деформирования, его реологии и условий нагружения. Показан дискретный характер распределения движений в зонах динамического влияния разломов, даны другие зависимости, определяющие регулярность сетки разломов земной коры. Акцентировано внимание на целесообразности учета факторов, "искажающих" наблюдаемые движения коры около больших разломов.

DOI: https://doi.org/10.2312/zipe.1989.102.03

Movements of the Earth's crust are most pronounced in fault zones. Irrespective of their age and morphogenetic type, faults are easily subjected to activation even in permanent stress fields and have considerable amplitudes of vertical and horizontal movements. Moreover, faults have the zones of their dynamic effect, movements of the crust within which are of complex and ambiguously interpreted pattern. They differ from crust movements associated with the geotectonic regime of the whole region.

Studying current crust movements by geodetic methods and interpreting recent geodynamic data, one should consider peculiarities of faulting and displacements within the limits of fault zones.

Undoubtedly, faulting in the continental lithosphere obeys physical laws of deformation and destruction in Maxwell viscoelastic body. Mapping shows that the continental fault net is systematic in directions, intervals between faults, their lengths, and in other factors. The exception is few global faults with the lengths over several thousands of kilometers. They are not always coordinated with the general orientation of lineaments, and their parameters sometimes disagree with those of other faults.

In this paper, I discuss the quantitative expression of systematic faulting in the continental crust that should be taken into account in geodynamic investigations, including the analysis of recent crust movements.

To describe physical peculiarities of faulting, quantitative criteria are used, that are parameters of faults, such as length, depth of penetration, amplitude of displacement, interval between parallel faults of commensurable length, width of the zone of their dynamic effect, and others.

The less studied and most important for the discussed problem is the parameter of the zone of dynamic effect of faults. It is a three-dimensional body surrounding the fault where plastic and fracture or elastic deformations result from fault development and displacements along the fault plane (Sherman et al., 1983). In plane it is an ellipsoid area within which the field of stress and deformation

DOI: https://doi.org/10.2312/zipe.1989.102.03

changes due to dynamic effect of the fault. The width of this zone depends on the morphogenetic type of the fault, the thickness of the layer or layers involved in deformation, the rate of deformation, rheology, and some other factors (Fig. 1).

Direct geologic methods generally give ambiguous values of the width of the zone of dynamic effect of the fault and do not reveal its dependence on other parameters of faults. Structural and other geological criteria affecting the width of this zone are studied by physical modeling (Sherman et al., 1983). This method allowed us to estimate ratios between the width of the zone of dynamic effect and the above-mentioned parameters of faults (Fig. 2). We extrapolated the obtained values on real geologic situations using the theory of similarity. We suggest that in the near-fault zone there are certain additional deformations,"disturbing" the general pattern of crust movements in the region. The width of the near-fault zone is suggested several tens or hundreds of meters for local faults and tens or a hundred of kilometers for global faults. Diagrams in Figure 2 show the principal factors regulating the width of the zone of dynamic effect of the fault.

It is important to know the real values of displacements and their relations with other parameters. Investigations of peculiarities of the Earth crust destruction show the existance of systematic relationships between parameters of faults, that are relatively uniform within large regions and most probably depend on geotectonic regimes.

The relationship between the length of faults and the amplitude of strike-slip displacement seems particularly interesting. Figure 3 shows the relationships between these parameters after V.V.Ruzhich and S.I.Sherman (1978). The diagrams are based on the results of structural mapping of metamorphic and igneous rocks, diverse in composition and age, in the Pribaikalje and Zabaikalje regions. Fault slips of several centimeters and hundreds of meters which are well fixed in the outcrops were measured, as well as the local and regional faults of some tens of kilometers, formed by tangential stress. It was established that amplitudes of displacement along the fault strike range from zero at the fault ends to a maximum

DOI: https://doi.org/10.2312/zipe.1989.102.03

value in its centre. Statistical analysis of the data reveals the correlation between the length of shear faults and the amplitude of displacement given by

$$a = 0.08\ L^{0.77}$$

where a is the amplitude of displacement in cm, L is the length of the fault in cm. The amplitude of displacement is 1-8 % of the fault length. This equation is applicable to the faults with the length up to tens of kilometers.

It is more difficult to obtain a similar ratio for longer faults, because they generally evolve over a significant period of time, during which the direction of displacement may have changed. Total displacement along great faults is a summary result of movements during several tectonic periods, when slip in the opposite direction was possible. With respect of these difficulties and probable ambiquity of results, we analyzed the parameters of a number of great faults. The ratio of the amplitude of displacement and the length of the faults over 75-100 km appeares to increase significantly. This tendency is rather stable.

We discuss this ratio on three examples of great faults. The Main Sayan fault evolving since the early Proterozoic is one of the largest faults in the East Siberia. It has 1000 km length and the amplitude of horizontal displacement from 40 to 80 km or 4-8 % of the fault length. The amplitudes of displacement are 10-25 % of the length of the Sikhote-Alin (L = 500 km, a = 120-140 km) and the Fudzino-Iman (L = 200-400 km, a = 40 km) faults (Pushcharovsky, 1972). Figure 3 shows the increase of the ratio a/L for higher values of the fault length and time of their development.

Faults of the late Cenozoic activation associated with great earthquakes are characterized by the other ratio a /L. The analysis of the data on the Gobi-Altai 1957 earthquake (Gobi-Altaiskoe ..., 1971), Anotolia, Caucasus, and Hindu-Kush (Nowroozi, 1971) shows that the ratio a /L is about 0.0001-0.0007 or 0.01-0.07 %.

Comparison of the above-mentioned data and the analysis of the curves (see Fig. 3) reveals that faulting is strongly de-

DOI: https://doi.org/10.2312/zipe.1989.102.03

pendent on the deformation rate. If tectonic stress is released quickly, i.e. by earthquakes, elastic properties of rocks predominate, brittle destruction occurs and the ratio a /L has small values. Slow and long-term realization of tectonic stresses induce processes of quasi-plastic deformation and even ductile flow. In this case, the contribution of brittle destruction in total displacement is considerably smaller. The ratio a /L increases.

On the whole, irrespective of tectonic development of the region, there appeares to be a general correlation between the length of faults and the amplitude of displacement given by

$$a = kL^b$$

where k and b vary within the ranges 0.01-0.08 and 0.8-1.2 respectively.

Thus, there is a correlation between displacement along strike-slip faults and their length and degree of their activation. Along the fault strike, the values of displacement change from a maximum in the centre to a minimum at the fault ends. However, this change is not uniform. Basing on physical experiments, V.A.Sanjkov and K.Zh.Seminsky (1988) reveal the distribution of amplitudes of displacement along faults in the elastic and viscoelastic models and compare it with the field observations (Fig. 4). The general statistic tendency of a maximum amplitude of displacement to the centre of the fault is well proved. At the same time, the discrete pattern of distribution of amplitudes along the fault strike is clearly observed.

Therefore, when studying the Earth crust movements and controlling measurement sites along great strike-slip faults, one should take into account irregular changes of absolute values of horizontal displacements, so that not to interpret them as specific properties of the crust movements. Considering crust movements a precursor of great earthquakes, we should locate an observation net in zones of dynamic effect of faults.

Going back to the zone of dynamic effect of the fault and the distribution of amplitudes of displacements, for instance

DOI: https://doi.org/10.2312/zipe.1989.102.03

horizontal ones, we clearly observe that across the strike of this zone, amplitudes of displacement grow from zero at the ends of the zone to a maximum value at the fault axis. Their distribution is not regular.

Let us discuss some other peculiarities of the Earth crust destruction, that are not so closely connected with crust movements.

In practical terms, among the parameters of a systematic net of faults the most important one is the interval or mean distance between subparallel faults of commensurable lengths. For a number of regions of the world, empirical relations between the interval and the length of faults were obtained (Fig. 5). In different regions, these analytical relationships slightly differ in values of coefficients of proportionality. For the whole Eurasia, this relationship is given by

$$\bar{M} = 4.5\ L^{0.45}\ \text{(in km)}$$

with the coefficient of correlation $r = 0.7 \pm 0.3$. 161 measurements were used for $50 < L < 650$ km.

The interval between faults of the same range of length depends on the distribution of stress fields and the thickness of deformed layers. Without examining the physics of the process of deformation, we suggest the general relationship between the interval M and the fault length L given by the following equation :

$$M = kL^{c}$$

where k and c are the coefficients of proportionality that vary within the ranges 0,3-0.5 and 0.5-0.95 respectively. These data should be taken into account for location of stationary nets for observation of the Earth crust movements.

General pattern of faulting is strongly affected by the relation between the length and the number of faults (Sherman, 1977)(Table 1), as well as the distribution of the Earth crust blocks according to their size (Sadovsky et al., 1987). Special attention should be given to recent studies of faulting in permanent stress fields. A.N.Adamovich (1988) presents a theoretical model of this process and proves the above-

DOI: https://doi.org/10.2312/zipe.1989.102.03

mentioned suggestion of irregular time-pattern of development of seismogenic faults in a permanent stress field (Fig. 6). The obtained data show that even in weak permanent stress fields, dynamic equilibrium of environment is periodically disturbed and activation of faults takes place in long time intervals. Rate of activation, its increase, and the release of tension itself are not regular in time.

Thus, zones of dynamic effect of faults are characterized by the ununiform distribution of horizontal and vertical displacements in time and space. Values of these displacements and their deviations from a general regional pattern of the crust movements depend on the scale of faults, the stage of development of the deformation cycle, and other factors associated with physical laws of destruction of elastic and viscoelastic bodies. Geologic formations and peculiarities of geologic situations in the region are of minor importance. They determine the state of the substance and sources of deformation.

Movements of the Earth crust and the whole lithosphere are one of the principal criteria of recent geodynamics of the lithosphere. It is natural that analysis of the crust movements and establishement of their relations with a complex of other geological processes and structures are given much attention. Amplitudes and rates of displacements are indices of activity of recent crust movements which characterize current geodynamic situation.

Absolute values of the crust movements increase or decrease, depending on the zone of dynamic effect of the fault and other quantitative factors of faults. With respect of aims of investigations, one should exclude the zones of dynamic effect of the faults from the analysis or study them for a more precise evaluation of processes, for example, displacements before earthquakes.

Now it seems possible to eliminate some errors in evaluation of amplitudes and rates of displacements because of peculiarities of the crust movements in the zones of dynamic effect of faults. Modern tectonophysical concepts of

DOI: https://doi.org/10.2312/zipe.1989.102.03

faulting in the continental lithosphere and kinematics of movements along faults should be considered for correct interpretation of displacements in the near-fault zones and other processes.

Literature

Adamovich A.N. Matematicheskoe modelirovanie tektonicheskoj aktivnosti razlomov. Irkutsk, Institute of the Earth Crust, 1988, 17 p. (in Russian).

Gobi-Altaiskoe zemletryasenie. Moskva, Izdatelstvo Akademii nauk SSSR, 1963, 391 p. (in Russian).

Nowroozi A.A. Seismotectonics of Persian Plateau, Eastern Turkey, Caucasus and Hindu-Kush regions. Bull. Seismol. Soc. Amer., 1971, v. 61, No. 2, pp. 317-343.

Pushcharovsky Yu.M. Vvedenie k tektonike Tikhookeanskogo segmenta Zemli. Moskva, Nauka, 1972, 222 p. (in Russian).

Ruzhich V.V. and Sherman S.I. Otsenka svyazi mezhdu dlinoj i amplitudoj razryvnykh narushenij. In : Dinamika zemnoj kory Vostochnoj Sibiri. Novosibirsk, Nauka, 1978, pp. 52-57 (in Russian).

Sadovsky M.A., Bolkhovitinov L.G. and Pisarenko V.F. Deformirovanie geofizicheskoj sredy i seismicheskij protsess. Moskva, Nauka, 1987, 100 p. (in Russian).

Sanjkov V.A. and Seminsky K.Zh. Analiz smeshchenij po razryvam v zone formiruyushchegosya transformnogo razloma. Geologiya i razvedka, 1988, No. 4, pp. 10-18 (in Russian).

Sherman S.I. Fizicheskie zakonomernosti razvitiya razlomov zemnoj kory. Novosibirsk, Nauka, 1977, 101 p. (in Russian).

Sherman S.I., Bornyakov S.A. and Buddo V.Yu. Oblasti dinamicheskogo vliyaniya razlomov. Novosibirsk, Nauka, 1983, 111 p. (in Russian).

Sieh K.E. Slip along the San Andreas fault associated with the great 1857 earthquake. Bull. Seismol. Soc. Amer., 1978, v.68, No. 5, pp. 1421-1448.

DOI: https://doi.org/10.2312/zipe.1989.102.03

Table 1

RELATIONSHIPS BETWEEN MAIN PARAMETERS OF FAULTS IN THE EARTH CRUST

Main parameters	Relations between them	Coefficients of proportionality
Width of the zone of dynamic effect of faults M in m for strike-slip faults (1), normal faults (2), and thrusts (3)	$M = aH + b \lg\eta + c \lg V$	$a_1 \sim 1.0\text{-}1.5$ $a_2 = 0.9\text{-}1.0$ $a_3 = 1.0$ $b_{1,2,3} = 0.004\text{-}0.009$ $c_{1,2,3} = 0.003\text{-}0.009$
Amplitude of displacement a in km with respect to the fault length L in km	$a = kL^b$	$k = 0.01\text{-}0.08$ $b = 0.8\text{-}1.2$
Interval m in km between faults of a given length L in km	$m = kL^c$	$k \sim 0.3\text{-}0.5$ $c \sim 0.5\text{-}0.95$
Length L and number of faults N in the regions with similar geotectonic regimes	$L = a / N^b$	a-depends on length of faults $b \sim 0.4$

DOI: https://doi.org/10.2312/zipe.1989.102.03

FIGURE CAPTIONS

S.I.Sherman. Faulting in the continental lithosphere and movements in the near-fault zones

Fig. 1. Morphogenetic types of faults and zones of dynamic effect of strike-slip faults (type I) (a), normal faults (b), strike-slip faults (type II) (c), and thrusts (d).

Fig. 2. Width of the zone of dynamic effect of faults M versus the model thickness H_m(1), its viscosity in Pa•s (2), and deformation rate V in ms^{-1} (3) for strike-slip faults (type I) (I), thrusts (II), normal faults (III), and strike-slip faults (type II) (IV).

Fig. 3. Relations between length of strike-slip faults and amplitudes of displacements along shear joints and strike-slips (1) and seismically active wrench faults (2).

Fig. 4. Distribution of amplitudes of displacements along faults in the elastic (1) and viscoelastic (2,3,4) models (after V.A.Sanjkov and K.Zh.Seminsky, 1988) and along the San Andreas fault, 1857 earthquake (after K.E.Sieh, 1978) (5).

Fig. 5. Interval between faults versus fault length in the Baikal rift zone (a), Altai-Sayan folded region (b), East African rift zone (c), and Eurasian plate (d).

Fig. 6. The model of fault development in a permanent stress field (after A.N.Adamovich, 1988). Nondimentional curves show time-dependent depth of penetration of the fault (a) and rate of increase of penetration depth versus time (b).

DOI: https://doi.org/10.2312/zipe.1989.102.03

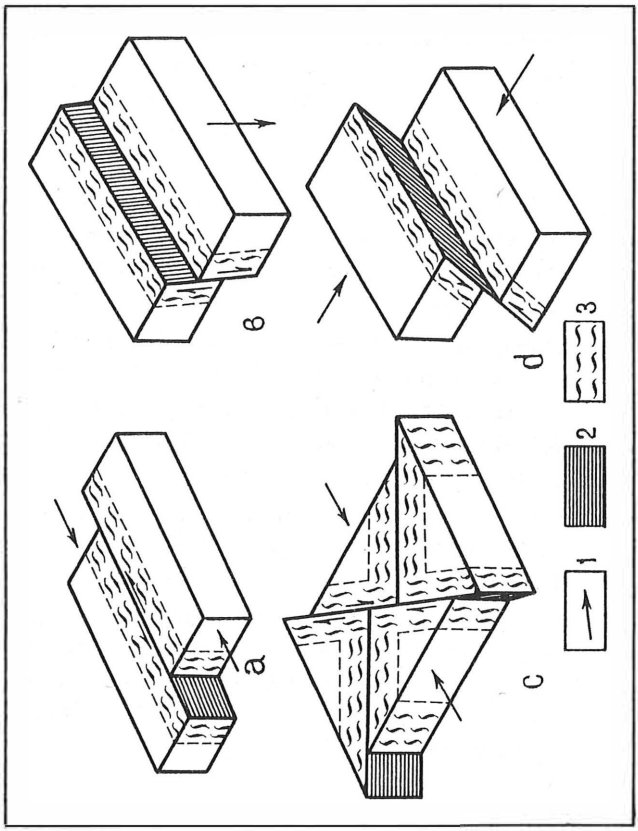

Fig.1

DOI: https://doi.org/10.2312/zipe.1989.102.03

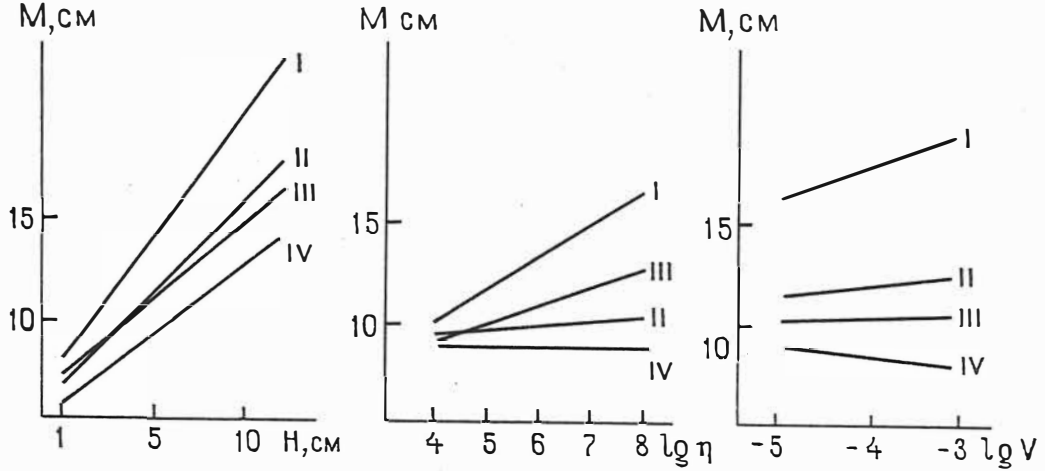

Fig.2

DOI: https://doi.org/10.2312/zipe.1989.102.03

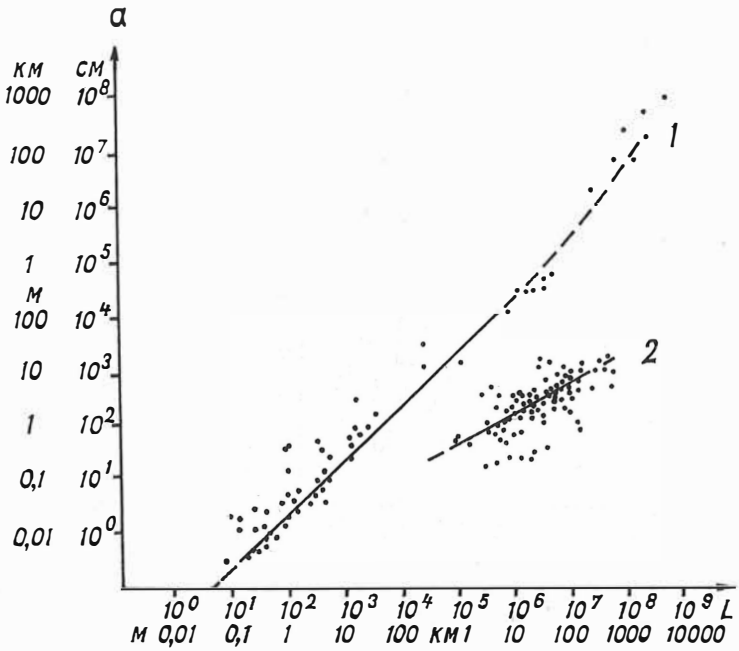

Fig. 3

DOI: https://doi.org/10.2312/zipe.1989.102.03

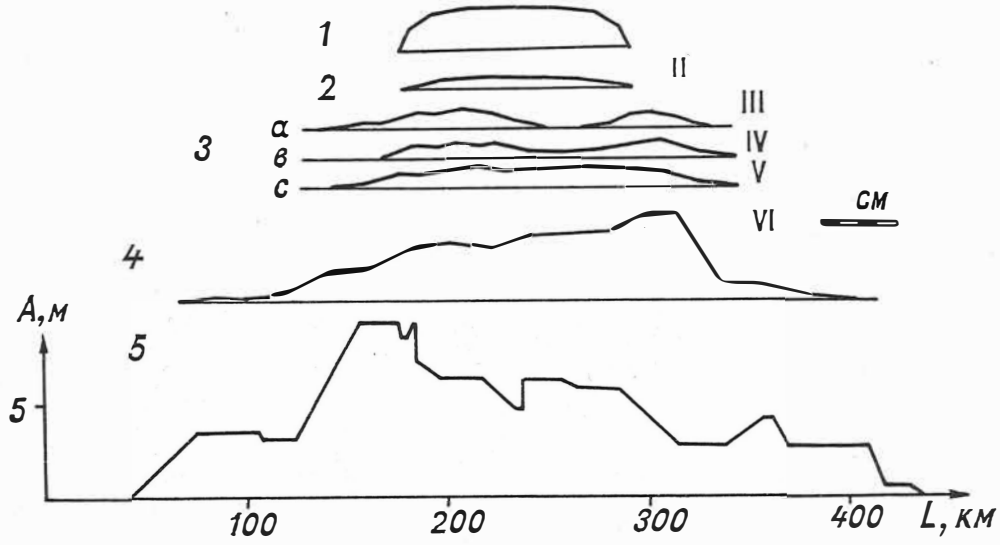

Fig. 4

DOI: https://doi.org/10.2312/zipe.1989.102.03

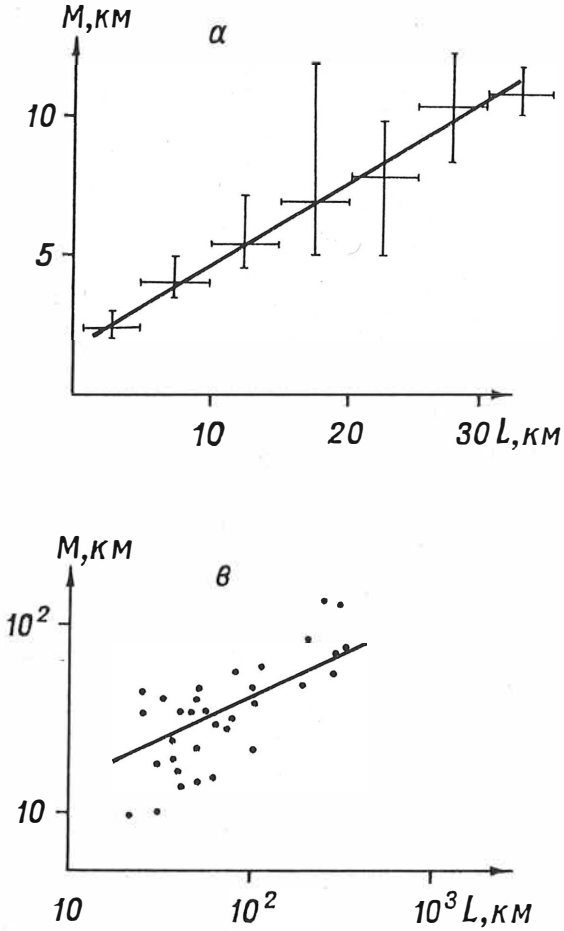

Fig.5

DOI: https://doi.org/10.2312/zipe.1989.102.03

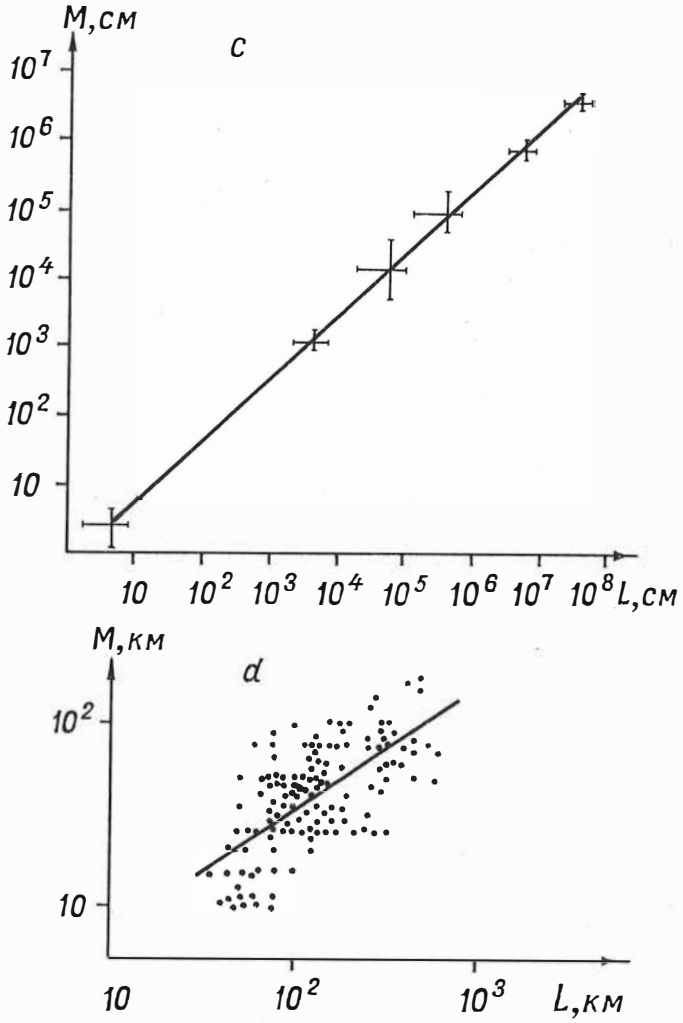

Fig. 5

DOI: https://doi.org/10.2312/zipe.1989.102.03

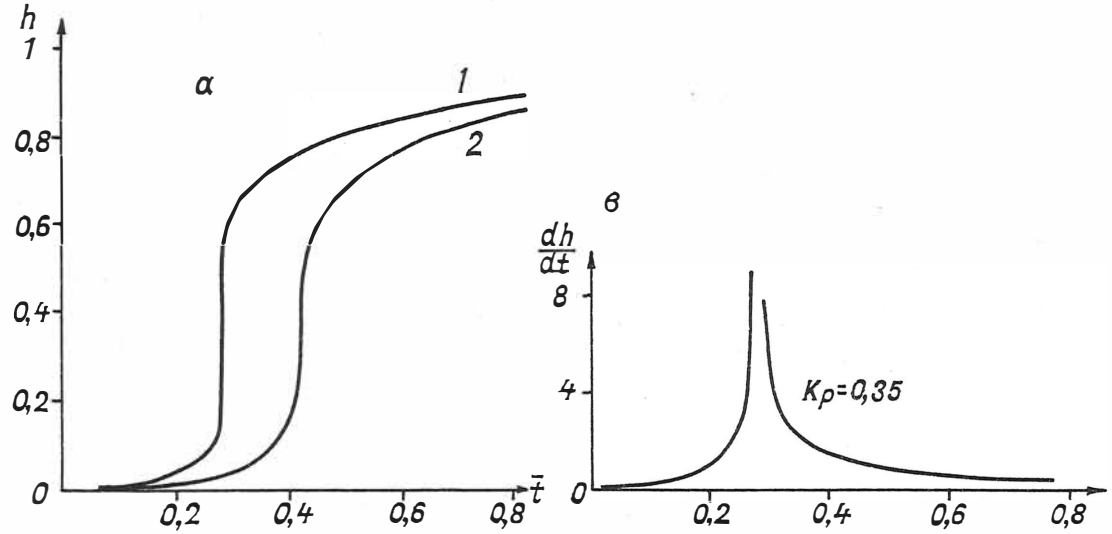

Fig. 6

DOI: https://doi.org/10.2312/zipe.1989.102.03

ИССЛЕДОВАНИЕ ДЕФОРМАЦИОННЫХ ПРОЦЕССОВ ВБЛИЗИ ВРАНЧЕСКОЙ ОЧАГОВОЙ ЗОНЫ ВЫСОКОТОЧНЫМИ НАКЛОНОМЕРАМИ

Шляховый В.П.*, Черный В.И.**
Островский А.Е.***

С 1983 г. под Кишиневом на глубине 75 м действует наклономерная станция сейсмопрогностической направленности. Наблюдения выполняются высокоточными наклономерами. Исследуются: земные приливы, спектры в дробносуточных диапазонах, наклоны - предвестники Вранческих землетрясений.

При современных геофизических исследованиях, связанных с изучением деформационных процессов на земной поверхности, важное место занимают наклономерные измерения. Они широко используются при исследованиях земноприливных явлений, резонансных эффектов внутреннего ядра Земли, блоковой структуры земной коры и верхней мантии и пр. Очень важное значение этот метод приобретает в связи с усилившейся в последнее время разработкой научных и практических вопросов проблемы прогноза землетрясений. Связано это с тем, что по своей природе наклономерные измерения относятся к классу деформационных методов изучения геофизических явлений, а, как следует из литературных данных [I], именно

* Полтавская гравиметрическая обсерватория Института геофизики им. С.И. Субботина АН УССР.

** Молдавская опытно-методическая партия Института геофизики и геологии АН МССР.

*** Институт физики Земли им. О.Ю. Шмидта АН СССР.

DOI: https://doi.org/10.2312/zipe.1989.102.03

деформационные методы имеют наибольшую информативность и надежность по отношению к предвестниковым явлениям, генерируемых аномальным напряженно-деформируемым состоянием глубинных пород очаговых зон. Естественно, наблюдения наклонов земной поверхности наряду с другими высокоточными измерениями составляют неотъемлемую часть любой реальной программы поиска предвестников землетрясений. Сейчас такие наблюдения проводятся практически во всех сейсмоактивных зонах мира. Причем, если раньше наблюдения велись на единичных наклономерных пунктах, то сейчас в каждом сейсмопрогностическом регионе должно предусматриваться создание сетей таких станций.

Юго-западная часть территории Украины и Молдавии, примыкающие к Вранческой сейсмогенной очаговой зоне, относятся к одним из наиболее сейсмоопасных регионов европейской части СССР. Поэтому проблема прогнозирования землетрясений здесь имеет важное значение и для ее решения разработана и осуществляется научная программа. В рамках этой программы предусмотрено развитие широкой сети комплексных станций режимных наблюдений за поведением различных геофизических полей, вариации которых могут служить предвестниками землетрясений. Проведение высокоточных наклономерных наблюдений - важная составная часть этой программы, в связи с чем начато создание сети наклономерных пунктов.

Станция "Кишинев", введенная в действие в конце 1983 г., является первым пунктом такой сети. Организована она совместно Полтавской гравиметрической обсерваторией АН УССР и Молдавской опытно-методической партией ИГГ АН МССР. Станция оснащена современными высокоточными наклономерами автокомпенсационного типа, разработанными в ПГО АН УССР. Чувствительная к наклонам аппаратура установлена на глубине свыше 75 м от дневной поверхности в

DOI: https://doi.org/10.2312/zipe.1989.102.03

тупиковом штреке шахты по добыче известняка. Здесь имеются достаточно стабильные внешние условия, что обеспечило высокую помехозащищенность измерительных каналов. В нас нет возможности останавливаться на описании условий наблюдений и используемого наклономерного оборудования. Эти вопросы отражены в работах [2,3]. Заметим только, что, исключая установочный период и редкие случайные сбои в работе наклономеров по организационно-техническим причинам, весь измерительный комплекс обеспечивает высококачественную регистрацию наклонов земной поверхности. Имеется возможность дальнейшего улучшения качества наблюдательного материала: если сейчас достигнуто разрешение до 0,1 мс. (по деформациям это соответствует 10^{-10}), то в недалеком будущем чувствительность регистрации будет увеличена еще на 0,5 порядка и более. С момента ввода станции сейчас уже накоплен значительный объем экспериментального материала пригодного для изучения геофизических эффектов деформационного типа. Ниже представлены результаты исследований земных приливов, спектрального состава наклонов в дробносуточном диапазоне, а также случаев аномального поведения наклонов-деформаций перед сильными землетрясениями.

Земные приливы

Имеется несколько аспектов в исследованиях земных приливов по наклономерных наблюдениях. Одна из основных задач при таких исследованиях заключается в получении экспериментальных данных, характеризующих распределение амплитуд и фаз главных волн земного прилива в неисследованных ранее регионах земной поверхности. Это позволяет исследовать упругие свойства Земли в региональном и глобальном масштабах, а также возможные вариа-

DOI: https://doi.org/10.2312/zipe.1989.102.03

ции этих свойств от региона к региону. Не менее важной по значению задачей, решаемой при таких исследованиях, по нашему мнению, является изучение нелинейных и неупругих эффектов внутрикорового и мантийного происхождения. Практическое и научное значение этих исследований исключительно важно для физики очаговых зон землетрясений [4,5]. При земноприливных исследованиях могут также рассматриваться и другие актуальные задачи геодинамики.

Параметрами, характеризующими упругость Земли, являются амплитудный фактор γ и фазовое запаздывание $\Delta\varphi$. Для их определения данные наклономерных наблюдений были разбиты на месячные серии и подвергнуты гармоническому анализу методом Матвеева [6]. По полученным месячным значениям параметров γ и $\Delta\varphi$ вычислены средневекторные величины для 8 главнейших приливных волн суточного и полусуточного диапазонов. Такие вычисления пока проведены по материалам первого двухлетнего ряда наблюдений. Анализ полученных результатов показывает, что по всем волнам получены достаточно надежные значения упругих параметров, которые для одного любого направления взаимно согласованы. С наиболее высокой точностью ($\sim 0{,}5\%$) они определены для волны M_2: направление В-З - $\gamma = 0{,}699$; $\Delta\varphi = 5{,}46^{\circ}$, направление С-Ю - $\gamma = 0{,}576$; $\Delta\varphi = -15{,}33^{\circ}$. Как видим, упругие параметры в направлении В-З соответствуют аналогичным величинам, полученным экспериментально на территории Украины [7], а также глобальным значениям этого параметра. Значения параметров в направлении С-Ю существенно отличаются от своих глобальных значений. Отличие это столь значительно, что явно выходит за пределы возможных ошибок. Наличие значительной аномалии земноприливных парамет-

DOI: https://doi.org/10.2312/zipe.1989.102.03

ров свидетельствует о аномально большой податливости породного массива на ст. "Кишинев" в направлении С-Ю. Вероятными причинами появления этих аномалий могут быть следующие факторы: близлежащие разломы, влияние Врачской очаговой зоны и эффект полости. Для выяснения причин аномалий требуются дополнительные исследования.

Спектральный состав наклонов исследовался преимущественно с целью выделения гармоник на неприливных частотах (например, нелинейных гармоник земноприливного происхождения), а также изучения характера распределения упругой энергии деформаций в дробносуточном диапазоне. Для анализа массивы данных разбивались на 6-месячные серии. По ним вычислялись спектры Фурье, а затем и энергетические спектры. Они вычислялись по данным наблюдений в обоих направлениях. Результирующий энергетический спектр в направлении В-З представлен на рис. I. Из него видно, что на некоторых участках дробносуточного диапазона имеются гармоники, заметно выделяющиеся на общем фоне. В третьсуточном и более высокочастотных диапазонах помимо земноприливной волны M_3. заметно выделяются гармоники неприливного происхождения. Наиболее сильно выделяются компоненты с частотами кратными солнечному циклу (45,0; 60,0; 75,0 град/час,...).
Указанные гармоники имеют солнечное происхождение. Причины их появления достоверно не установлены и требуются дополнительные исследования для их выяснения, хотя можно высказать ряд предположений об этом [4,5,8,9].

Главным направлением наклономерных исследований в Кишиневе является решение сейсмопрогностических задач. При наклономерных наблюдениях перед землетрясениями могут регистрироваться необычные деформационные процессы. Часть из них можно использо-

DOI: https://doi.org/10.2312/zipe.1989.102.03

вать в качестве предвестников землетрясений. Для долгосрочного и среднесуточного прогноза уже используются или предполагается использовать данные о ходе медленных наклонов земной поверхности, вариации амплитудных параметров главных приливных волн и пр. Для целей оперативного прогноза пригодны к использованию короткопериодные аномалии в наклонах, имеющие различный характер, а именно, бухтообразные и флуктуирующие наклоны, аномалии в поведении комбинационных гармоник, обязанных нелинейному взаимодействию в земноприливном сигнале и др.

Так как все перечисленные предвестниковые эффекты имеют вероятностно-статистический характер и пока не подтверждены экспериментально, то основной задачей первого этапа настоящих наблюдений является обнаружение и выделение наиболее достоверных предвестниковых эффектов, изучение их характерных особенностей. Поэтому при анализе материалов наблюдений приоритет здесь отдан изучению относительно краткосрочных деформационных процессов, имевших место в пределах от нескольких часов до $2^x - 3^x$ суток перед землетрясениями. Такие аномалии часто обнаруживаются перед местными (Вранческими) землетрясениями. Регистрируются аномальные наклоны в виде нерегулярностей на обычно гладкой кривой приливного наклона. Чаще всего они имеют флуктуирующий характер, бывает в виде бухт наклонов, иногда и то и другое. Для местного прогноза наибольший интерес представляют случаи появления аномалий перед Вранческими землетрясениями. Они почти всегда имеют место перед землетрясениями с $M > 5$. За период с 1984-1986 гг. установлено 4 почти бесспорных события этого рода. Аномалии наблюдались перед землетрясениями происшедшими: I - 14.05. 84 г. ($M \geq 4{,}7$); II - 1.08. 85 г. ($M \geq 5{,}2$); III - 21.02. 86 г. ($M \geq 5$); IV - 31.08. 86 г. ($M \geq 6{,}9$). На

DOI: https://doi.org/10.2312/zipe.1989.102.03

рис. 3 и 4 представлены записи двух наиболее интересных случаев хода наклона с аномалиями.

Анализируя эти и другие случаи появления аномалий, можно отметить следующее. Аномалии наклонов перед сильными местными землетрясениями хорошо выделяются на фоне приливного наклона. Каждая аномалия кроме общих черт имеет и существенные индивидуальные особенности. Наибольший размах этих аномалий не превышает единиц, в лучшем случае пары десятков миллисекунд. Абсолютная величина в наклонах по составляющей С–Ю в несколько раз больше, чем в направлении В–З. Сопоставляя этот факт с тем, что в этом же направлении обнаружена сильная аномальность земного прилива, по-видимому, следует заключить, что это совпадение неслучайно: большая податливость земной коры по С–Ю должна приводить здесь к повышенной деформируемости земной коры. Обнаруженное совпадение, если оно в дальнейшем будет подтверждено продолжающимися наблюдениями, имеет сейсмопрогностическое значение при поиске прогнозных пунктов.

В заключение отметим, что опыт выполненных высокоточных наблюдений позволяет нам сделать нижеследующие замечания. Использование данных наклономерных наблюдений для сейсмопрогностических целей имеет многоплановый характер, а потенциальные возможности таких наблюдений реализованы еще очень слабо. Чтобы с максимальной эффективностью реализовать эти возможности необходимо применительно к региону и имеющимся условиям наблюдений разработать и внедрить соответствующую методику проведения высокоточных измерений наклонов. Первостепенное внимание следует уделить выбору высокоточного и надежного оборудования, стабилизации условий наблюдений, выбору месторасположения наклономерного пункта. При надлежащем качестве приборов основным

DOI: https://doi.org/10.2312/zipe.1989.102.03

фактором, ограничивающим точность наклономеров, а следовательно и возможности изучения тонких геофизических эффектов, есть помехи метеорологического происхождения, локализованные вблизи станции. Снижение всевозможных помех является обязательным для каждой наклономерной станции, работающей на прогноз.

Ссылки

I. Рикитаке Т. Предсказание землетрясений. - М., Мир, 1979, 388 с.

2. Шляховый В.П., Островский А.Е. Наклономер автокомпенсационного типа и перспективы его применения для целей прогноза землетрясений. - /Развитие сейсмопрогностических исследований на Украине: Сб. научн. тр. Киев: Наук. думка, 1984, с. 99-104.

3. Шляховый В.П., Островский А.Е., Сковитин А.И., Черный В.И. О наблюдениях наклонов на станции "Кишинев". - /Изучение современных геодинамических процессов в связи с проблемой прогноза: Сб. научн. тр. Киев: Наук. думка, 1987, с. 67-70.

4. Шляховый В.П. О сезонных искажениях параметров основных земноприливных волн на ст. "Судиевка" по наблюдениям с автокомпенсационными наклономерами. - //Вращение и приливные деформации Земли, - 1983 - вып. 15, с. 30-37.

5. Шляховый В.П. Приливные сигналы в нелинейных системах и вопросы прогноза землетрясений. - /Современная геодинамика и прогноз землетрясений на Украине: Сб. научн. тр. Киев: Наук. думка, 1985, с. 85-90.

6. Матвеев П.С. Гармонический анализ месячной серии наблюдений

DOI: https://doi.org/10.2312/zipe.1989.102.03

земных приливов. - /Земные приливы. Сб. научн. тр. Киев: Наук. думка, 1966, с. 51-79.

7. Баленко В.Г. Исследования наклонов земной поверхности по профилю Киев-Артемовск. - Киев: Наук. думка, 1978, - 184 с.
8. Дычко И.А., Шляховый В.П. Оценка эффекта экранирования в наблюдениях земных приливов. - //Вращение и приливные деформации Земли, 1978, вып. 10, с. 39-48.
9. Simon Z., Kostelesky J., Zeman A. On the gravitation absorption hypothesis.-/ Studia geoph. at geod., 1988, N32, p. 16-23.

DOI: https://doi.org/10.2312/zipe.1989.102.03

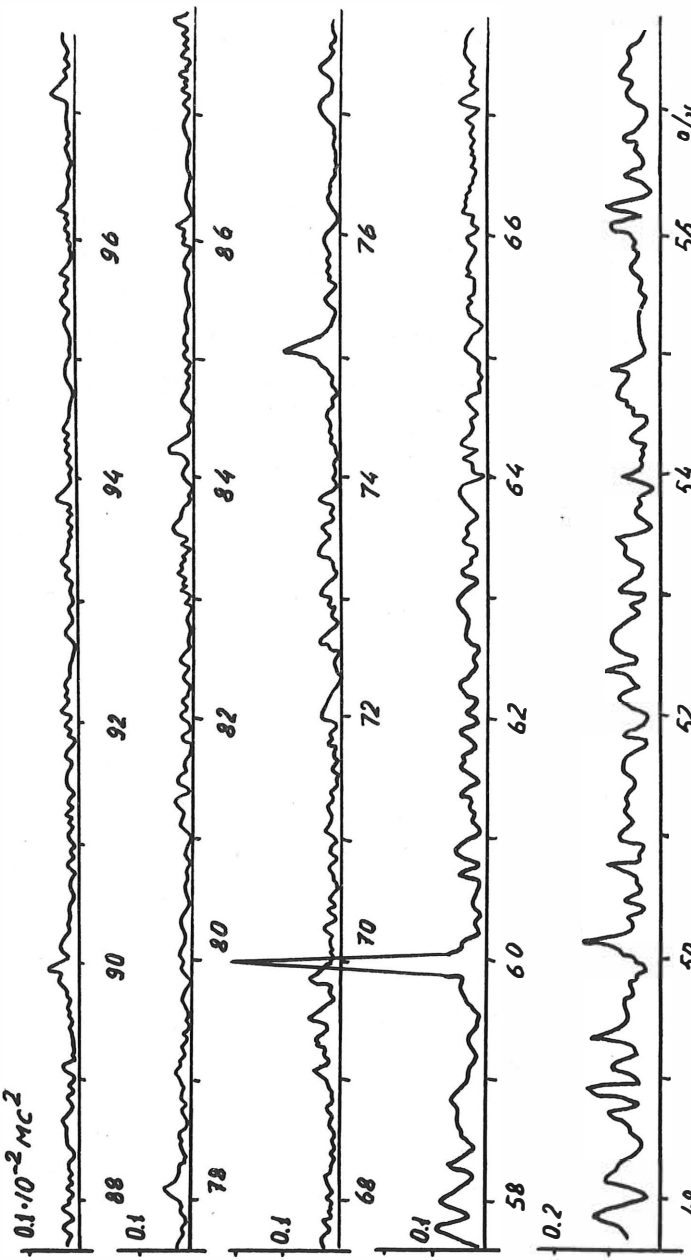

Рис.1. Энергетический спектр наклонов в дробносуточных диапазонах. Направление В-З.

DOI: https://doi.org/10.2312/zipe.1989.102.03

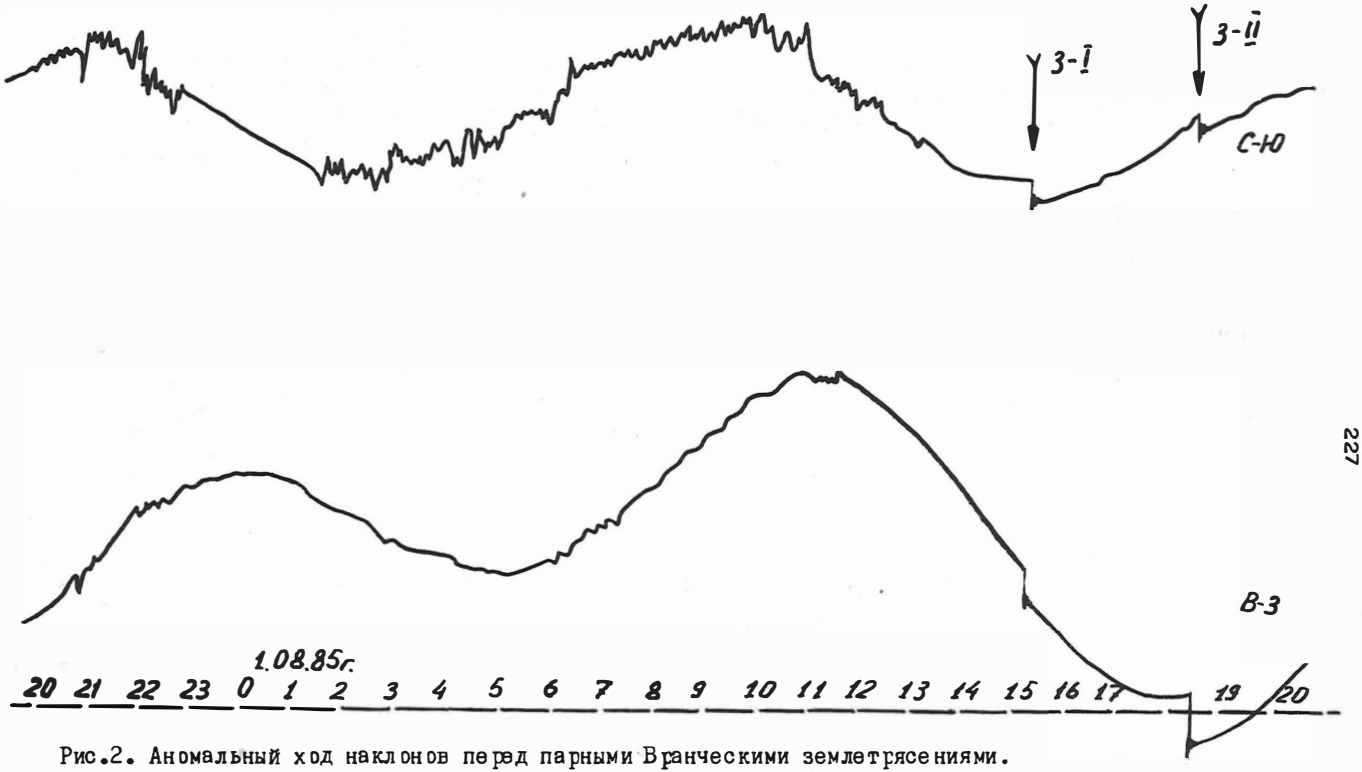

Рис.2. Аномальный ход наклонов перед парными Вранческими землетрясениями.
(1.08.1985 г., ИТ 11ч.17м.,М=5.2; ИТ= 14ч. 35м. , М= 5.1)

DOI: https://doi.org/10.2312/zipe.1989.102.03

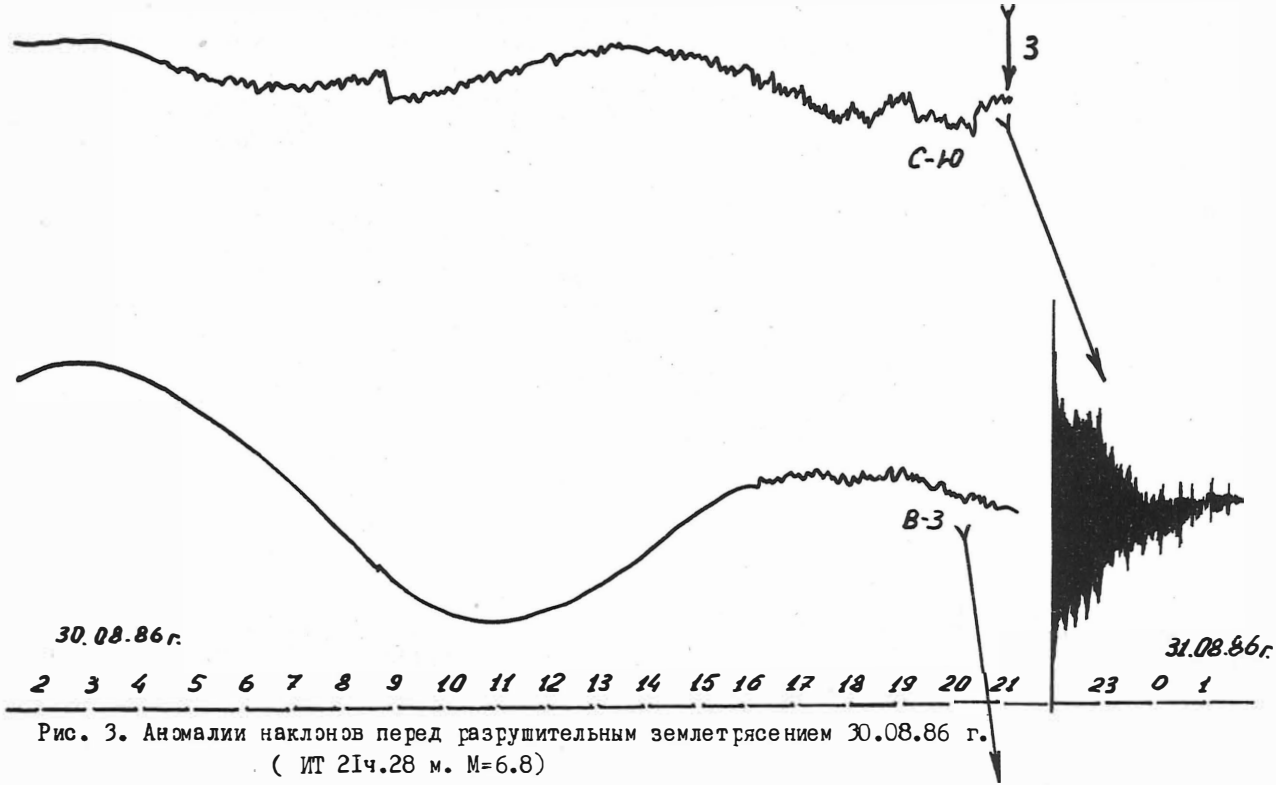

Рис. 3. Аномалии наклонов перед разрушительным землетрясением 30.08.86 г. (ИТ 21ч.28 м. М=6.8)

DOI: https://doi.org/10.2312/zipe.1989.102.03

Prof. Dr.-habil. Janusz ŚLEDZIŃSKI
Doz. Dr.-habil. Marcin BARLIK
Doz. Dr.-habil. Jerzy ROGOWSKI

Warsaw University of Technology
Institute of Higher Geodesy
and Geodetical Astronomy

SATELLITE-GEODETIC TRAVERSES SAGET IN CENTRAL AND SOUTHERN POLAND

Summary

The works concerning the establishment of the geodynamical network SAGET /Satellite-Geodetic Traverses/ in Central and Southern Poland initiated in 1986 at the Institute of Higher Geodesy and Geodetical Astronomy of the Warsaw University of Technology have been shortly presented in the paper. The network of SAGET join geodetic stations of three main tectonic units of Central Europe which meet on the territory of Poland i.e. East European Platform, Paleozoic Platform of Central and Western Europe and Alpine Orogeny. Scientific programme of geodetic and geodynamical investigations is briefly pointed out. Project of SAGET is planned as a long term work. Geodetic, astronomic, satellite and gravimetric observations will be carried out permanently or periodically. First points of the traverses were established and first measurements were made in 1988.

DOI: https://doi.org/10.2312/zipe.1989.102.03

In 1986 the Institute of Higher Geodesy and Geodetical Astronomy of Warsaw University of Technology took up works aimed at establishing geodynamical traverses in the Central and Southern Poland. The works have been planned for several years and are sponsored by the Space Research Center of the Polish Academy of Sciences.

The position of Poland is very interesting concerning the tectonic processes which occur on the European continent. On the territory of Poland the boundaries of three great tectonic units of various age meet, i.e. the East European Precambrian Platform, Paleozoic Platform of the Central and Western Europe and South-European Alpine Orogeny. The location of these units have been presented in Fig. 1. The territory of Poland is also crossed by the Teisseyre-Tornquist zone which is well known to geologists and those dealing with tectonics.

DOI: https://doi.org/10.2312/zipe.1989.102.03

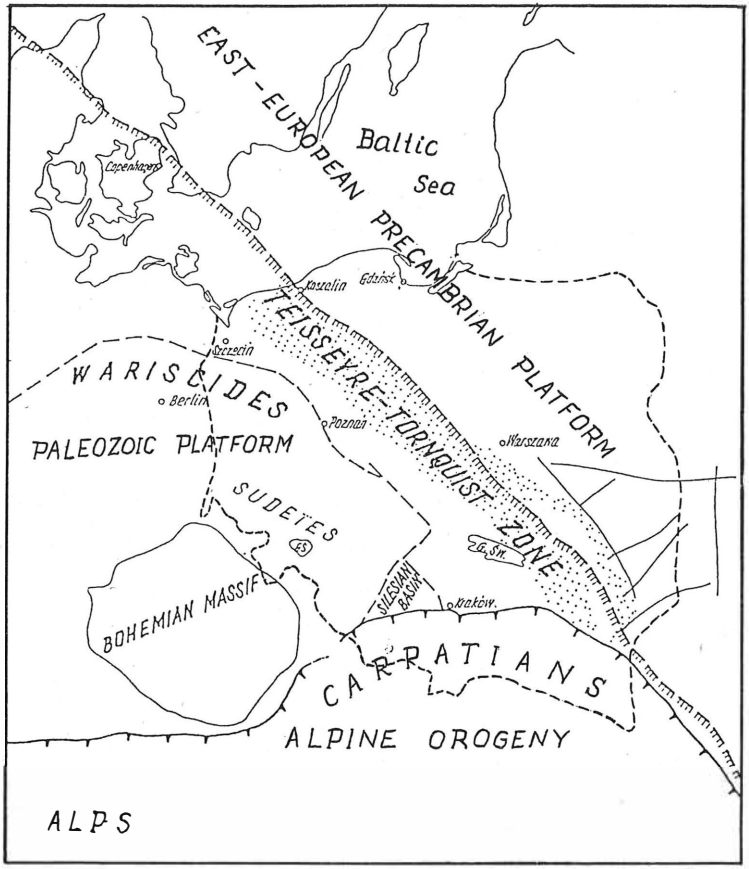

Fig. 1. Territory of Poland and major tectonic units of Central Europe.

DOI: https://doi.org/10.2312/zipe.1989.102.03

Considering the geological situation of Poland, in 1986 a multifunctional project of a geodynamical network including the points situated on all the geological structures was worked out. SAtellite-GEodetic Traverses SAGET crossing all the interesting boundaries between the geological zones will be basic elements of this network.

The aims of establishing such a multifunctional geodetic network in the Central and Southern Poland are as follows:

1. to obtain a frame for long term experimental geodynamical investigations and investigations of the deep tectonic structures,
2. to investigate the geoidal heights by applying classical methods and modern satellite techniques; to compare the effectiveness of various methods of determining the geoidal heights and their time variations,
3. to investigate the relationship between the local natural coordinate systems and the global reference frame for the needs of establishing the national first order control networks and for the needs of geodynamical investigations,
4. to test the scale of the horizontal control network by means of classical and satellite methods,
5. to obtain an accurate test field and test traverses for testing and developing the technologies for the establishment and densification of networks under special conditions, e.g. establishment of networks by classical and satellite methods in the areas with lack of dense gravity field data. The test field will be also used for testing the measuring technologies of absolute and relative point positioning,
6. to investigate the new methods of satellite and inertial point positioning for developing countries,

DOI: https://doi.org/10.2312/zipe.1989.102.03

7. to reconnaissance the geological structures using satellite remote sensing techniques in the areas covered by the traverses of the SAGET project,
8. to carry out the complex investigations of the recent vertical movements of the Earth's crust along the selected sections of the SAGET traverses.

The satellite geodetic network SAGET will consist of the following basic stations:

1. Borowa Góra - Astronomical-Geodetic Observatory of the Institute of Geodesy and Cartography,
2. Borowiec - Astronomical Latitude Observatory of the Polish Academy of Sciences,
3. Grybów - Branch of the Astronomical Observatory of Warsaw University of Technology,
4. Józefosław - Astronomical-Geodetic Observatory of Warsaw University of Technology,
5. Olsztyn - Satellite Observatory of the Academy of Agriculture,
6. Śnieżka /the Karkonosze Mts / - Meteorological Observatory.

Such stations as Borowiec, Grybów and Józefosław are the points of the International West-East European Doppler Network WEDOC. The coordinates of these stations will be also determined in the system of Doppler precise ephemeris. The station Borowa Góra is the reference point of the national astronomical-geodetic control network and it is included in the network of points at which Doppler observations are carried out within MERIT campaign. Doppler station receivers DOG-3, constructed in Poland, have been installed and work permanently at such stations as Borowa Góra, Borowiec, Józefosław and Olsztyn. Most of the above mentioned basic stations are connected with the Doppler points in other countries /e.g. Wettzell, Hannover, Graz, Penc, Metsahovi, Jänhiälä and others/.

DOI: https://doi.org/10.2312/zipe.1989.102.03

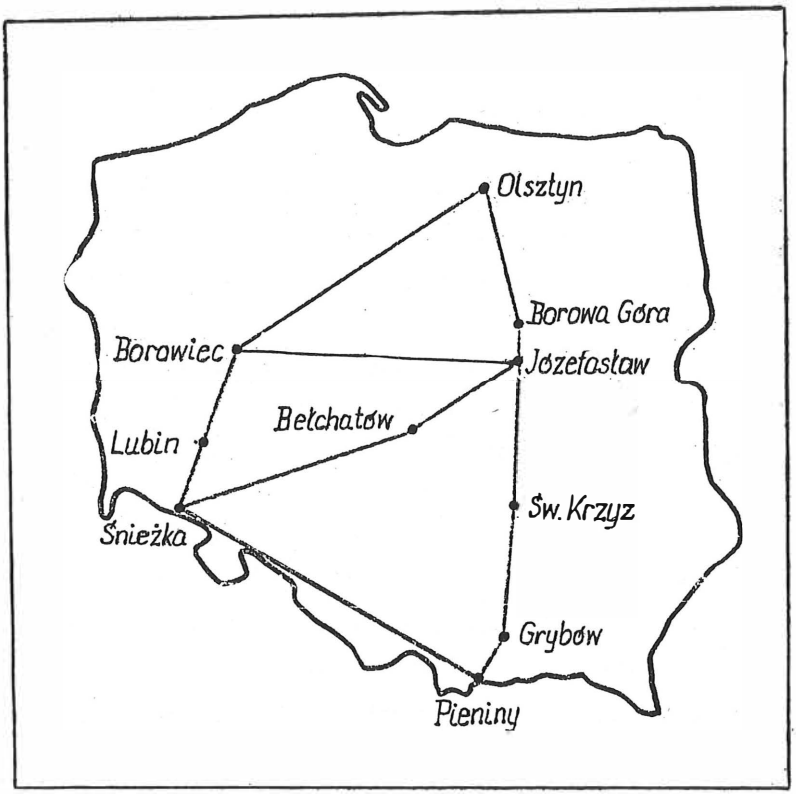

Fig. 2. The SAGET traverses

DOI: https://doi.org/10.2312/zipe.1989.102.03

Further international Doppler connections of these points are being planned.

The network will consist of the following basic traverses /Fig. 2/:

1. Olsztyn - Borowa Góra - Józefosław - Św. Krzyż /The Świętokrzyskie Mts / - Grybów.
2. Grybów - The Pieniny Mts. - Upper Silesia /hard coal mine region/ - Lower Silesia - Śnieżka /The Karkonosze Mts./.
3. Józefosław - Bełchatów /brown coal mine region/ - Śnieżka /The Karkonosze Mts/.
4. Józefosław - Borowiec.
5. Śnieżka /The Karkonosze Mts/ - Lubin /copper ore mine region/ - Borowiec - Olsztyn.

In the SAGET network satellite, geodetic /linear-angular and levelling/, astronomical and gravimetric observations will be carried out permanently or periodically.

At the basic stations of the network satellite Doppler, gravimetric and astronomical observations will be made periodically. At such stations as Borowa Góra, Borowiec, Józefosław and Olsztyn Doppler observations are carried out permanently, permanent astronomical observations of latitude are also carried out at Borowiec and Józefosław. There are plans to carry out and repeat periodically absolute gravimetric measurements at some points of the network /e.g. Borowa Góra, Borowiec, Grybów/.

Along the traverses of SAGET periodical measurements will be performed. The frequency of these measurements will depend on the kind of measurements and the needs of collecting observational data for the analysis and interpretation.

DOI: https://doi.org/10.2312/zipe.1989.102.03

The emphasis will be particularly put on the following measurements:

1. geodetic linear-angular measurements /a laser/microwave distancemeter/,
2. gravimetric measurements along the traverses and their surroundings,
3. astronomical measurements of astronomical latitude and longitude at the astronomical points situated at the distances of about 50-70 km along the traverses,
4. Doppler satellite measurements at the points mentioned in p. 3,
5. satellite GPS measurements along the traverses,
6. measurements of high precision levelling aimed at connecting the points of the traverses to the existing vertical precise control network,
7. inertial measurements on the selected sections of the traverses and in their surroundings.

The establishment and measurement of the whole satellite-geodetic network as presented in Fig. 2 are planned as a programme for several years. Till now /August, 1988/ the points of the traverses have been established on the following sections:
Borowa Góra - Józefosław - Św. Krzyż /The Świętokrzyskie Mts/,
Józefosław - Bełchatów, as well as
Grybów - Pieniny Mts.
The first measurements on theses sections were carried out already in 1988, among them: Doppler measurements /6 points/, astronomical observations /4 points/, linear-angular measurements of the traverses /a distancemeter AGA6 and Wild T3/ and a gravimetric measurement which was carried out twice.

DOI: https://doi.org/10.2312/zipe.1989.102.03

There are also plans to carry out a geodetic satellite GPS measurement between the stations of Borowiec and Józefosław this year. This measurement will be performed in cooperation with the foreign research institutions.

The aim of this paper is to provide some information on the works undertaken and their range. The Institute of Higher Geodesy and Geodetical Astronomy of the Warsaw University of Technology wishes to invite all those who are interested in our programme to come into cooperation with the Institute in all aspects of our programme. All those who are interested in the cooperation are kindly requested to contact the Institute.

Address:

Warsaw University of Technology
Institute of Higher Geodesy
and Geodetical Astronomy
Plac Jedności Robotniczej 1
00-661 Warszawa Warsaw/POLAND
Phone: 25-85-15
Telex: 81-33-07 pw pl

DOI: https://doi.org/10.2312/zipe.1989.102.03

THE PREDESTINATION ROLE OF NEOGENE-QUATERNARY WITH RESPECT TO RECENT TECTONIC MOVEMENTS AND SOME APPLICATIONS TO THE EARTHQUAKE-RESISTENT BUILDING CONSTRUCTION IN THE TRANSITIONAL PERIPLATFORM-OROGENETIC REGION OF THE BLACK SEA COAST

Ivan Nik. Totomanov

Bulgarian Academy of Sciences - Central Laboratory
for Geodesy, Block No 1, 1113 Sofia

Abstract. The study of the neotectonic Z and the recent X vertical Earth's crustal movements and the establishment of a stable or variable structure of the relation between them are both of fundamental and scientific-applied significance to the assessment of the earthquake hazard and to the microseismic zoning. With respect to this, a detailed investigation on the dependence between X and Z is carried out for an intensively developed industrial and mineral-deposit exploitation region of the Black Sea coast where, in recent years, the antropogenetic activity plays the role of a catalyzer to the natural seismicity. This region is of considerable scientific interest, too, being an integral part both of the periplatform southern edge of the Moesian plate, and of the mobile orogenetic space between the latter and the Thrace Median Massif. Based on locally-smoothed estimates of X and Z related to 12 independent model areas, the marginal and the joined sampling distributions of the two-dimensional random variable (X,Z) are determined and studied. The statistical and information relation between X and Z is demonstrated by means of

DOI: https://doi.org/10.2312/zipe.1989.102.03

an entropy test of independence. A close positive and statistically significant correlation between them is discovered. The best fitting mathematical-stochastic polynomial model, with its parameters for the regression equation $\bar{x} = \bar{x}(z)$, as well as the accuracy of the respective forecast are determined. The established space-time interrelation between X and Z elucidates the regional geodynamics of the Eastern Fore-Balkan and will contribute to the earthquake-resistent building construction within the region under investigation.

ПРЕДОПРЕДЕЛЯЮЩАЯ РОЛЬ НЕОГЕН-ЧЕТВЕРТИЧНЫХ ПО ОТНОШЕНИЮ К СОВРЕМЕННЫМ ТЕКТОНИЧЕСКИМ ДВИЖЕНИЯМ И НЕКОТОРЫЕ ПРИМЕНЕНИЯ ДЛЯ ЦЕЛЕЙ СЕЙСМОСТОЙКОГО СТРОИТЕЛЬСТВА В ПЕРЕХОДНОМ ПЕРИПЛАТФОРМЕННОМ-ОРОГЕННОМ РАЙОНЕ ПОБЕРЕЖЬЯ ЧЕРНОГО МОРЯ. РЕЗЮМЕ. Изучение неотектонических Z и современных X вертикальных движений земной коры и установление стабильной или переменной структуры связи между ними имеет как фундаментальное, так и научно-прикладное значение для оценки сейсмической опасности и для сейсмического районерования. В связи с этим, сделано детальное исследование зависимости между X и Z в интенсивно развитом промышленном и горно-добывающем районе Черноморского побережья, где в последних годах антропогенная деятельность является катализатором естественной сейсмичности. Этот район представляет и значительный научный интерес, являясь интегральной частью как периплатформенной южной граничной зоны Мизийской плиты, так и подвижного орогенного пространства между ней и Фракийским срединным массивом. На основе ло-

DOI: https://doi.org/10.2312/zipe.1989.102.03

кально-изгладенных оценок для X и Z из 12 независимых модельных областей, определены и исследованы эмпирические одномерные и совместное двумерное распределения случайной величины (X, Z). Статистическая и информационная связь между X и Z доказана при помощи энтропийного теста независимости. При том установлена сильная положительная и статистически значимая корреляция между ними. Определена и наиболее подходящая математико-стохастическая модель с ее параметрами для уравнения регрессии $\bar{x} = \bar{x}(z)$ и точность соответствующего прогноза. Установленная пространственно-временная связь между X и Z объясняет региональную геодинамику Восточного Предбалкана и вносит вклад в сейсмостойкое строительство в исследуемом районе.

DOI: https://doi.org/10.2312/zipe.1989.102.03

1. Introduction

The modern methods of seismic zoning related to the earthquake-resistent building construction (Ризниченко , 1979) which are based on the assumption for a stationary character of the processes generating and accompanying a determined earthquake regime, assess the long-term mean seismic hazard with its probability measure - the sheakability B=B(J) where by J a suitably defined parameter-intensity is designated. To this end two types of data are used: a) for the maximum magnitude Y=(K-4)/1.8 of the possible earthquakes with energy $E=10^k$ joules where k is the respective maximum energetical class, and b) for the long-term source seismicity and for the fading law of J related to the increasing distance to the hypocentre.

When mapping Y versatile geophysical, geologo-geomorphological and geodetic information is used (e.g. Bonćev et al, 1982; Гитис et al., 1982): geostructure position, type of contact between the geotectonic structures, geotectonic inhomogeneities, active faults, nodes of fault-crossing, neotectonic vertical deformation Z of the peneplain, contrast of the relief of Z, vertical velocity X of the recent Earth's crustal movements, depth of the seismoactive layer, depth of the boundary of Mohorovićić, Bouguer gravity anomalies, etc. At this X and Z prove to be among the most informative parameters of the forecasting function Y= = Y(X, Z, ...). The study of the dependence of Y upon its parameters, and of the weight gradation of the respective initial data is quite important with regard to the determination of an adequate mathematical model and to the application of this function (Totomanov, 1985a). The dependence of Y upon X has been

DOI: https://doi.org/10.2312/zipe.1989.102.03

object of a number of investigations (Totomanov, 1984a, 1984b, 1985b, 1985c, etc.) of a regional character. By the present work, with regard to the fundamental researches assigned by the Ministry of Culture, Science and Education, concerning the geodetic methods of searching earthquake precursors, these elaborations, and the first of its kind quantitative investigation (Totomanov, 1988b) on the relation between X and Z, are carried on and extended.

2. Balkanide orogen, Moesian platform, and the Shoumen Transitional Zone between them

The nowadays Balkanides are the northern branch of the Alpo-Himalayan orogen within the eastern part of the Balkan peninsula, within the so called Balkanide Mobile Space. The latter is situated in the collision zone between two lithospheric plates with Precambrian stabilization. These are: southwards - the steady rising thick but light (of sial type) Earth's crust of the Pannono-Thrace-Anatolian plate, and northwards - the steady sinking Moesian platform with a considerably heavier (of mafic type) Earth's crust of the Ponto-Caspian lithospheric plate (Бончев , 1987) By the process of isostasy, together with its movement against, and with the quasisubduction of the platform beneath the Thrace Mediane Massif, the Balkanide Fold Belt is developed, as a reflection of the lineament bundle, of the same name, which marks a deep breaking of the lithosphere. From the multiple geosyncline development of this bundle, only the final neotectonic epizode of the late phase of the Alpian stage is noted here. The epizode embraces the Neogene (initiating about the Middle Myocene, with an absolute age of nearly 15 millions of years), the Pliocene (aged about 5-10 millions of years) from the Terciar period, and the Pleistocene (aged 2-1.5 millions of years) from

DOI: https://doi.org/10.2312/zipe.1989.102.03

the Quaternary period of the Cenozoic era; within the Quaternary, following immediately the Pleistocene, is the recent epoch, according to the geochronological scale.

Between the Middle and the Upper Myocene, resulting from a general denudation flattening of the dryland, the initial flattening surface - peneplane is formed (География на България ,1982). In the beginning of the Quaternary, caused by a new tectonic activation with intensive vertical crustal movements Z, rise the nowadays Balkanide, Sredna-Gora and other orogenetic systems, with deep new depressions within the interstitial zones. In this way the continuous development of the Bulgarian land completes, as a result of which the present relief, and the related to it physical-geographical and structure appearance of this country, are created. It is evident that the recent X vertical movements (during the last century) are a manifestation, only in the final moment, of the 10-15 millions of years development of the neotectonic (Neogene-Quaternary) Z-dynamics of these lands. It is this very aspect which determines the considerable scientific and applied interest of discovering regularities in the interralation between X and Z.

According to the modern genetic point of view, the Balkanides comprise Stara Planina (the Balkan), southwards, and the Fore-Balkan, northwards. The latter lengthwise is divided into two structural zones: the Proper Fore-Balkan (neighbouring the Balkan), and the Transitional Zone situated between it and the Moesian platform (Fig. 1). The present work deals with the Transitional Zone of the Eastern Fore-Balkan, known as Shoumen Transitional Zone (Бончев , 1987). Its structure comprises a

DOI: https://doi.org/10.2312/zipe.1989.102.03

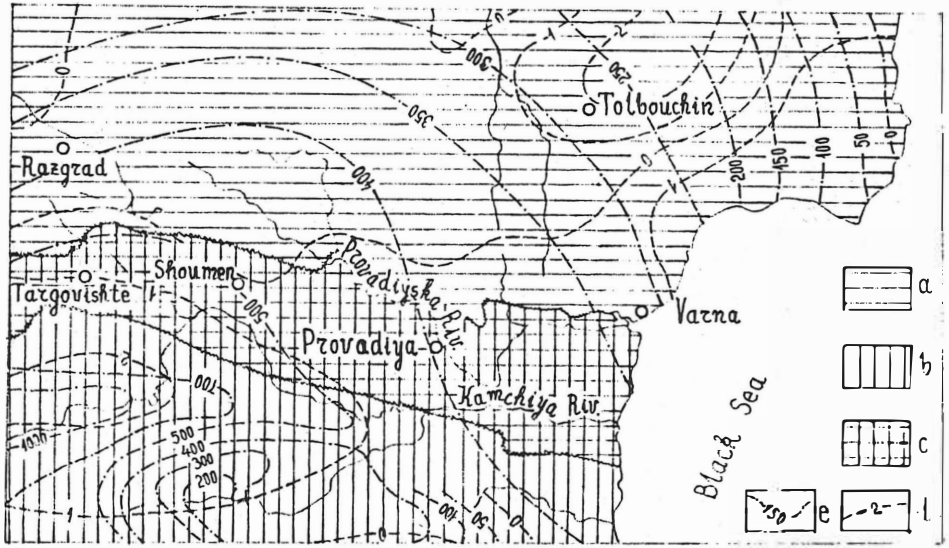

Fig. 1. Tectonic structure and vertical Earth's crustal movements in Northeastern Bulgaria. Structural zones: a - Moesian platform, b - Eastern Balkanides, c - Shoumen Transitional Zone. Isolines of the movements: d - velocity of recent movements ($mm.a^{-1}$), e - amplitude of neotectonic deformations of the initial smoothing surface - peneplane (m).

DOI: https://doi.org/10.2312/zipe.1989.102.03

number of wide and shallow synclines and anticlinal swells on the northern coast and its continuation to east within the shelf-aquatory of the Black Sea. This zone is of an unique periplatform-orogenetic character: it is an integral part both of the Moesian platform and of the northern strip of the Fore-Balkan which makes it quite interesting for fundamental scientific investigations. The intensively developed chemical, mineral-deposit and other industry in the regions of the towns of Varna, Devnya (the ancient Marcianopolis), Provadiya and Shoumen, endue the geodynamic studies with a considerable practical actuality concerning a future and more refined seismic zoning of this territory. This is connected, too, with the interesting and disturbing fact that, in recent years, the anthropogenetic activity within this zone manifests itself as an intensifying catalyzer of the natural seismicity. Owing to all these reasons, together with the prospects of a long-term and considerable development and extension of the economic basement, and with the necessity of a reliable earthquake-resistent building construction, and a damage-protected exploitation of the available and future industrial eneterprises and great engineering structures and complexes, the present geodynamic investigations about X and Z within the Shoumen Transitional Zone are undertaken.

3. Statistical relation between neotectonic Z and recent X vertical kinematics of the Shoumen Transitional Zone

3.1. Initial data, model areas and sampling distribution of X and Z

The neotectonic movements are determined by means of geologo-geomorphological studies and mapping of the summary amplitude Z of the vertical deformation of the peneplane (География на България , 1982; Vapcarov et al., 1974). The recent move-

DOI: https://doi.org/10.2312/zipe.1989.102.03

ments are studied by means of instrumental geodetic (precise geometric levelling) and oceanographic methods and measurements by which the vertical velocity X is mapped (ТОТОМАНОВ et al., 1978; Joo et al., 1979). A fragment of these maps, with isolines for X and Z within Northeastern Bulgaria, is shown in Fig. 1, the visual analysis of which makes possible to draw the following more important conclusions:

1. The geodynamic development of the Shoumen Transitional Zone manifests the features a) of the Moesian platform - for the neotectonic phase, and b) of the Balkanide space - for the nowadays phase.

2. Lengthwise the Shoumen Transitional Zone, in the east-west direction, a general quantitative particularity of the X- and Z-fields is present: a systematic decreasing of their values.

The second deduction can be connected with a hypothesis on the existence of a regional measurable regular relation between the neotectonic and the recent kinematics of the studied region. In order to check and, if corroborated as true, to put into practice this hypothesis, the zone is divided into n=12 independent trapezium-shaped model areas i=1,2,...,n of dimensions 20x21 km lengthwise the meridian and the parallel, respectively (Fig. 2). For these areas, by means of two sets of 105 symmetric independent readings on the two maps, generalized locally-smoothed estimates X_i and Z_i are determined (Totomanov, 1988 b); these very estimates are the variants of the sampling distribution of the two-dimensional random variable (X,Z). In Fig. 3 is plotted the stereohystogramme of the relief of the frequencies $n_{k\ell}$ of the realizations of this variable within the respective site ($x_k \pm d_x$, $z_\ell \pm d_z$) with a central point (x_k , z_ℓ) and semi-widths d_x =

DOI: https://doi.org/10.2312/zipe.1989.102.03

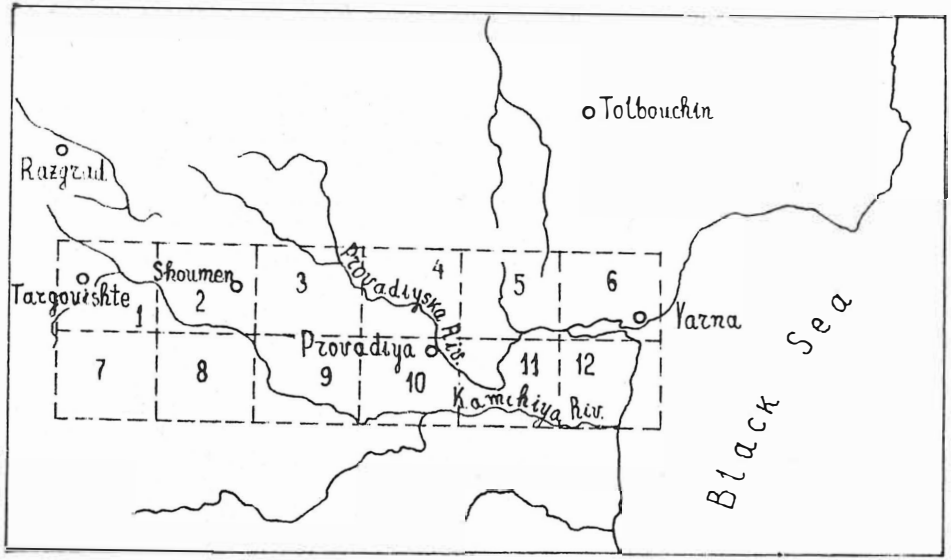

Fig. 2. Model areas of studying the relation between the recent and neotectonic Earth's crustal movements within the Shoumen Transitional Zone.

DOI: https://doi.org/10.2312/zipe.1989.102.03

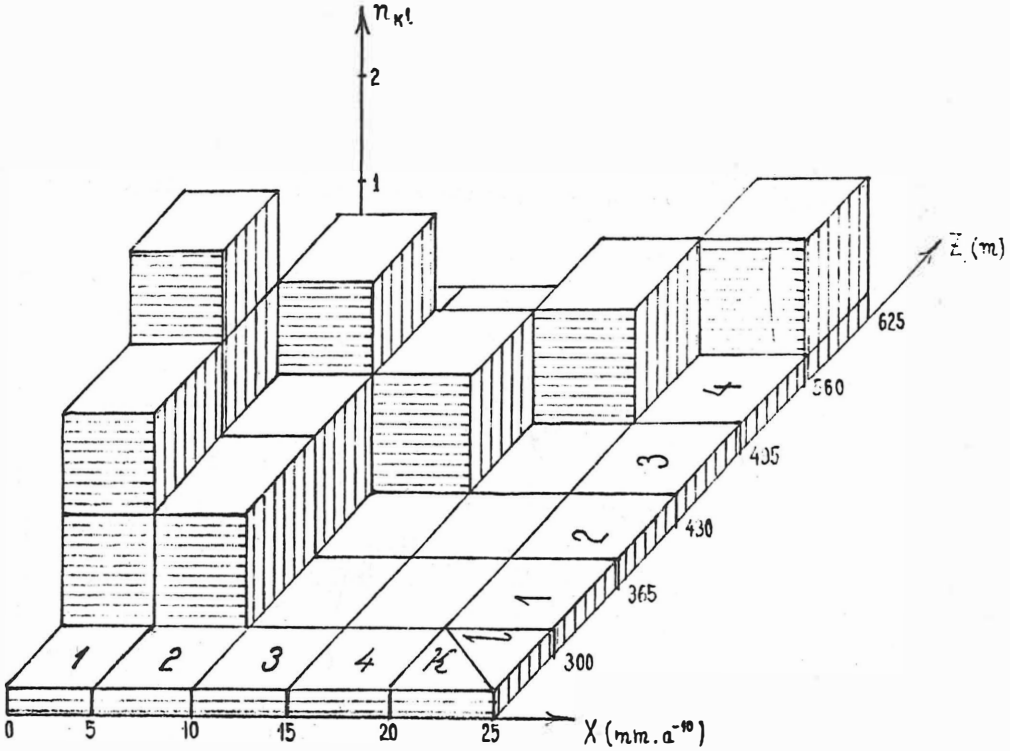

Fig. 3. Stereohystogramme of the joint differential distribution of the recent X and neotectonic Z vertical Earth's crustal movements within the Shoumen Transitional Zone.

DOI: https://doi.org/10.2312/zipe.1989.102.03

= 0,5 mm.a^{-1} and d_z = 65 m of the intervals, with numbers in sequence k = 1,2,...,n_x and l = 1,2,...,n_z, of data grouping respectively for X and Z.

The visual analysis of the stereohystogramme, with its distinctly expressed ridge (from the joint minimum towards the joint maximum of X and Y) in the relief of n_{kl} is a convincing corroboration of the hypothesis on the existence of a regular relation between X and Z, and gives grounds to search a positive correlation between them. However, a more objective quantitative corroboration on the existence of such a regularity within the Shoumen Transitional Zone will preliminarily be searched for.

3.2. Entropy test of independence of X and Z

In order to check this hypothesis, here is applied the new quantitative approach (Totomanov, 1988 a) suggested to assess both the general statistical and the information relation among the components of the initial data of the seismic zoning.

The two-dimensional random variable (X,Z) with possible states (x_k , z_l) and respective probabilities $p_{kl} = P(x_k, z_l)$ can be considered (e.g. Вентцель , 1964) as a physical system to which an inner degree of indefiniteness is inherent. This indefiniteness is measured by the entropy of the system given by

$$(1) \qquad H(X,Z) = -\sum_{k=1}^{k=n_x} \sum_{l=1}^{l=n_z} p_{kl} \log_a p_{kl}$$

where usually a = 2. For the separate random variables X and Z the entropy is

$$(2) \qquad H(X) = -\sum_{k=1}^{k=n_x} p_k \log_a p_k \ , \quad H(Z) = -\sum_{l=1}^{l=n_z} p_l \log_a p_l .$$

DOI: https://doi.org/10.2312/zipe.1989.102.03

At this, the entropy numerically is equal to the information quantity which is necessary for an exhausted study of the respective physical system. From eqs. (1) and (2) besides a number of other useful properties, the additivity of the entropy

$$H(A,B) = H(A) + H(B) \tag{3}$$

follows when creating, by means of two simple independent systems A and B, of a composed system (A,B).

If for (X,Z) eq. (3) is valid, the checked hypothesis on the the existence of some relation between X and Z within the Shoumen Transitional Zone should be rejected as contradictory to the data (x , z) of the sample studied, and vice-versa.

The calculations for the entropy within the region under examination are given in Tabs 1-3 according to the sampling probabilities

$$p_\kappa = \Big(\sum_{\lambda=1}^{\lambda=n_\lambda} n_{\kappa\lambda}\Big)/n = n_\kappa/n, \quad p_\lambda = \Big(\sum_{\kappa=1}^{\kappa=n_\kappa} n_{\kappa\lambda}\Big)/n = n_\lambda/n, \tag{4}$$
$$p_{\kappa\lambda} = n_{\kappa\lambda}/n$$

determined by means of the stereohystogramme (Fig. 3) of the joint distribution of X and Z, by which the respective table is used (Miller et al., 1979). In Tab. 3, for each cell kl are given two values: of $p_{\kappa\lambda}$ in the numerator, and the respective component $-p_{\kappa\lambda}\log_a p_{\kappa\lambda}$ in the denominator. By such a manner the following values

$$H(X) = 1.9485 \quad , \quad H(Z) = 2.1243, \tag{5}$$
$$H(X,Z) = 2.8524$$

for the entropy are calculated, from which

$$H(X) + H(Z) = 4.0728 \tag{6}$$

DOI: https://doi.org/10.2312/zipe.1989.102.03

Table 1. Entropy of the simple (one-dimensional) physical system X ($mm.a^{-1}$)

Interval for X			Sampling probabilities p_k	$-p_k \log_2 p_k$
No. k	from	to		
1	0.00	0.50	0.416 667	0.5262
2	0.50	1.00	0.333 333	0.5283
3	1.00	1.50	0.083 333	0.2980
4	1.50	2.00	0.083 333	0.2980
5	2.00	2.50	0.083 333	0.2980
	$\sum_{k=1}^{k=5}$		0.999 999	1.9485

Table 2. Entropy of the simple (one-dimensional) physical system Z (hm)

Interval for Z			Sampling probabilities p_l	$-p_l \log_2 p_l$
No. l	from	to		
1	3.00	3.65	0.250 000	0.5000
2	3.65	4.30	0.333 333	0.5283
3	4.30	4.95	0.250 000	0.5000
4	4.95	5.60	0.083 333	0.2980
5	5.60	6.25	0.083 333	0.2980
	$\sum_{l=1}^{l=5}$		0.999 999	2.1243

DOI: https://doi.org/10.2312/zipe.1989.102.03

Table 3. Entropy of the composed (two-dimensional) physical system (X, Z)

Intervals			for	X (mm. a^{-1})					$\sum_{K=1}^{K=5}$
			No. k	1	2	3	4	5	
			from	0.00	0.50	1.00	1.50	2.00	
for	No. l	from	to	0.50	1.00	1.50	2.00	2.50	
Z (km)	1	3.00	3.65	0.166 667 / 0.4312	0.083 333 / 0.2980	0 / 0	0 / 0	0 / 0	0.250 000 / 0.7292
	2	3.65	4.30	0.250 000 / 0.5000	0.083 333 / 0.2980	0 / 0	0 / 0	0 / 0	0.333 333 / 0.7980
	3	4.30	4.95	0 / 0	0.166 667 / 0.4312	0.083 333 / 0.2980	0 / 0	0 / 0	0.250 000 / 0.7292
	4	4.95	5.60	0 / 0	0 / 0	0 / 0	0.083 333 / 0.2980	0 / 0	0.083 333 / 0.2980
	5	5.60	6.25	0 / 0	0 / 0	0 / 0	0 / 0	0.083 333 / 0.2980	0.083 333 / 0.2980
$\sum_{l=1}^{l=5}$				0.416 667 / 0.9312	0.333 333 / 1.0272	0.083 333 / 0.2980	0.083333 / 0.2980	0.083333 / 0.2980	0.999 999 / 2.8524

DOI: https://doi.org/10.2312/zipe.1989.102.03

is obtained.

From (5)

(7) $$H(Z) > H(X)$$

follows which designates that the quantity of information necessary for an exhausted study of Z is greater than the respective quantity for X.

The comparison of (5) and (6) results in

(8) $$H(X,Z) << H(X) + H(Z)$$

which contradicts the null-hypothesis in eq. (3). This means that the sampling data for the general population (X,Z) demonstrate convincingly the verity of the checked hypothesis on the existence of a statistical relation between X and Z within the region under investigation.

The results of this study are a new firm information-statistical argument for the first express study (Totomanov, 1988b) and for the following quantitative geodynamic researches on X and Z in the present work.

3.3. Intensity, significance and type of correlation between X and Z

As was already emphasized, the stereohystogramme (Fig. 3) of the sampling distribution of (X,Z) gives grounds to search a positive correlation between X and Z. The assessment of the closeness of this relation by means of some appropriate measure for its intensity depends essentially upon the type of the distribution of (X,Z), and in particular - upon the degree of the deviation of this distribution from the normal one. The acceptance, or the rejecting, of the assertion on the normality of the distribution of a two-dimensional random variable is, however, con-

DOI: https://doi.org/10.2312/zipe.1989.102.03

nected with checking of a great number (at least four - see Totomanov, 1985 b) statistical hypothesis and, due to the restricted volume and the purposes of the present investigation, here an approximate but quite efficient approach of the correlation analysis is adopted; the results of the application of this approach are corroborated in the following, when modelling the regression of X with respect to Z.

The well-known by the theory (e.g. Paradine & Rivett, 1962) statement that the regression is linear (i.e. that the respective two-dimensional distribution is normal - see e.g. Вентцель , 1964 too) provided only if the two correlation Pearson's ratios η numerically are equal to the correlation coefficient between the two random variables of which the two dimensional random variable is composed.

Making use of the data for the sampling frequencies $n_{k\ell}$ according to the hystogramme (Fig. 3), the correlation coefficient ρ_{xz} between X and Z is calculated as follows

$$\rho_{xz} = \left(\sum_{k=1}^{k=n_x}\sum_{\ell=1}^{\ell=n_z} n_{k\ell}\, x_k\, z_\ell / n - a_x a_z\right) / s_x s_z \pm \tag{9}$$

$$(1-\rho_{xz}^2)/\sqrt{n-1} = 0.798 \pm 0.109$$

where the sampling initial moments (mean values)

$$a_x = \left(\sum_{k=1}^{k=n_x} n_k\, x_k\right)/n = 0.791\,67 \text{ mm.a}^{-1},$$

$$a_z = \left(\sum_{\ell=1}^{\ell=n_z} n_\ell\, z_\ell\right)/n = 0.245\,83 \text{ km} \tag{10}$$

DOI: https://doi.org/10.2312/zipe.1989.102.03

and standard deviations

$$s_x = \sqrt{\left[\sum_{k=1}^{k=n_x} n_k (x_k - a_x)^2\right] / (n-1)} = 0.655\,69 \text{ mm.a}^{-1},$$

$$s_z = \sqrt{\left[\sum_{l=1}^{l=n_z} n_l (z_l - a_z)^2\right] / (n-1)} = 0.806\,07 \text{ km} \quad (11)$$

of the marginal distributions of X and Z are designated.

The Pearson's correlation ratios

$$\eta_{\bar{x}/z} = \sqrt{\left[\sum_{l=1}^{l=n_z} n_l (\bar{x}_l - a_x)^2\right] / (n-1)} \; / \; s_x \pm$$

$$(1 - \eta^2_{\bar{x}/z}) / \sqrt{n-1} = 0.943 \pm 0.033,$$

$$\eta_{\bar{z}/x} = \sqrt{\left[\sum_{k=1}^{k=n_x} n_k (\bar{z}_k - a_z)^2\right] / (n-1)} \; / \; s_z \pm \quad (12)$$

$$(1 - \eta^2_{\bar{z}/x}) / \sqrt{n-1} = 0.875 \pm 0.071$$

are determined similarly by which the interval mean values

$$\bar{x}_l = \left(\sum_{k=1}^{k=n_x} n_{kl}\, x_k\right) / n_l,$$

$$\bar{z}_k = \left(\sum_{l=1}^{l=n_z} n_{kl}\, z_l\right) / n_k \quad (13)$$

and the marginal frequencies n_k and n_l (4) are used.

The sampling marginal distributions of X and Z, together with the calculations for $\eta_{\bar{x}/z}$ and $\eta_{\bar{z}/x}$ are given in Tabs 4 and 5. Based on the comparison of eqs (9) and (12), the following deductions are drawn:

DOI: https://doi.org/10.2312/zipe.1989.102.03

Table 4. Sampling distribution of X and computations for the correlation ratio $\eta_{z/X}$

Interval		Frequency				
No. k	middle x_k (mm.a^{-1})	n_k	$n_k x_k$	$\bar{z}_k$ (km)	$\bar{z}_k - a_z$	$n_k(\bar{z}_k - a_z)^2$
1	0.25	5	1.25	3.715	- 0.530 83	1.408 90
2	0.75	4	3.00	4.138	- 0.107 83	0.046 51
3	1.25	1	1.25	4.625	0.379 17	0.143 77
4	1.75	1	1.75	5.275	1.029 17	1.059 19
5	2.25	1	2.25	5.925	1.679 17	2.819 61
	$\sum_{k=1}^{k=5}$	12	9.50	23.678	2.448 85	5.477 98

$a_x = 9.50 / 12 = 0.791\,67$ mm.a^{-1} ,

$\eta_{\bar{z}/X} = \sqrt{5.477\,98 / 11} \;/\; 0.806\,07 = 0.875\,47$

DOI: https://doi.org/10.2312/zipe.1989.102.03

Table 5. Sampling distribution of Z and computations for the correlation ratio $\eta_{\bar{x}/Z}$

Interval		Frequency				
No. k	middle z_ℓ (hm)	n_ℓ	$n_\ell z_\ell$	$\bar{x}_\ell$ mm.a^{-1}	$\bar{x}_\ell - a_x$	$n_\ell (\bar{x}_\ell - a_x)^2$
1	3.325	3	9.975	0.417	- 0.374 67	0.421 13
2	3.975	4	15.900	0.375	- 0.416 67	0.694 46
3	4.625	3	13.875	0.917	0.125 33	0.047 12
4	5.275	1	5.275	1.750	0.958 33	0.918 40
5	5.925	1	5.925	2.250	1.458 33	2.126 73
	$\sum_{\ell=1}^{\ell=5}$	12	50.950	5.709	1.750 65	4.207 84

a_z = 50.950 / 12 = 4.245 83 hm

$\eta_{\bar{x}/Z}$ = $\sqrt{4.207\ 84 / 11}$ / 0.655 69 = 0.943 27

DOI: https://doi.org/10.2312/zipe.1989.102.03

a. ρ_{XZ} , $\eta_{\bar{x}/Z}$ and $\eta_{\bar{z}/X}$ are determined with a relative root mean square error 3.5-13.7% which is an indication for the reliability of these estimates. Their statistical significance can be corroborated by means of checking some statistical hypotheses.

b. A closeness of the estimates $\rho_{XZ} \approx 0.8$ and $\eta \approx 0.9$ is established which testifies on the validity of the assertion (Totomanov, 1988 b) that the distribution of (X,Z) within the Shoumen Transitional Zone is close to the normal one. Based on this statement, the conclusions follow that,

- the correlation coefficient can be accepted as a measure for the intensity of the statistical relation between X and Z;

- a linear mathematical model can be applied, at least as a first approximation, for the regression equations.

It should be emphasized that these two consequences are exercised by the first express study (Totomanov, 1988 b) in which all the calculations are made directly by the original data X_i and Z_i. On that account the estimates determined (including the ones for α_x , α_z and ρ_{XZ} =0,987) in this study differ from the estimates calculated in the present paper which is based on the processing of the data x_k and z_l for the respective intervals of grouping.

c. Although not quite considerable, a difference between the values both of ρ_{XZ} , on the one hand, and of $\eta_{\bar{x}/Z}$ and $\eta_{\bar{z}/X}$ - on the other hand (together with their dispersions) is established. This very difference determines the approximate character of the deduction of point "b" in the preceding text. A reliable solution of the problem treated for the normality of the distribution of (X,Z) by means of a comparison of ρ

DOI: https://doi.org/10.2312/zipe.1989.102.03

and η requires additional elaborations. With regard to this the following procedure with checking of statistical hypotheses is suggested here:

- the sample (X_i, Z_i) is distributed, according to some (real or formal) sign, to a quantity (X_{ij}, Z_{ij}) of samples at $j=1,2,\ldots,m$;

- from these samples the respective estimates ρ_j and $\eta^{(j)}_{\bar{x}/\bar{z}}$, $\eta^{(j)}_{\bar{z}/X}$ are determined;

- these estimates are treated as samples from general populations of normal distributions $N_\rho(\tilde{\rho}, \tilde{S}^2)$, $N_{\eta x}(\tilde{\eta}_{\bar{x}/\bar{z}}, \tilde{S}^2_{\bar{x}/\bar{z}})$, $N_{\eta z}(\tilde{\eta}_{\bar{z}/X}, \tilde{S}^2_{\bar{z}/X})$ with parameters determined by the use of the respective samples;

- the statistical hypothesis on the equality of the mathematical expectations of these general populations, is checked, similarly to the study (Totomanov et al., 1987) on the module of the horizontal gradient of X. The rejecting of this hypothesis, at a level of significance α, will repudate in the same time the normality of (X,Z) with a probability $P=1-\alpha$ and, therefore, will indicate a rejection of the linear model for the regression equations; and vice versa.

The realization of this new statistical solution of the problem for the normality of a two-dimensional distribution cannot be included in the present work. On that account here a traditional approach will be used once again, and additional data for the solution of the problem mentioned, in the case of the random variable (X,Z) studied, will be obtained.

The type of the regression is expressed more clearly by an appropriate generalization (smoothing or grouping) of the initial data, especially when it concerns the processing of great

DOI: https://doi.org/10.2312/zipe.1989.102.03

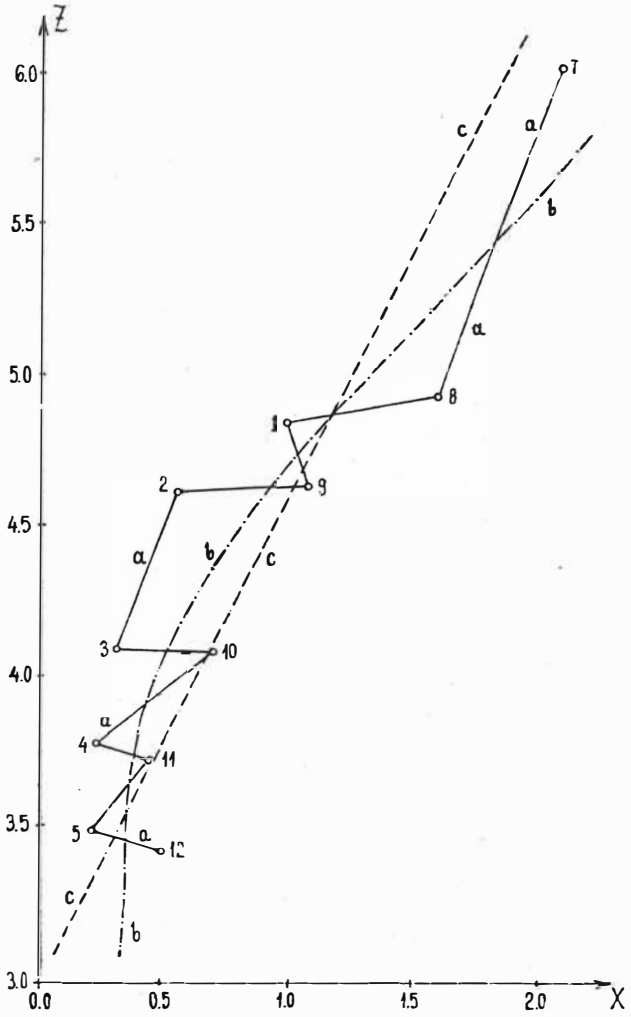

Fig. 4. Regression of X ($mm.a^{-1}$) with respect to Z (hm). a - sampling polygon of the variants (X_i, Z_i) related to the model areas with numbers i = 1, 2,..., 12 (see Fig. 2). Graphical approximation of the equation aimed to forecast mean values $\bar{X} = \bar{X}(Z)$: b - by means of a best fitting curve line, c - by means of a best fitting straight line.

DOI: https://doi.org/10.2312/zipe.1989.102.03

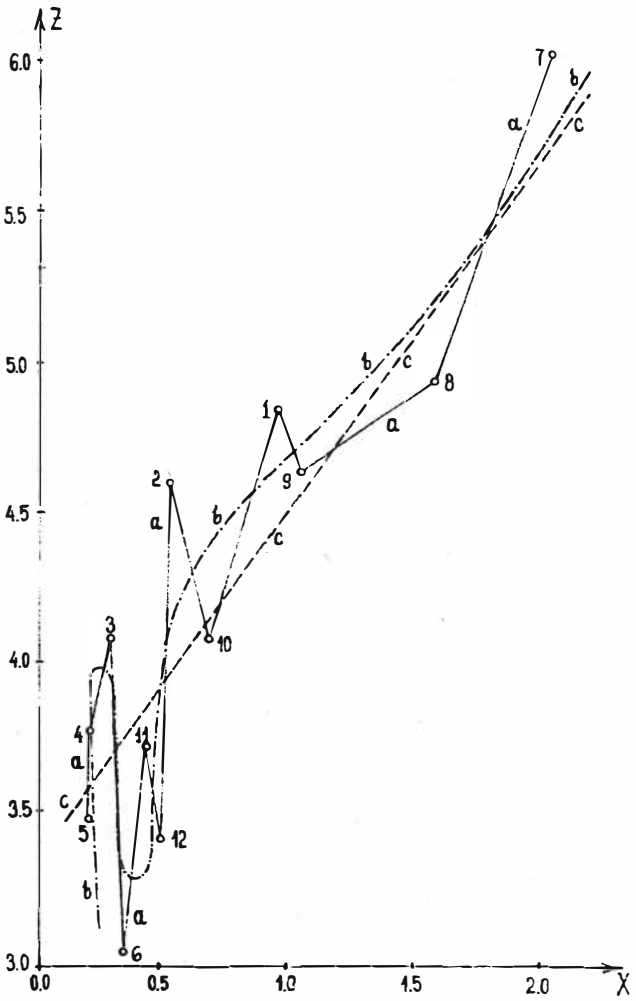

Fig. 5. Regression of Z (hm) with respect to X ($mm.a^{-1}$). a - sampling polygon of the variants (X_i, Z_i) related to the model areas of numbers i = 1, 2,..., 12 (see Fig. 2). Graphical approximation of the equation aimed to forecast mean values $\bar{Z} = \bar{Z}(X)$: b - by means of a best fitting curve line, c - by means of a best fitting straight line.

DOI: https://doi.org/10.2312/zipe.1989.102.03

samples in which the multiple random and some systematic unknown great deviations frequently disguise the manifestation even of determined, close to or practically functional regularities. In the case examined, the joint smoothing and grouping of the original 2 x 105 cartometric readings into a 5 x 5 - table of (x_k, z_ℓ) - frequencies $n_{k\ell}$ for the distribution of X and Z, by the use of which frequencies the stereohystogram in Fig. 3 is plotted, gives grounds for the statement, and later on - for the corroboration of the hypothesis on the existence of a strength positive correlation between X and Z in the studied region. This generalization, however, with the used till now traditional apparatus, seems to be quite synthetizing, with a view to a more detailed determination of the type of the regression mathematical model. On that account it is appropriate to study the regression over again directly by means of the sample itself (X_i, Z_i) of the smoothed 2 x 12 original estimates for the model areas i. Exactly with this very aim the sampling polygons (X_i, Z_i) of the regressions between X and Z are plotted in Figs. 4 and 5, according to the data of the respective table (Totomanov, 1988b). The two figures corroborate the admissibility of the use of a linear model for the regression, but at the same time gives grounds to check non-linear mathematical models, too (in particular - quadratic, and for Fig. 5 - even cubic and biquadratic ones). The next section of the present work deals with investigations on the efficiency of such a mathematical model complication.

3.4. Mathematical model of the regression of X with respect to Z

The regression equation $\bar{x} = \bar{x}(z)$ which determines the mean values $\bar{x}$ for X by means of given values z for Z is the quanti-

DOI: https://doi.org/10.2312/zipe.1989.102.03

Table 6. Coefficient of the approximating power polynomials aimed to model the dependence of X upon Z

Power of the polynomial λ	Coefficients f_r for r				
	0	1	2	3	4
0	0.737 500	-	-	-	-
1	- 1.788 698	0,591 846	-	-	-
2	2.536 451	- 1.403 485	0,221 657	-	-
3	10.821 990	- 7.169 514	1.524 292	- 0.095 552	-
4	- 29.941 428	31.374 083	11.882 618	1.937 504	- 0,013 418

DOI: https://doi.org/10.2312/zipe.1989.102.03

tative expression of the established regular dependence of the recent kinematics upon the Neogene-Quaternary regional vertical Earth's crustal one. A priori useful information on the mathematical model of this equation is not available, however, because of the absence of any experience and results of similar investigations both in other regions in the world and for the territory examined. On that account, the searched for relation will be approximated by a power polynomial

$$\bar{X} = \sum_{z=0}^{z=\lambda} f_{\lambda z} Z^z \tag{14}$$

where λ and f are unknown. With the aim to determine the best fitting polynomial, similarly to ТОТОМАНОВ (1978) and Totomanov (1984, 1985b), some indices depending on λ have been studied. To this end the respective f are calculated by means of an adjustment by the method of least squares, of the data $(X_i Z_i)$ according to the sample (Totomanov, 1988 b) of the general population (X,Z). These data are treated as measurements, and the respective correction equations for X_i are formed and solved. The results of these calculations are presented in Tab 6. In the same time, or based on the polynomial obtained, the following values are determined:

quadratic form

$$\psi_\lambda = \sum_{i=1}^{i=n} \left(\sum_{z=0}^{z=\lambda} f_{\lambda z} Z_i - X_i \right)^2, \tag{15}$$

sampling standard deviation

$$\mu_\lambda = \sqrt{\psi_\lambda / (n - z - 1)} \tag{16}$$

DOI: https://doi.org/10.2312/zipe.1989.102.03

and the following criteria for the conditioning of the matrices N_λ of the coefficients before the unknowns in the systems of normal equations: the determinant of N_λ, the Turing's (1948) M-number

$$M_\lambda = M(N_\lambda).M(N_\lambda^{-1})/(\lambda+1) \tag{17}$$

and the Totomanov's (1984b) ρ-number

$$\rho_\lambda = \sqrt[\lambda+1]{\det N_\lambda} = \sqrt[\lambda+1]{\rho_1 \rho_2 \dots \rho_{\lambda+1}}. \tag{18}$$

Here the M-norms (Фадеев & Фадеева, 1960)

$$M(N_\lambda = \| a_{ij} \|) = (\lambda+1) \max_{ij} | a_{ij} |,$$
$$M(N_\lambda^{-1} = \| b_{ij} \|) = (\lambda+1) \max_{ij} | b_{ij} | \tag{19}$$

of the respective matrices, and the eigen-values ρ of the matrix N_λ are introduced. The Yule's coefficient R_λ,

$$R_\lambda^2 = 1 - U_\lambda / n\sigma_z^2 = 1 - \sum_{i=1}^{i=n} v_{i\lambda}^2 / n[\sum_{i=1}^{i=n}(X_i - \bar{X})^2/n] =$$
$$1 - \sum_{i=1}^{i=n}(X_i - \bar{x}_{\lambda i})^2 / \sum_{i=1}^{i=n}(X_i - \frac{1}{n}\sum_{i=1}^{i=n} X_i)^2, \tag{20}$$

for the model determination (Yule & Kendall, 1950) is calculated too. Here this coefficient is described, in the spirit and letter of the original cited, by the corrections v, and the forecasted values x for X. With a view to the symbolics adopted here from eqs (14), (15) and (19) the expression

$$R_\lambda = \sqrt{1 - \psi_\lambda / \psi_0} \tag{21}$$

DOI: https://doi.org/10.2312/zipe.1989.102.03

Table 7. Criteria for selecting the most appropriate degree λ of the polynomial approximating the regression equation $\bar{x} = \bar{x}(z)$

λ	ψ_λ	$\varkappa_\lambda$	μ_λ	$\det \mathbf{N}_\lambda$	ρ_λ	$M(N_\lambda)$	$M(N_\lambda^{-1})$	...
0	3.614	11	0.573	12.000	12.000	12.000	0.083	
1	0.707	10	0.266	99.592	9.980	453.847	4.577	
2	0.358	9	0.199	706.490	8.906	14 912.437	167.856	
3	0.315	8	0.198	3 292.221	7.575	497 277.651	6 677.950	
4	0.286	7	0.202	7.688.930	5.987	17 304 549.900	284 987.614	

...	M_λ	R_λ
	11.0	0.000
	11 038.6	0.897
	834 380.7	0.949
	830 198 822.4	0.955
	986 004 995 570.8	0.960

DOI: https://doi.org/10.2312/zipe.1989.102.03

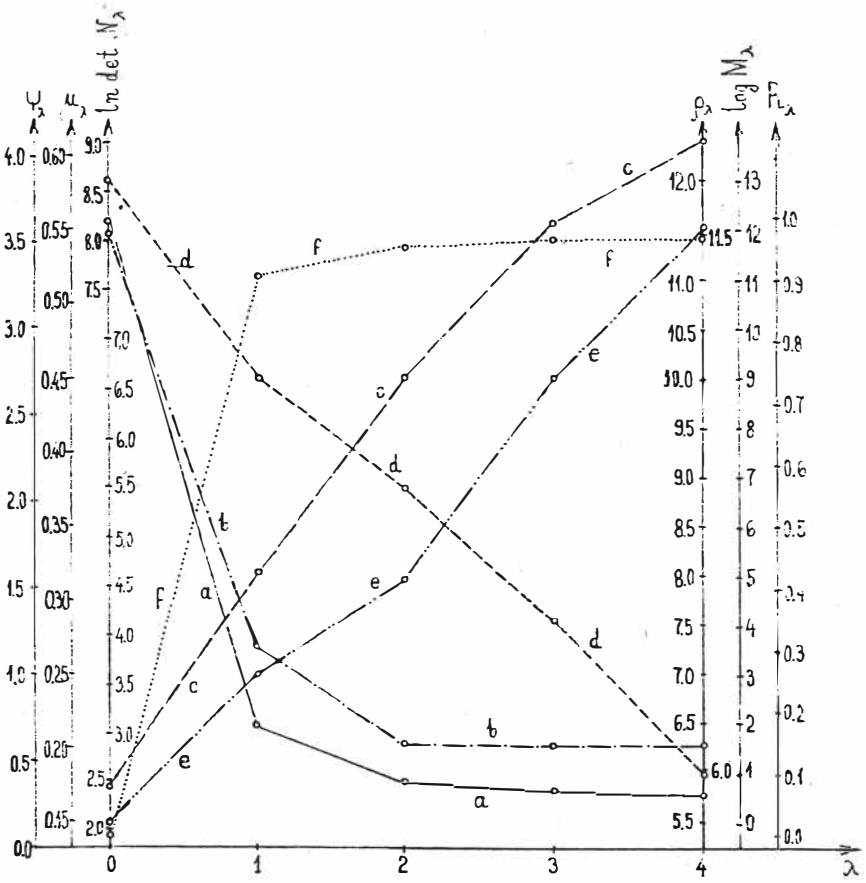

Fig. 6. Criteria of selecting the degree λ of the best fitting polynomial approximating the sampling dependence of X upon Z (see the text): a - quadratic form ψ_λ, b - standard deviation μ_λ, c -transformed determinant of the matrix N_λ of coefficients before unknowns in the system of normal equations, d - eigenvalue ρ -number for N_λ, e - transformed Turing's M-number for N_λ, f - Yule's coefficient of model determination.

DOI: https://doi.org/10.2312/zipe.1989.102.03

follows which is used in the present work.

Some of the essential interim and final results of all these calculations are given in Tab. 7. Partially suitably transformed (for det N_λ - in ln det N_λ , and for M_λ - in log M_λ), these data are plotted in Fig. 6.

The analysis of Tab. 7 and Fig. 6 allow to draw the following more important conclusions for the degree λ of the polynomial approximating the regression equation $\bar{x} = \bar{x}(z)$:

a. The criteria det N, ρ and M in the present study (in contrast to other similar elaborations - see Totomanov, 1984b, for instance) manifest a low informativity. With a view to ρ and M, the transit from the linear to a quadratic model is of low efficiency compared to the transit both from the point to a linear and from the quadratic to a cubic and to a biquadratic model. With a view to det N, the increasing of λ to 3 is connected with an uniform decreasing of the stability (conditioning) of the numerical solutions, and the further model complication surprisingly impede the development of the effect of this risk factor.

According to the complex of these three criteria, the linear model is quite satisfactory; this model is argued, by the use of other means, and successfully applied in the first express study mentioned (Totomanov, 1988 b) on the relation between X and Z.

b. The criteria ψ , μ and R manifest a very high informativity in the present study. It is evident that the transit from the linear to a quadratic model (especially with regard to μ) is quite well grounded; a further increasing of λ , however, practically has not any positive effect.

According to these three criteria, the quadratic model is the best fitting one.

DOI: https://doi.org/10.2312/zipe.1989.102.03

c. The joint consideration of the behaviour of all 6 criteria studied convincingly demonstrate the admissibility of the linear and the optimum type of the quadratic model as well as the following, from the latter conclusion, actually curvilinear, but quite close to a normal one, correlation between X and Z.

4. Regression equation and accuracy of the forecast of recent vertical Earth's crustal movements by means of Neogene-Quaternary ones

On the basis of these final studies, according to Tab. 6 and the established optimum degree $\lambda = 2$, it can already be ascertained that the best fitting the sampling data polynomial prognosticating mean values $\bar{x}$ ($mm.a^{-1}$) for X, by means of given values z(hm) for Z, within the Shoumen Transitional Zone is

$$\bar{x} = 2.536 - 1.404z + 0.222\,z^2 \tag{22}$$

at a root mean square error $m_{\bar{x}}$ for $\bar{x}$ determined by the formula

$$m_{\bar{x}}^2 = 0.224\,53 - 2.009\,80\,z + 0.677\,67\,z^2 - 0.100\,90\,z^3 + 0.005\,60\,z^4 . \tag{23}$$

Equations (22) and (23) are namely the searched for quantitative expression of the directly demonstrated for the first time here regular dependence of the recent X upon the neotectonic Z Earth's crustal movements.

The graph of the new quadratic equation (22), together with the confidence areas

$$\bar{x} - t_\gamma m_{\bar{x}} < X < \bar{x} + t_\gamma m_{\bar{x}} \tag{24}$$

DOI: https://doi.org/10.2312/zipe.1989.102.03

related to the standard confidence probabilities

$$(25) \qquad P(|X - \bar{x}| < t_{\gamma(q)} m_{\bar{x}}) = \gamma_q$$

are plotted in Fig. 7. Here γ_1 = 99,7%, γ_2 = 95,4% and γ_3=68,3% according to the "rule of $q m_{\bar{x}}$" , at q = 1,2,3 for sufficiently great samples from normal general populations.

In the examined case, however, the volume n = 12 of the sample studied is small, and by means of the Student's t-distribution, at γ_q and the number of the degrees of freedom $\mathcal{E}$=n-m= =12-3=9 (here m is the number of the parameters estimated in the model adopted of the regression equation), by means of the respective tables, the values $t_{\gamma(1)}$ =4,0211 (Бронштейн & Семендяев, 1986), $t_{\gamma(2)}$ =2,330 (Янко , 1961) and $t_{\gamma(3)}$ = 1,058 (Христов , 1965) are determined. With these values, according to eq. (24), 13 confidence intervals related to each one from the three standard probabilities mentioned are calculated, and the respective confidence areas of the quadratic approximating polynomial (24) for the regression equation $\bar{x} = \bar{x}(z)$ are plotted.

Aimed to compare with the results of the new study, the graph of the same regression equation but for a linear model (Totomanov, 1988b) is plotted too, with its confidence area related to the probability γ_1 = 99,7%. In this case, at $\mathcal{E}$ = = 12-2=10, by the use of the Student's t-distribution, the value $t_{\gamma(1)}$ = 3,892 (Бронштейн & Семендяев,1986) is determined.

It could be clearly seen in Fig. 7 that the transit from a linear to a quadratic mathematical model of the regression equation is not connected with some considerable decreasing of the confidence area of the prognosis. The comparison of Fig. 7

DOI: https://doi.org/10.2312/zipe.1989.102.03

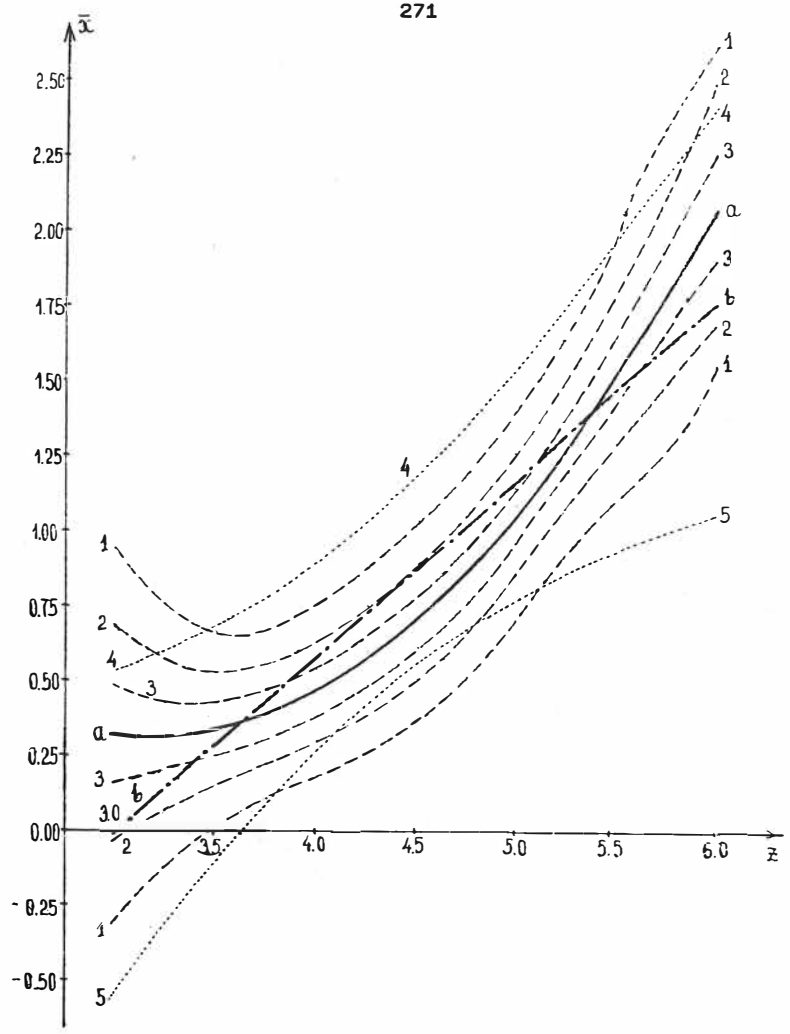

Fig. 7. Best prognosis of mean values $\bar{x}$ (mm.a^{-1}) of the recent Earth's crustal movements, by means of given values z (hm) of the neotectonic ones, within the Shoumen Transitional Zone. Admissible linear model: b - graph of the equation; border lines of the confidence area at probability 99.7 %: 4 - upper, 5 - lower. Optimum curvilinear model: a - graph of the equation; border lines of the confidence area of the prognosis at: 1 - probability 99.7 %, 2 - probability 95.4 %, 3 - probability 68.3%

DOI: https://doi.org/10.2312/zipe.1989.102.03

and Fig. 4, however, and making use of the data in Tab. 7, by taking into consideration Fig. 6, demonstrates the considerably better characteristics of the quadratic approximation of the sampling data compared to the linear one. This analysis elucidates the meaning of the conclusions made in the preceding text on the satisfactory effect of the linear, and the optimum effect of the quadratic model for the regression of X with respect to Z.

Finally it should be emphasized that the established close positive correlation between X and Z together with the reliable forecast of X by means of Z really are the first quantitative assessment of the degree of predestination of the recent by the Neogene-Quaternary vertical kinematics of the Shoumen Transitional Zone. This predestination is manifested by a regular maintenance during the nowadays epoch, too, of the main neotectonic tendencies of the geodynamic development during the final 10-15 millions of years, of the Earth's crust within the region under examination. On the other hand, the results obtained for this periplatform-orogenetic zone, demonstrate the necessity of a territorial extension of the investigations. It is appropriate, in particular, to study the relation between the Neogene-Quaternary and the recent dynamics of the neighbouring to this zone regions of the Moesian platform and of the Eastern Balkanides, with the aim to elucidate the specific role which the two respective types of Earth's crust play in the tectonic processes of the northern Black-Sea coast. This will contribute both to the fundamental scientific elaborations related to the region studied, and to an establishment of more general regularities of planetary character, by means of comparison and discovering of similar particularities within other regions of the same type in the world.

DOI: https://doi.org/10.2312/zipe.1989.102.03

REFERENCES

Bončev, E., Bune, V.J., Christoskov, L., Karagjuleva, J., Kostadinoov, V., Reisner, G.J., Rizhikova, S., Shebalin, N.V., Sholpo, V.N., Sokerova, D. 1982. A method for compilation of seismic zoning prognostic maps for the territory of Bulgaria. - Geologica Balcanica, t. 12, No. 2, 3-48

Joo, I. (ed.-in-chief), Jovanović, P., Somov, V.I., Thury, J., Totomanov, I.N., Vanko, J., Wyrzykowski, T., Visarion, M (eds.). 1979. Map of recent vertical crustal movements in the Carpatho-Balkan region. Scale 1:1 000 000. Budapest, National Office of Lands and Mapping - Cartographia, 2 sheets

Müller, P., Neumann, P., Storm, R. 1979. Tafeln der mathematischen Statistik. 3. verbesserte Auflage. Leipzig, VEB Fachbücher Verlag, 270 S.

Paradine, C.G., Rivett, B.H.P. 1962. Statistical methods for technologists. 2nd ed. London, The English University Press Ltd., 288 p.

Totomanov, I.N. 1984a. On the statistical dependence between long-term seismic activity and recent tectonic movements in Bulgaria. - Comptes rendus de l'Académie bulgare des Sciences, t. 37, No. 1, 39-42

Totomanov, I.N. 1984b. A study on the relationship between the seismic hazard and the recent Earth's crustal movements in Bulgaria. - Viša geodezija (Geodesy), No. 10, 72-80

Totomanov, I.N. 1985a. Dependence of seismic activity upon recent tectonic movements in Bulgaria. - Geologica Balcanica, t. 15, No. 3, 33-44

Totomanov, I.N. 1985b. Relation between earthquake focal intensity and recent vertical Earth's crustal movements in the Rila-Rhodope seismic region. - Veröffentlichungen des Zentralinstituts für Physik der Erde, Nr. 81, Teil III, Potsdam. Akademie der Wissenschaften der DDR, 148-155

DOI: https://doi.org/10.2312/zipe.1989.102.03

Totomanov, I.N. 1985c. Regional field and correlation features of the maximum earthquake magnitude and recent vertical crustal movements in Southwestern Bulgaria. - Bâlgarsko geofizično spisanie (Bulgarian geophysical journal), t. XI, No. 4, 123-129

Totomanov, I.N. 1988a. Information approach to the assessment of the dependence of earthquake focal intensity upon recent tectonic activity. - Comptes rendus de l'Académie bulgare des Sciences, t. 41, No. 7, 47-49

Totomanov, I.N. 1988b. Space-time effects in the interrelation between Neogene-Quaternary and recent tectonic movements within the Eastern Fore-Balkan. - Comptes rendus de l'Académie bulgare des Sciences, t. 41, No. 11, in print

Totomanov, I.N., Georgiev, N.I., Raev, P.S., Jovev, Il., Bončev, E.S., Christoskov, L.Vl., Petkov, I.N., Vaptsarov, I.N. 1987. Geodynamic studies in the region of Sofia - argumentation, results and prospects. - Geologica Balcanica, t. 17, No. 2, 3-14

Turing, A.M. 1948. Rounding-off errors in matrix processes. - Quarterly journal of mechanics and applied mathematics, t. 1, 287-308

Vapcarov, I., Galabov, J., Michev, K., Georgiev, M., Vrablianski, B. 1974. Neotectonic map of Bulgaria. - In: Proceedings of the Seminar on the seismotectonic map of the Balkan region (Dubrovnik, 1973). Skopje, UNESCO, Appendix No. 11

Yule, G.U., Kendall, M.G. 1950. An introduction to the thepry of statistics. 14th ed., revised and enlarged. London, Ch. Griffin and Co., Ltd., 780 p.

Бончев, Е. 1987. Балканидите. Геотектонско положение и развитие. София, БАН, 273 с.

Бронштейн, И.Н., Семендяев, К.А. 1986. Справочник по математике для инженеров и учащихся втузов. Изд. 13-ое исправл. Москва, Наука, 544 с.

Вентцель, Е.С. 1964. Теория вероятностей. Изд. 3-ье, исправл. Москва, Наука, 576 с.

DOI: https://doi.org/10.2312/zipe.1989.102.03

Г е о г р а ф и я н а Б ъ л г а р и я в т р и т о м а . Том I - Физическа география. Природни условия и ресурси. 1982. Под ред. на Ж. Гълъбов и др. София, БАН, 514 с.

Г и т и с , В . Г . , М и р о н о в , М . А . , Б у н а , В . И . , В ы ч е в , В . Т . 1982. Построение карты M_{max} землетрясений на основе метода аппроксимации интервальных экспертных оценок. - Известия АН СССР. Физика Земли, т. 18, № 4, 3-14

Р и з н и ч е н к о , Ю . В . /отв. ред./. 1979. Сейсмическая сотрясаемость территории СССР. Москва, Наука, 192 с.

Т о т о м а н о в , И . Н . 1978. Някои проучвания за съвременните менните вертикални движения на земната кора и релефа на физическата земна повърхност в България. - Висша геодезия, № 4, 21-32

Т о т о м а н о в , И . Н . , В р ъ б л я н с к и , Б . Г . , М л а д е н с в с к и , М . М . 1978. Изследване и картиране на съвременните вертикални движения на земната кора в България. - Проблеми на географията, № 3, 68-74

Ф а д д е е в , Д . К . , Ф а д д е е в а , В . Н . 1960. Вычислительные методы линейной алгебры. Москва, Физматгиз, 656 с.

Х р и с т о в , В л . К . 1965. Изравнение по метода на най-малките квадрати. София, Техника, 171 с

Я н к о , Я . 1961. Математико-статистические таблицы. Пер. с чешск. Москва, Госстатиздат, 244 с.

DOI: https://doi.org/10.2312/zipe.1989.102.03

STRESS FIELD IN THE LITHOSPHERE DUE TO TOPOGRAPHY AND DENSITY INHOMOGENEITIES

Jiří Trešl
Geophysical Institute Czechosl.Acad.Sci.,
Boční II, Spořilov, CS - 141 31 Praha 4

S u m m a r y: Stress and strain fields in the incompressible elastic plate floating at the fluid basement are investigated. It is assumed the stress sources are terrain topography and crustal density inhomogeneities. The expressions are derived for two-dimensional stress and displacement components. Calculations performed along the Carpathian profile KP III show the maximum horizontal stress 70 MPa in this region.

Р е з ю м е: Исследуются поля напряжений и деформаций с помощью модели несжимаемой упругой плиты на жидком основании. Источниками напряжений является совместное влияние нагрузок от рельефа местности и от плотностных неоднородностей земной коры. Выведены выражения для компонент двумерного напряжения и смещения. Из расчетов на Карпатском траверсу КП 3 вытекает, что горизонтальные напряжения в этой области достигают значений 70 МПа.

1. INTRODUCTION

One of the most important tasks of geophysics to-day is the determination of stress and strain fields in the lithosphere. In principle, the lithospheric stress field may be generated either due to various forces acting at the upper and bottom boundary or as a result of body forces in the interior [1] . Only the upper part of the lithosphere can be treated as an elastic layer in geological time scale; in the lower part the stress relaxation probably occurs due to solid body creep [2] .

The purpose of this paper is to study the stress field generated by the topography and crustal density inhomogeneities. The influence of topography itself was investigated by several

DOI: https://doi.org/10.2312/zipe.1989.102.03

authors [3] , [4] , [5] . The results obtained are only weakly dependent on the compressibility and an incompressible model may be used for the load wavelengths up to several hundreds kilometres. On the other hand, the distribution of crustal density inhomogeneities can strongly influence the primary stress field generated by terrain topography and cannot be neglected.

2. MATHEMATICAL ANALYSIS

We shall study two-dimensional deformation of an incompressible elastic plate with density ρ floating at a fluid basement with density $\rho_f > \rho$ (Fig.1). The plate density may be written

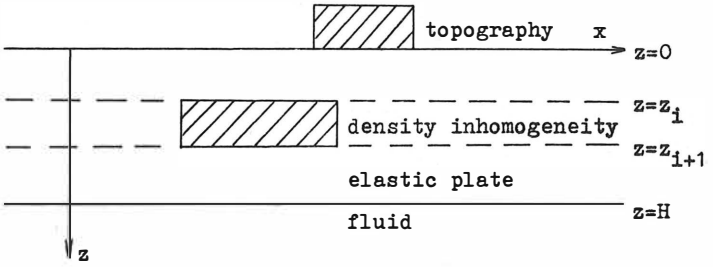

Fig.1

$$\rho(x,z) = \rho_0 + \rho_1(x,z)$$

where ρ_0 is initial density and ρ_1 the density perturbation resulting from crustal inhomogeneities. Initially, the plate is in the state of hydrostatic equilibrium. The state of deformation under this initial stress is taken as the reference state. The additional stress and displacement fields are measured from this reference state. The equations of static equilibrium are [6]

$$(1) \quad \partial\sigma_{xx}/\partial x + \partial\sigma_{xz}/\partial z = 0$$

$$(2) \quad \partial\sigma_{xz}/\partial x + \partial\sigma_{zz}/\partial z + \rho_1 g = 0$$

where σ_{xx}, σ_{zz} , σ_{xz} are components of the total perturbation stress and g is the gravity acceleration, which is supposed to be constant. The stress-strain relations for an incompressible

DOI: https://doi.org/10.2312/zipe.1989.102.03

medium are [6]

(3) $\sigma_{xx} = -p + 2\mu\, \partial u/\partial x$

(4) $\sigma_{zz} = -p + 2\mu\, \partial w/\partial z$

(5) $\sigma_{xz} = \mu(\partial u/\partial z + \partial w/\partial x)$

Here u,w are the displacement vector components, p the unknown pressure and μ Lame's elastic constant. The equilibrium equations in displacements become

(6) $-\partial p/\partial x + \mu \Delta u = 0$

(7) $-\partial p/\partial z + \mu \Delta w + \rho_1 g = 0$

Further, the incompressibility condition

(8) $\partial u/\partial x + \partial w/\partial z = 0$

provides the third equation for the determination of three unknowns u, w, p. We may express the displacements in terms of a potential Ψ

(9) $u = -\partial\Psi/\partial z \qquad w = \partial\Psi/\partial x$

and, after elimination of pressure terms we arrive at

(10) $\Delta\Delta\Psi = -(g/\mu)\,\partial\rho_1/\partial x$

On the other hand, eliminating displacements terms, we obtain

(11) $\Delta p = g\,\partial\rho_1/\partial z$

Now, we shall suppose crustal density inhomogeneities are generalized with the help of a layered model. The perturbation density ρ_1 is supposed to be independent of z-coordinate within each layer. We shall solve Eqs.(10),(11) for a harmonic density perturbations

(12) $\rho_1 = \rho_1^0 e^{ikx}$

keeping in mind the fact, each real density perturbation may be expressed as a superposition of harmonic terms. The general solutions of Eqs.(10),(11) are then

(13) $\Psi = (Ae^{kz} + Be^{-kz} + Cze^{kz} + Dze^{-kz} - ig\rho_1^0\mu^{-1}k^{-3})e^{ikx}$

(14) $p = 2\mu k(Ce^{kz} + De^{-kz})ie^{ikx}$

DOI: https://doi.org/10.2312/zipe.1989.102.03

where A,B,C,D are arbitrary constants for each layer. From Eqs. (3),(4),(5),(9) we obtain final expressions for the stress tensor components

$$(15)\quad \sigma_{xx} = -[ae^{kz} - be^{-kz} + c(2+kz)e^{kz} + d(2-kz)e^{-kz}]e^{ikx}$$

$$(16)\quad \sigma_{zz} = [ae^{kz} - be^{-kz} + ckze^{kz} - dkze^{-kz}]e^{ikx}$$

$$(17)\quad \sigma_{xz} = [ae^{kz} + be^{-kz} + c(1+kz)e^{kz} - d(1-kz)e^{-kz} + \rho_1^0 g k^{-1}]ie^{ikx}$$

and for the displacement vector components

$$(18)\quad u = (2\mu k)^{-1}[ae^{kz} - be^{-kz} + c(1+kz)e^{kz} + d(1-kz)e^{-kz}]ie^{ikx}$$

$$(19)\quad w = (2\mu k)^{-1}[ae^{kz} + be^{-kz} + ckze^{kz} + dkze^{-kz} + 2\rho_1^0 g k^{-1}]e^{ikx}$$

New constants a,b,c,d are connected with old ones as

$$(20)\quad (a,b) = 2i\mu k^2 (A,B) \qquad (c,d) = 2i\mu k (C,D)$$

We must determine altogether 4n unknown constants if we employ n layers in our model. The boundary conditions at the upper surface read

$$(21)\quad \sigma_{zz}(x,0) = \rho g w(x,0) - \rho g h(x)$$

$$(22)\quad \sigma_{xz}(x,0) = 0$$

The physical meaning of the first condition is the vertical stress balances surface load due to topography h(x) and the weight of displaced elastic plate.

The boundary conditions at the lower surface are

$$(23)\quad \sigma_{zz}(x,H) = -(\rho_f - \rho) g w(x,H)$$

$$(24)\quad \sigma_{xz}(x,H) = 0$$

Here the vertical stress balances the buoyancy force at the bottom side of the elastic plate. Finally, the continuity of stresses and displacements at internal layer boundaries demands

$$(25)\quad \sigma_{zz}^{(i)}(x,z_i) = \sigma_{zz}^{(i+1)}(x,z_i)$$

$$(26)\quad \sigma_{xz}^{(i)}(x,z_i) = \sigma_{xz}^{(i+1)}(x,z_i)$$

DOI: https://doi.org/10.2312/zipe.1989.102.03

(27) $u_i(x,z_i) = u_{i+1}(x,z_i)$

(28) $w_i(x,z_i) = w_{i+1}(x,z_i)$

The boundary conditions (21)-(28) represents altogether 4n linear algebraic equations for the 4n unknown constants.

3. THE STRESS FIELD ALONG THE PROFILE KP III ZAKOPANE - SALGÓTARJÁN

The overall length of the profile was 400km (-150km≤x≤250km), of which 150km are on the territory of Poland, 120km on the territory of Czechoslovakia and 130km on the territory of Hungary (Fig.2). The Czechoslovakian section of this profile is bounded by 0 km≤x≤120km .The following reference densities were adopted:

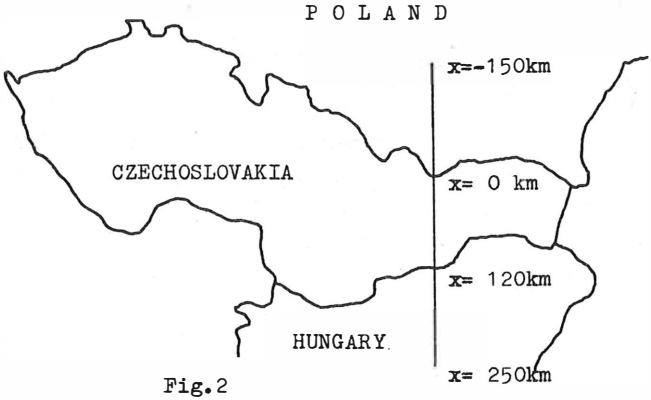

Fig.2

ρ_1 = 2700 kg/m^3 for 0 km < z < 10 km ,
ρ_2 = 2800 kg/m^3 for 10 km < z < 20 km ,
ρ_3 = 3000 kg/m^3 for 20 km < z < 30 km ,
ρ_f = 3200 kg/m^3 for z > 30 km .

The elastic layer thickness H=30km and μ =3 x 10^{4}MPa [2].

Approximation rectangles with a constant base 10km and variable height equal to the mean sea elevation of the terrain were established for computing the effect of the terrain topography. The elastic plate was divided into 6 layers with uniform thicknesses 5km. In each layer, generalized density inhomogeneities

DOI: https://doi.org/10.2312/zipe.1989.102.03

were created from actual ones taken from [7].

Surface loads and generalized density inhomogeneities were expressed by Fourier series using interval length L=2000km, much lomger than the profile lengfh. Stress and displacement fields have been computed for x = -150,-140,...240,250km and for z = 0, 5,...25,30km. All computations were performed in two variants:

A/ The source of stress field is only topography,

B/ The source of stress field is topography and crustal density inhomogeneities.

The basic results may be formulated in this manner:

1/ Along the profile given, the elastic lithosphere behaves like "thin plate". It means that the horizontal stress component σ_{xx} is dominant. For given x, σ_{xx} is maximum at the upper and bottom boundary of the plate, but with opposite direction.

2/ The horizontal stress component σ_{xx} at z=0 along the profile KP III is illustrated in Fig.3. In the A-variant, compressible horizontal stress reaches maximum value 140 MPa at the boundary between Czechoslovakia and Poland (the High Tatras), whereas tensional stresses with maximum value 42 MPa are generated at Hungary. In the B-variant, maximum compressible stress is reduced to 72 MPa and shifted to x=55km (Vepor deep-fault). On the contrary, maximum tensional stress is increased to 74 MPa for x=200km (Balaton lineament).

3/ The vertical displacement of the bottom boundary is shown in Fig.4. In the A-variant, the maximum deflection 570m occurs at the boundary between Czechoslovakia and Poland. In the B-variant, the maximum deflection reduces to 270m and is practically unshifted. The maximum uplift 140m is generated for x=230km.

R E F E R E N C E S

[1] BOTT,M.-KUSZNIR,N.: The origin of tectonic stress in the lithosphere. Tectonophysics 105(1984),1.
[2] TURCOTTE,D.-SCHUBERT,G.: Geodynamics. Wiley,New York 1982.
[3] COMER,R.: Thick-plate flexure. Geophys.J:RAS 72(1983),101.
[4] WOLF,D.: Thick-plate flexure re-examined. Geoph.J.RAS 80(1985).
[5] TREŠL,J.-MARVANOVÁ,V.: Stresses and displacements in the floating lithosphere due to terrain topography. Studia geoph.et geod.32(1988),in press.
[6] ERINGEN,A.: Mechanics of continua. Wiley,New York 1967.
[7] BIELIK,M.et al.: Density models along the profiles crossing the West Carpathians. PFUK Bratislava 1988,in press(in Slovak).

DOI: https://doi.org/10.2312/zipe.1989.102.03

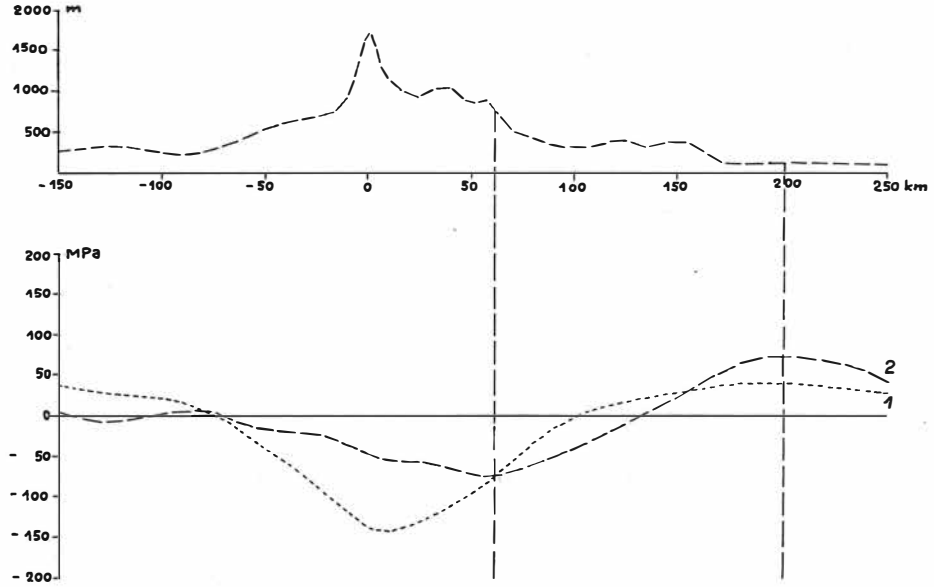

F i g. 3 Horizontal stress along the profile KP III.
1 - topography, 2 - topography and density inhomogeneities
Above topography elevations.

DOI: https://doi.org/10.2312/zipe.1989.102.03

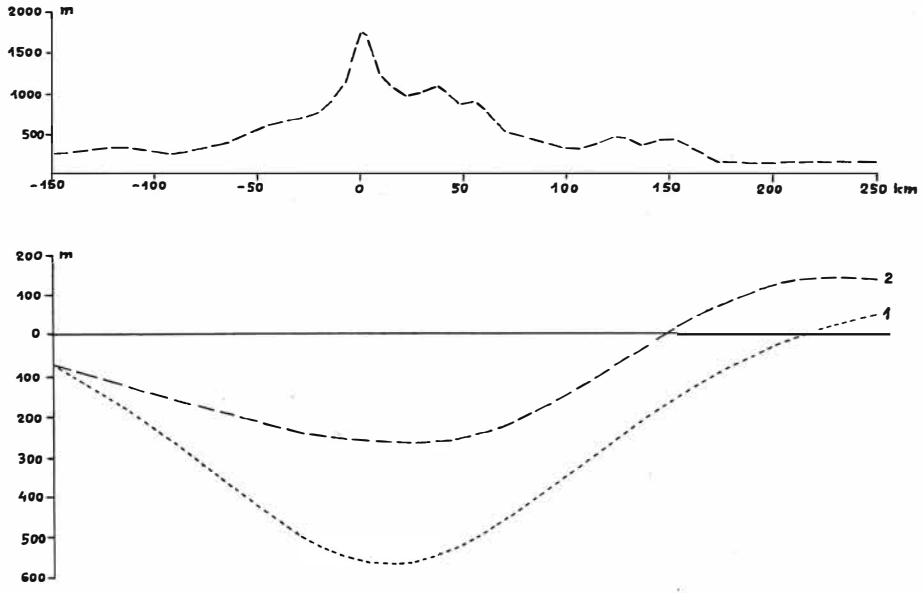

F i g. 4 Vertical displacement w along the profile KP III.
1 - topography, 2 - topography and density inhomogeneities
Above topography elevations.

DOI: https://doi.org/10.2312/zipe.1989.102.03

RECENT CRUSTAL MOVEMENTS IN THE LIGHT OF EARTH EXPANSION THEORY

Klaus Vogel, Gabelsbergerstraße 27, Werdau GDR-9820

Abstract

The theory of Earth expansion is starting from the assumption that Pangaea covered completely the surface of a smaller Earth till Mesozoic. By growing volume of the Earth due to endogenic processes this crust broke to pieces and the continual widening gaps developed to the oceans of today.

A reconstruction of this crust is represented at a globe with 60 % and the stage of the half opened oceans with 75 % of the present Earth diameter. These globes are enclosed within transparent spheres of the modern Earth to compare the starting positions with the present situation. It is visible that the continents in general seem to be fixed at the substratum, retaining their positions to each other. Herewith the recent crustal movements are mainly determined by radial outward pressing of the continents and filling the growing gaps by new oceanic crust accordimg to seafloor spreading. A series of photos gives a survey of this development.

The question arises whether this process will be detectable by modern methods of intercontinental measurements in a foreseeable future, especially whether the Pacific is shrinking or widening by some cm per year.

Zusammenfassung

Die Theorie der Erdexpansion geht davon aus, daß die Pangaea bis zum Mesozoikum die kleinere Erde völlig bedeckte. Durch Wachsen des Erdvolumens wurde diese Kruste von innen heraus zerrissen und die sich weitenden Bruchspalten entwickelten sich zu den heutigen Ozeanen.

Eine Rekonstruktion dieser Urkruste ist auf einer Kugel mit 60 % und das Stadium halb geöffneter Ozeane mit 75 % des heutigen Erddurchmessers dargestellt. Zum Vergleich mit dem Jetztzustand wurden diese Globen zentral in die durchsichtige heutige Erde eingefügt. Hierbei erscheinen die Kontinente auf ihrem Substrat fixiert, so daß sie ihre Lage zueinander weitgehend beibehalten haben. Die rezenten Krustenbewegungen sind hauptsächlich durch das strahlenförmige Herausheben der Kontinente gekennzeichnet. Dazwischen entsteht durch Seafloorspreading neue Kruste. Eine Fotoserie zeigt dies im Überblick.

Es erhebt sich die Frage, ob dieser Vorgang durch die modernen Methoden der interkontinentalen Messungen in absehbarer Zeit nachweisbar ist, vor allem, ob der Pazifik schrumpft oder sich jährlich um einige cm ausweitet.

DOI: https://doi.org/10.2312/zipe.1989.102.03

The aim of this contribution is to point to the possibility of the expanding Earth as an alternative model to the plate tectonics theory and its implications to recent crustal movements. The Earth expansion theory is starting from the assumption that the archaic Earth had only about half of its present diameter and the surface was completely covered with continental crust. In consequence of a slow growth originated from the core, this crust became disrupted and the widening gaps were filled with new crust from still continental components. During the Mesozoic with more than 60 % of the present diameter due to the accelerating rate of expansion, the fragments of continental crust separated, by roughly remaining constant in their shape and size. Between the fragments new oceanic crust originated, representing now the beginning of seafloor spreading. The axes of the midoceanic ridges essentially followed the old fracturelines and are today the main expansion joints of the expanding Earth. No surplus oceanic crust is formed which demands a subduction at other places.

On global models with increasing diameters the fit of the continets and the development of the oceans are represented, showing the accordance of the growing surface and the pattern of seafloor spreading. These globes are enclosed within transparent plastic globes of the modern Earth for comparison of the starting positions with the present distribution of the continents. It is visible that the kinematics of the crustal fragments is mainly determined by radial outward movements during expansion. Simultaneously the distances of the continental fragments at the surface are increasing, but their arrangement to each other remains nearly unchanged. Hereby the recent crustal movements are resulting from horizontal and vertical components which both are caused by the

DOI: https://doi.org/10.2312/zipe.1989.102.03

expansion of the Earth. Based on these models the direction and magnitude of the movements supposed today can be estimated for the diffenrent regions of the crust. This is especially clear on the southern hemisphere with the dismemberment of Gondwana. It is estimated that the annual growth of the South Atlantic is 2 cm, of the Indic is 3 cm and the South Pacific is 7 cm. That means that the growth of the circumference in about 30 degrees southern latitude is 12 cm, if no subduction of ocean floor takes place. Calculated for the equator it is adequate to an annual radius increase of 2 - 2,5 cm. According to this the circumference of the circles of longitude must increase as well. This mainly takes place in the circumantarctic systems of rifts extending the southern oceans parallel to the latitudes. This is one reason for the asymmetric distribution of continents and oceans.

Because of this the surface of the southern hemisphere is more expanding than the northern hemisphere. Therefore at the latter the circles of latitude are migrating to the south. In addition compensating movements by horizontal shifting and opening of wedgeshaped gaps result from geometrical reasons. They are also influenced by different strength of the lithosphere, the interactions between stress and strain and the magnitude of friction between the crust and mantle within the asthenosphere. Important examples of these movements are the shearing of West- and East Antarctica or the huge parallel shifting (megashear) between the westcoast of North America and the northcoast of Asia in connection with the forming of the Pacific. The San Andreas fault of California today may be an aftereffect of this displacement.

Starting from the estimate that the Earth radius increased by 2500 km during the last 200 million years the average annual increase is 1,25 cm. We must suppose that during this period the rate of expansion accelerated. Therefore the above mentioned amount of 2 - 2,5 cm may be convenient for today.

DOI: https://doi.org/10.2312/zipe.1989.102.03

Recently Dr. W.D. Parkinson calculated with the help of values of intercontinental measuerements by the NASA an annual radius increase of 2,8 ± 0,8 cm (Carey 1988). This corresponds very well with the two values estimated beforehand.

The fit of the continents on a smaller globe and from there the development of the oceans according the pattern of seafloor spreading demonstrate a high degree of probability for a considerably expanding Earth, regardless of some more supporting arguments from other fields. On the other hand there are also strong objections against an expansion in the magnitude postulated above mainly from physical viewpoints. They concentrade on questions of gravitation, length of the day, celestial mechanics or the suggested increase of mass of the Earth parallel to its expansion.

Summarized it is very important whether in the course of the next years the continuation of the intercontinental measurements will confirm the trend of Dr. Parkinson's calculation. The deciding question is whether in accordance with the expectation of the plate tectonics the Pacific diminishes by some cm per year or whether instead of this an increase in the sense of the Earth expansion theory will be demonstrated. Especially the distance between Australia respectively New Zealand and South America is of uppermost interest.

THE GLOBAL MODELS

The presented global models show two different stages of the expanding Earth:

- The fit of the continents to a closed crust on the surface with a diameter of roughly 60 % of today (before Trias).
- The partly opened oceans on the planet with a diameter of 75 % (Cretaceous).
- These globes enclosed within a transparent modern Earth showing the development of the oceans and the outward movement of the continents to their present positions caused by expansion.

DOI: https://doi.org/10.2312/zipe.1989.102.03

REFERENCES

Bretterbauer, K.: Expandiert die Erde? - ÖZfVuPh 72. Jahrg. (1984) 3 p. 81-93.

Bretterbauer, K.: Geodäsie und Erdgeschichte - Vermessungstechnik, Berlin 35 (1987) 5, p.146-149.

Carey, S.W.: The Expanding Earth.-Devel. Geotectonics, 10 Amsterdam 1976 488 p.

Carey, S.W.: (Ed.) The Expanding Earth - a Symposium, Hobart, Univ.Tasmania 1983, 423 p.

Carey, S.W.: Diapiric Krigogenesis. In: F.-C. Wezel (Ed.): The Origin of Arcs. Devel. Geotectonics, 21 Amsterdam 1986 p. 1-40.

Carey, S.W.: Theories of the Earth and Universe. - Stanford University Press 1988, 413 p.

Crawford, A.R.: The Origin of the Pacific on an expanding Earth. In: F.-C. Wezel (Ed.) The Origin of Arcs.- Devel. Geotectonics 21, Amsterdam 1986 p.423-434.

Hilgenberg, O.C.: Vom wachsenden Erdball, - Berlin 1933.

Milanovskij, E.E.(Ed.):Problems of Expansion and Pulsation of the Earth.- Nauka Moskva 1984. 190 p. (in Russian).

Osipishin, N.Ya. and Blinov, V.F.: Age zonation of oceanic crust and its connection with Earth expansion. Byull Mosk Ova Ispyt Prir Otd Geol.(1987)62.4, p.18-30 (in Russian).

Pfeufer, J.: Die Gebirgsbildungsprozesse als Folge der Expansion der Erde.-Essen: Verl.Glückauf, 1982 128 p.

Scalera, G.: Nonconventional Pangea reconstructions: new evidence for an expanding Earth. Tectonophysics 146, (1988) p. 365-383.

Vogel, K.:Global models and Earth expansion. In:S.W.Carey(Ed.) The Expanding Earth, Hobart, Univ.Tasmania 1983 ,p.17-27.

Vogel, K.: Beiträge zur Frage der Expansion der Erde auf der Grundlage von Globenmodellen. Z.geol.Wiss., Berlin 12 (1984) 5 p. 563-573.

Wegener, A.: Die Entstehung der Kontinente und Ozeane. 4.Aufl. Braunschweig: Verl. Vieweg & Sohn, 1929. 231 p.

Wolf, H.: Moderne Methoden der geodätischen Ortsbestimmung. Naturwissenschaften 73, (1986) p. 292-298.

DOI: https://doi.org/10.2312/zipe.1989.102.03

CRUSTAL MOVEMENTS AT SEISMOACTIVE AREA OF CHEB - WESTERN BOHEMIA

Pavel Vyskočil, Research Institute of Geodesy, Topography and Cartography, Zdiby, Czechoslovakia

ABSTRACT

One of the seismoactive zone of Czechoslovakia is the area Cheb-Kraslice, at the western border with GDR and FRG. The occurence of earthquake swarms is typical there, and the last swarm occured in the winter 1985/86. Consequences of some main shocks affected buildings in the Cheb vicinity and the quakes were registered also in central part of Bohemia. No special geodetic measurements were performed before the swarm, but the available data of triangulation can serve for analysis of the dynamical properties of the area under study. In present paper the three repeated triangulations performed in 1870, 1930 and 1947 are analyzed at the background of the map of vertical movements, based on the levellings from 1930-1950 and 1975-1984. The derived field of horizontal deformations as well as the isolines of vertical movements are in good agreement with the geological structure and situation of the seismoactive faults. In addition, the extremal uplift of the area under study could be considered as the pre-seismic deformation. In order to support this assumption, the new repeated measurements are in progress.

DOI: https://doi.org/10.2312/zipe.1989.102.03

INTRODUCTION

The seismoactive area of Cheb-Kraslice is situated at the crossing of the Jáchymov-Mariánské Lázně fault system in NW direction, and Podkrušnohorský fault zone in NE direction. All seismic events - earthquake swarms - are shallow (of about 10 km or less) and the epicenters of main shocks occure either at the territory of Czechoslovakia or at the territory of GDR. The earthquake swarm of 1985/86 was relatively strong with damages at buildings and sounds similar to thunder (Procházková, 1986). Two workshops were organized to this swarm during 1986 (Proceedings, 1986a, 1986b) and the scientific interest was focused at this area. In addition to seismolcgical and other geophysical studies, the results of repeated geodetic measurements were analyzed with respect to the occurence of the swarm. The first results were published at mentioned above workshops (Vyskočil, P., 1986a, 1986b). The following presentation could be considered as the continuation of previous work, summarizing all available data in one analysis.

The properties of horizontal component are given in the field of deformation determined for the epochs 1870-1930 and 1930-1947 separately. The annual velocities of vertical movements are given by the isolines with the interval 0.1mm/a and cover the epoch 1945 - 1980.

VERTICAL MOVEMENTS

The data on vertical movements are derived using repeated levellings performed in years 1939-1950 (average 1945) and 1975-1984 (average 1980), at whole territory of Czechoslovakia. After the careful chioce of proper benchmarks, the network was adjusted and values of annual velocities of vertical movements were determined relatively to the Fundamental

DOI: https://doi.org/10.2312/zipe.1989.102.03

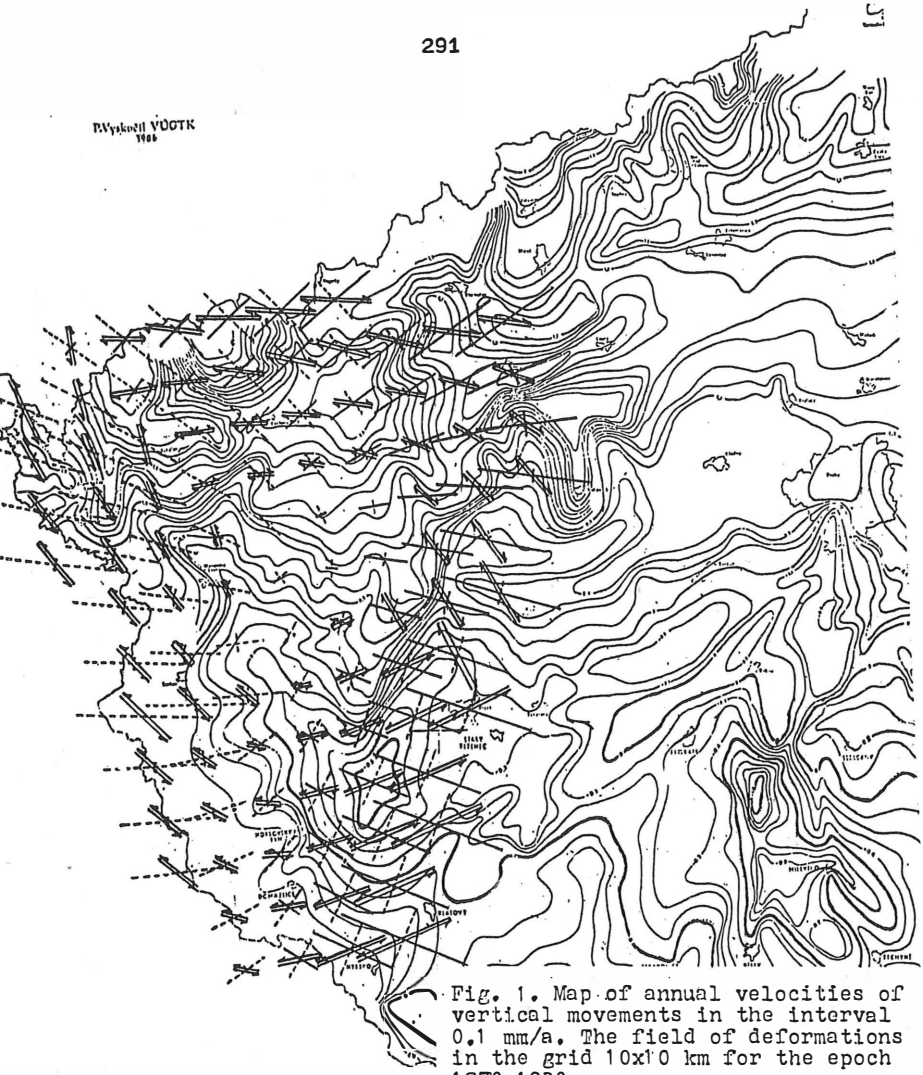

Fig. 1. Map of annual velocities of vertical movements in the interval 0.1 mm/a. The field of deformations in the grid 10x10 km for the epoch 1870-1930.

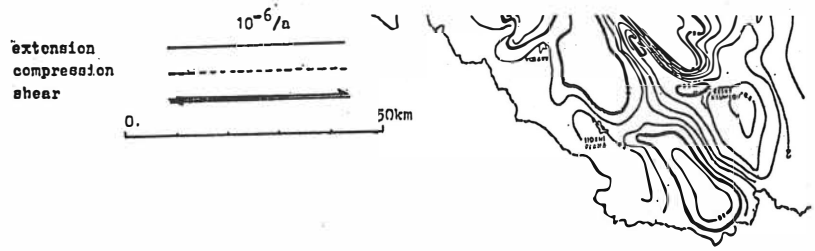

DOI: https://doi.org/10.2312/zipe.1989.102.03

Levelling Benchmark Želešice, situated in the structures of the Bohemian Massif southern from Brno in the central part of Czechoslovak territory (Vanko, J., Vyskočil, P., 1987). The adjusted values in very dense network served for compilation of the map of annual relative velocities of vertical movements, constructed orginally in the scale 1:200 000. For isolines was chosen the interval 0.1 mm/a. The western part of this map is the basis for present analysis of vertical movements in the area under study (Fig. 1.). In comparison with the map constructed early (Vyskočil, P., Kopecký, A., 1974) for previous epoch, the area under study tends to strong uplifts for last years before the earthquake swarm. This uplift is distinct especially in the area of Kraslice and can be considered as the preseismic movement.

In order to separate the main trends of vertical movements and their residuals, the second order polynomian approximation was applied. The trend of vertical movements is given in Fig. 2 and demonstrate the systematical tilt from NW to SE with the maximum values 1.5 mm/a at NW border and 0.4 mm/a at the SE border of the area. The residuals are given in Fig. 3. The uplift of area Kraslice by NW border is evident with the strong tendencies to subsidences towards SW, where the isolines follow the seismoactive fault zones by Cheb, where the main quakes of the swarm 1985/86 took place. At SE side follow isolines the direction of the Podkrušnohorský fault zone interrupted by uplift between Kraslice vicinity and Doupovské hory Mts. (+0.5 mm/a). Following the SE continuation of seismoactive zones, the subsidences in Marianské Lázně fault are evident. With respect to the fact that the map of this part is based on relevellings from 1984, we can suppose the whole picture as the preseismic movements in the vertical direction.

DOI: https://doi.org/10.2312/zipe.1989.102.03

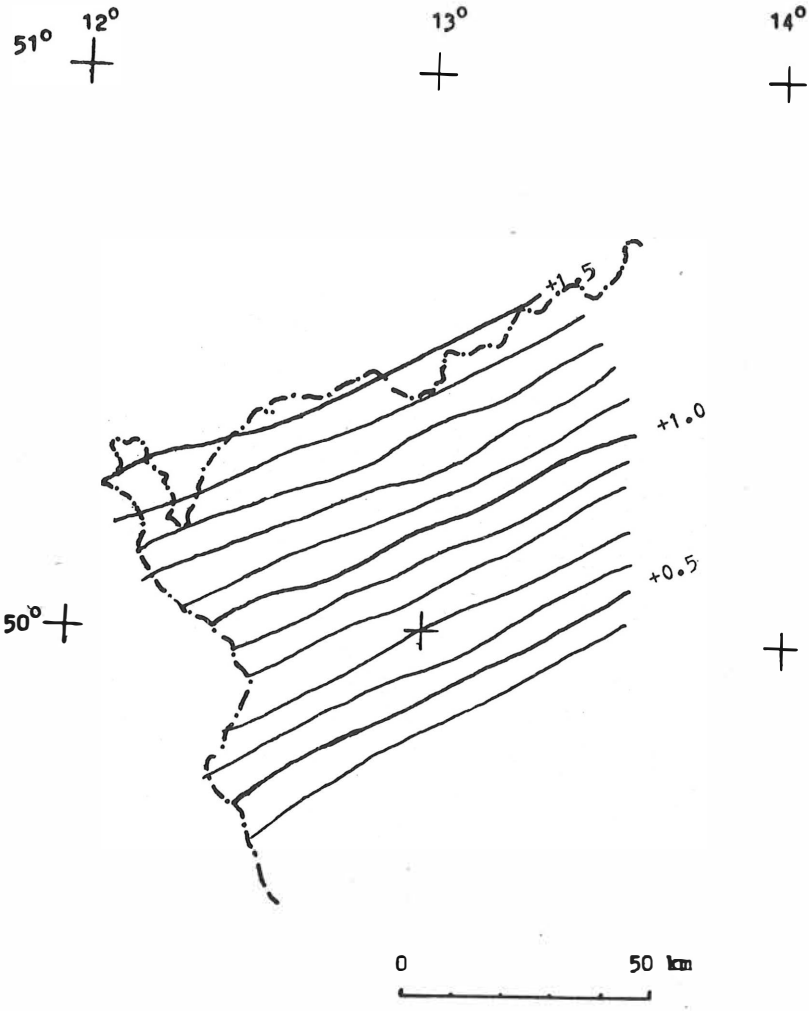

Fig. 2. The trend of annual velocities of vertical movements in the vicinity of the seismoactive area Cheb-Kraslice. Isolines given in the interval 0.1 mm/a.

DOI: https://doi.org/10.2312/zipe.1989.102.03

Fig. 3. The residuals in the trend analysis od annual velocities of vertical movements. Full lines uplifts, Dashed lines subsidences. Isolines given in the interval 0.1 mm/a.

DOI: https://doi.org/10.2312/zipe.1989.102.03

HORIZONTAL DEFORMATIONS

As has been stated early, the results of three repeated triangulations were used for our present analysis. The network used for the epoch 1930-1947 is more dense in the area under study than the for the epoch 1870-1930. It is why the area covered by our results for epoch 1870-1930 is broader. By the initial processing the single triangulations were adjusted separately as the free networks. Applying the Helmert´s transformation the coordinates of 1930 were transformed into the system 1870, and the coordinates of 1947 into the system 1930. The average accuracy in determination of coordinate differences for the epoch 1870-1930 is given by the value $m_x \doteq m_y = 4.5$ mm/a and for the epoch 1930-1947 $m_x \doteq m_y = 3.8$ mm/a. The average lateral displacement for the epoch 1870-1930 is given by the value of $dx \doteq dy = 6.9$ mm/a and for the epoch 1930-1947 $dx \doteq dy = 10.7$ mm/a. The presented accuracy gives the evidence that the determined coordinate differences can be consider as horizontal movements.

By the further processing of available data, the horizontal movements for the epoch 1870-1930 were trasformed in areal field of horizontal deformations using third order polynomian approximation. The field of deformations, i.e. the main axis of compression and/or extension and shear deformation, were computed in the grid 10x10 km. The area covered by computations was extended especially southward in comparison with the data set used by Vyskočil (1986b). The results of computations are given in Fig. 1. at the background of the map of annual velocities of vertical movements. It must be point out that the orientation of shear deformations in Cheb area is in the direction of seismoactive fault system as well as in the direction of crossing Podkrušnohorský fault zone.

The main parameters of deformation for the epoch 1930-1947 were determined within separate triangles only.

DOI: https://doi.org/10.2312/zipe.1989.102.03

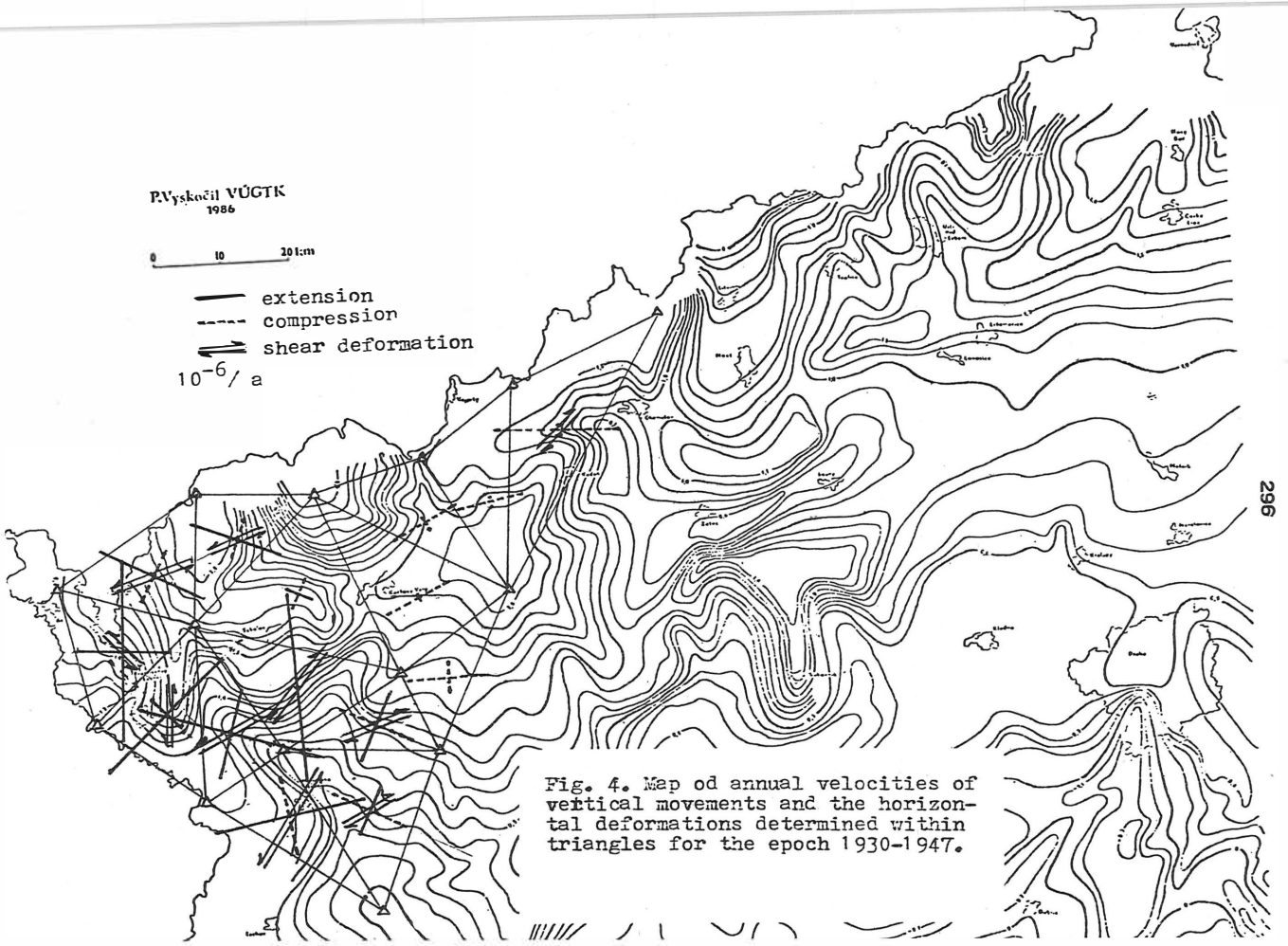

Fig. 4. Map od annual velocities of vertical movements and the horizontal deformations determined within triangles for the epoch 1930-1947.

DOI: https://doi.org/10.2312/zipe.1989.102.03

The results are given in Fig. 4, also at the background of the part of the map of annual velocities of vertical movements. The orientation of the shear deformation in the area under study is similar to the deformations given for the epoch 1870-1930 in Fig. 1.

DISCUSSION OF RESULTS

Comparing the results of analysis in both horizontal and vertical directions of movements or deformations we can find the common features. Especially, it is the evidence of seismoactive fault system in NW direction resulting from orientation of isolines of vertical movements residuals and orientation of shear deformations in the same directions in both epoch of retriangulation. By the same way are evident the vertical movements and horizontal deformations along the part of the Podkrušnohorský fault zone in NE direction. The interruption of deformation and movements at this fault zone towards NE is also evident. This probably connected to the presence of neovulcanits in Doupovské hory Mts. area.

As concerns the vertical component of movements it should be point out the extremal uplift in the area of Kraslice and the large gradient across the seismoactive faults system. The levelling measurements were performed in this part in 1984 and can be accompanied to the stage of preparation of earthquake swarm. Some detail analysis along separate levelling lines are in agreement with this assumption and were published earlier (Vyskočil, P., 1986a). This preliminary statement should be tested at further repeated levellings performed or planned after the swarm 1985/86.

In comparison with the vertical component, the horizontal deformation are not related to the earthquake swarm under study. Moreover, during the large time interval 1870-1930 occured there the other swarms, comparable with the last one(1897, 1900, 1903, 1908, 1911, 1929). In the

DOI: https://doi.org/10.2312/zipe.1989.102.03

epoch 1930-1947 occured only two small swarms (1930 and 1936). It means that the field of deformations given either in Fig. 1. or in Fig. 4. reflects only the main tendencies of horizontal deformations in the area under study. From this viewpoint it is important the agreement in the direction of the shear deformations in both epochs. But, comparing the main axes of deformation we can recognize the tendencies to compression in 1870-1930 and for extension in 1930-1947. This difference can be considered as not identical number and intensity of swarms occured in both epochs. In addition, it can be supposed the connection of these differences and variations of the state of stress in various stages of seismic activity. The answer on this open question can be given also by detail studies of horizontal deformations. The measurements focused at this problem are planned for the next year.

The mechanism of the earthquakes in the stage of their prepartion is difficult to discuss now. Nevertheless, it can be supposed that the deformations determined at the area under study are the result of main compressional pressure from the Alps, affecting especially the central part of the border with FRG towards NE (Vyskočil, P. 1988). This main force is then distributed by separate blocks of the Bohemian Massif including the blocks of the area under study. The direction of deformations than can varried with respect to the orientation of borders of separate crustal blocks.

CONCLUSION

The results of analysis of vertical movements as well as horizontal deformations in the area of Cheb-Kraslice are presented. The results of the analysis of vertical movements allow us to suppose the connection between the uplifts and strong gradients at seismoactive faults system and the occurence of the earthquake swarm 1985/86. The mentioned above pheno-

DOI: https://doi.org/10.2312/zipe.1989.102.03

mena can be considered as the pre-seismic movements due to the stress accumulation in shallow parts of the crust. The horizontal deformations are also in good agreement with the geolcgical structure of the area under study, and reflects the difference in orientation of seismoactive faults system and Podkrušnohorský fault zone. Due to other time intervals, the horizontal deformations themselfs are not related to present earthquake swarm. Nevertheless, the variation in dilatation and similarities in shear deformations allow us to suppose the mutual connection between the seismic activity and variations of stress in the crust.

With respect to the importance of the vicinity of the seismic area under study (mineral waters, mining activity etc.) the detail studies of its seismicity is very desirable. It is why the system of levelling lines and trigonometric stations was established there in 1987 and 1988 in order to increase the number of new data on the vertical and horizontal movements before the next earthquake swarm. In this direction it could be also recommended to connect the present network in Cheb-Kraslice area to the network in test area Vogtland in the DDR (Ergebnisse, 1985). These works and studies can essentially contribute to the understanding of the mechanism of erthquake swarms in the stage of their preparation and occurence.

REFERENCES

Proceedings, 1986a : Počítačové spracovanie údajov Česko-slovenskej siete. SAV, ČSAV, Bratislava (in Czech).

Proceedings, 1986b : Earthquake swarm 1985/86 in Western Bohemia. ČSAV - Geophysical Inst., Praha.

DOI: https://doi.org/10.2312/zipe.1989.102.03

Ergebnisse, 1985: Ergebnisse der Untersuchungen rezenter Erdkrustenbewegungen in Testgebieten der DDR. Geo-Geodätische und geophysikalische Veröffentlichungen, Reihe III, Heft 52, Berlin.

Procházková, D., 1986: Processing results of macroseismic data on the 1985/86 Earthquake swarm in Western Bohemia. In: Proceedings (1986b).

Vanko, J., Vyskočil, P.:1987: The map of vertical crustal movements in Czechoslovakia and its interpretation. Journal of Geodynamics 8, 143-150, Amsterdam.

Vyskočil, P. 1986a: Probable indications of a swarm occurence derived from analysing repeated geodetic measurements. In: Proceedings (1986a).

Vyskočil, P., 1986b: Horizontal recent tectonic deformations in Western Bohemia. In: Proceedings (1986b).

Vyskočil, P., Kopecký, A., 1974: Neotectonics and recent crustal movements in the Bohemian Massif. Edition of the Research Inst. of Geodesy, Topography and Cartography (VÚGTK). Monographical Publication. Praha.

Vyskočil, P., 1988: To the dynamics of the Bohemian Massif. Journal of Geodynamics,(in print), Amsterdam.

DOI: https://doi.org/10.2312/zipe.1989.102.03

THE PRESENT STATE OF CRUSTAL MOVEMENT STUDIES AT KALABSHA AREA, ASWAN, EGYPT

P. Vyskočil

International Centre On Recent Crustal Movements, Zdiby, Prague, Czechoslovakia,

R.M. Kebeasy , A. Tealeb and S.M. Mahmoud

National Research Institute of Astronomy and Geophysics, Helwan, Cairo, Egypt

ABSTRACT

Aswan lake is the second largest man-made reservoir in the world. Its filling started 1964 and earthquake of magnitude 5.6 took place in 1981 at Kalabsha fault area. Since then, seismicity continuous to occur around the fault in that area.

Local geodetic network of 16 points was established in 1983 around Kalabsha fault for monitoring vertical and lateral movements. Five repeated horizontal and two repeated levelling measurements were performed since 1984. The analysis of these measurements revealed remarkable horizontal and vertical changes.

INTRODUCTION

On November 14, 1981 a moderate earthquake with a local magnitude of 5.6 occured at the unpopulated area of Kalabsha, along the Kalabsha fault, 70 km southwest of Aswan City (Kebeasy et al.,1982 , Kebeasy et al.,1987). This earthquake was considered as a very important event as it is located not far from the Aswan High Dam. Due to its possible association with the impoundment of Lake Nasser, especially the water activity in and around this lake, and as the Aswan High Dam is the single dam which affects the whole country, several programms, such as monitoring seismicity, underground water behaviour, strong motion effects on important structures and crustal deformation by means of geodetic methods were initiated.

DOI: https://doi.org/10.2312/zipe.1989.102.03

In order to monitor continuously the earthquake activity around the lake and to investigate its relationship with water activity in and around the lake, a radio-telemetry network of 13 seismic stations (fig.1) were established around the northern part of the lake and has operated since July 1982 (Kebeasy et al., 1987 , Simpson et al.,1987). The seismic events are recorded telemetry at the Regional Seismological Center at Aswan.

Eight strong motion accelerographs were installed on the Aswan High Dam, old dam and free fields in order to record the acceleration due significant earthquakes and to study soil and structural response.

A network of 6 piezometers (fig.1) constructed in 1983 and 1985 around the northern part of the lake. The purpose of this network is to investigate the relationship between the hydrological regime of underground water and the earthquake activity in and around the lake. This investigation is to assess the underground water level and its role in the pore-pressure changes in the Nubian formation. The data from the six piezometers (water level, temperature and pressure of underground water) are transmitted telemetry into the Regional Seismological Center at Aswan.

In order to monitor horizontal and vertical crustal movements, using geodetic methods, around the northern part of Lake Nasser to investigate their possible association with the earthquake activity and the water loading in the lake and to understand the geodynamics of the area, a long term study program was planned (Kebeasy et al.,1984 , Vyskočil and Tealeb,1985 , Vyskočil et al.,1987). This programm includes establishments and measurements of local and regional geodetic networks around potential faults. The first local geodetic network (Kalabsha network) was established around an active part of the Kalabsha fault in November 1983 (fig.1). The network consist of 16 geodetic points for horizontal measurements and two levelling lines (fig.2). The initial measurements were carried out in

DOI: https://doi.org/10.2312/zipe.1989.102.03

December 1984. The measurements were repeated in February 1986, January 1987, September 1987 and January 1988.

This paper focuses on the present state of crustal movement studies at Kalabsha area using the precise geodetic measurements. The work includes short notes about the geology, structure and seismicity of the area to the south of Aswan and around Lake Nasser. The preliminary results of adjustments and interpretations of the geodetic measurements are also discussed. The aim of the whole studies carried in the area is a better understanding about the cause of the earthquake occurance and its origin and also earthquake prediction in order to diminish the seismic risk within the area of Aswan as well as the safety of the Aswan High Dam and its economic resources.

HISTORICAL VIEW , GENERAL GEOLOGY AND STRUCTURES OF THE AREA SOUTH OF ASWAN

1. Aswan Lake (Lake Nasser): Throughout history of Egypt, the River Nile have ever been the source of gift. Floods of the River Nile were known in some years, while in the other years drought has prevailed. The water income to the Nile is irregular, i.e. its yield varies daily, monthly, seasonly and annually. The idea of constructing a High Dam at Aswan for high level storage was brought up in 1952. Such a dam would guarantie supplying Egypt with the required amount of water for agricultural expansion and protecting the country from the periods of high floods. Besides, the dam would also provide the country by clean hydroelectric power essential for industry, agriculture and national development.

The Aswan High Dam is considered as a unique structure among all the large irregation and electric power projects in the world. It is rockfill and concrete type structure, 110 m height. It is located above the first cataract of the Nile, 15 km south of Aswan City. The dam impounds the second largest man-made reservoir in the world extending about 500 km in southern Egypt and northern Sudan, 350 km of them extends in the Egyptian teritories along the main course of the River Nile. The reservoir, over most of

DOI: https://doi.org/10.2312/zipe.1989.102.03

its length, has a width of about 10 kms. The only major exptions to this is the embayments to the west of Wadi Kurkur and Wadi Kalabsha (fig.1). The reservoir began to be filled early in 1964 and the level rose gradually with annual irrigation cycles and reached a maximum level of 177.48 m in November 1978.

2. General Geology and Structures : The area of southern Egypt is belong to the so-called Arabio-Nubian Massif. To the east, the lake overlies mainly Pre-Cambrian rocks and contacts mainly Pre-Cambrian granits and metamorphyics. To the west, the lake covers the Nubian sandstone formations.

In the area to the northwest of Lake Nasser a sequence of sedimentary rock units, consists mainly of the Nubian formations, ranging in age from late Cretaceous to Eocene unconformably overlies Pre-Cambrian basement rocks. The Nubian formation is composed of fine- to course-grained sandstone with some shale and siltstone intercalations. The information from boreholes indicates that the Nubian formation is approximately 500 m thick.

The tectonic setting of the area is characterized by the presence of two main sets of fault system and regional uplift of the basement rocks (Issawi, 1968, 1971, 1978). These sets are the north-south and the east-west fault systems (fig.1). The Kalabsha fault is located on the western side of the River Nile and was identified as the source of the 14 November 1981 earthquake (Kebeasy et al.,1982 , Kebeasy et al.,1987). This fault is well-expressed on aerial photographs and associated with en-enchelon folds. Its total length is approximately 300 kms. Geologic, seismologic and geomorphic evidences indicate that the fault is a right-slip fault. The Seiyal fault is located approximately 12 km north of the Kalabsha fault. It is also right-slip fault. The north-trending fault system affect the Nubian formation and includes the Gebel el-Barqa, Kurkur, Khor el-Ramla, Gazelle and Abu-Dirwa faults (fig.1).

DOI: https://doi.org/10.2312/zipe.1989.102.03

PREVIOUS AND RECENT STUDIES IN THE AREA SOUTH OF ASWAN

1. Seismicity: Until recently no significant earthquakes were reported to have take place around the Lake Nasser. Moreover, the lake area was regarded as aseismic area (Gutenberg and Richter, 1954). Microearthquake survey carried out around Abu-Simbel in 1981 (Gibowicz et al., 1982) shows that all the microearthquakes originated either directly under or close to the reservoir.

The Kalabsha area is the most recently active area. It lies on a large western embayment of Lake Nasser. Earthquakes were estimated to have occurred near the epicentre of the main earthquake of 1981. Earthquake activity in the area is continuing at a low level till now. The 14 November 1981 earthquake was occurred in Kalabsha area along the Kalabsha fault near Gebel Marawa, 70 km southwest of Aswan City. Extensive ground craking were occurred in the desert within the epicentral area. This earthquake was preceded by three foreschockes,on November 9 (magnitude 3.6 and 4.2) and on November 11 (magnitude 4.5), and followed by a tremendous number of afterschocks. The 14 November 1981 earthquake is the most significant signal earthquake in the region because of its proximity to the Aswan and High Dams and because of its possible association with the reservoir induced seismicity.

The activity is believed to be triggered by the lake (Kebeasy et al.,1982) because: there is no significant earthquake has been located in the lake area throughout history, the epicenter of this earthquake is located near a considerably wide area of the lake, water penetration in the fractured near-surface rocks and the increased pore-pressure and the lake is very large and relatively deep.

Analysis and interpretation of seismograms, recorded by the telemetry network, shows that the seismicity clusters are in three main zones (fig.1). The first- and most active zone extends WSW-ENE for about 14 kms along the Kalabsha fault approximately

DOI: https://doi.org/10.2312/zipe.1989.102.03

beneath Gebel Marawa. The hypocenters are concentrated at two depth intervals: from 14 to 22 km, and from 4 to 7 km. The second zone extends for 8 km along another segment of Kalabsha fault which is closer to the old stream of the Nile. In this zone, the activity is confined to depths from 4 to 6 km. Regarded the foci distribution in these two zones, a gradual decrease in depths from west to east is observed. The third zone is located at Wadi Kurkur in the northwestern part of the lake and about 15 km south of the Aswan High Dam. This zone is characterized by low seismicity (Kijko et al., 1985) and shallower events at a depth of about 12 km.

The predominat focal mechanism of the activity at Kalabsha is a right-lateral strike slip faulting on an east-west fault plane. The epicentral distributions of earthquakes, occurred in the Kalabsha area from July, 1982 to December, 1987 are given in figure 3 (Kebeasy et al., 1987).

It is expected that the filling of Lake Nasser will alter the distribution of stresses in the subsurface beneath the lake and its vicinity. Also, the load of the water may change the total stresses on the surface of the area under investigation. Therefore, the water level in the reservoir and the number of earthquakes as well as their magnitudes, which occurred in the area, are continuosly recorded. An example of these data for the period from July, 1982 to March, 1988 are given in figure 4 (Kebeasy et al., 1988). From these data, it is noticed that the increase of earthquake activity in the area follows a high rate of change in the water level of the lake. This phenomenon is clear in the increased seismicity of : February 1983, December 1983- January 1984 and June 1987.

2. Hydrological Regime : Analysis of the data from the piezometers (water level, temperature and pressure of underground water) show that there is a relationship between the change of the water level in the lake and the underground water level around the lake for a long period, whereas for the short periods (monthly, seasonally and annually) there is no remarkable relation.

DOI: https://doi.org/10.2312/zipe.1989.102.03

The increase of the earthquake activity in Kalabsha area in Febraury 1983, December 1983 - January 1984 and June 1987 were followed a high rate of change in the water level in the lake, while the underground water level does not show remarkable change. Therefore, no clear conclusion could be drawn between the underground water regime and earthquake activity in Kalabsha area. This may be due to the existance of various north-south and east-west trending sets of faults which could act as barries. This conclusion leads to a fact that, the relationship between the underground water regime and the water level in the lake as well as the earthquake activity still needs more studies.

RECENT CRUSTAL MOVEMENT STUDIES

The recent crustal movement study in the northwestern area of Lake Nasser contributes successiful example for the studies of seismo-active areas in Africa. The aim of these studies are the mapping of the tectonic elements presented within the area, to understand the geodynamics of the region and to have a better understanding about the cause of the earthquake occurence and its origin. The scientific use of the informations and results of the above mentioned studies contribute a good base in earthquake prediction in order to diminsh the seismic risk within the area of Aswan and the safety of the Aswan High Dam and its economic resources.

The monumentation of the geodetic points in the desert condition is not so easy according to the problem of transportation in the desert. The benchmarkes were prepared from concrete fixed to a depth reaching the consolidated hard rocks (Vyskočil, 1984 a, Vyskočil and Tealeb, 1985). The marks for the horizontal and vertical measurements were installed at the top of the concrete. Carriying out the geodetic measurements in the desert conditions as at Aswan region, where the measurements are taken, is also not easy. The geodetic field works are laborious and slow. The one-second theodolite Kern DKM-2A and the electro-optical distancemeter Kern DM 503 with an accuracy of $\pm$ 3 mm were used

DOI: https://doi.org/10.2312/zipe.1989.102.03

for the precise angles and distance measurements. The precise automatic level Kern GK 2A, invar rodes of 3 m length and heavy footplates were used for monitoring the vertical movements.

The Kalabsha network (fig.2), 16 points for horizonta. measurements and two levelling lines crossing the fault, was established early in 1983. The initial measurements was performed in December 1984 and the measurements were repeated in February 1986, January 1987, September 1987 and January 1988. For the purpose of adjustment of the horizontal movements in the different epochs, the Kalabsha local network was considered as a free network.

Vertical Movements : The initial levelling measurements along the levelling lines (fig. 2 and 5) were carried out during January 1986. Repeated levelling measurements were performed in October 1987 and January 1988. The levelling measurements in the different epochs show a high accuracy of measurements. The relative vertical movement between the different benchmarks of the levelling profiles were determined considering the benchmark No. 13 as an initial level (fig.5). High rate of subsidence in Kalabsha area was recorded in the southwestern part of the network as represented by the areal projection of the vertical movement in figure 6.

In figure (5), the division of the network into two areas with different mean values of height changes in millimeter for the time interval from January 1986 to January 1988 and zone of maximal gradient of elevation changes are shwon. The elevation changes and the zone of maximal gradient of elevation changes are also clear along the profile extends from point No. 52 to point No. 13 crossing the Kalabsha fault (fig.7).

The trend of changes in elevations at several points were studied. In figure 8, the trend of height changes for the time interval from January 1986 to January 1988, at the mid point between 52 and 12 was represented. Annual height change of - 1.7 mm was recorded at this point.

DOI: https://doi.org/10.2312/zipe.1989.102.03

Horizontal Movements : Processing of four horizontal measurements (distances and angles) were performed in 1987. The processing includes :

1) the separate adjustment of the horizontal measurements of 1984, 1986, 1987 I,and 1987 II as a free network.
The results of adjustments of the horizontal measurements of the the different epochs show a high accuracy of measurements (Vyskočil et al. 1987 , Mahmoud, 1988).

2) the transformation of coordinates of the different epochs, 1986, 1987 I and 1987 II into the system of coordinates of 1984 using the Helmert' s transformation (Vyskočil, 1984 b).
The re-adjustments of the Kalabsha network improved the accuracy of measurements (Vyskočil et al., 1987 , Mahmoud, 1988).

3) the evaluation of the results of adjustment and transformation, using the error criteria given by Vyskočil (1984 a), (mean square error and confidence interval).

The displacement vectors of the Kalabsha local network were computed from the coordinate changes considering the usual assumption that the changes of coordinates after the transformation give the information on the displacements of the geodetic points during the considered time interval.

The displacement vectors for the epochs 1986, 1987 I and 1987 II are represented in figures 9, 10 and 11 respectively. Considering the confidence limit, most of these displacements vectors can be attributed mainly as the movement occured within the considered area in the different epochs of measurements.

The horizontal distances between each two points of the Kalabsha network were determined and the tendencies of horizontal movements within the considered network were computed from the horizontal distances which determined in the different epochs. In figure 12, the rate of annual deformation in millimeter are represented at each side of the different triangles of Kalabsha network. Different annual rates of displacements (extension and compression) were recorded. From this figure, the distance between points 52 and 51 shows a higher value of the annual rate of

DOI: https://doi.org/10.2312/zipe.1989.102.03

displacement (extension). The distances between the points which are close to the fault show a relatively small values of annual rate of displacement. Two examples for the main pronounced tendency in case of extension and compression (shortening) are given in figures 13 and 14 respectively.

Considering the results of tendencies of distance changes in time, the southern part of the Kalabsha network show a maximum trend of horizontal changes, whereas the northern part of the network and distances close to the trace of the fault show a relatively minimum trend of horizontal changes (fig.12). These results are in good agreement with the results of the vertical movement which in turn shows a high rate of subsidence in the area to the south of the network and a relatively small rates of subsidence in the northern part of the network (fig.5).

The initial information for the original displacements at the points of the network for the different epochs shown in figures 9, 10 and 11 were used for the determination of the displacements in grid of 1x1 km. The interpolated displacements of horizontal movements for the epochs 1986, 1987 I and 1987 II are given in figures 15, 16 and 17 respectively. These displacements were also used for the determination of the main axis of horizontal deformation fields (extensions and compressions) in the same grid. Results of these analysis are shown in figures 18, 19 and 20, where the main axis of horizontal deformation feilds for the epochs 1986, 1987 I and 1987 II are given respectively.

The analysis of the interpolated displacements of the horizontal movements in the different epochs show a general trend of regular pattern of movement. The points nearly to the south of Kalabsha fault, have an easterly motion, whereas the points to the north of the fault, have approximately westwards movements. In general, the area of Kalabsha network seems to move anticlockwise with a small component of rotation. The difference between the displacements from the epoch 1987 I to the epoch 1987 II could be according to accumulation of energy in the subsurface preceded the earthquake activity of June 1987 (fig.4). The values of

DOI: https://doi.org/10.2312/zipe.1989.102.03

strain parameters (figures 18, 19 and 20) indicate that, the area of the Kalabsha network got strained from one epoch to another and to rotate approximately anticlockwise.

The analysis of information from geology, seismicity, water level in the lake, underground water table and geophysical study with the results of deformations should be carried out after the performance of several geodetic measurements.

CONCLUSIONS

Monitoring of recent crustal movements (horizontal and vertical) was carried out at one of the most seismo-active area along the northwestern part of Lake Nasser (Kalabsha area) south of Aswan City in Egypt. This work was begon after the occurance of a moderate earthquake, with a magnitude of 5.6, on November 14, 1981 in the area along the Kalabsha fault 70 km southwest of the city of Aswan. A local network of 16 geodetic benchmarks and two levelling lines crossing the fault was established on a part of the Kalabsha fault early in 1983. The initial measurements were carried out in December 1984. The measurements were repeated in February 1986, January 1987, September 1987 and January 1988.

Although the period of the field observations is relatively short, the analysis of the obtained data indicated a significant evidence of both horizontal and vertical movements during the considered time interval. The preliminary analysis of the first four measurements show the following results :

1) The vertical movements indicates a maximum rate of subsidence at the southern part of the network and a minimum rate of subsidence in its northern part.
2) High rate of subsidence in Kalabsha area was recorded in the southwestern part of the network.
3) Zone of maximal gradient of elevation changes was determined, which could be correlated with the well-known trace of the fault.
4) Maximum trend of horizontal movements was determined in the southern part of the network.
5) Minimum trend of horizontal movements was recorded relatively

DOI: https://doi.org/10.2312/zipe.1989.102.03

in the northern part of the network and close to the trace of the fault.

6) The most of the area of the Kalabsha network, has got strained from one epoch to another and seems to rotate approximately anticlockwise.

7) The results of the vertical movements are in a good agreement with those of the horizontal movements.

In order to make it clear, the relation between these movements and the change of the water level in the lake, the underground water table as well as the seismicity of the area, it is planned to continue the precise geodetic measurements. Also, it was decided to extend stepwise the system of geodetic network containing some other local networks situated at the other faults and connected them by regional network to cover the whole area of the northern part of the lake. The study of the problem of geodetic refraction for this part of the Egyptian desert is in stage of data analysis. Detailed geophysical studies of the whole area includes gravity and magnetic surveys as well as seismic refraction and electric sounding along various profiles are also planned.

REFERENCES

Gibowicz, S.J. , Droste, Z. , Kebeasy, R.M. , Ibrahim, I.M. and Albert, R.N.H. ,(1982), A micro-earthquake survey in Abu-Simble area in Egypt. Engineering Geology 19, pp. 95 - 109.

Gutenberg, B. and Richter, C.F. ,(1954), Seismicity of the earth and associated phenomena. Princeton Univ. Press.

Issawi, B. ,(1968), The geology of Kurkur-Dungul area. General Egyptian Organization for Geological Researh and Mining, Geological Survey, Cairo, Paper No. 46, 101 p.

Issawi, B. ,(1971), Geology of the Darb el-Arabin, Western desert. Annals of the Geological Survey of Egypt.

Issawi, B. ,(1978), Geology of Nubia west area, Western desert. Annals of the Geological Survey of Egypt.

Kebeasy, R.M. , Maamoun, M. and Ibrahim, E.M. ,(1982), Aswan Lake induced earthquakes. Bull. Inter. Inst. of Seismology and Earthquake Engineering, Tokyo,19.

DOI: https://doi.org/10.2312/zipe.1989.102.03

Kebeasy, R.M. , Tealeb, A. and Vyskočil, P. ,(1984), Joint research project for monitoring recent crustal movements at Aswan. NRIAG (Egypt) , ICRCM (Prague). (not published).

Kebeasy, R.M. , Maamoun, M. , Ibrahim, E.M. , Megahed, A. , Simpson, D. and Leith, W. ,(1987), Earthquake studies at Aswan reservoir. Journal of Geodynamics 7,PP.173-193.

Kebeasy, R.M. , Tealeb, A. , Gharib, A.A. and Mahmoud, S.M. , (1988), Water loading is an effective factor in inducing seismicity around Aswan Lake. Paper presented at the 6th Annual Meeting of the E.G.S., Cairo, March 1988.

Kijko, A. , Dessoky, M.M. , Kebeasy, R.M. and Haseab, G.H. , (1985), Preliminary estimation of seismic hazard in the Aswan Lake in Egypt. Acta Geophys. 33, No.3,pp.270-277.

Mahmoud, S.M. ,(1988), Crustal deformation measurements in the southwestern part of Egypt based on observations of local seismic and geodetic networks. M.SC. Thesis submitted to the Faculty of Science,Ain Shams Univ.,Cairo.

Simpson, D.W. , Kebeasy, R.M. , Nicholson, C. , Maamoun, M. , Albert, R.N.H. , Ibrahim, E.M. , Megahid, A. , Gharib, A. and Hussain, A. ,(1987), Aswan telemetered seismograph network. Journal of Geodynamics 7, pp. 195-203.

Vyskočil, P. ,(1984 a), Procedures for monitoring recent crustal movements. IAG, CRCM, ICRCM, Prague, 73 p.

Vyskočil, P. ,(1984 b), Results of recent crustal movement studies. Academia Nakladatesltui CS, Akademie VED, Ročnik 94, Sesit 8, Prague, 103 p.

Vyskočil, P. , Tealeb, A. ,(1985), Report on :Activities for monitoring recent crustal movements at Aswan in the period 1983 - 1985. Bull. Helwan Inst. of Astronomy and Geophysics V, Ser. B.

Vyskočil, P. ,(1987), Recommendation on the project of monitoring of crustal movements in the western part of the Aswan region in Egypt. Journal of Geodynamics 7, pp. 257-259.

Vyskočil, P. , Tealeb, A. , Kebeasy, R.M. and Mahmoud, S.M. , (1987), Recent crustal movement studies along the western bank of Lake Nasser, Egypt. Proc. of the 5th Annual Meeting of the E.G.S., Cairo, March 1987.

DOI: https://doi.org/10.2312/zipe.1989.102.03

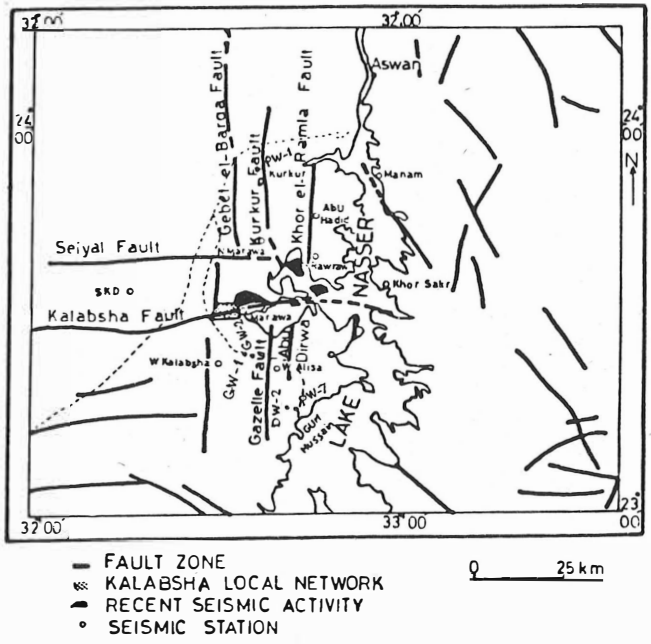

Fig.(1) Geologic structure of the northwestern area of Lake Nasser, location of Kalabsha network, Zones of recent seismic activity and location of seismic stations .

DOI: https://doi.org/10.2312/zipe.1989.102.03

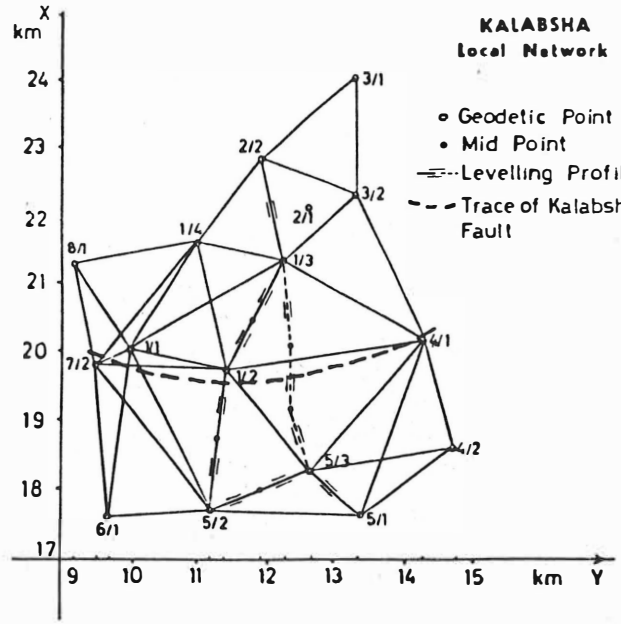

Fig.(2) Geometric configuration of Kalabsha geodetic network (16 benchmarks for horizontal measurements and 2 levelling lines crossing the Kalabsha fault) .

DOI: https://doi.org/10.2312/zipe.1989.102.03

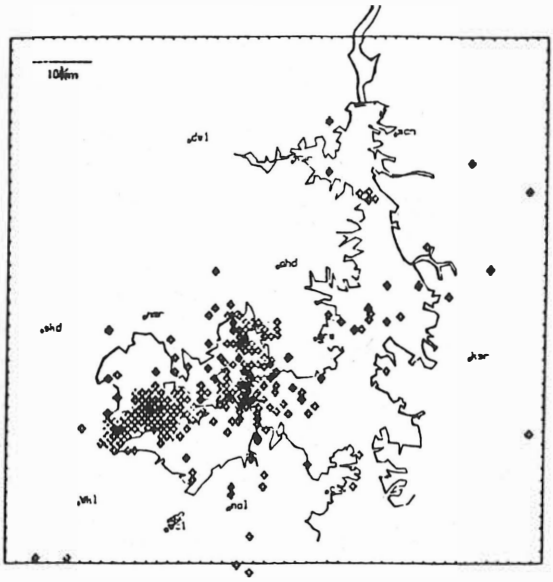

Fig.(3) Epicentral distribution of the earthquakes occured in the northwestern area of Lake Nasser for the period from July 1, 1982 to December 1987 .

DOI: https://doi.org/10.2312/zipe.1989.102.03

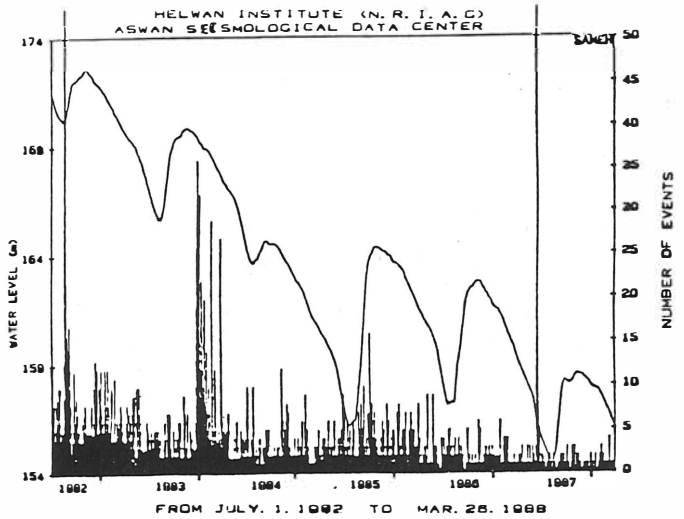

Fig.(4) Water level in the reservoir and number of earthquakes occured within the considered area for the period from July1. 1982 to March 26, 1988 .

DOI: https://doi.org/10.2312/zipe.1989.102.03

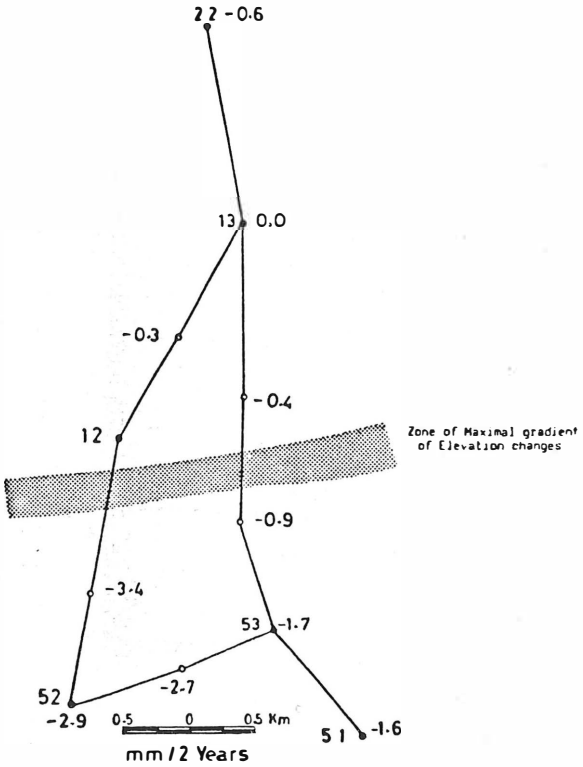

Fig.(5) Division of the Kalabsha network into two areas with different mean values of the height's changes in m m for time interval from January 1986 to January 1988 .

DOI: https://doi.org/10.2312/zipe.1989.102.03

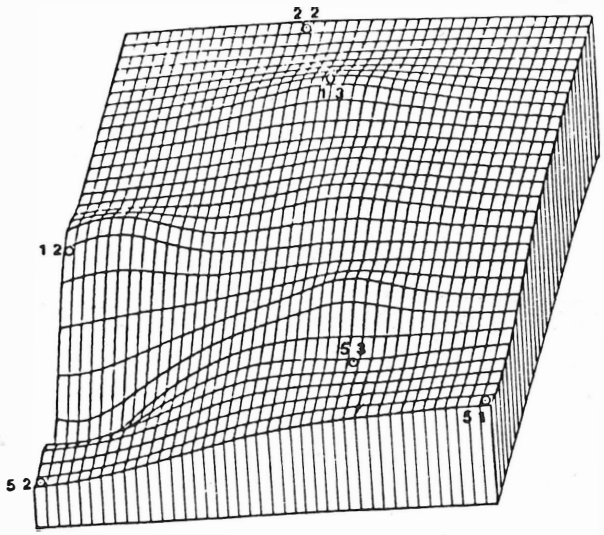

Fig.(6) An areal projection of vertical movements at Kalabsha network .

DOI: https://doi.org/10.2312/zipe.1989.102.03

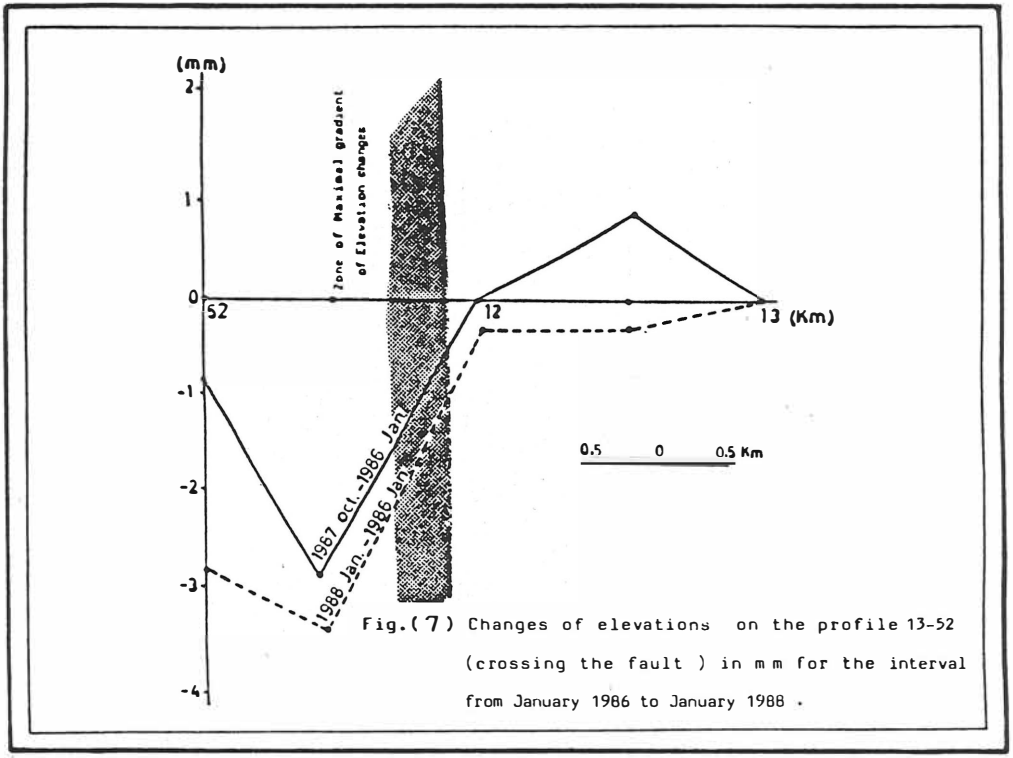

Fig.(7) Changes of elevations on the profile 13-52 (crossing the fault) in m m for the interval from January 1986 to January 1988 .

DOI: https://doi.org/10.2312/zipe.1989.102.03

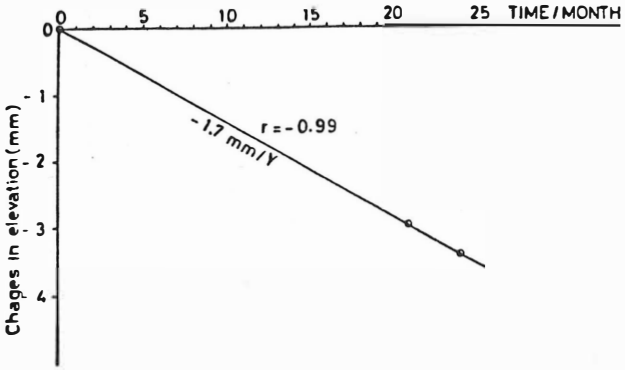

Fig.(8) The trend of height changes in time at mid- point between 52 and 12 .

DOI: https://doi.org/10.2312/zipe.1989.102.03

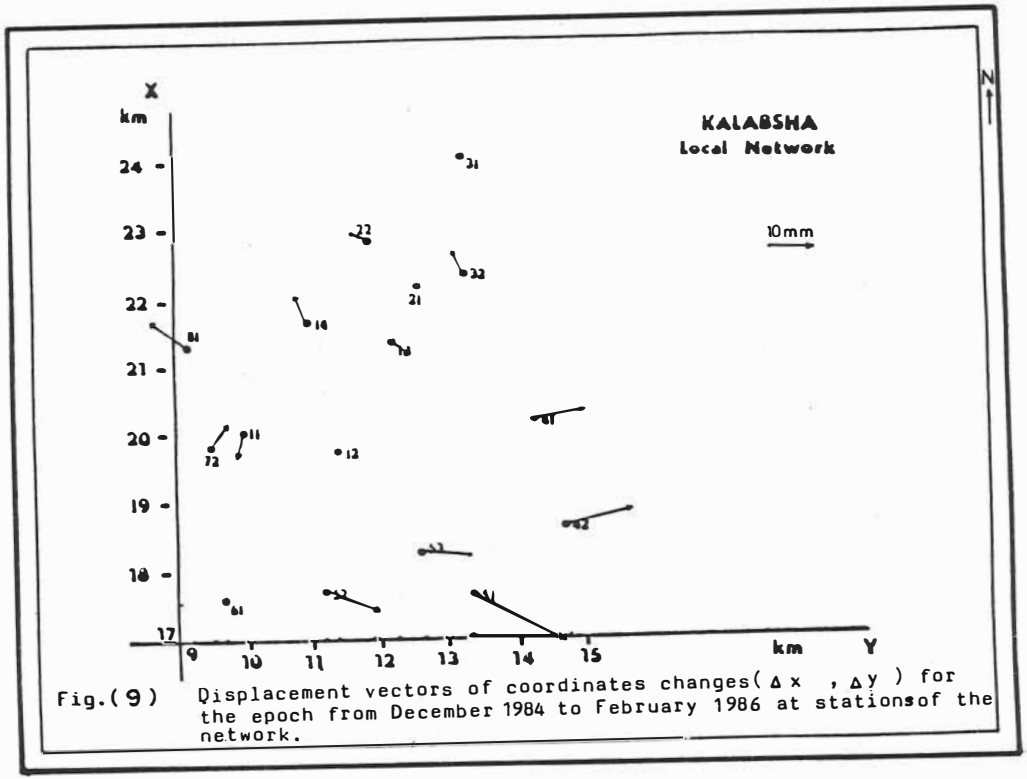

Fig.(9) Displacement vectors of coordinates changes(Δx , Δy) for the epoch from December 1984 to February 1986 at stations of the network.

DOI: https://doi.org/10.2312/zipe.1989.102.03

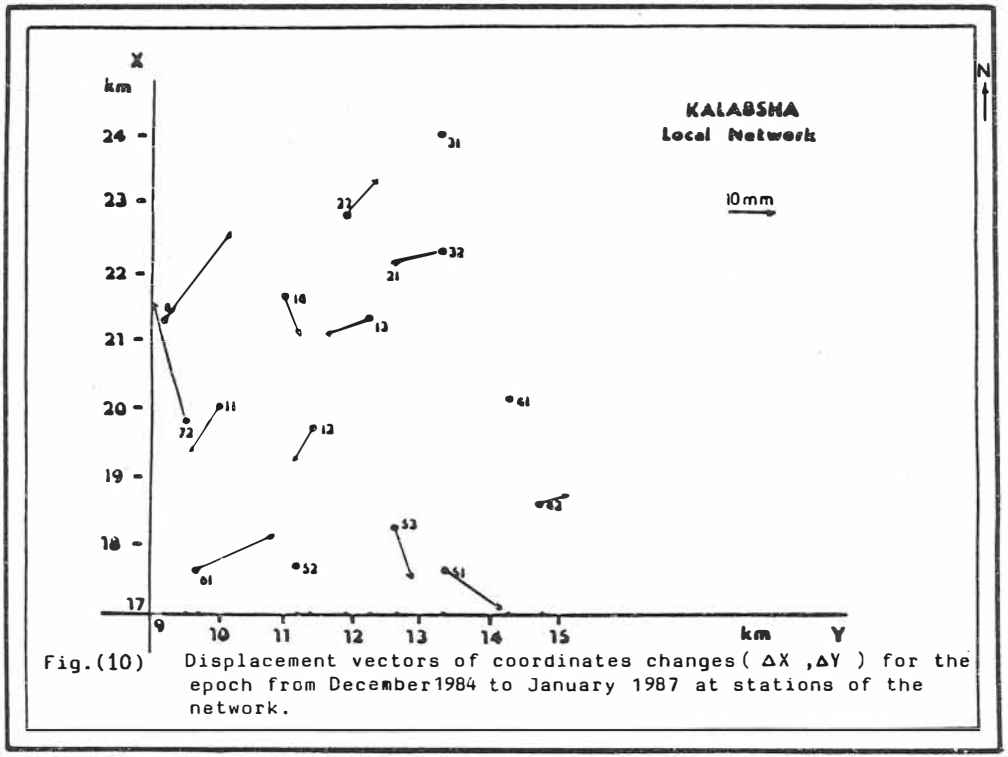

Fig.(10) Displacement vectors of coordinates changes (ΔX ,ΔY) for the epoch from December1984 to January 1987 at stations of the network.

DOI: https://doi.org/10.2312/zipe.1989.102.03

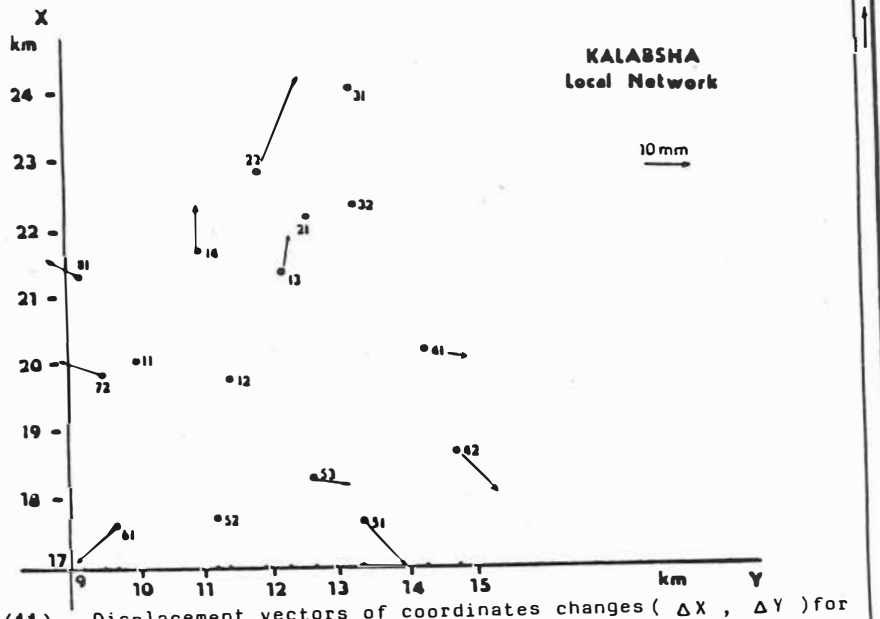

Fig.(11) Displacement vectors of coordinates changes (ΔX , ΔY) for the epoch from December 1984 to September 1987 .

DOI: https://doi.org/10.2312/zipe.1989.102.03

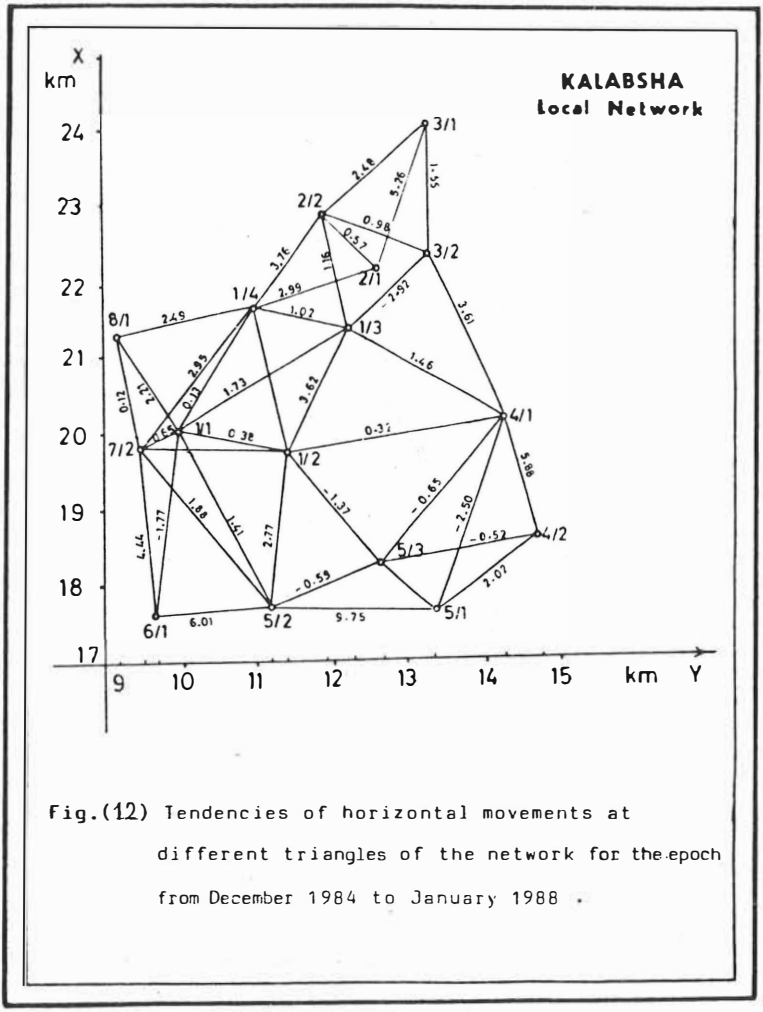

Fig.(12) Tendencies of horizontal movements at different triangles of the network for the epoch from December 1984 to January 1988 .

DOI: https://doi.org/10.2312/zipe.1989.102.03

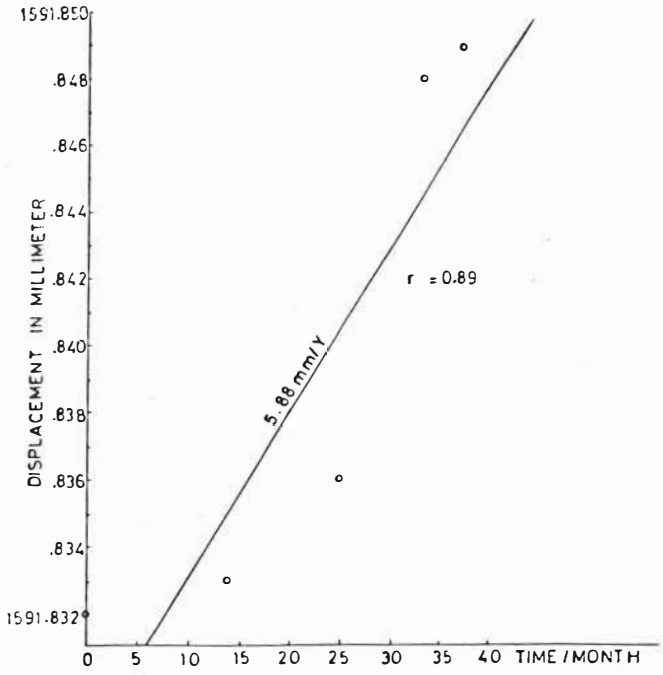

Fig.(13) Tendency of distance changes in time (in case of extension) for the distance between 41 - 42 in the epoch from December 1984 to January 1988 .

DOI: https://doi.org/10.2312/zipe.1989.102.03

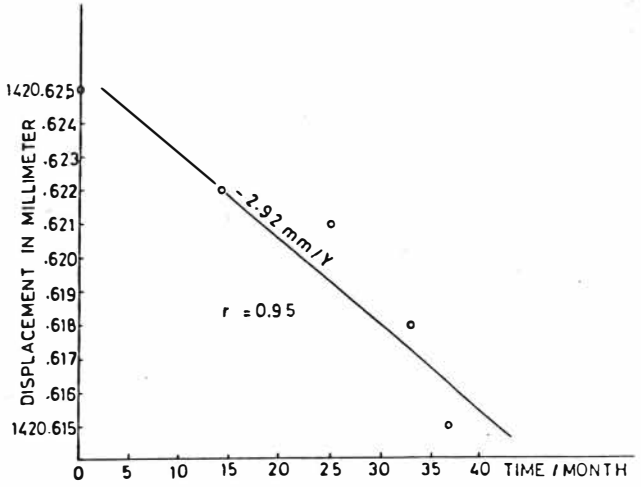

Fig.(14) Tendency of distance changes in time (in case of compression) for the distance between 13 - 32 in the epoch from December 1984 to January 1988 .

DOI: https://doi.org/10.2312/zipe.1989.102.03

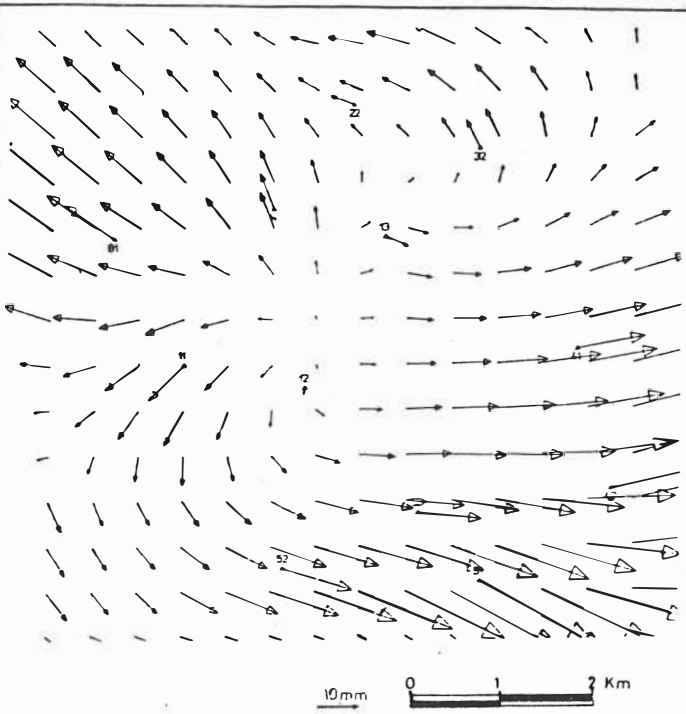

Fig.(15) Horizontal movements of the network for the epoch from December 1984 to February 1986 , computed on a grid 1 x 1 Km .

DOI: https://doi.org/10.2312/zipe.1989.102.03

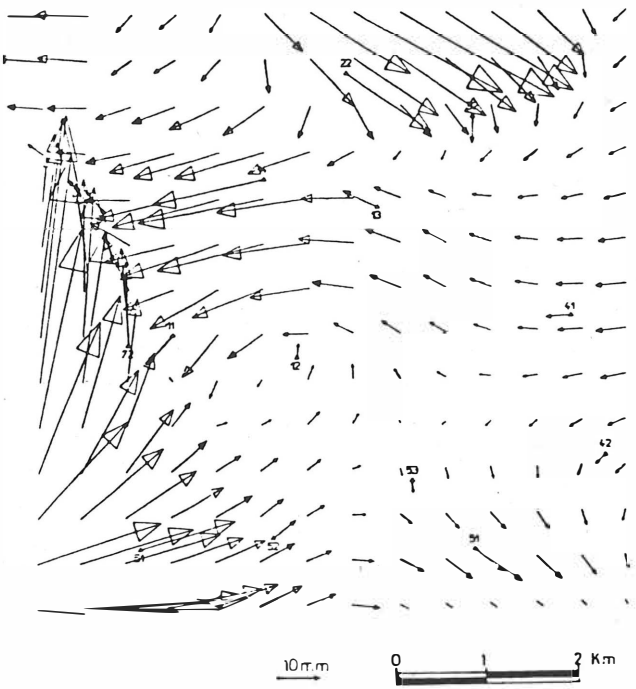

Fig.(16) Horizontal movements of the network for the epoch from December 1984 to January 1987, computed on a grid 1 x1 Km

DOI: https://doi.org/10.2312/zipe.1989.102.03

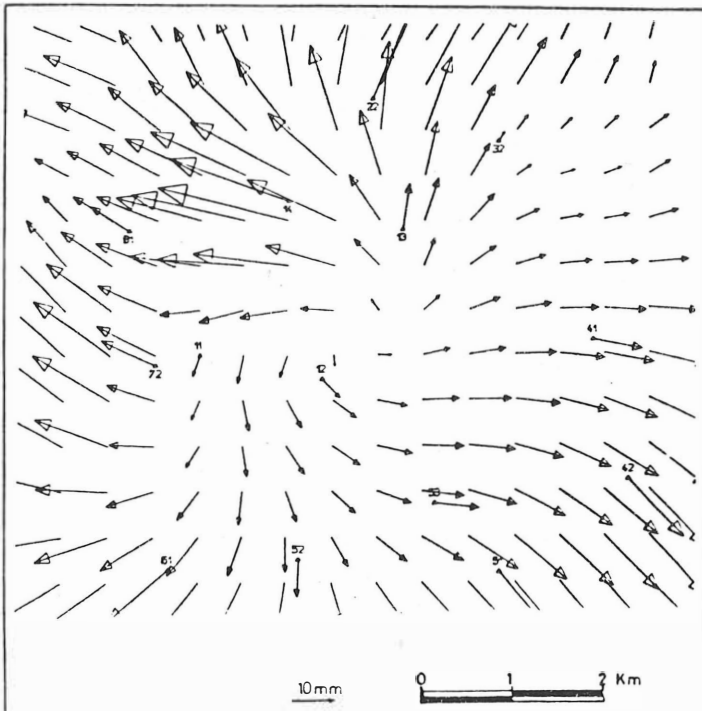

Fig.(17) Horizontal movements of the network for the epoch from December 1984 to September 1987, computed on a grid 1 x 1 km .

DOI: https://doi.org/10.2312/zipe.1989.102.03

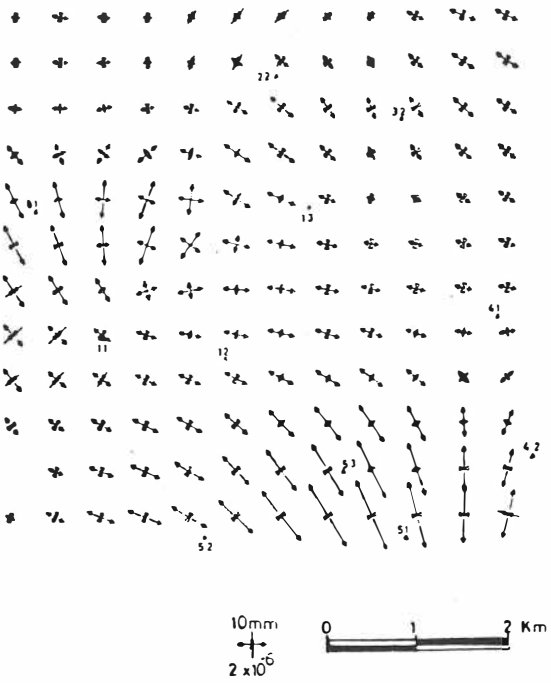

Fig.(18) Main axis of horizontal deformation fields (compression ; extension) for the epoch from December 1984 to February 1986 , computed on a grid 1 x 1 km .

DOI: https://doi.org/10.2312/zipe.1989.102.03

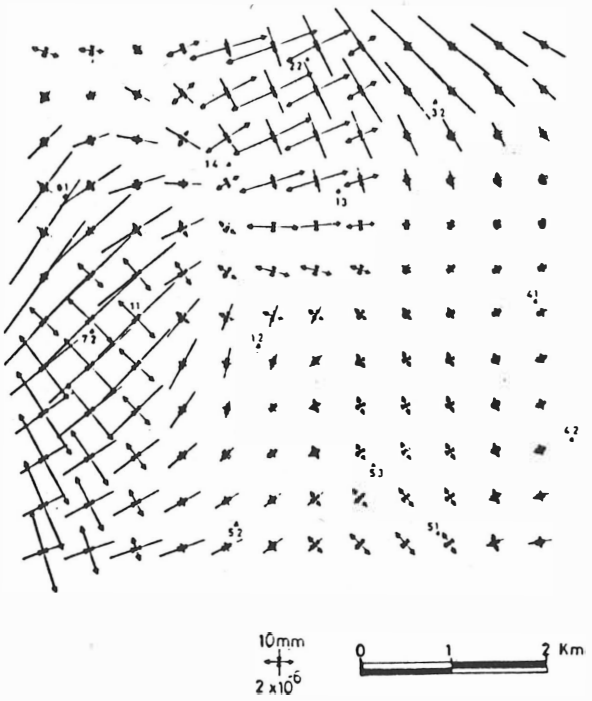

Fig.(19) Main axis of horizontal deformation fields (compression ; extension) for the epoch from December 1984 to January 1987, computed on a grid 1 x 1 km .

DOI: https://doi.org/10.2312/zipe.1989.102.03

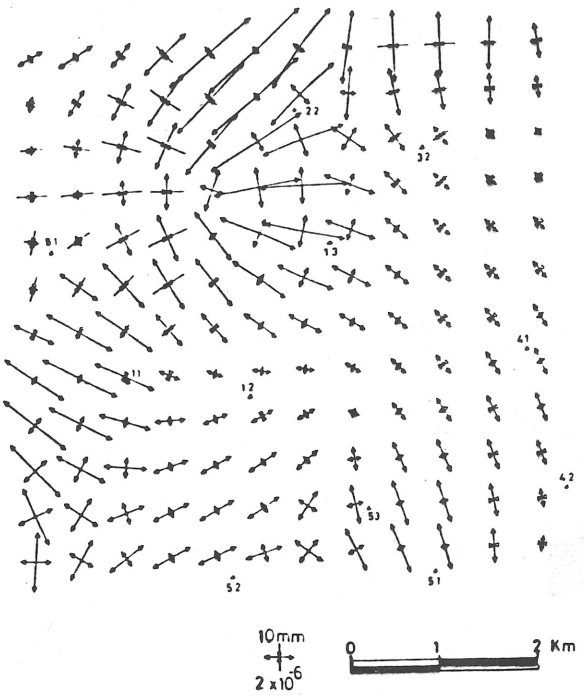

Fig.(20) Main axis of horizontal deformation fields (compression ; extension) for the epoch from December 1984 to September 1987, computed on a grid 1 x 1 km .

DOI: https://doi.org/10.2312/zipe.1989.102.03

NOTIZEN

DOI: https://doi.org/10.2312/zipe.1989.102.03

NOTIZEN

DOI: https://doi.org/10.2312/zipe.1989.102.03